Investigation of the leukaemic activity of MLL-fusions in human haematopoietic cells

Hikari Osaki

Molecular Haematology and Cancer Biology

Institute of Child Health

University College London

PhD thesis for a Degree for Doctor of Philosophy

September 2011

DECLARATION

I, Hikari Osaki, confirm that the work presented in this thesis is my own. Where information has been derived from other sources, I confirm that this has been indicated in the thesis.

ABSTRACT

The mixed lineage leukaemia (*MLL*) gene is frequently the target of chromosomal translocation in infant leukaemia. Translocation results in an in-frame chimeric fusion gene which is implicated in both ALL and AML, with particularly poor prognoses. It is widely accepted that MLL has a crucial role in regulating haematopoiesis. Our lab has previously developed a murine model for conditional expression of MLL-fusions to establish a list of transcriptional target genes using Affymetrix GeneChip analysis. In order to study the role of MLL-fusion target genes in human leukaemia cells, we generated four independent immortalised myeloid cell lines from human cord blood, using the MLL-AF9 fusion, by means of lentiviral transduction. The transduced cells proliferated exponentially in liquid culture and were found to cause leukaemia upon xenotransplantation into immunodeficient mice. One of the target genes up-regulated by the MLL-fusions, *RUVBL2*, encodes an ATPase belonging to AAA^+ family that has multiple roles in telomerase and chromatin-remodelling complexes. In this study, we demonstrate that *RUVBL2* is also up-regulated by MLL-AF9 in human immortalised myeloid cells. shRNA knock down of *RUVBL2* expression in these cells, and in the human leukaemia cell line THP-1, results in decreased cell proliferation and clonogenic potential, accompanied by an increase in apoptosis and differentiation, as judged by CD15 expression. Furthermore, inhibition of *RUVBL2* expression in THP-1 cells leads to a reduction in *hTERT* mRNA expression and telomerase activity. Together, these data demonstrate the requirement of RUVBL2 to mediate *MLL*-fusion induced telomerase activity in human cells, and suggest the possibility of targeting RUVBL2 as a potential therapeutic strategy for MLL-fusion associated leukaemia.

TABLE OF CONTENTS

TABLE OF FIGURES

LIST OF TABLES

ABBREVIATIONS

4-OHT	4-Hydroxy-tamoxifen
AAA+	ATPases belonging to the ATPAse associated with various cellular activities
AF4	*MLL* translation partner on chromosome 4q2, also known as AFF1, AF4/FMR2 family member1
AF9	*MLL* translocation partner on chromosome 9p22 also known as MLLT3, myeloid/lymphoid or mixed-lineage leukaemia translocated to 3
AF6	*MLL* translocation partner on chromosome 6q11 also known as MLLT4, myeloid/lymphoid or mixed-lineage leukaemia translocated to 4
AF10	*MLL* translocation partner on chromosome 10q11 also known as MLLT10, myeloid/lymphoid or mixed-lineage leukaemia translocated to 10
AGM	aorta-gonad-mesonephros
ALL	acute lymphoid leukaemia
AML	acute myeloid leukaemia
ASH2L	(absent, small, or homeotic)-like
Bad	Bcl-2 antagonist of cell death
Bax	BCL-2-associated X
Bid	BH3-interacting domain death agonist
BCR	breakpoint cluster region
BFU-E	burst-forming unit-erythroid
BSA	Bovine serum albumin
CAFC	Cobblestone area-forming colony
CB	cord blood
CBP	CREB-binding protein
CD	cluster of differentiation
cDNA	complementary deoxyribonucleic acid
CFC	colony forming cell
CFU	colony formation unit

CFU-E	CFU-erythroid
CFU-GEMM	CFU-granulocyte/erythoroid/macrophages/megakaryocyte
CFU-GM	CFU-granulocyte/macrophage
CFU-Mk	CFU-megakaryocyte
CHIP	chromatin immunoprecipitation
CLP	common lymphoid progenitor
CMP	common myeloid progenitor
CMV	cytomegalovirus
CtBP	C-terminal-binding protein
CSC	cancer stem cell
CYP	cyclophilin
DAPI	4', 6-diamidino-2-phenylindole
DC	dendritic cells
DMNT	DNA methyltransferase
DNA	deoxyribonucleic acid
dNTPS	deoxyribonucleotide triphosphates
Dot1l	Disruptor of telomeric silencing-1
Dox	doxycycline
DSIF	DRB sensitivity-inducing factor
DTT	dithiothreitol
E	embryonic day
EAP	ENL-associated protein
EBFAF	ENL associated BRG1- or hbrm-associated factors
EGFP	enhanced green fluorescent protein
ENL	eleven-nineteen leukaemia, also known as MLLT1, myeloid/lymphoid or mixed-lineage leukaemia translocated to 1
env	envelope proteins
ESET	ERG-associated protein with SET domain
FAB	French-American-British
FCS	foetal calf serum
FcγR II/III	Fcγ receptor II/III

FLT3L	FMS-related tyrosine kinase 3 ligand
E-LTC-IC	extended long-term culture-initiating cell
gag	group antigens
GATA-1	GATA binding factor 1
G-CSF	granulocyte colony-stimulation factor
GMLP	granulocyte/monocyte/lymphoid progenitor
GMP	granulocyte/monocyte progenitor
H3K4	histone 3 lysine 4
H3K79	histone 3 lysine 79
HAT	histone acetyl transferase
hCD2	human CD2
HDAC	histone deacetylase
HLA	human leukocyte antigen
HOX	homeoprotein
HPC	haematopoietic progenitor cell
HPGM™	Haematopoietic Progenitor Growth Medium
HRP	horseradish peroxidase
HSC	Haematopoietic stem cells
IL-7αR	interleukin-7 α receptor
IMAGE	Integrated Molecular Analysis of Genomes and their Expression
IMDM	Iscove's modified Dulbecco's medium
IRES	internal ribosome entry site
LEDGF	lens epithelium derived growth factor
Lin	lineage-associated-surface markers
LMPP	lymphoid primed multipotent progenitor
LSC	leukaemic stem cell
LTC-IC	long-term culture-initiating cell assay
LT-HSC	long-term repopulating HSC
MACS	magnetic activated cells sorting
MBII	c-Myc domain box II

MEIS1	mouse ecotropic integration site
MEP	megakaryocytic/erythroid progenitor
MFI	mean florescence intensity
MGG	May-Grünwald-Giemsa
miR30	micro RNA 30
MLL	mixed lineage leukaemia
MLL^{C}	C-terminal fragment of MLL
MLL^{N}	N-terminal fragment of MLL
MOF	males absent on the first
MPP	multipotent progenitor
ms	millisecond
MYB	myeloblastosis viral oncogene homolog
MYC	myelocytomatosis viral oncogene homolog
NEB	New England Bio Labs
NELF	negative elongation factor
NHEJ	non-homologous end joining
NK	natural killer
NOD	non-obese diabetic
MoLV	Moloney murine leukemia virus
NSG	NOD-scid-gmma (NOD.Cg-$Prkdc^{scid}$ $Il2rg^{tm1Wjl}$/SzJ)
ODN	oligodeoxyribonucleotide
OH	hydroxyl
PAF1C	mammalian PAF elongation complex
PBS	phosphate buffered saline
PcG	polycomb group proteins
PCR	polymerase chain reaction
PHD	plant homeodomain
Plat-GP	platinum-GP
PMA	Phorbol 12-myristate 13-acetate
Pol II CTD	polymerase II C-terminal domain kinase

pTEFb	positive transcription elongation factor b
PVDF	polyvinylidenefluoride
RBBP5	retinoblastoma binding protein 5
RD	repression domain
rh	recombinant human
RISC	RNA-induced silencing complex
RNA	ribonucleic acid
RNP	ribonucleoprotein
rpm	revolutions per minutes
RPMI	Roswell Park Memorial Institute medium
RRM	RNA recognition motif
RTA	relative telomerase activity
Sca-1	stem cell antigen-1
SCF	stem cell factor
SCID	severe combined immunodeficiency
SD	standard deviation
SDS	Sodium Dodecyl Sulfate
SDS-PAGE	SDS- polyacrylamide gel electrophoresis
SET	su(var)3-9, enchancer-of-zeste, trithorax
SFFV	spleen focus-forming virus
shRNA	short-hairpin ribonucleic acid
siRNA	small interfering ribonucleic acid
SL-IC	SCID-leukaemia initiating cell
SNL	sub-nuclear localisation domain
SRC	SCID repopulating cell
ST-HSC	short-term HSC
SWI-SNF	SWItch/Sucrose NonFermentable
TD	Transactivation domain
TERC	telomerase RNA component
TERT	telomerase reverse transcriptase

tGFP	turbo green fluorescent protein
TPO	thrombopoietin
tTA	tetracycline-controlled transactivator protein
TRE	tetracycline-responsive promoter element
Trx	*Trithorax*
Trx-G	*Trithorax* group
VSV-G	Vesicular stomatitis virus Glycoprotein
WBBP5	retinoblastoma binding protein 5
WDR5	WD repeat domain 5
WHO	World Health Organisation
YEATS	Yaf9, ENL, AF9, Taf14, and Sas5

ACKNOWLEDGEMENTS

First of all, I would like to express my sincere gratitude to my principle supervisor, Dr. Owen Williams, for dedicating so much time, and providing me with invaluable support throughout the four years of my PhD. Without his inspirational guidance, enthusiasm and encouragement, this thesis would not have been possible. I am also deeply grateful to my secondary supervisor, Dr. Jonathan Ham, for his continuous support and encouragement throughout.

I am thankful to all my colleagues and friends in the Molecular Haematology and Cancer Biology Unit, Institute of Child Health. I would especially like to thank Dr. Jasper De Boer and Dr. Vanessa Walf-Vorderwülbecke for sharing their expertise in many experimental procedures and providing me with constant support with patience. Also I wish to thank Mr Maurizio Mangolini for kindly performing some experiments.

I would also like to acknowledge Great Ormond Street Hospital for funding my PhD and the Institute of Child Health, University College London, for giving me the opportunity to carry out this research.

Finally, I would like to thank my family, especially my mother, for giving me unequivocal support throughout. Above all, I would like to thank Rick Hayes for his patience, endless support, and his never failing faith in me.

CHAPTER 1. INTRODUCTION

1.1. Ontogeny of haematopoiesis

Haematopoiesis refers to a highly organised maturation process of blood cells. Haematopoietic diversity originates from haematopoietic stem cells (HSCs), which by definition, have the ability to self-renew and to differentiate into multiple progenitor cells that eventually terminally differentiate into mature cells [reviewed in (Orkin, 2000; Iwasaki and Akashi, 2007)]. Haematopoiesis occurs in two distinct waves. Primitive haematopoiesis refers to the initial transient red blood cell production necessary to oxygenate the rapidly growing embryo, while definitive haematopoiesis refers to production of long-term repopulating HSCs (LT-HSC), that later on replace primitive haematopoiesis to generate multipotent haematopoietic progenitors (Cumano and Godin, 2001; Orkin and Zon, 2008). Although most of what we know about haematopoiesis is derived from studies in mouse models, there are many similarities between mouse and human haematopoiesis, suggesting that this process is highly conserved [reviewed in (Marshall and Thrasher, 2001; Tavian and Peault, 2005)]. In mice, primitive haematopoietic cells are first observed in the primitive streak after gastrulation, at embryonic day seven (E7), and then migrate into the yolk sac where primitive haematopoiesis is initiated (Palis et al., 1999) (Figure.1.1). Definitive haematopoiesis, on the other hand, derives from the aorta-gonad-mesonephros (AGM) region of the mouse embryo at E10.5 (Muller et al., 1994; Medvinsky and Dzierzak, 1996; de Bruijn et al., 2000). The emerging HSC subsequently colonise the placenta, foetal liver, thymus, spleen and then the bone marrow (Muller et al., 1994; Medvinsky

and Dzierzak, 1996; Gekas et al., 2005). A diagram summarising mouse and human haematopoiesis is shown in Figure 1.1.

In the highly organised hierarchy of haematopoiesis, LT-HSCs give rise to short-term repopulating HSCs (ST-HSCs). Unlike LT-HSC, ST-HSCs have limited self-renewal ability (Morrison and Weissman, 1994). Two distinct lineages then derive from ST-HSCs. The common lymphoid progenitors (CLPs) generate all lymphoid cells, including T cells, B cells and Natural killer (NK) cells (Kondo et al., 1997). The common myeloid progenitors (CMPs) produce granulocyte/monocyte progenitors (GMPs) which differentiate into monocytes and granulocytes. These then mature into macrophages, and neutrophils, eosinophils and basophils, respectively (Akashi et al., 2000). Megakaryotic/erythroid progenitors (MEPs) in contrast, give rise to megakaryocytes/platelets and erythrocytes (Akashi et al., 2000). All of these progenitors show a limited self renewing capacity upon transplantation into lethally irradiated mice (Akashi et al., 2000). Finally, dendritic cells (DC) have been reported to derive both from CMPs and CLPs (Traver et al., 2000).

1.2. Haematopoietic assays

Several methods have been developed to assay haematopoietic lineages. In order to determine lineage restricted progenitors, a short-term *in vitro* assay is used, known as the colony forming cell (CFC) assay [reviewed in (Coulombel, 2004)]. This assay determines the ability of single cells, or colony forming units (CFU), to form colonies in semi-solid media.

Figure 1.1. Establishment of primitive definitive haematopoiesis in mouse and human embryos [adapted from (Mikkola et al.,2006)]

The diagram illustrates haematopoiesis in mouse and human embryos at different age stages. Red bars indicate active haematopoietic differentiation, yellow bars represent generation of HSCs, and blue bars represent adult LT-HSCs. Broken yellow bars represent *de novo* HSC generation that has not been experimentally shown.

Several types of progenitors including CFU-erythroid (CFU-E), burst-forming unit-erythroid (BFU-E), CFU-granuclocyte/macrophage (CFU-GM), CFU-granulocyte/erythoroid/macrophages/megakaryocyte (CFU-GEMM), CFU-preB and CFU-megakaryocyte (CFU-Mk), can be observed using this assay (technical manual from Stem cells Technology, Sheffield, UK). This assay can be used to study both mouse and human myeloid progenitors (Coulombel, 2004). The CFC-U assay, however, is not appropriate for more immature haematopoietic cells, since the semi-solid media can only support viable cells for approximately 2 weeks. This is not sufficient for HSC to generate lineage committed progenitor cells and self-renew (Coulombel, 2004).

In contrast to the CFC-U assay, the long-term bone marrow culture assay enabled immature haematopoietic cells to persist longer in culture by co-culturing them on a layer of adherent cells (stromal feeders) isolated from bone marrow. The adherent cells support haematopoietic cell growth and together they recreate some aspects of the physiology found in the bone marrow microenvironment (Dexter et al., 1977). The stromal feeder based assay was adapted and modified to detect more primitive progenitor cells known as the long-term culture-initiating cells (LTC-IC) (Sutherland et al., 1989; Sutherland et al., 1990). LTC-ICs are immature haematopoietic cells that are able to produce CFC-U beyond 5 weeks. LTC-ICs are detected by co-culturing immature hematopoietic cells on pre-irradiated adherent cells from mouse or human bone marrow. The long culture period allows LTC-IC to properly propagate while promoting all other committed progenitors to terminally differentiate (Sutherland et al., 1989). Another way to assess primitive haematopoietic cells is the cobblestone area-forming cell (CAFC) assay, in which HSCs integrate into the stromal feeder layer,

resulting in the formation of cobblestone-like patches. This formation provides a visual indication of immature cell propagation (Ploemacher et al., 1989). The extended LTC-IC (E-LTC-IC) assay was used to identify more primitive haematopoietic cells that proliferate longer in the culture than the LTC-IC cells. This assay used human bone marrow or cord blood and supplemented the LTC-IC assay with cytokines and had an extended culture period beyond 8 weeks. The immature cells detected using this assay were more quiescent than those from LTC-ICs, suggesting that these cells represent more primitive haematopoietic cells (Hao et al., 1996). Overall, these studies indicate the importance of stroma based assays to support both mouse and human haematopoiesis *in vitro*.

However, none of these *in vitro* assays are fully able to recapitulate the bone marrow microenvironment. For this reason, transplantation of isolated mouse haematopoietic cells into lethally irradiated recipient mice is the most commonly used method to assess HSC activity (Spangrude et al., 1988; Morrison and Weissman, 1994). This is assessed by measuring homing of HSC to the bone marrow, long-term engraftment of HSC and multi-lineage repopulation of recipient mice. Since this technique is not possible in the human system, xenotransplantation using immunodeficient recipient mice or foetal sheep has been performed to examine the activity of human HSCs [reviewed in (Bonnet, 2005)]. Initially, severe combined immunodeficiency (SCID) mice were used as recipients for engraftment of human bone marrow (Kamelreid and Dick, 1988; Lapidot et al., 1992) and cord blood cells (Vormoor et al., 1994). These immature haematopoietic cells, that are able to propagate in recipient mice, were termed SCID-repopulating cells (SRC). The engraftment efficiency in this model, however, was sub-optimal due to residual NK cell activity in SCID mice [reviewed in (Bonnet, 2002;

Dick, 2008)]. In order to overcome this problem, non-obese diabetic (NOD)/SCID mice, that have additional deficiencies in NK cell and macrophage activity, were generated, and this strain has been shown to provide higher engraftment of human cells (Shultz et al., 1995).

1.3. Mouse haematopoiesis

In mouse haematopoiesis, HSCs were first identified in the bone marrow as being negative for the expression of lineage-associated-surface markers (Lin), while expressing stem cell angtigen-1 (Sca-1) and c-Kit. This population is now known as the LSK (Lin^- $Sca\text{-}1^+$ $c\text{-}Kit^+$) bone marrow fraction (Spangrude et al., 1988; Ikuta and Weissman, 1992). Approximately 0.05% of mouse bone marrow cells have multi-lineage differentiation capacity, as shown by *in vivo* reconstitution assays (Spangrude et al., 1988). Within the LSK fraction, LT-HSCs are found within a fraction of $CD34^-$, (Osawa et al., 1996), $Thy1.1^{lo}$ (Morrison and Weissman, 1994) and $CD38^+$ (Randall et al., 1996) cells. In contrast, ST-HSCs are found to reside in the $CD34^+$ (Osawa et al., 1996) and $CD38^-$ fraction (Randall et al., 1996). Due to the transient repopulating activity of ST-HSCs, these cells are also referred to as multipotent progenitors (MPP). Despite some attempts to differentiate these two populations, primarily using CD4 and CD11b expression (Morrison et al., 1994; Morrison et al., 1997), no distinctive functional differences have been reported [reviewed in (Iwasaki and Akashi, 2007)].

The first lineages derived from the LSK fraction are CLPs and CMPs (Kondo et al., 1997; Akashi et al., 2000). CLPs were originally isolated by virtue of interleukin-7α

receptor (IL-7αR) expression and defined as the IL-7α^{+} Lin^{-} Sca-1^{lo} c-Kit^{lo} population of cells. CLPs have the ability to give rise to lymphoid cells but are unable to generate myeloid progenitrors (Kondo et al., 1997). CMPs on the contrary, reside in the IL-7Rα^{-} fraction (Akashi et al., 2000). This IL-7Rα^{-} Lin^{-} Sca-1^{-} c-Kit^{+} population exclusively possesses myeloid colony forming potential and can be divided into subgroups using expression of the Fcγ receptor II/III (FcγR II/III or CD16/32) and CD34. Thus, CMPs are FcγR II/III^{lo} CD34^{+}, whereas MEP are FcγR II/III^{lo} CD34^{-} and GMP are FcγR II/III^{hi} CD34^{+} (Akashi et al., 2000). The discovery of CMP and CLP led to the classical pathway hypothesis that down-stream myeloid and lymphoid progenitors only rise from CMP and CLP, respectively (Iwasaki and Akashi, 2007). A simple diagram illustrating this original model is shown in Figure1.2A.

In recent years there have been a number of reports suggesting possible alternative haematopoietic pathways and challenging the original classical pathway of haematopoiesis. This was due to the discovery that MPPs/ST-HSCs were in fact more heterogeneous in myeloid/lymphoid commitment than originally thought (Adolfsson et al., 2005). Cells within the LSK population with high expression levels of the FMS-related tyrosine kinase 3 (Flt3) were found to have lost the ability to mature into MEP, when compared to a population without Flt3 expression (Adolfsson et al., 2005). This subpopulation of LSK cells with Flt3 expression was named the lymphoid primed multipotent progenitor (LMPP), because although this population preferentially differentiates into lymphoid progenitors, it still possesses the potential to mature into GMP (Adolfsson et al., 2005).

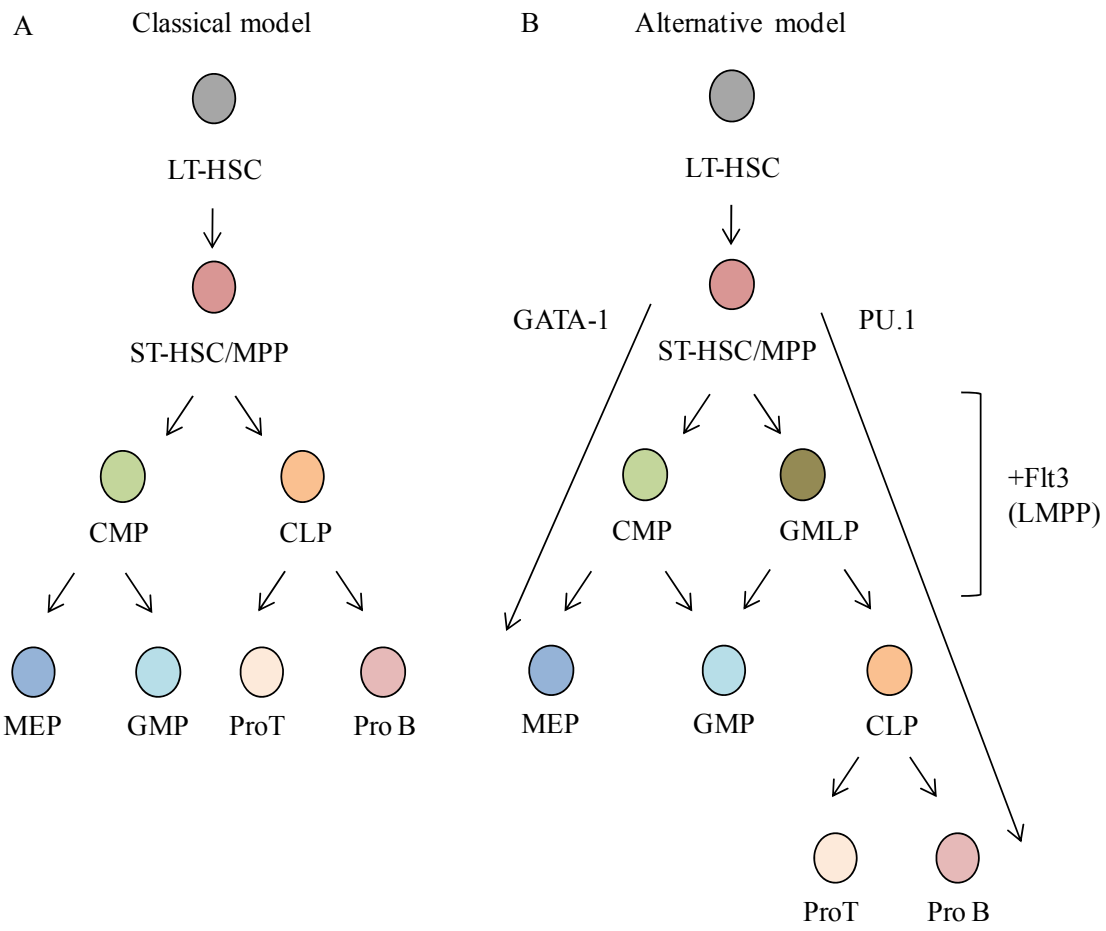

Figure 1.2. Classical model and alternative model of mouse haematopoiesis [adapted from (Arinobu et al., 2007)]

A) The diagram illustrates the classic model for mouse haematopoiesis. LT-HSC, long-term repopulating haematopoietic stem cells; ST-HSC, short-term repopulating haematopoietic stem cells; MPP, multipotent progenitors; CMP, common myeloid progenitor; GMP, granulocyte/monocyte progenitor and MEP, megakaryotic/erythroid progenitor. B) The diagram illustrates the alternative model for mouse haematopoiesis. LMPP, lymphoid primed multipotent progenitor.

This observation suggests that MEP potential is first lost from the ST-HSC/MPP population, and this is the first step towards lineage commitment (Adolfsson et al., 2005). Arinobu *et al* further investigated this possible alternative pathway of haematopoiesis by analysing expression of the GATA binding factor (GATA-1) and PU.1 transcription factors (Arinobu et al., 2007). PU.1 belongs to the ETS family of transcription factors and its expression is essential for HSC renewal and CMP and CLP development (Iwasaki et al., 2005). GATA-1, on the other hand, is a transcription factor regulating MEP development (Fujiwara et al., 1996). $PU.1^+$ MPP/ST-HSCs were found to give rise to granulocyte/monocyte/lymphoid progenitors (GMLP), that in turn are restricted to GMP and CLP production like the LMPP, while $GATA\text{-}1^+$ MPP/ST-HSCs gave rise to both MEPs and GMPs, and were functionally identical to conventional CMPs (Arinobu et al., 2007). The new model of haematopoietic differentiation is shown in Figure1.2B. Note that, unlike the conventional model, this new model suggests that GMP development can be achieved from both CMPs and GMLPs (Arinobu et al., 2007).

1.4. Human haematopoiesis

Although there are many similarities between haematopoietic pathways in humans and mice, considerable differences have also been reported [reviewed in (Iwasaki and Akashi, 2007)]. For example, LT-HSCs are found in the $CD34^-CD38^+$ population in mice, while the $CD34^+CD38^-$ population marks the LT-HSCs in human haematopoiesis (Terstappen et al., 1991; Okuno et al., 2002). Indeed, CD34 was found to be expressed in most CLPs, CMPs, and approximately 30% of MEPs [(Okuno et al., 2002); also reviewed in (Iwasaki and Akashi, 2007)]. However, there is some evidence that human

LT-HSCs devoid of CD34 expression also show repopulating property *in vivo* (Goodell et al., 1997; Bhatia et al., 1998). This Lin^- $CD34^-$ $CD38^-$ population showed limited clonogenic potential *in vitro*, unlike $CD34^+$ cells, indicating that it is a distinct subset of cells (Bhatia et al., 1998). This evidence, together with the existence of mouse $CD34^-$ LT-HSCs, indicates that the Lin^- $CD34^-$ $CD38^-$ subpopulation may represent a more immature form of LT-HSC [reviewed in (Bonnet, 2002)].

In human myelopoiesis, $CD34^+CD38^-CD90^+CD45RA^-$ HSCs give rise to CMPs, expressing CD38, low CD123, while losing CD90 expression ($CD34^+CD38^-CD90^-CD45RA^-CD123^{lo}$) (Manz et al., 2002). CMPs have the ability to differentiate into GMPs, which acquire the expression of CD15 and CD45RA ($CD15^+CD34^+CD38^+CD90^-CD45RA^+CD123^{lo}$). GMPs then give rise to monoblasts and myeloblasts. Monoblasts are characterised by the expression of CD14 and CD11b and the ability to differentiate into monocytes, while myeloblasts, which are CD14 negative, terminally differentiate into neutrophils. A schematic diagram of human myelopoiesis and expression markers of each stage is shown in Figure 1.3.

1.5. Cancer stem cells (CSC)

Following the discoveries in normal haematopoiesis, it became apparent that normal stem cell properties in many ways resemble those of cancer cells. For example, both HSCs and a subpopulation of cancer cells can generate more differentiated progeny, and both cells have a prolonged self-renewal ability [reviewed in (Reya et al., 2001)].

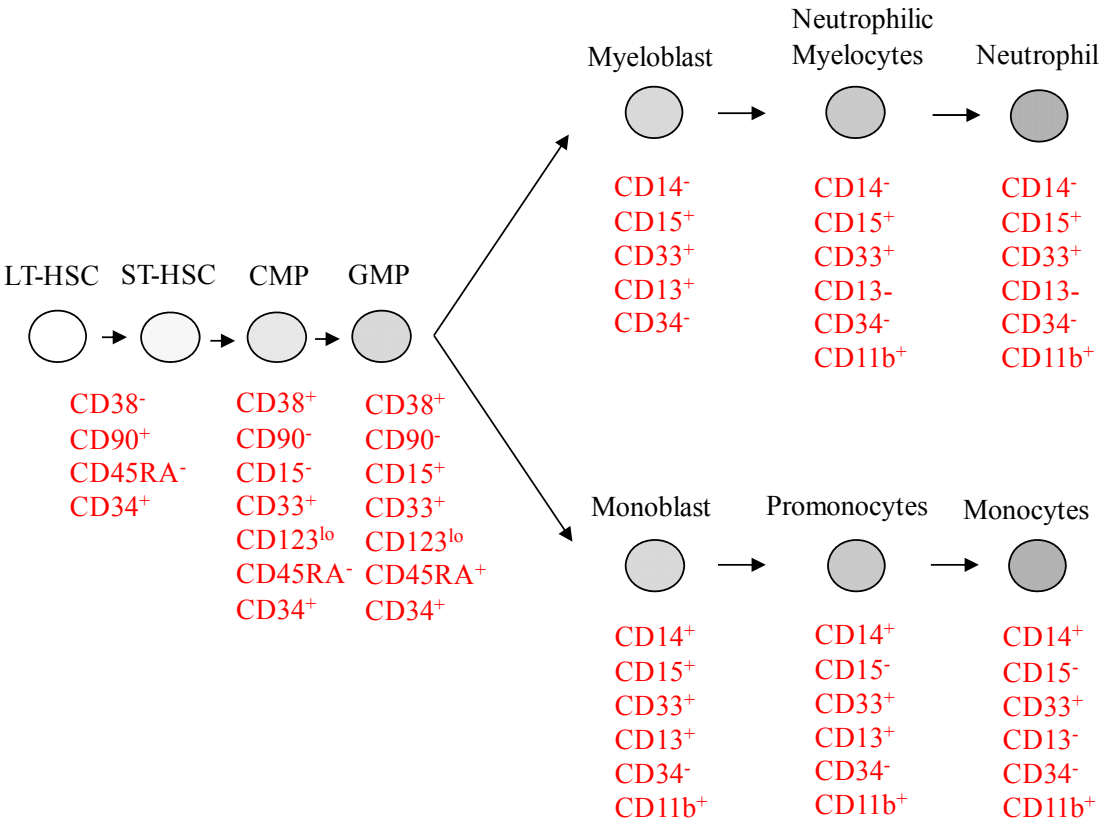

Figure 1.3. Human myelopoiesis (Adapted from KEGG pathway; http://www.genome.jp/kegg/pathway/hsa/hsa04640.html and Manz et al., 2002)

The diagram illustrates the human myelopoiesis and expression of associated surface antigen markers. LT-HSC, long-term repopulating haematopoietic stem cell; ST-HSC, short-term repopulating haematopoietic stem cell; MPP, multipotent progenitor; CMP, common myeloid progenitor; GMP, granulocyte/monocyte progenitor and MEP, megakaryotic/erythroid progenitor.

These observations were brought together into one hypothesis that cancer cells may derive from a small population of cancer stem cells (CSC), which have stem cell-like properties and can give rise to the entire cancer cell population [reviewed in (Reya et al., 2001)]. Evidence for this hypothesis was first observed in leukaemia (Lapidot et al., 1994; Bonnet and Dick, 1997). In these studies, only sorted $CD34^{+}CD38^{-}$ cells from patient AML samples were successfully engrafted onto SCID (Lapidot et al., 1994) or NOD/SCID (Bonnet and Dick, 1997) mice to develop acute myeloid leukaemia (AML), and these cells could also be serially transplanted (Bonnet and Dick, 1997). This was consistent regardless of the different AML types analysed. Based on these observations, the term SCID leukaemia-initiating cells (SL-IC) was adapted for the engrafting cells (Lapidot et al., 1994). Moreover, immunophenotype and morphological analysis of transplanted mice both suggested that this population gave rise to leukaemia progeny that highly resembled the disease from the donor AML patients (Bonnet and Dick, 1997). An initial model for leukaemic stem cells (LSCs) proposed that leukaemogenesis creates LSC from the most primitive stage of haematopoiesis, the $CD34^{+}CD38^{-}$ HSC, and that LSC are generated as a consequence of the HSC acquiring transforming mutations (Bonnet and Dick, 1997) (Figure 1.4). Since then, the LSC concept has been adapted to other cancers and CSCs have been discovered in solid cancers, such as breast and brain malignancies (Al-Hajj et al., 2003; Singh et al., 2003).

However, accumulating evidence suggests that more committed progenitors are also able to undergo transformation to give rise to LSCs [reviewed in (Bonnet, 2005; Huntly and Gilliland, 2005)]. Cozzio *et al* used retroviral transduction of the leukaemic fusion gene *MLL-ENL* to demonstrate that GMPs and CMPs, but not MEPs, could be transformed and induce leukaemia (Cozzio et al., 2003).

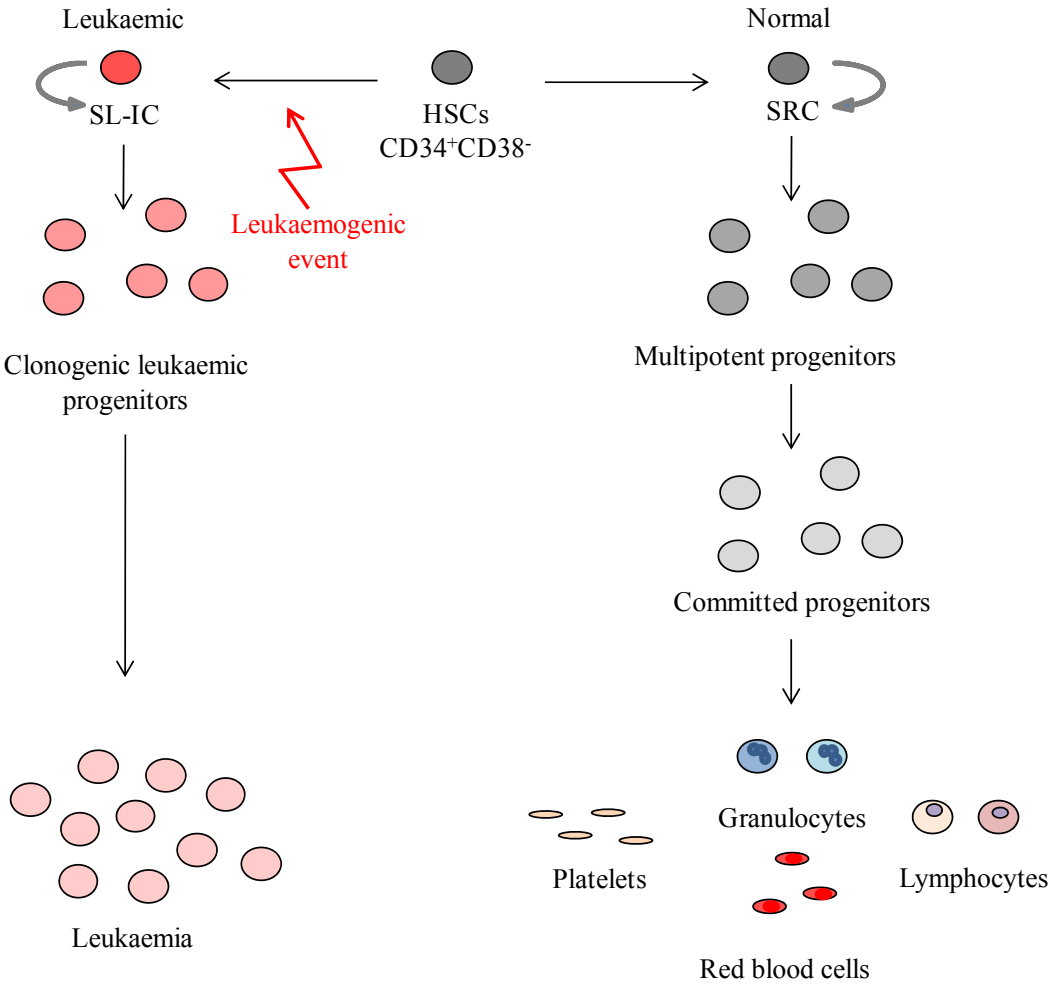

Figure 1.4. Original cancer stem cell model [adapted from (Bonnet et al., 1997)]

The diagram illustrates the original model of cancer stem cell organisation. The model proposed that both SCID leukaemia initiating cells (SL-IC) and SCID repopulating cells (SRC) are both derived from $CD34^{+}CD38^{-}$ HSC. During normal haematopoiesis, SRC give rise to multipotent progenitors and more committed progenitors. These cells eventually differentiate into different lineages. Leukaemogenic events in $CD34^{+}CD38^{-}$ cells initiate SL-IC. SL-IC give rise to clonogenic leukaemic progenitors, which eventually cause leukaemia.

Huntly *et al* also demonstrated that these committed progenitors can be transformed by the *MOZ-TIF2* oncogenic fusion gene, but not with *BCR-ABL*, suggesting that this effect does not apply to all oncogenes (Huntly et al., 2004). In addition, transformation of GMP has also been shown using *MLL-AF9* (Krivtsov et al., 2006). These studies suggest that it is probable that LSC may arise from more than one population from the haematopoietic hierarchy, and this depends on various factors, such as the nature of the leukaemia and the oncogenes involved.

1.6. Acute myeloid leukaemia (AML)

Abnormalities in haematopoiesis are implicated in various blood disorders, including leukaemia. Leukaemia develops as a result of the uncontrolled expansion of lymphoid or myeloid progenitors and is characterised by a block at particular stages of differentiation [reviewed in (Pui, 1995)]. AML is not an exception to this, and these phenomena result in haematopoietic insufficiency, such as granulocytopenia, thrombocytopenia and anemia together with, or without, leukocytosis [reviewed in (Lowenberg et al., 1999)]. The initial diagnosis of AML relies on the finding of leukaemic myeloblasts, which are characterised by round or irregular nuclei, distinctive nucleoli and a very small area of cytoplasm. According to the World Health Organisation (WHO), the definitive diagnosis following the initial diagnosis of AML depends on blast count (with more than 20% blasts identified in the bone marrow), lineage commitment and the degree of differentiation of the blasts. These criteria are recognised using morphological, cytochemical and immunophenotypic assays, accompanied with analysis of genetic abnormalities (Lowenberg et al., 1999; Harris et al., 2000). AML is a heterogeneous disease displaying various stages of differentiation

blocks and hence variability in the leukaemia morphology. In order to sub-group AML, one of the most frequently employed systems is the French-American-British (FAB) system. The FAB system categorises AML into 9 subtypes according to morphological appearance of the cells and cytochemistry [reviewed in (Lowenberg et al., 1999; Estey and Dohner, 2006)] (Table 1.1).

FAB	Morphology and common name
M0	Acute myeloblastic leukaemia with minimal myeloid differentiation
M1	Acute myeloblastic leukaemia without maturation
M2	Acute myeloblastic leukaemia with maturation
M3	Acute myeloblastic leukemia
M4	Acute myelomonocytic leukaemia
M4Eo	Acute myelomonocytic leukaemia with abnormal eosinophils
M5	Acute monocytic leukaemia
M6	Erythroleukaemia
M7	Acute megakaryocytic leukaemia

Table 1.1. FAB classifications of AML [adapted from (Lowenberg et al,. 1999)]

Identification of any cytogenetic abnormalities associated with a particular AML helps predict a patient's outcome. More than half of AML patients carry various degrees of karyotypic abnormalities at diagnosis and these are often used as independent prognostic indicators [reviewed in (Scandura et al., 2002; Estey and Dohner, 2006)] (Table 1.2). For example, the t(8;21) translocation is largely associated with the M2 subtype of AML and is often correlated with a good prognosis in adults. The inv(16) abnormality is less common, but found in the M4Eo subtype of AML, and is also associated with a relatively good outcome [reviewed in (Scandura et al., 2002)]. Additional information, such as the identification of specific secondary mutations, can be used to subdivide these prognostic categories.

Translocation/inversion	Genes involved	FAB/Leukaemic subtype	Cytogenetic prognosis
t(8;21)(q22;q22)	*AML1-ETO*	M2	good
inv(16) (p13;q22) or t(16;16)(p13;q22)	*CBFβ-MYHI1*	M4Eo	good
t(15;17)(q22;q11-21)	*PML-RARAα*	M3	Good
t(9;11)(p22;q23)	*MLL-AF9*	M4, M5	Poor/intermediate
t(6;11)(q27;q23)	*MLL-AF6*	M4, M5	poor
Inv(3) (q21q26) or t(3,3)(q21;q26)	*EVI1*	M1, M4, M6	Poor
t(6;9)(q23;q34)	*DEK-CAN*	M2, M4	Poor

Table 1.2. Common chromosomal aberrations in AML and their associated cytogenetic prognosis [modified from (Estey and Dohner, 2006; Scandura et al., 2002)]

For example, mutations in the *KIT* gene have been shown to worsen the prognosis of both inv(16) and t(8,21) AML. AML with a normal karyotype is normally categorised into an intermediate group. In contrast, poor prognosis occurs in patients with translocations involving inv(3), t(3,3), or del(5q). These translocations tend to be found in older patients and also in secondary AML, presenting an overall survival rate of less than 20% over 5 years - suggesting that current therapies are not effective in these cases (Lowenberg et al., 1999). On the whole, the strong association between cytogenetic abnormalities and the clinical outcome of patients emphasizes the importance of accurate detection of specific cytogenetic abnormalities in order to treat AML appropriately. Furthermore, it suggests an urgent need to develop translocation-specific molecular therapy.

1.7. *MLL* rearranged leukaemia

One of the most common features of acute leukaemia in infants is the chromosomal translocation of the mixed lineage leukaemia (*MLL*) gene. As its name suggests, translocations of the *MLL* gene are associated with lymphoid leukaemia (ALL), AML, and bi-phenotypic leukaemia [reviewed in (Ayton and Cleary, 2001; Daser and Rabbitts, 2005)]. *MLL* rearrangements are only found in approximately 10% of all adult and childhood acute leukaemias [reviewed in (Krivtsov and Armstrong, 2007)]. In contrast, in infants 60-70% of acute leukaemia cases are caused by *MLL* rearrangements [Reviewed in (Biondi et al., 2000; Krivtsov and Armstrong, 2007)]. Of these *MLL*-associated infant leukaemias, 50-80% consist of ALL and 34-50% of AML [reviewed in (Felix and Lange, 1999; Biondi et al., 2000)].

The most frequently occurring *MLL* translocations are with partner genes on chromosomes 4q21 (*AF4*), 9p22 (*AF9*), 19p13.3 (*ENL*), 10q12 (*AF10*) and 6q27 (*AF6*). These give rise to the *MLL-AF4*, *MLL-AF9*, *MLL-ENL, MLL-AF10 and MLL-AF6* fusion genes and together account for approximately 80% of *MLL*-associated leukaemia (Huret et al., 2001; Meyer et al., 2006) (Table 1.3). In terms of lineage distribution, fusion partners are strongly correlated with the phenotypes of leukaemia, for instance, *MLL-AF9* is predominantly found in AML, *MLL-AF4* in ALL, and *MLL-ENL* is found in both AML and ALL [reviewed in (Ayton and Cleary, 2001)].

The early onset of infant leukaemia suggests that the *MLL*-associated translocations occur during pregnancy [reviewed in (Eguchi et al., 2003)].

Translocation	Resulting fusion gene	Localization of fusion partner protein	FAB/leukaemic subtype
t(4;11)(q21;q23)	*MLL-AF4*	Nuclear	Most commonly ALL
t(9;11)(p22;q23)	*MLL-AF9*	Nuclear	M4 or M5
t(11;19)(q23;p13.3)	*MLL-ENL*	Nuclear	Biphenotypic, pre-B ALL, M4 or M5
t(10;11)(p12;q23)	*MLL-AF10*	Nuclear	M4 or M5
t(6;11)(q27;q23)	*MLL-AF6*	Cytoplasm	M4 or M5 (and T-ALL)

Table 1.3. The five most common translocations bearing MLL [modified from (Estey and Dohner, 2006; Scandura et al., 2002)]

Evidence for the origin of *MLL* translocations came from twin studies and the use of PCR-based methods to look at DNA from neonatal blood spots (Gurthrie cards) (Ford et al., 1993; Gale et al., 1997). These studies together suggested that *MLL* rearrangement was not inherited but acquired. In addition, results from three pairs of twins showed that the *MLL* translocation breakpoints were identical in each pair, suggesting that *MLL* rearrangement occurs *in utero* and that sibling disease is caused by spreading of the aberrant clone through a process called intra-placental metastasis (Ford et al., 1993).

1.8. MLL structure and function

The *MLL* gene was cloned by four independent groups, as the target of leukaemia-associated 11q23 translocations (Zieminvanderpoel et al., 1991; Djabali et al., 1992; Gu et al., 1992; Tkachuk et al., 1992). Following its cloning, it was discovered that *MLL* was a homolog of the *Drosophila Trithorax* gene (*Trx*). The *Trx* gene is a family member of the *trithorax* group (trx-G) and is a DNA-binding transcription factor implicated in homeoprotein regulated segmentation and early embryogenesis (Mazo et

al., 1990). *MLL* is widely expressed in various organs and tissues such as brain, spinal cord, liver, spleen, thymus, kidney, heart, testis, lungs and skeletal muscles in humans (Butler et al., 1997). In haematopoiesis, *MLL* is expressed both in adult and foetal lymphoid and myeloid progenitor cells, but not in mature erythroid cells, indicating that its expression is essential for early maintenance of haematopoiesis, but not for terminal differentiation (Hess et al., 1997; Ernst et al., 2004).

The *MLL* gene is approximately 90kb in size, with 36 exons and around 12kb of coding sequence [reviewed in (Eguchi et al., 2003)]. *MLL* encodes a protein containing 3968 amino acids with an estimated size of 431kDa. This large protein is proteolytically cleaved in the cytoplasm by a protease called Taspase1, which generates two MLL fragments of 320kDa [N-terminal fragment of MLL (MLL^N)] and 180kDa [C-terminal fragment of MLL (MLL^C)] (Yokoyama et al., 2002; Hsieh et al., 2003a). These two post-translationally processed fragments are stabilized by forming a complex through interaction of the FYRN domain of the MLL^N and the FYRC domain of the MLL^C. This complex is then co-localized into sub-nuclear compartments of the cell (Hsieh et al., 2003b).

The MLL protein contains several functional domains. Adjacent to the N-terminus of MLL, there are three AT-hooks which are able to bind to the minor groove of AT-rich DNA, by recognizing the DNA structure, rather than binding in a sequence-specific manner (Zeleznikle et al., 1994). Next to these AT hooks, there are two sub-nuclear localisation domains (SNL-1, SNL-2), which determine the localisation of MLL protein within the nucleus [reviewed in (Hess, 2004; Daser and Rabbitts, 2005)]. A transcriptional repression domain is positioned next to SNL-1 and SNL-2. This

repression domain contains two functional sub-units known as repression domain one and two (RD-1 and RD-2). RD-1 displays homology with the cysteine-rich CxxC zinc finger motif of DNA methyltransferase (DMNT) (Prasad et al., 1995). In addition, RD-1 interacts with the polycomb group proteins (PcG) HPC2 and BMI-1, and the co-repressor C-terminal-binding protein (CtBP) (Xia et al., 2003). RD-2 plays a role in transcriptional repression via interaction with the histone deacetylases, HDAC1 and HDAC2. There are three plant homeodomain (PHD) zinc finger motifs that are homologous to domains in *Drosophila* TRX. The third PHD finger interacts with nuclear cyclophilin (Cyp33) (Fair et al., 2001). Cyp33 possesses an RNA recognition motif (RRM) and its over-expression is inversely correlated with homeoprotein (hox) *HOXC8* and *HOXC9* mRNA expression (Fair et al., 2001). Adjacent to the PHD domains, there is a bromo-domain. This domain interacts with the carbonyl-amide moiety of acetylated lysine, which may have a role in chromatin association (Schultz et al., 2001). The transactivation domain (TD) is conserved in vertebrates, but is not found in *Drosophila* TRX [reviewed in (Daser and Rabbitts, 2005)]. The TD is known to interact with the co-activator CREB-binding protein (CBP), which is an acetyltransferase. This binding is required for correct transcriptional activation of target genes (Ernst et al., 2001). Towards the end of the C-terminus of MLL, there is the su(var)3-9, enchancer-of-zeste, trithorax (SET) domain. The highly conserved SET domain possesses MLL histone 3 lysine 4 (H3K4) methyltransferase activity, which is associated with transcriptional activation, and was shown to be responsible for H3K4 methylation of MLL target gene promoters (Milne et al., 2002; Nakamura et al., 2002). In addition, the SET domain was also found to interact with the SWItch/Sucrose Non Fermentable (SWI-SNF) chromatin re-modelling complex in yeast and *Drosophila*, via the INI-1 protein, which is implicated in ATP-dependent nucleosome remodelling and RNA polymerase activity (Rozenblatt-Rosen et al., 1998). Overall, MLL^N has a net

repressive effect on transcription, due to recruitment of PcG and CtBP proteins, as well as HDAC1 and 2 (Fair et al., 2001; Yokoyama et al., 2002; Xia et al., 2003). However, when MLL^N undergoes heterodimerization with MLL^C, the resulting complex then has an overall positive effect on transcription due to chromatin remodelling [reviewed in (Hess, 2004)]. A schematic diagram of the MLL protein is shown in Figure 1.5.

1.9. Normal function of MLL

A study using *Drosophila* demonstrated that the *trx* mutation is embryonic lethal and that mutant embryos have abnormal segmentation (Mazo et al., 1990). Knockout of the mouse *Mll* gene is embryonic lethal between E10.5 and E16.5, and embryos showed skeletal malformation and misregulation of *Hox* gene expression (Yu et al., 1995; Hess et al., 1997; Yagi et al., 1998; McMahon et al., 2007). $Mll^{-/-}$ mice were able to initiate correct *Hox* gene expression, but were unable to sustain this expression during embryogenesis, suggesting that MLL has an important role in maintaining *Hox* gene expression. Indeed, *Hox* genes are major target genes of MLL, as will be discussed later.

The MLL protein was discovered to be a part of macromolecular complexes with several different proteins. These complexes were found to be responsible for methyltransferase activity and other chromatin modifications involved in transcriptional regulation (Nakamura et al., 2002). Several proteins have been discovered to associate with the MLL protein.

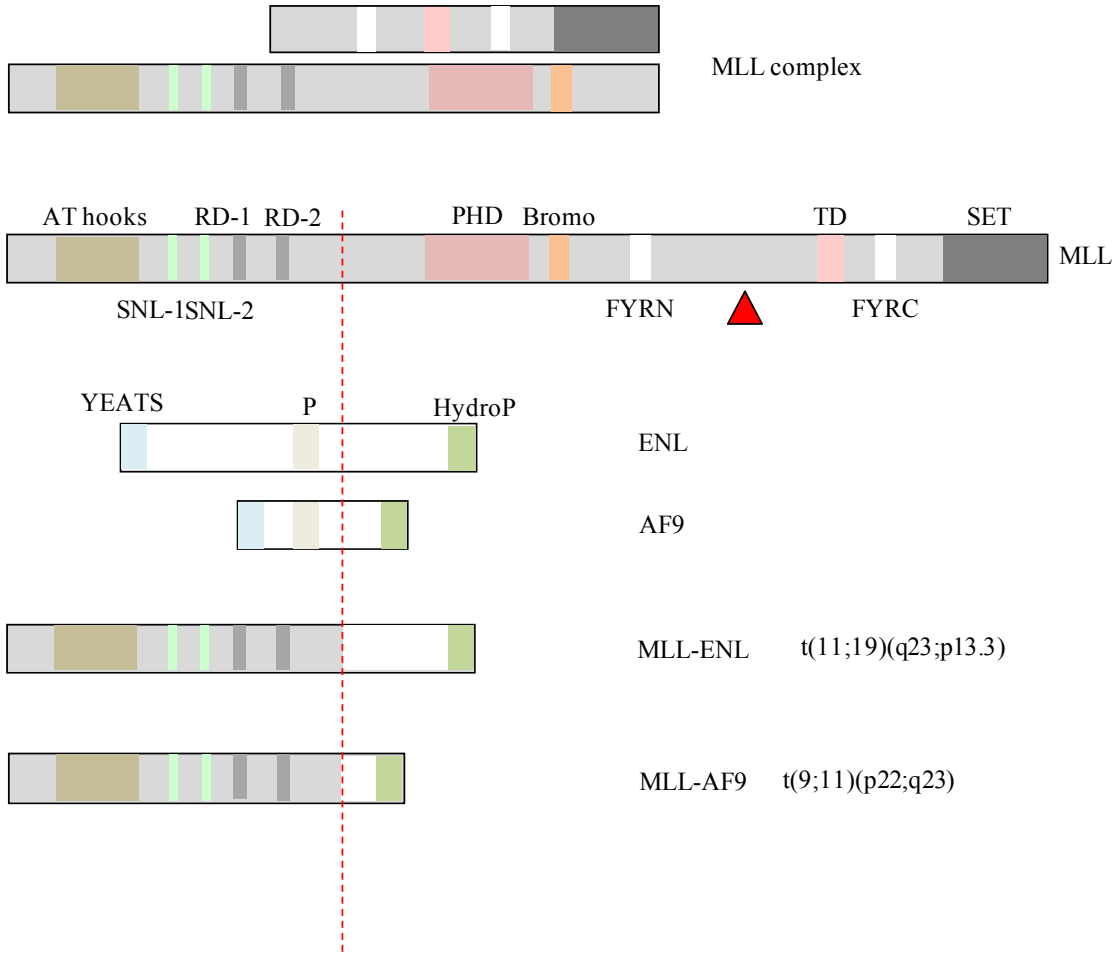

Figure 1.5. Schematic diagram of MLL and MLL-fusion proteins

The MLL protein consists of several domains: From the N-terminus: AT hooks, sub-nuclear localization 1 and 2 domains (SNL-1, SNL-2), repression domain 1 and 2 (RD1, RD2), trithrax plant homeodomain (PHD), bromo-domain (bromo), FYRN domain, transactivation domain (TD), FYRC domain, su(var)3-9, enchancer-of-zeste, trithorax (SET) domains. The red triangle represents the protelolytic cleavage site which produces the MLL complex. The red dotted line indicates the break cluster region (BCR). ENL and AF9 both possess a YEATS (Yaf9, ENL, AF9, Taf14, and Sas5) domain, a proline/serine (P) rich region and a hydrophobic region (HydroP). The MLL-ENL chimeric fusion is created by the translocation t(11;19)(q23;p13.3). The MLL-AF9 chimeric fusion protein is created by the translocation t(9;11)(p22;q23).

Proteins that associate with MLL^c include the H4K16 acetyltransferase, MOF, which has a role in neutralising histone charges to unwind chromatin structure (Dou et al., 2005), and the WDR5 protein, which interacts with Histone 3 to present the lysine 4 side chain for further methylation to take place (Ruthenburg et al., 2006). In addition, ASH2L and RBBP5 stabilize the active MLL complex to initiate efficient methyltranferase function (Yokoyama et al., 2004; Southall et al., 2009). Collectively, this complex induces trimethylation of H3K4, which is required for active transcription. MLL^N on the other hand, associates with proteins required for targeting the MLL complex to specific loci. The tumour suppressor protein menin, which is a product of the *Men1* gene, interacts with a region of MLL^N between amino acid residues 5 and 44 (Caslini et al., 2007). Its physical interaction was shown to be important for MLL-fusion mediated oncogenic transformation (Yokoyama et al., 2005; Caslini et al., 2007). Furthermore, MLL and menin provide a surface for interacting with the lens epithelium derived growth factor (LEDGF), which in turn tethers the MLL complex to chromatin (Yokoyama and Cleary, 2008). The MLL macro-complex co-ordinates chromatin remodelling through several activities, including methylation and acetylation, in order to initiate transcription. A schematic diagram of the MLL protein is shown in Figure 1.6. The recruitment of this complex may be regulated by several transcription factors, for example p53 and β-catenin (Dou et al., 2005; Sierra et al., 2006; Wang et al., 2010).

1.10. MLL fusions and their transcriptional targets

Based on sequencing analysis of patients diagnosed with 11q23-associated leukaemia, a common target region of *MLL* rearrangement was found (Gu et al., 1994).

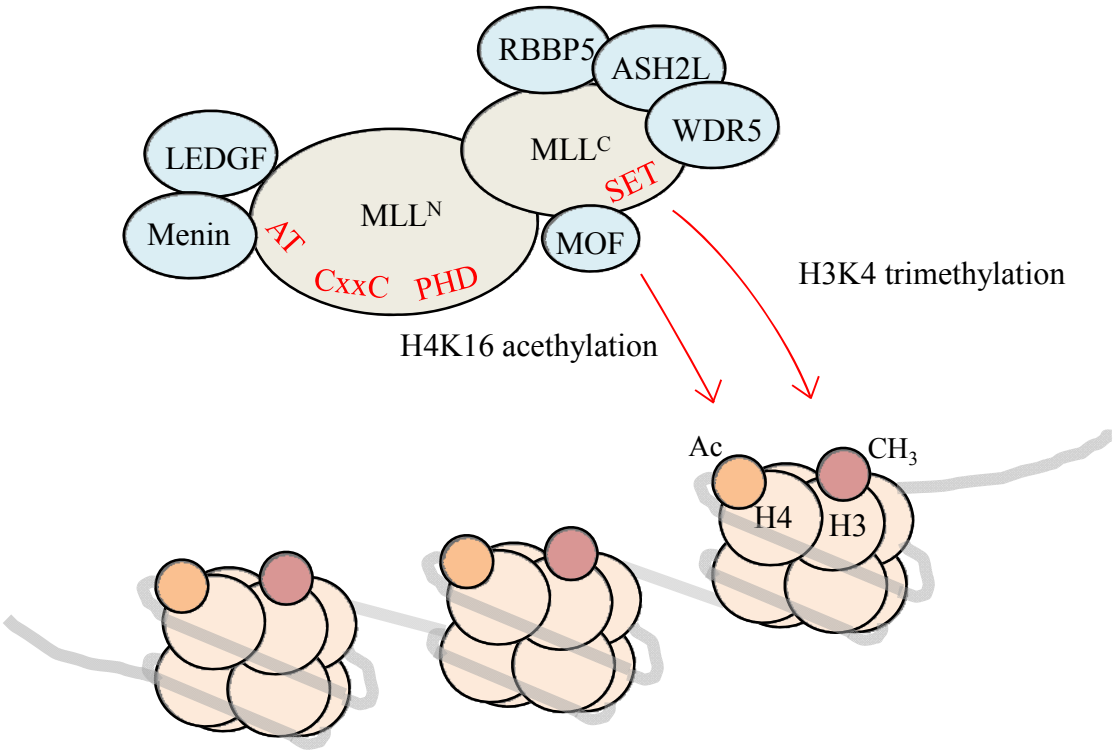

Figure 1.6. The normal function of the MLL complex [adapted from (Slany et al., 2009)]

The schematic diagram illustrates the normal function of the MLL complex. The proteolytically cleaved MLL forms a macromolecular complex with several other proteins. This complex has a role in H3K4 trimethylation and H4K16 acetylation to assist chromatin remodelling and transcriptional initiation. LEDGF, lens epithelium derived growth factor; PHD, plant homeodomain; MLL^N, N-terminal fragment of MLL; MLL^C, C-terminal fragment of MLL; SET, su(var)3-9, enchancer-of-zeste, trithorax; H, histone; Ac, acetylation; CH3, trimethylation; ASH2L, (absent, small, or homeotic)-like; MOF, males absent on the first; RBBP5, retinoblastoma binding protein 5; WDR5, WD repeat domain 5.

This 8.3kb breakpoint cluster region (BCR) lies between exons 8 and 13 of the *MLL* gene, next to sequences encoding the PHD zinc finger motifs, and includes topoisomerse II cleavage sites (Hars et al., 2006). Although there is no conclusive evidence, the fact that this region contains topoisomerase II cleavage sites indicates that double strand breaks may be involved in initiation of the translocation events (Libura et al., 2005). An alternative hypothesis is that the translocation is a result of early apoptotic events that preferentially cause breaks in the BCR of *MLL*. In cells that ultimately survive, these breaks are repaired, but may result in translocations in a small fraction of cells (Betti et al., 2001). In either case, it is likely that non-homologous end joining (NHEJ) is involved in this process since the BCR contains filler nucleotides which are also present and involved in the generation of T and B cell receptor diversity, a process that is known to use the NHEJ pathway (Gillert et al., 1999).

Re-arrangement of the *MLL* gene is frequently characterised by a balanced in-frame translocation between *MLL* and a fusion partner gene. Together they produce a fusion gene that encodes an MLL-chimeric fusion protein. Generally, these MLL-fusion proteins retain the N-terminus of MLL, with the ATH1-3, SNL1-2 and RD1-2 domains, while losing the TAD and SET domains and the rest of the C-terminus. In addition, all the MLL-associated translocations disrupt the Taspase 1 proteolytic cleavage site [reviewed in (Daser and Rabbitts, 2005)]. Although there is some evidence that the reciprocal fusion product of the MLL-AF4 translocation, the AF4-MLL fusion, may contribute to ALL, there is no evidence of any other reciprocal fusion being implicated in MLL-associated leukaemia [(Bursen et al., 2010; Benedikt et al., 2011)].

It is likely that MLL-fusions exert their effects as a result of a gain-of-function rather than a loss-of-function. There are several lines of evidence to support this. Firstly *Mll*$^{-/-}$ knockout mice exhibited defective haematopoietic progenitors rather than increased numbers (Hess et al., 1997; Yagi et al., 1998; Ernst et al., 2004). Furthermore, *Mll*$^{+/-}$ mice and truncated *MLL-myc(tag)* knock-in mice do not exhibit an increase in leukaemia incidence (Corral et al., 1996), suggesting that loss of one *MLL* allele or *MLL* truncation is not sufficient for leukaemogenesis. However, when the *AF9* gene was introduced into the *Mll* locus by homologous recombination, to generate an *Mll-AF9* in-frame knock-in model, the resulting mice developed AML, demonstrating that the presence of fusion partner is essential for leukaemia induction (Dobson et al., 1999). Collectively, this evidence suggests that oncogenic transformation by MLL-fusions is a consequence of gain-of-function activity.

Hox genes are some of the most studied MLL target genes and MLL has been found to bind directly to promoter regions of specific *Hox* genes (Milne et al., 2002). *Hox* genes are a highly conserved family of transcription factors that are expressed in embryogenesis as well as in various adult tissues, such as bone marrow (Pineault et al., 2002). There are 39 recognised *Hox* genes in mice and humans and they are classified into 4 different clusters (A, B, C and D) (Pineault et al., 2002). In haematopoiesis, different *Hox* genes are required for various stages of haematopoiesis, usually being up-regulated in early stages of haematopoiesis and down-regulated upon differentiation (Sauvageau et al., 1994; Lawrence et al., 1996).

1.11. MLL fusion partners

To date, at least 73 different *MLL* translocations have been described and 54 *MLL* fusion partners have been identified [reviewed in (Slany, 2009)]. These fusion partners can be grouped into several categories. The most common fusion partners encode nuclear proteins which include AF4, AF9, AF10 and ENL, associated with four of the five most common MLL-rearranged leukaemia subtypes [reviewed in (Krivtsov and Armstrong, 2007)]. Interestingly, most of these nuclear proteins are themselves also involved in transcriptional activation and elongation (Bitoun et al., 2007; Mueller et al., 2007). AF9 is a proline/serine rich nuclear protein and is responsible for gene activation (Erfurth et al., 2004). Interestingly, an *Af9* knockout study showed that *Af9* expression is required for controlling pattern formation in normal embryogenesis (Collins et al., 2002). AF9 and ENL both have a highly conserved region at their C-termini, the 84 amino-acid domain and this domain in ENL is enough to cause transformation when fused to the N-terminal MLL fragment (Slany et al., 1998). Indeed, AF9 and ENL share structural similarity and protein-protein interactions [reviewed in (Schulze et al., 2009)]. The C-termini of AF9 and ENL (hydrophobic region) were shown to interact with other fusion partners of MLL, such as AF4 and AF5q31 (Prasad et al., 1995; Zeisig et al., 2005; Bitoun et al., 2007). The N-termini of AF9 and ENL contain the highly conserved YEATS (Yaf9, ENL, AF9, Taf14, and Sas5) domain which is responsible for histone H3 and H1 binding (Zeisig et al., 2005). Moreover, AF9 and ENL were both found to be recruited to the SWI-SNF complex and ENL was found to participate in a SWI-SNF-like complex, called ENL-associated BRG1- or hbrm-associated factors (EBFAF) (Nie et al., 2003). AF4 is also a proline/serine rich nuclear protein containing a transactivation domain and was shown be required for lymphoid development (Isnard et al., 2000). AF4 belongs to the

FMR2/LAF4 protein family together with two other fusion proteins, AF5q31 and LAF4. (Erfurth et al., 2004). In addition, AF4 has been shown to interact directly with AF9, affecting subnuclear co-localization of the MLL-AF4 fusion protein (Erfurth et al., 2004; Zeisig et al., 2005). AF10 interacts with ENL and the AF9 homolog GAS41, which also interacts with SWI-SNF complex (Debernardi et al., 2002). In addition, AF10 was recently found to interact with the histone 3 lysine 79 (H3K79) methytransferase, Dot1l, which was shown to be essential for MLL-fusion mediated transformation (Okada et al., 2005).

A second group of fusion partners are cytoplasmic proteins, such as AF6, GAS7 and EEN. These cytoplasmic proteins were shown to induce oligomierisation, mediated by coiled coil domains, and this is required for MLL-associated transformation by these fusions (So et al., 2003). Septins are a small group of MLL fusion partners, including SEPT2, 5 6, 9 and 11. They are also cytoplasmic proteins and have several functional roles such as cell cycle regulation, vehicle trafficking and GTP hydrolysis. However, the functional significance of these activities in MLL-fusion associated leukaemogenesis is unknown (Hall and Russell, 2004). The final group of fusion partners includes p300 and CBP, both of which are acetyltransferases and also found to interact with normal MLL, via the TD domain, which is lost in the MLL-fusions (Ida et al., 1997; Rowley et al., 1997; Taki et al., 1997).

1.12. Regulation of transcription by MLL-fusions

Despite the large number of different MLL-fusions, many of the MLL-associated leukaemias share a common gene expression signature, suggesting that many of the fusions may have a similar mechanism of action (Armstrong et al., 2002). For the nuclear protein MLL-fusions there has been some progress in understanding this mechanism, with the discovery that the fusion partners AF9, ENL, AF4 and AF10 could interact with each other and that ENL could bind to histone H3. This suggested that all of these fusion partners may have a common chromatin re-modelling function (Zeisig et al., 2005). The complex containing these fusion partners was then named ENL-associated protein (EAP) and this complex was also discovered to bind the C-terminal kinase domain of RNA polymerase II (RNA pol II CTD), the positive transcription elongation factor b (pTEFb) and the H3K79 histone methyltransferase Dot1l (Bitoun et al., 2007; Mueller et al., 2007). pTEFb is a heterodimeric complex of cyclin-dependent kinase 9 (CDK9) and cyclin T1, which phosphorylates the RNA pol II CTD, and the DRB sensitivity-inducing factor (DSIF) and negative elongation factor (NELF). This process is necessary for efficient elongation (Bitoun et al., 2007). This evidence suggests that these common nuclear fusion partner proteins are essential for H3K79 methylation during transcriptional elongation. The model for normal transcriptional elongation is shown in Figure 1.7. In this model, the normal MLL complex is recruited to RNA pol II, located at a promoter region, to trimethylate H3K4. The MLL complex-associated protein, MOF, acetylates H4K16 to neutralize histone charges, in order to unwind the chromatin structure. The negative elongation factors, DSIF and NELF, are also associated with RNA pol II, ensuring its transcriptional arrest

Figure 1.7. The normal function of the MLL complex and EAPs in the transcriptional elongation process [modified from (Bitoun et al., 2007)]

The schematic diagrams illustrate the normal function of the MLL complex in the transcriptional elongation process. The MLL complex is recruited to RNA pol II to trimetylate H3K4 and acetylate H4K16, to neutralise histone charges (Top diagram). pTEFb is recruited to phosphorylate RNA pol II, DSIF and NELF to release the arrested RNA pol II. Meanwhile, ENL-AF9 form a complex with H3 to recruit AF10 to the AF4 and ENL-AF9 complex. This AF10-ENL-AF9 interaction recruits Dot1l to RNA pol II to cause H3K79 methylation (Middle). RNA pol II initiates elongation and MLL and other complexes leave the elongation complex (Bottom). Pol II, RNA polymerase II; MLL^N, N-terminal fragment of MLL; MLL^C, C-terminal fragment of MLL; DSIF, DRB sensitivity-inducing factor; NELF, negative elongation factor; P, phosphorylation; pTEFb, Positive transcription elongation factor b; Dot1l, Disruptor of telomeric silencing-1.

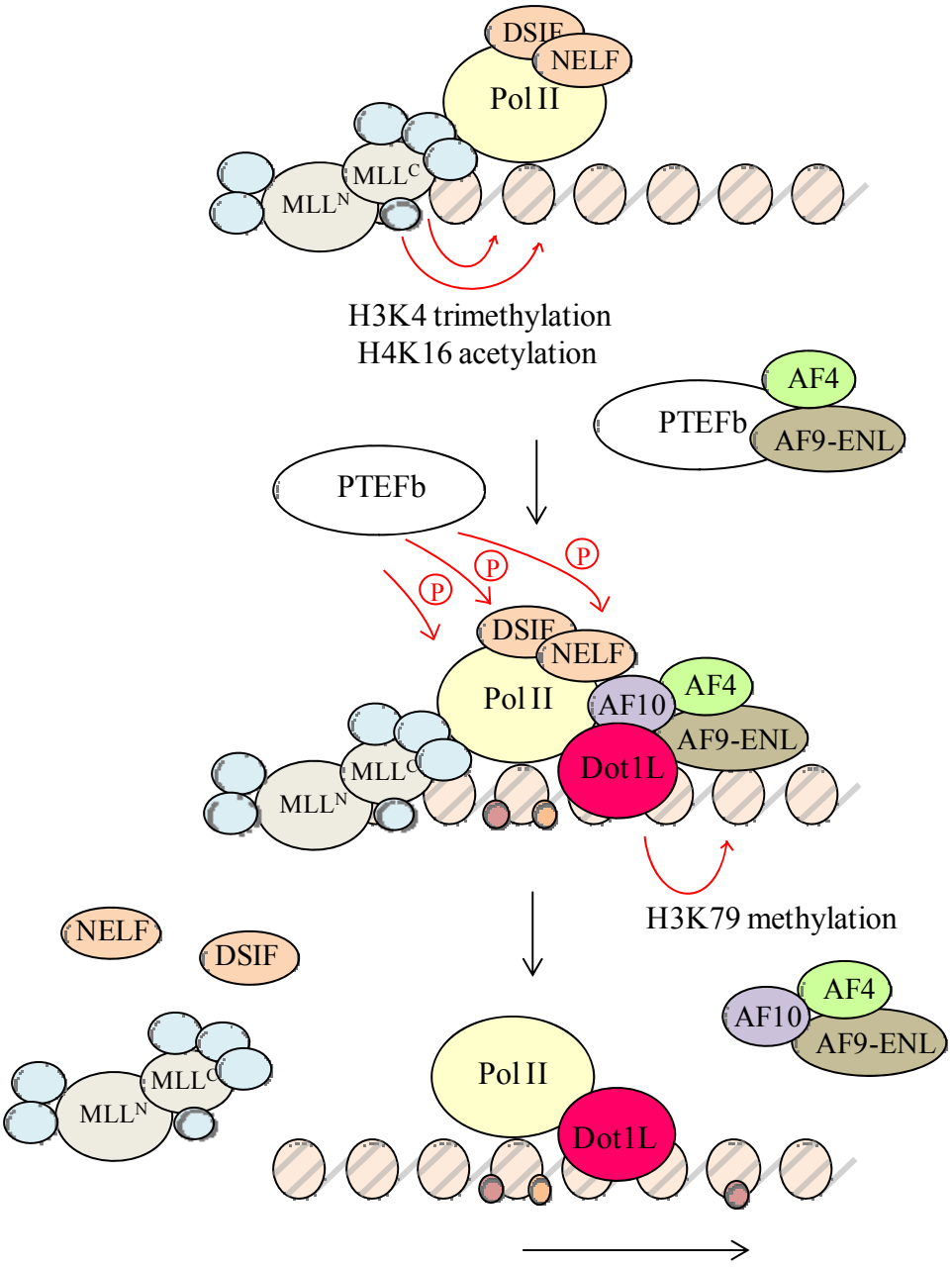
DSIF
NELF
Pol II
MLL^C
MLL^N
H3K4 trimethylation
H4K16 acetylation
AF4
PTEFb
AF9-ENL
PTEFb
P
P
P
DSIF
NELF
Pol II
AF10
AF4
AF9-ENL
Dot1L
MLL^C
MLL^N
H3K79 methylation
NELF
DSIF
AF4
AF10
AF9-ENL
Pol II
Dot1L
MLL^C
MLL^N

.

When pTEFb, in a complex with AF4 and ENL-AF9, is recruited to the RNA pol II complex, it phosphorylates the RNA pol II CTD, DSIF and NELF, to release the arrested polymerase. At the same time, ENL-AF9 dissociates from pTEFb and instead complexes with H3, to recruit AF10 to the AF4 and ENL-AF9 complex. This interaction between AF10 and ENL-AF9 results in recruitment of Dot1l to the RNA pol II complex. Dot1l in turn, methylates H3K79 and initiates elongation. When elongation proceeds, MLL leaves the active elongation complex (Bitoun et al., 2007).

However, fusion of MLL to the nuclear partners disrupts this highly organised process. The MLL-fusion itself binds to Dot1l and pTEFb, due to the presence of the appropriate fusion partner domain within the fusion protein. This results in aberrant and elevated H3K79 methylation and deregulated transcriptional elongation by RNA pol II at MLL-fusion target loci (Bitoun et al., 2007; Yokoyama et al., 2010) (Figure 1.8).

Recently, wild type MLL was also found to be implicated in the leukemogenic activity of MLL-fusions. Milne *et al* showed that MLL-fusion proteins are unable to bind the *Hoxa9* promoter region in the absence of wild type MLL (Milne et al., 2010). In the proposed model, wild type MLL protein is first recruited by the mammalian PAF elongation complex (PAF1C) and di- or trimethylates H3K4 at the *HoxA9* promoter. This recruitment of wild type MLL releases the binding by repressor proteins such as the ERG-associated protein with SET domain (ESET), which is an H3K9 methyltransferase. As a result, the MLL-fusion can then bind to an open chromatin conformation (Milne et al., 2010). This model is also supported by other studies. Thiel *et al* demonstrated that Menin recruits both wild type MLL and MLL-fusions to the *Hoxa9* promoter region (Thiel et al., 2010).

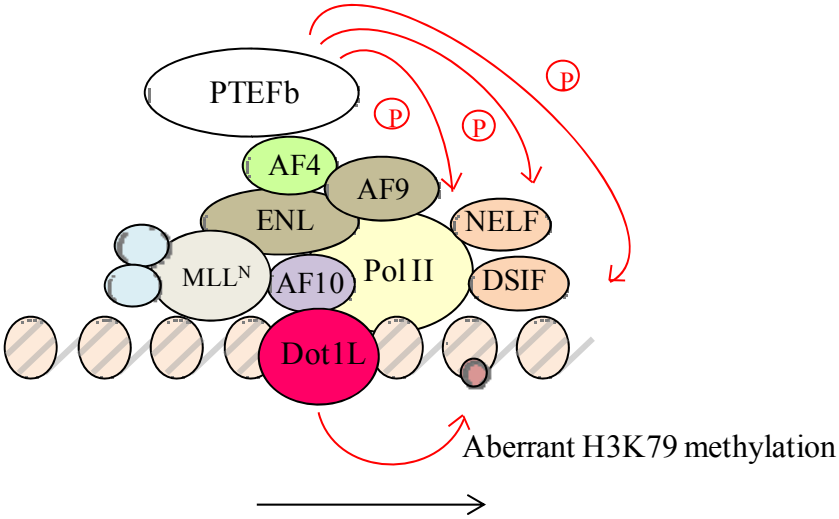

Figure 1.8. The proposed abnormal function of MLL-fusions in transcriptional elongation

The schematic diagram illustrates the proposed abnormal function of MLL-fusions in transcriptional elongation. The MLL-fusion binds to Dot1l and pTEFb due to its fusion partners. This abnormal complex causes aberrant H3K79 methylation and deregulated transcriptional elongation by RNA pol II at MLL-fusion target loci. Pol II, RNA polymerase II; MLL^N, N-terminal fragment of MLL; DSIF, DRB sensitivity-inducing factor; NELF, negative elongation factor; P, phosphorylation; ; Dot1l, Disruptor of telomeric silencing-1.

This study also showed that *MLL-AF9*-transduced mouse bone marrow cells require wild type MLL to maintain over-expression of *Hoxa9*, proliferation, survival and transformation (Thiel et al., 2010). Taken together, all of this evidence indicates that the MLL complex is involved in transcriptional initiation and chromatin remodelling in a highly regulated manner, and that MLL-fusions, assisted by the wild type MLL complex, function by 'hijacking' the machinery to cause aberrant regulation of MLL target genes, such as the *Hox* genes.

1.13. Transcriptional down-stream targets of MLL-fusions

Since both the normal MLL complex and the MLL-fusion complex share the N-terminus of MLL, it is highly probable that they share common target genes. Indeed, this was shown to be the case, at least for *HOX* genes (Armstrong et al., 2002; Yokoyama et al., 2002). Up-regulation of *HOX* gene expression, particularly *HOXA7, HOXA9* and their dimerization partner, mouse ecotropic integration site *(MEIS1)*, are consistently observed in 11q23-associated leukaemia (Armstrong et al., 2002). In addition, human patients with MLL-associated leukaemia also frequently have elevated expression of *HOXA7*, *HOXA9* and *MEIS1* (Yeoh et al., 2002). *Hoxa9* and *Meis1* are restricted in their expression in early haematopoietic cells (Pineault et al., 2002). Several studies using murine MLL-fusion models suggest that *Hoxa9* and *Meis1* are major target genes of MLL-fusions and are required for induction of MLL-associated leukaemia (Ayton and Cleary, 2003; Zeisig et al., 2004; Krivtsov et al., 2006; Faber et al., 2009; Kumar et al., 2009). Continued expression of *MLL*-fusions was also shown to be required for maintenance of *Hox* gene expression in transformed cells (Horton et al., 2005). In addition, ectopic expression of *Hoxa9* and *Meis1* in mouse bone marrow was

shown to transform haematopoietic cells and induce AML, with features resembling MLL-associated leukaemia (Kroon et al., 1998). In fact, MLL-ENL binds to promoter regions of both *Hoxa9* and *Meis1*, and expression of these two genes substitute for MLL-ENL in maintaining transformation (Zeisig et al., 2004; Milne et al., 2005). These studies confirm that *Hoxa9* and *Meis1* are key transcriptional targets of MLL-fusions. Further studies demonstrated that *c-Myb* was found to be one of the down-stream target genes of *Hoxa9* and *Mies1*, suggesting that *Hoxa9* and *Meis1* mediate leukaemia through deregulated *c-Myb* expression (Hess et al., 2006).

Apart from *Hoxa9* and *Meis1*, MLL-fusions are thought to regulate a large number of other genes. In a mouse model of MLL-rearranged ALL, genome-wide chromatin immunoprecipitation (ChIP) analysis showed MLL-AF4 binding to, and increased H3K79 methylation in, more than 1000 promoters, indicating deregulated expression of many other genes (Krivtsov et al., 2008). In contrast, ChIP analysis in a human leukaemia cell line, suggested that MLL-AF4 bound the promoters of less than 200 genes (Guenther et al., 2008). Furthermore, a recent study using a conditional mouse model demonstrated that only a small proportion of MLL target genes were bound by MLL-fusions, resulting in increased H3K79 methylation and upregulated expression (Wang et al., 2011). This suggests that MLL-fusions may act through the direct deregulation of a relatively small number of key target genes, that in turn cause changes in the expression of a large number of downstream genes.

1.14. Models for MLL-fusion induced leukaemia

In order to understand the molecular pathogenesis of MLL-fusion associated leukaemia, several groups have generated murine models, using different approaches (Figure1.9). The classical model was generated utilizing homologous recombination in embryonic stem (ES) cells, to knock-in the human *AF9* gene into exon 8 of the endogenous mouse *Mll* locus, achieving endogenous expression of *Mll-AF9* (Corral et al., 1996; Dobson et al., 1999; Dobson et al., 2000). These chimeric ES cells were injected into blastocysts and chimeric mice were produced. The resulting knock-in chimeric mice and their heterozygous offspring developed predominantly AML, and occasionally ALL, with extended latency, suggesting the possible requirement of secondary mutations for leukaemia development. The advantage of the knock-in model is that *Mll-AF9* expression is driven by the endogenous *Mll* promoter and the resulting mice contain only one wild type *Mll* allele. However, using this knock-in approach, the *Mll-AF9* gene is expressed ubiquitously like *Mll* itself, and is not restricted to haematopoietic cells.

In order to achieve tissue-specific expression of the MLL-fusion, the same group elegantly used interchromosomal recombination to generate a conditional model of *Mll-Af9* (Collins et al., 2000) and *Mll-Enl* (Forster et al., 2003) expression. In this model, recombination was mediated by the Cre-loxP system, whereby Cre recombinase facilitates *de novo* site-specific chromosomal recombination of loxP sites, introduced into the appropriate chromosomes in the mice. In addition, the tissue specificity of these conditional knock-in mice was achieved by driving Cre recombinase expression from the *Lmo2* promoter, which is expressed in HSC (Forster et al., 2003).

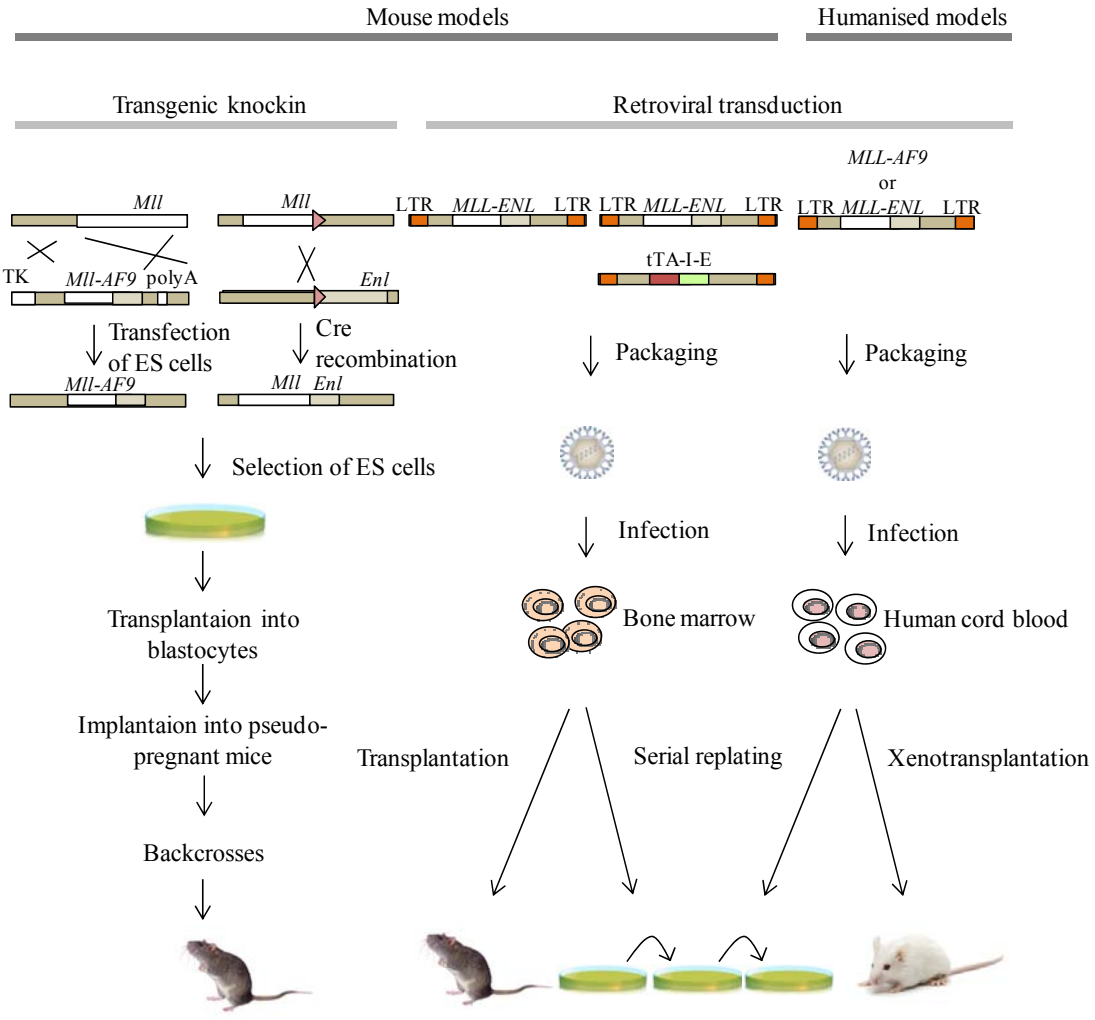

Figure 1.9. Models for MLL-fusions [modified from (Marschalek., 2011)]

The schematic diagrams illustrate different models for MLL-fusions in human and mice cells. The models can be classified into transgenic models and retroviral transduction models. Knock-in mouse was generated using homologous recombination. Intrerchromosomal recombination was used to generate a conditional knock-in model using Cre recombinase. Retroviral transduction was used to create both constitutive and conditional expression of MLL-fusions. The retroviral transduction system was also used to generate a model for MLL-fusions using human cord blood. TK, herpes simplex virus thymidine kinase gene; polyA, simisimian virus 40 (SV40) poly(A) site; ES, embryonic stem; LTR, long terminal repeat, tTA-I-E, t tetracycline transactivator-IRES-EGFP.

This model gave rise to rapid AML, with a latency of approximately two to four months, suggesting that this rare somatic recombination event is enough, possibly without a secondary mutation, to induce leukaemia (Forster et al., 2003).

An alternative approach was used to generate a murine model of *MLL-ENL* induced disease by retroviral transduction of mouse bone marrow haematopoietic progenitor cells (Lavau et al., 1997; Slany et al., 1998). In this model, the transduced cells were immortalised *in vitro* and gave rise to rapid AML upon transplantation into irradiated recipient mice. Several other MLL-fusions have been modelled using this retroviral transduction approach, such as MLL-AF9 (Somervaille and Cleary, 2006), MLL-EEL (DiMartino et al., 2000; Lavau et al., 2000b) and MLL-CBP (Lavau et al., 2000a). In addition, pro-B cell ALL development was demonstrated using MLL-ENL (Zeisig et al., 2003). This approach was also used to show that committed progenitors expressing MLL-ENL (Cozzio et al., 2003) and MLL-AF9 (Krivtsov et al., 2006) were able to induce AML. Tamoxifen-inducible retroviral expression models were then generated and used to demonstrate the dependence of transformed cells on continued MLL-fusion expression (Ayton and Cleary, 2003; Zeisig et al., 2004). In this system, a mutant human estrogen binding domain, which is responsive to 4-hydroxyl-tamoxifen (4-OHT), was fused with the C-terminus of the MLL-ENL. As a result, the MLL-ENL protein was in an inactive state, due to complex formation with heat shock proteins, and only became active once it was released from the complex in the presence of 4-OHT (Zeisig et al., 2004).

Our lab has used a modified retroviral approach to generate a conditional murine model of *MLL-ENL* expression, regulated by the 'Tet-Off' system (Horton et al., 2005). In this

model, the tetracycline-responsive promoter element (TRE) drives *MLL-ENL* expression, which is dependent on binding of the tetracycline-controlled transactivator protein (tTA). In the presence of doxycycline (dox), tTA undergoes a conformational change that prevents it from binding to the TRE and therefore blocks the expression of MLL-ENL. Using this model, it was demonstrated that maintenance of *MLL-ENL* expression is obligatory for the survival and proliferation of immortalized cells *in vitro* and for leukaemia progression *in vivo* (Horton et al., 2005; Horton et al., 2009). Although these mouse models have yielded valuable information on the mechanism of MLL-fusion mediated leukaemia, the use of inbred mice has important limitations in recapitulating human disease. Therefore, generation of a human MLL-fusion model was necessary to compliment the work with mouse cells.

In contrast to the large body of data using murine MLL-fusion models, there are comparatively few publications concerning human models. The first model to examine the consequences of expressing MLL-fusions in human primary cells was generated by Barabe *et al* (Barabe et al., 2007). This study transduced lineage-depleted human umbilical cord blood cells with retroviral vectors expressing *MLL-ENL* and *MLL-AF9*. Sublethally irradiated immunodeficient mice transplanted with the transduced cells developed disease with hallmarks of human acute leukaemia (Barabe et al., 2007). Interestingly, only ALL developed from the cells transduced with MLL-ENL, while features of both AML and ALL were observed from cells transduced with MLL-AF9. The transduced cells expressing MLL-ENL and MLL-AF9 continued to proliferate *in vitro* for approximately 100 and 125 days, respectively (Barabe et al., 2007).

Following this study, Wei *et al* was the second group to generate a human model of MLL-AF9 associated leukaemia using retroviral transduction of human $CD34^+$ cord blood (Wei et al., 2008). They also transplanted the transduced cells into sublethally irradiated immunodeficient mice to show the induction of acute leukaemia. Interestingly, they demonstrated that the generation of ALL or AML by the MLL-AF9 expressing cells was dependent on the strain of immunodeficient mice used in the transplantation experiment. In contrast to the work of Barabe *et al*, the MLL-AF9 transduced cells proliferated indefinitely *in vitro* (Wei et al., 2008). Together, these two studies established the possibility of using human primary cells to generate models that can be used to study the leukaemogenic activity of MLL-fusions.

1.15. Telomerase activity and MLL-fusion associated leukaemia

Telomeres are non-coding short repeated DNA sequences at the ends of eukaryotic chromosomes that have a role in protecting these regions [reviewed in (Blackburn, 1991; Blackburn, 2001)]. The mammalian telomere sequence consists of TTAGGG tandem repeats and the telomere ends are protected by a 6 protein subunit called shelterin [reviewed in (Martinez and Blasco, 2011)]. Shelterin caps and shapes the ends of chromosomes into t-loops and this confirmation is important for stabilizing chromosome ends and preventing their end-to-end fusion, degradation, chromosomal recombination and recognition as damaged double stranded DNA. Since DNA polymerase cannot replicate DNA at the ends of chromosomes, telomeric DNA sequence is lost every time cells divide, a phenomenon known as 'the end replication problem' [reviewed in (Harley, 2008)]. In order to solve this problem, terminal telomeres are synthesized by a ribonucleoprotein (RNP) complex called telomerase, to

compensate for this loss (Blackburn, 1992). The major subunits of the telomerase complex consist of telomerase reverse transcriptase (TERT) and telomerase RNA component (TERC).

In general, telomerase activity is elevated in many cancers. It is believed that telomerase activity is essential for maintaining telomeres and the indefinite proliferation of cancer cells. Leukaemia is not an exception to this. Indeed, one study showed that although elevated telomerase activity in adult AML patients correlated with better prognosis and survival, elevated telomerase activity in paediatric AML was associated with poor prognosis and survival (Verstovsek et al., 2003). Several other studies also support this data (Ohyashiki et al., 1997; Xu et al., 1998; Engelhardt et al., 2000). Another study demonstrated the correlation between complete remission of acute leukaemia and decreased telomerase activity. An increase in telomerase activity in isolated $CD34^+$ cells from leukaemia patients has also been demonstrated (Ohyashiki et al., 1997; Engelhardt et al., 2000). Furthermore, transduction of cells from AML patient samples, with a dominant-negative *TERT* expression vector, resulted in reduced clonogenic potential in colony formation assays and delayed engraftment of leukaemia upon xenotransplantation (Roth et al., 2003). All this evidence supports the idea that telomerase activity is important in leukaemia progression.

Two studies reported an association between MLL-fusion induced leukaemia and elevated telomerase activity. Gessener *et al* showed decreased telomerase activity and *TERT* expression in human leukaemia cell lines upon siRNA-mediated inhibition of *MLL-AF4* expression (Gessner et al., 2010). HOXA7 was shown to bind to a region of the *TERT* promoter and *HOXA7* knockdown was shown to result in decreased *TERT*

expression and telomerase activity (Gessner et al., 2010). This suggested that MLL-fusions may regulate telomerase activity through transcriptional activation of their *HOXA* gene targets. Wei *et al* demonstrated elevated telomerase activity in their MLL-AF9 immortalized human cells (Wei et al., 2008). However, it is unclear how MLL-AF9 induced this elevated activity, since no increase in *TERT* expression was observed (Wei et al., 2008). However, these studies indicate that telomerase activity is highly likely to be involved in MLL-fusion associated leukaemia pathogenesis.

1.16. RUVBL1 and RUVBL2

RUVBL1 (also known as Tip49a, NMP238, ECP54, TAP54α, TIH1, Pontin and Rvb1) and RUVBL2 (also known as Tip49b, ECP51,CGI-46, INO80J, TIH2 Tip48, Reptin and Rvb2) are two related family members of ATPases associated with diverse cellular activities (AAA+) [reviewed in (Grigoletto et al., 2011)]. They are involved in many cellular processes and take part in the formation of multiple complexes. One of the characteristics of AAA+ proteins is the formation hexameric rings, mediated by the AAA+ domains [reviewed in (Huen et al., 2010a)] (Figure 1.10).

RUVBL1 and RUVBL2 contain conserved Walker A and Walker B domains which are responsible for ATP binding and ATPase activity (Mezard et al., 1997). Apart from their ATPase activity, RUVBL1 and RUVBL2 have both been suggested to have helicase activities [reviewed in (Grigoletto et al., 2011)].

Figure 1.10. Architecture of RUVBL1 and RUVBL2

A) Domain organisation of human RUVBL1 and RUVBL2. B) 3D structure of the human RUVBL1 monomer in a ribbon representation. Red arrow indicates the location of Walker A and Walker B motifs.[modified from (Matias et al., 2006; Huen et al., 2010b)]. C) 3D structure of human RUVBL1 hexamer (side view on the left, top view on the right) [B&C adapted from (Matias et al., 2006)]. D) Yeast Rvbl1-Rvbl2 structure shown using an electron microscope (adapted from [(Cheung et al., 2010)]. AAA+, ATPases belonging to the ATPAse associated with various cellular activities; aa, amino acid. N, N-terminal and C, C-terminus.

The ATPase and helicase activities of RUVBL1 and RUVBL2 are seen in several different protein complexes, involved in chromatin remodelling, transcriptional regulation and telomerase assembly (Baek, 2008).

The Ino80 complex is one example of a chromatin remodelling complex containing both RUVBL1 and RUVBL2. This complex is conserved from yeast to humans and is responsible for nucleosome mobilization as well as DNA repair and replication (Conaway and Conaway, 2009). TIP60 is another complex in which RUVBL1 and RUVBL2 are involved.

TIP60 is an evolutionally conserved histone acetyltransferase enzyme (HAT). The HAT activity of TIP60 plays a crucial role in DNA damage repair (Jha et al., 2008). DNA damage induces phosphorylation of the histone variant called H2AX, and its phosphorylation is required in order to recruit other proteins to amplify the damage signal and for damage repair to proceed. TIP60 and RUVBL1 were shown to be crucial in downregulation of phosphoH2AX following completion of DNA repair. In addition, RUVBL1 was suggested to play a role in efficient assembly and regulation of TIP60 (Jha et al., 2008).

RUVBL1 and RUVBL2 are also known to interact with many transcription factors such as c-Myc and β-catenin. Reporter gene assays were used to show that both RUVBL1 and RUVBL2 not only bound β-catenin, but also regulated its activity. Interestingly, in this study, RUVBL2 was shown to repress β-catenin mediated transcriptional activity, while RUVBL1 activates it (Bauer et al., 2000). The antagonistic function of RUVBL1

and RUVBL2 was also apparent in the regulation of the anti-metastatic gene *KAI-1* (Kim et al., 2005). Thus, RUVBL2 was found to repress *KAI-1* transcription by forming a complex with TIP60, whilst RUVBL1 activated its transcription by forming a complex with β-catenin (Kim et al., 2005).

Recently, RUVBL1 and RUVBL2 were both discovered to be a part of the telomerase complex (Venteicher et al., 2008). RUVBL1 was demonstrated to interact with TERT and to recruit RUVBL2 to the resulting complex. RUVBL1 and RUVBL2 were also found to interact with the TERC-binding protein dyskerin. Also, TERT-RUVBL1-RUVBL2 association was found to be regulated in a cell cycle-dependent manner, since this complex was specifically found in the S phase of the cell cycle (Venteicher et al., 2008). Depletion of RUVBL1 and RUVBL2 resulted in reduced telomerase activity. From these findings, the authors proposed that RUVBL1and RUVBL2 are required for assembly and remodelling of the telomerase complex, prior to TERT-TERC-dyskerin complex formation (Venteicher et al., 2008)

There are several lines of evidence indicating that *RUVBL1* and *RUVBL2* expression are regulated by c-Myc (Wood et al., 2000; Fan et al., 2010). Wood *et al* showed decreased *RUVBL1* and *RUVBL2* expression in *c-Myc* null rat fibroblasts (Wood et al., 2000). In addition, c-Myc binding sites were identified in both *RUVBL1* and *RUVBL2* promoters, suggesting that c-Myc transcriptionally regulates *RUVBL1* and *RUVBL2* expression (Fan et al., 2010). Interestingly, RUVBL1 and RUVBL2 protein expression have also been shown to be interdependent. Venteicher *et al* first demonstrated that depletion of *RUVBL1* by siRNA resulted in co-depletion of RUVBL2 protein expression, and the reciprocal result was also obtained upon depletion of *RUVBL2* (Venteicher et al., 2008).

A similar trend was observed in other cell lines including liver and breast cancer cell lines (Haurie et al., 2009). Haruie *et al* also found that depletion of *RUVBL1* does not affect the mRNA level of *RUVBL2* and *vice versa*, suggesting that this co-depletion was regulated by a post-translational mechanism, possibly proteasomal degradation (Haurie et al., 2009). Collectively, these studies demonstrate the tight co-regulation of RUVBL1 and RUVBL2 expression.

RUVBL1 and RUVBL2 are also implicated in cancer. RUVBL1 was shown to be required for c-Myc and β-catenin mediated transformation (Wood et al., 2000; Feng et al., 2003). Recently, *RUVBL2* was found to be over-expressed in gastric cancer and the clonogenic potential of gastric cancer cells was shown to depend on *RUVBL2* expression (Li et al., 2010). RUVBL2 function was associated with c-MYC mediated transcriptional regulation of *TERT* expression and resulting telomerase activity. Other studies also showed the importance of *RUVBL1* and *RUVB2* expression in hepatocellular carcinoma (Haurie et al., 2009; Menard et al., 2010). Together, these data have established the importance of *RUVBL1* and *RUVBL2* expression in several human cancers.

1.17. Aims and objectives

Using Affymetrix GeneChip expression analysis, our lab recently established a list of MLL-fusion target genes critical for oncogenic function in murine cells (Dr Vanessa Walf-Vorderwülbecke, PhD thesis). The aim of the present study was to establish whether the identified murine MLL-fusion target genes are also required in human immortalised cells. In order to achieve this, we planned to generate a human model to investigate the importance of the MLL-fusion target genes. Therefore, my objectives were:

1. Generate immortalised myeloid cell lines from human cord blood using MLL-fusions

2. Use patient-derived leukaemic cell lines to study MLL-fusion function

3. To investigate the role of the MLL-fusion target genes in human leukaemogenesis

CHAPTER 2. MATERIALS AND METHODS

2.1. Transformation of bacteria

Subcloning Efficiency DH5α™ chemically competent cells (Invitrogen, Paisley,UK) were used for transforming bacteria. 1µl of DNA (0.5µg/µl) was incubated in pre-chilled polypropylene round-bottom tubes (BD Bioscience [BD], Oxford, UK) together with the competent cells, previously thawed on ice. The mixture was incubated on ice for 30 minutes, followed by heat shock for 20 seconds in a 37°C waterbath. The mixture was subsequently incubated on ice for 2 minutes. 300µl of pre-warmed SOC outgrowth medium (New England Bio Labs [NEB], Ipswich, UK) was added to the mixture and shaken at 37°C for one hour at 225 rpm. The mixture was then plated onto LB agar plates containing LB agar (1.5g bacto Agar (BD) per 100ml LB broth (1% w/v Bacto Tryptone (BD), 0.5% w/v Bacto Yeast Extract (BD), 1% w/v Sodium Chloride (NaCl),[pH 7.0])) and 100µg/ml Ampicillin (Sigma-Aldrich, Dorset, UK) and incubated at 37°C overnight.

2.2. Isolation of plasmid DNA

Individual bacterial colonies were inoculated into 3ml LB broth with 100µg/ml Ampicillin and incubated in a shaker at 37 °C overnight, at 225 rpm. The bacterial cultures were then used to extract DNA using the QIAprep Spin Miniprep Kit (Qiagen, West Sussex, UK) according to the manufacturer's instructions. 1ml of bacterial culture was centrifuged at 300xg and the pellet was resuspended in 250µl buffer P1 and P2,

then thoroughly mixed. 350µl of buffer N3 was added to the mixture and then centrifuged at 17,900xg for 10 minutes. The supernatant was applied to a QIAprep spin column and centrifuged for 60 seconds and flow-through was discarded. The QIAprep spin column was washed by adding 0.5ml buffer PB and centrifuged as before, and the process repeated with 0.75ml of buffer PE. The QIAprep spin column was centrifuged for an additional 1 minute to remove excess buffer and then DNA was eluted with 30µl buffer EB. The concentration of extracted plasmid DNA was determined by measuring the absorbance at 260nm using a spectrophotometer (NanoDrop ND-1000, Lebtech International, East Sussex, UK). The ratio of absorbance between 260 and 280 was used to measure the purity of DNA. A ratio of approximately 1.8 was considered to be pure from protein contamination.

In order to obtain large quantities of plasmid DNA, required for transfections, individual bacterial colonies were inoculated into 3ml of LB broth with 100µg/ml Ampicillin and incubated in a shaker at 37 °C for 6 hours, at 225 rpm. This starter culture was then added to 250ml LB broth with 100µg/ml Ampicillin and incubated in a shaker at 37 °C overnight, at 225 rpm. The Genopure Plasmid Maxi Kit (Roche, Burgess Hill, UK) was used to isolate the plasmid DNA from the bacterial culture according to manufacturer's guidelines. The bacterial culture was centrifuged for 15 minutes at 15,000xg. The pellet was resuspended with 12ml of resuspension buffer and 12ml of lysis buffer and incubated for 2-3 minutes at room temperature. 12ml of neutralisation buffer was added to the mixture and incubated for 5 minutes on ice. The lysate was cleared by centrifugation at 15,000xg for 30 minutes and the supernatant was added to a pre-equilibrated column through a filter. The column was washed 3 times with 16ml wash buffer, then eluted with pre-warmed 15ml elusion buffer. The eluted plasmid DNA was

precipitated with 11ml isopropanol and centrifuged for 10 minutes at 15,000xg immediately. The plasmid DNA was washed with chilled 70% ethanol and centrifuged again at 15,000xg for 10 minutes. The DNA pellet was air-dried and re-dissolved in distilled water. The concentration of the plasmid DNA was measured using a spectrophotometer as per the methods given above.

2.3. Plasmid sub-cloning

2.3.1. Restriction enzyme digests

Restriction digestion of plasmid DNA was performed according to the manufacturer's instructions. In general, 10 µg of plasmid DNA was digested with 1µl of 10U/µl restriction enzyme, 20µl of 10x restriction enzyme buffer and 2µl of 10µg/µl BSA, in a final volume of 200µl, made up with H_2O. This was digested for 1-4 hours depending on the restriction enzyme used. Depending on the size of the fragment, the digested products were run on 0.7-1.2% w/v Agarose gels [Agarose (Invitrogen), 1x TAE buffer (National diagnostics, Hessle, UK), 0.5% Ethidium Bromide (Sigma)], in order to be visualised (UV1doc HD/26M, Cambridge, U) and isolated.

2.3.2. Blunt ending

Linearised DNA with a 5' overhang was filled with dNTPs (Promega) by T4 DNA polymerase (Promega), to generate fragmented DNA with a blunt end for some of the cloning procedures. Blunting was carried out according to manufacturer's protocols. In general, 2µg of fragmented DNA was filled in with 10 units of T4 DNA polymerase (Promega), 200µM of dNTPs and T4DNA polymerase reaction buffer was added to

make the final volume 100µl. The mixture was incubated for 15 minutes at 37C° and 4µl of 0.5M EDTA was added to stop the reaction. The blunt ended product was purified using the QIAquick Nucleotide removal kit (Qiagen) according to the manufacturer's instructions.

2.3.3. Gel extraction

Isolated digested product was purified from the Agarose gel using QIAquick Gel Extraction Kit (Qiagen) according to the manufacturer's guidelines. The DNA fragment was excised from the agarose gel. The excised gel fragment was weighed and 3 times the weight of buffer QG, to 1 times the weight of gel, was added and incubated at 50°C for 10 minutes, or until the gel was completely dissolved. 1 gel volume of isopropanol was added to the mix and transferred onto a QIAquick spin column and centrifuged at 17,900xg for 1 minute. The QIAquick spin column was centrifuged with 0.5ml of buffer QG for 1 minute to remove any trace of agarose, then centrifuged with 0.75ml of buffer PE for 1 minute to remove any salt contaminants. The QIAquick spin column was centrifuged for an additional 1 minute to completely remove ethanol from buffer PE. DNA was then eluted by centrifuging the QIAquick spin column with 30µl of buffer EB (10mM, Tris-Cl [pH8.5]).

2.3.4. Ligation

Following gel extraction, the linearised DNA fragment and vector were ligated to generate plasmid DNA. Depending on the cloning, the molar ratio between the fragment and the vector varied from 1:1, 3:1, and 10:1. The following formula was used to determine the mass of insert required for each ratio.

For example, for 3:1 ratio ligation:

$$ng_{\text{insert required}} = [(50ng_{\text{vector}} \times kb_{\text{insert}})/kb_{\text{vector}}]x3$$

50ng of vector and the required amount of insert were ligated with 5µl of 2x Rapid Ligation Buffer (Promega) and 1 weiss unit of T4 DNA ligase (Promega), in a total volume of 10µl, made up with H_2O. The mixture was incubated at room temperature for 5 minutes for sticky end ligation and 15 minutes for blunt end ligation, prior to transformation (Refer to 2.1).

2.4. Generation of retroviral expression constructs

A schematic diagram of the retroviral expression constructs generated and used is shown in Figure 2.1.

2.4.1. pMSCV-PGK-EGFP

The cDNA of the green fluorescent protein (EGFP) gene was amplified by PCR using MSCV-LMP (Open Biosystems, Surrey, UK) as a template. A 730bp fragment encoding EGFP was amplified using a forward primer incorporating a 5' HindIII site: 5' AGTAAGCTTCACGATGATAATATGGCCAC-3' and a reverse primer incorporating a ClaI site: 5'-ACTATCGATAATTCATTACTTGTACAGCT-3'. pMSCV-puro (Clontech, Nottinghamshire, UK) was then digested with HindIII and ClaI to excise the 650kb puromycin fragment. The 730bp EGFP gene was then sub-cloned into the pMSCV-puro vector.

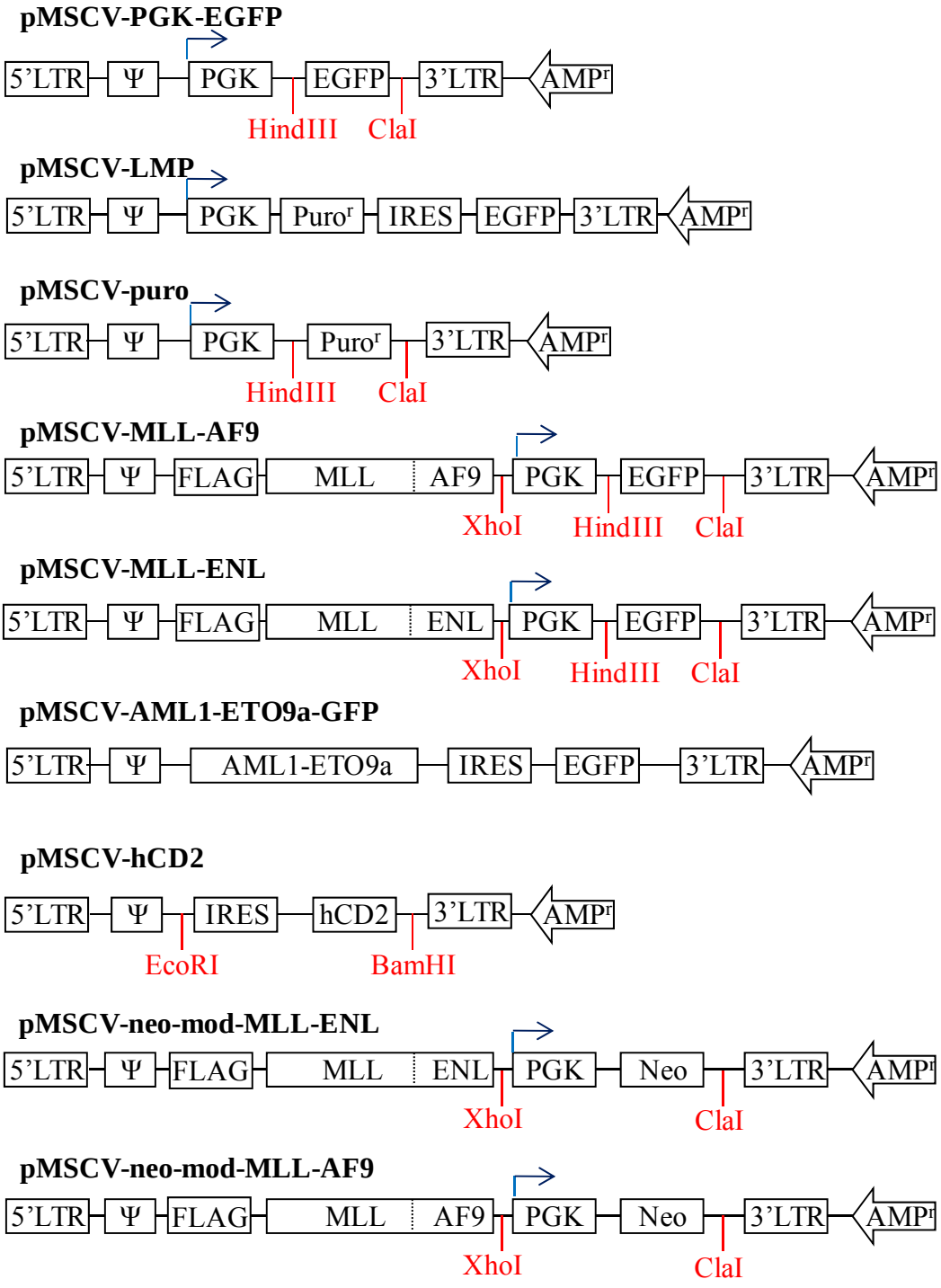

Figure 2.1. Retroviral expression vectors used in this study

LTR, long terminal repeat; Ψ, viral packaging signal; PGK, murine phosphoglycerate kinase promoter; EGFP, enhanced Green Fluorescent Proteins; AMP^r , ampicilin resistance gene.

2.4.2. pMSCV-PGK-MLL-ENL and pMSCV-PGK-MLL-AF9

pMSCV-PGK-EGFP was digested with XhoI and ClaI to release the 1,238bp fragment consisting of the 508bp PGK promoter and the 730 bp EGFP gene fragments. This 1,238bp fragment was then sub-cloned into pMSCV-neo-mod-MLL-ENL, or pMSCV-neo-mod-MLL-AF9, previously digested with XhoI and ClaI.

2.5. Generation of lentiviral vectors

A schematic diagram of the lentiviral constructs generated and used is shown in Figure 2.2.

2.6. shRNA

The shRNA vectors used in this study were derived from vectors previously described (Silva et al., 2005) . In this system, a specific short hairpin was implanted into the transcript of the naturally occurring micro RNA 30 (miR30), which was previously demonstrated to increase the efficiency of knock down of the gene expression (Silva et al., 2005). shRNA are delivered by lentiviral transduction and transcribed by RNA polymerase II to produce pre-mRNA (Figure 2.3). This is then cleaved by a microprocessor complex containing the RNAase III family enzyme, Drosha. The pre-mRNA is transferred into the cytoplasm via Exportin 5 and it is then further cleaved by Dicer to generate siRNA (Cullen, 2005; Leung and Whittaker, 2005; Rao et al., 2009).

Figure 2.2. Lentiviral expression vectors used in this study

LTR, long terminal repeat; Ψ, viral packaging signal; PGK, murine phosphoglycerate kinase promoter; EGFP, enhanced Green Fluorescent Protein; tGFP, turbo Green Fluorescent Protein; AMP^r , ampicilin resistance gene; UbiC, Ubiquitin-C promoter*;* WASP*,* Wriskott Aldrich syndrome promoter*;* SFFV, spleen focus-forming virus promoter; WRE, Woodchuck hepatitis virus regulatory element. Note that MLL-AF9 expression in FUGW-V6MA vector is driven by UbiC promoter in reverse direction i.e. AF9-MLL.

FUGW-V6MA

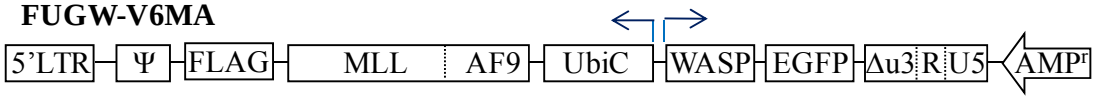

FUGW-V6

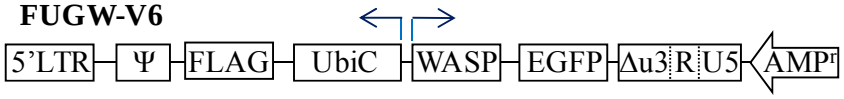

pGIPZ

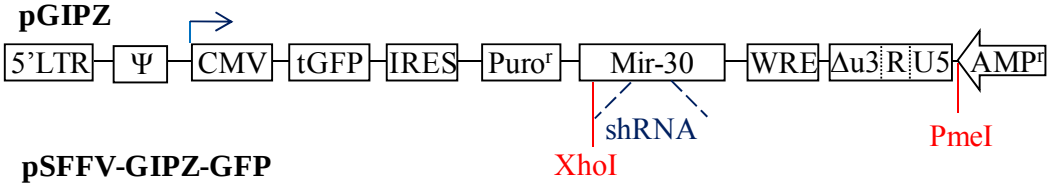

pSFFV-GIPZ-GFP

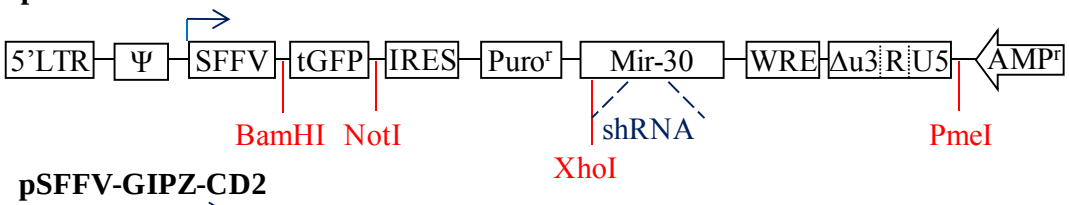

pSFFV-GIPZ-CD2

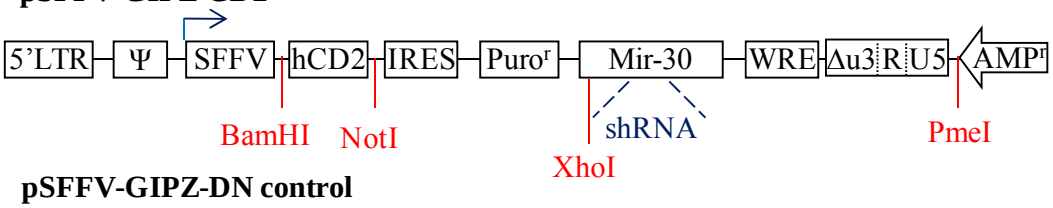

pSFFV-GIPZ-DN control

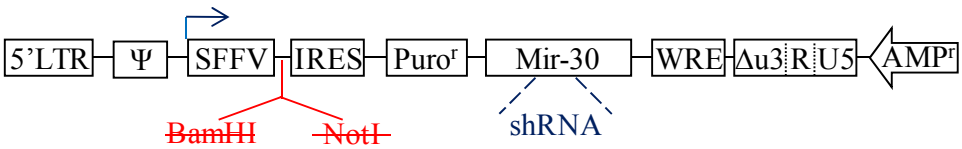

pSFFV-GIPZ-RUVBL1(D302N)

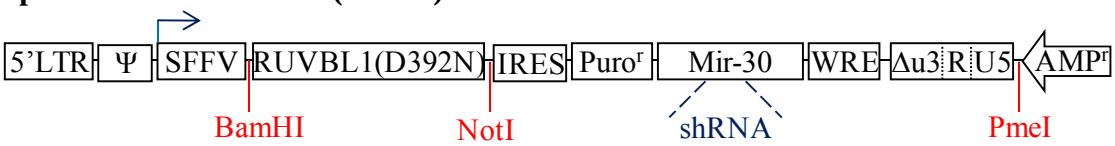

pSFFV-GIPZ-RUVBL2(D302N)

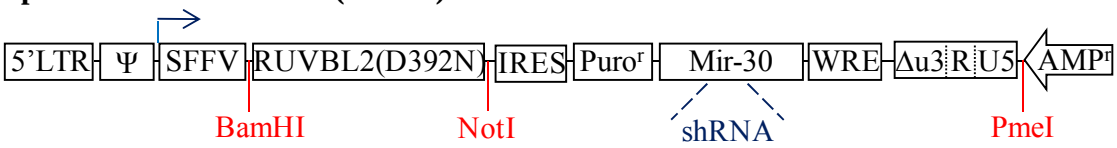

Figure 2.3. Sturcture of lentiviral shRNA used in this study (Diagram modified from OpenBiosystems)

siRNA is incorporated into the RNA-induced silencing comlex (RISC) where it unwinds and cleaves the target mRNA, and this process causes silencing of the target gene. shRNAs were purchased in the pGIPZ lentiviral vector from the GIPZ lentiviral shRNAmir library at UCL, Open Biosystems (Surrey, UK) (Table 2.1).

2.6.1. SFFV-GIPZ-GFP

Since the human cytomegalovirus (CMV) promoter contained in the pGIPZ vector was previously shown to be inefficient in haematopoetic cells (Sirven et al., 2001), shRNAs from the pGIPZ vector were cloned into the SFFV-GIPZ vector, in which the spleen focus-forming virus (SFFV) promoter was used to drive the expression of EGFP. For this cloning procedure, the pGIPZ vector with the shRNA of interest was digested with PmeI (NEB) and XhoI (Promega) to isolate the 1400bp fragment containing the shRNA and part of the vector backbone. This was then sub-cloned into the SFFV-GIPZ vector pre-digested with PmeI and XhoI.

2.6.2. SFFV-GIPZ-CD2

The cDNA was amplified by PCR using the pMSCV-IRES-CD2 vector as a template. The human CD2 (hCD2) cDNA used in our experiments is 'tailless' hCD2, which codes for a truncated CD2 protein, lacking most of its cytoplasmic domain (Deftos et al., 1998). A 839bp fragment encoding hCD2 was amplified using a forward primer incorporating a 5 BamHI site: 5'-CGGGATCCGCCACCATGGGCTTTCCATG TAAATTTGTAGCC AGC-3' and a reverse primer incorporating a NotI site: 5' CGGCGGCCGCTTAGGAAGTTGCTGGATTCTGAGGG-3' (refer to 2.28).

Gene (Asession no)	Sequence (5'-3') (mir-30-sense-loop-antisense-mir-30)
GAPDH (NM_002046)	TGCTGTTGACAGTGAGCGAGCTCATTTCCTGGTATGACAATAGTGAAGCCACAGATGTA TTGTCATACCAGGAAATGAGCGTGCCTACTGCCTCGGA
HOXA9.4 (NM_152739)	TGCTGTTGACAGTGAGCGCCTCCTCCAGTTGATAGAGAAATAGTGAAGCCACAGATGTA TTTCTCTATCAACTGGAGGAGATGCCTACTGCCTCGGA
HOXA9.5 (NM_152739)	TGCTGTTGACAGTGAGCGATCCCGTGCAGCTTCCAGTCCAAAGTGAAGCCACAGATGTA TTGGACTGGAAGCTGCACGGGCTGCCTACTGCCTCGGA
HOXA9.6 (NM_152739)	TGCTGTTGACAGTGAGCGTCAACAAAGACCGAGCAAAAGTGAAGCCACAGATGTA TTTGCTCGGTCTTTGTTGATGCCTACTGCCTCGGA
MYC.1 (NM_002467)	TGCTGTTGACAGTGAGCGCCCGTCCAAGCAGAGGAGCAAATAGTGAAGCCACAGATGTA TTTGCTCCTCTGCTTGGACGGATGCCTACTGCCTCGGA
MYC.2 (NM_002467)	TGCTGTTGACAGTGAGCGCCGAGAACAGTTGAAACACAAATAGTGAAGCCACAGATGTA TTTGTGTTTCAACTGTTCTCGTTGCCTACTGCCTCGGA
MYC.3 (NM_002467)	TGCTGTTGACAGTGAGCGAGGAACTCTTGTGCGTAAGGAATAGTGAAGCCACAGATGTA TTCCTTACGCACAAGAGTTCCGTGCCTACTGCCTCGGA
MLL.2 (NM_005933)	TGCTGTTGACAGTGAGCGCCTGCAAGATTGAGAAGAGTAATAGTGAAGCCACAGATGTA TTACTCTTCTCAATCTTGCAGATGCCTACTGCCTCGGA
MLL.5 (NM_005933)	TGCTGTTGACAGTGAGCGCGGAGATAAGATCAAGAAGAAATAGTGAAGCCACAGATGTA TTTCTTCTTGATCTTATCTCCATGCCTACTGCCTCGGA
RUVBL1.1 (NM_003707)	TGCTGTTGACAGTGAGCGACCGGCCAACTTGCTTGCTAAATAGTGAAGCCACAGATGTA TTTAGCAAGCAAGTTGGCCGGGTGCCTACTGCCTCGGA
RUVBL1.2 (NM_003707)	TGCTGTTGACAGTGAGCGAAAGACAGAAATCACAGACAAATAGTGAAGCCACAGATGTA TTTGTCTGTGATTTCTGTCTTCTGCCTACTGCCTCGGA
RUVBL1.3 (NM_003707)	TGCTGTTGACAGTGAGCGCTACCTGGTGTGTTTTCTATAATAGTGAAGCCACAGATGTA TTATAGAAAACACACCAGGTATGCCTACTGCCTCGGA
RUVBL2.3 (NM_006666)	TGCTGTTGACAGTGAGCGACAGCGAGAAAGACACGAAGCATAGTGAAGCCACAGATGTA TGCTTCGTGTCTTTCTCGCTGTTGCCTACTGCCTCGGA
RUVBL2.4 (NM_006666)	TGCTGTTGACAGTGAGCGACACGCAGTACATGAAGGAGTATAGTGAAGCCACAGATGTA TACTCCTTCATGTACTGCGTGGTGCCTACTGCCTCGGA
RUVBL2.5 (NM_006666)	TGCTGTTGACAGTGAGCGACCGGAGATCCGTGATGTAACATAGTGAAGCCACAGATGTA TGTTACATCACGGATCTCCGGGTGCCTACTGCCTCGGA
RUVBL2.6 (NM_006666)	TGCTGTTGACAGTGAGCGATTCCTCTTCAACGAACTCAAATAGTGAAGCCACAGATGTA TTTGAGTTCGTTGAAGAGGAAGTGCCTACTGCCTCGGA
RUVBL2.7 (NM_006666)	TGCTGTTGACAGTGAGCGATCCAGATTGATCGACCAGCAATAGTGAAGCCACAGATGTA TTGCTGGTCGATCAATCTGGATTGCCTACTGCCTCGGA

Table 2.1. shRNA mir30 sequences used in this study

The SFFV-GIPZ vector was digested with BamHI and NotI to release the 698bp fragment encoding turbo GFP (tGFP). The 839bp fragment encoding hCD2 was then sub-cloned into the SFFV-GIPZ vector.

2.7. Mutagenesis

Point mutations were introduced within the conserved Walker B sequence both in *RUVBL1* and *RUVBL2* cDNA containing Integrated Molecular Analysis of Genomes and their Expression (IMAGE) clones pOTB7 vector [(Source BioScience, Nottingham, UK (Wood et al., 2000)]. The QuikChange® Site-Directed Mutagenesis Kit (Strategene, Cheshire, UK) was used to introduce a Guanine (G) to Adenine (A) bp point mutation, resulting in an Aspartic acid (D) to Asparagine (N) substitution at aa residue 302 and 299 in RUVBL1 and RUVBL2, respectively. Mutated *RUVBL1* and *RUVBL2* cDNA were amplified by PCR and these amplified products were digested with BamHI (Promega) and NotI (Promega) to release the entire *RUVBL1* and *RUVBL2* cDNA fragments, which were 1371bp and 1404bp respectively. The SFFV-GIPZ vector was then digested with BamHI and NotI to release the 698bp fragment encoding tGFP. *RUVBL1* and *RUVBL2* cDNA fragments were sub-cloned into the SFFV-GIPZ vector. Table 2.2 shows the primers used for this mutagenesis.

RUVBL1

Purpose	Direction of the primers	Sequence (5'-3')
mutagenesis	forward	CGGGTGTGCTGTTTGTTAATGAGGTCCACATGCTG
mutagenesis	reverse	CAGCATGTGGACCTCATTAACAAACAGCACACCCG
PCR	forward	CGGGATCCATGAAGATTGAGGAGGTGAAG
PCR	reverse	CGGCGGCCGCTCACTTCATGTACTTATCCTGC
sequencing-1	forward	AGATTGAGGAGGTGAAGAGC
sequencing-2	reverse	GACAGCTCTTCCAGCCATTT
sequencing -3	forward	TTGGGCTGCGAATAAAGGAG
sequencing -4	forward	CATCCAAGATGTGACCTTGC
sequencing -5	forward	ATCCGGACCATGCTGTATAC

RUVBL2

Purpose	Direction of the primers	Sequence (5'-3')
mutagenesis	forward	GGAGTGCTGTTCATCAACGAGGTCCACATGC
mutagenesis	reverse	GCATGTGGACCTCGTTGATGAACAGCACTCC
PCR	forward	CGGGATCCTTGGTGAGCATCATGGCAAC
PCR	reverse	CTGCGGCCGCCAGGAGGTGTCCATGGTCTC
sequencing-1	forward	TACAGCCACAACCAAAGTCC
sequencing-2	reverse	CAATCTTCCCTTCCCGGATC
sequencing -3	forward	AAACTGACCCTCAAGACCAC
sequencing -4	forward	ACGAGATCGACGTCATCAAC
sequencing -5	forward	AGATGTGGAGATGAGTGAGG

Table 2.2. Primers used for mutageneis in this study

2.8. Cell culture and cell lines

Human leukaemic cell lines (The German Resource Centre for Biological Material, DSMZ, Braunschweig, Germany) were cultured in Roswell Park Memorial Institute (RPMI) medium (Invitrogen), supplemented with 10% heat-inactivated FCS, 100U/ml Penicillin (Invitrogen), 100µg/ml Streptomycin (Invitrogen) and 2mM L-glutamine (Invitrogen) (complete RPMI). Each human leukaemic cell line was seeded at between 0.1-0.5 $x10^6$/ml and sub-cultured every two to three days according to the supplier's instructions (DSMZ). The MLL-AF9 immortalised myeloid cells derived from human CB in this study were cultured in Iscoves Modified Dulbeccos Medium (IMDM) (Invitrogen) with 20% FCS, 100U/ml Penicillin, 100µg/ml Streptomycin and 2mM L-glutamine (complete IMDM), supplemented with 100ng/ml recombinant human (rh) Thrombopoietin (TPO) (Miltenyi Biotec), 100ng/ml rh FMS-related tyrosine kinase 3 ligand (FLT3L) (R&D systems), 100ng/ml rh stem cell factor (SCF) (R&D systems, Abingdon, UK), 10ng/ml rhIL-3 (R&D systems) and 10ng/ml rhIL-6 (R&D systems). Human CB cells were seeded at 0.5 $x10^6$/ml and sub-cultured every two to three days.

2.9. Culture of packaging cell lines and NIH-3T3 fibroblast cells

The LinXE (Genetica, Hannon *et al*, 1999), Platinum-GP (Plat-GP) (Cell Biolab, Cambridge, UK), GP2-293 (Clontech) and 293FT (Invitrogen) packaging cell lines and NIH-3T3 mouse embryonic fibroblast cells (DSMZ), were cultured in Dulbecco's Modified Eagle's medium (DMEM, Invitrogen), supplemented with 10% heat-inactivated FCS (Sigma-Aldrich, Dorset, UK), 100U/ml Penicillin (Invitrogen), 100µg/ml Streptomycin (Invitrogen) and 2mM L-glutamine (Invitrogen) (complete

DMEM). LinXE cells were maintained with 7.5µg/ml Hygromycin (Invivogen). Plat-GP cells were maintained with 10µg/ml Blasticidin (Invitrogen).

2.10. Transfection of packaging cell lines

LinXE cells were seeded without Hygromycin at a density of 0.5-0.75x10^6 per 10cm petri dish (Thermo Fisher Scientific, Leicestershire, UK), three days before the transfection for production of retrovirus. A total of 10µg of expression vector was incubated in 1.5ml of Optimen (GIBCO) and 36µl of Lipofectamine 2000 reagent (Invitrogen) was incubated in 1.5ml of Optimem for 5 minutes at room temperature. These two mixtures were then combined and incubated for 20 minutes at room temperature. Meanwhile, the packaging cells were harvested and re-suspended at a density of 1.2x10^6 per ml. 5ml of the cells was then plated with 5ml of complete DMEM medium and DNA-Lipofectamine 2000 complexes. Lipofectamine containing medium was then replaced with 8ml of complete DMEM medium on the second day of transfection. For retroviral transduction using GP2-293 cells, the cells were seeded at a density of 0.5x10^6 in 10ml medium, three days before the transfection. For Plat-GP cells, the cells were seeded without Blasticidin at a density of 1x10^6 in 10ml medium, three days before the transfection. 8µg of expression vector and 2µg of envelope construct were used for both GP2-293 and Plat-GP cells. For lentiviral packaging cell line transfection, 293FT cells were seeded at a density of 4x10^5 in 10ml medium, three days before transfection for the production of lentivirus. For lentiviral transfection, 5µg of expression vector, 3.75µg of psPAX2 (kindly supplied by Professor Didier Trono, Lausanne, Switzerland) and 1.5µg of envelope construct were used.

2.11. Retroviral and lentiviral transduction of human myeloid leukaemic cells

Retroviral and lentiviral supernatants were harvested 48 hours after transfection. For human leukaemic cells, $1x10^4$ cells were plated out at 100µl per well in a complete RPMI, supplemented with 5µg/ml polybrene, and were transduced by spinoculation at 700g, for 45 minutes at 25 ºC. 24 hours after the transduction, 100µl per well of complete RPMI was added. In some experiments, the transduced cells were selected with 2µg/ml puromycin for 3 days. In all cases, the transduced leukaemic cells were used for further experiments 5 days after transduction.

2.12. Isolation of human $CD34^+$ CB cells

Frozen human cord blood mononuclear cells ($150x10^6$ cells per sample) (Stem Cell Technologies, Sheffield, UK) were thawed and $CD34^+$ cells were purified by magnetic activated cell sorting (MACS) (Miltenyi Biotec, Surry, UK) using the human CD34 microbead kit, according to the manufacturer's protocol. Purified $CD34^+$ cord blood ($CD34^+$ CB) cells were maintained at a density of $1\text{-}2x10^5$ per ml in Hematopoietic Progenitor Growth Medium (HPGM™) (Lonza, Sough, UK) supplemented with 100ng/ml rhSCF, 100µg/ml rhTPO, and 100ng/ml rhFLT3L. The cells were cultured for two days before transduction. The number of cells isolated and the corresponding purity of $CD34^+$ cells after sorting are shown in Table 2.3.

CB sample Number	Total cell count before sorting	Total cell count after sorting	% $CD34^+$ cells (purity)	Cell line generated
A	$73x10^6$	$1x10^6$	87%	-
B	$90x10^6$	$0.4x10^6$	93%	-
C	$90x10^6$	$0.4x10^6$	93%	-
1	$77x10^6$	$0.8x10^6$	90%	V6.1/V6MA1
2	$110x10^6$	$0.2x10^6$	21%	V6.2/V6MA2
3	$77x10^6$	$0.6x10^6$	62%	V6.3/V6MA3
4	$90x10^6$	$2.3x10^6$	86%	V6.4/V6MA4

Table 2.3. Cord blood samples used in this study

2.13. Retroviral and lentiviral transduction of human $CD34^+$ CB cells

One day before transduction, retronectin (Takara Bio Inc, Shiga, Japan) coated plates were prepared. 250µl per well of retronectin (80µg/ml) in phosphate buffered saline (PBS) was coated onto non-tissue culture treated 48-well plates (Thermo Fisher Scientific). The retronectin-coated plate was incubated at 4ºC overnight. The retronectin-coated plate was blocked with PBS containing 0.3mM bovine serum albumin (BSA) for 30 minutes at room temperature and then washed with PBS. Retroviral or lentiviral supernatant was collected 48 hours after transfection and filtered through a 0.45µm filter (Sartorius, Surry, UK). 250µl of filtered virus was added to each well of the retronectin-coated plate and the plate was centrifuged at 1,500g for two hours at room temperature. The supernatant was removed and the wells were washed

with PBS twice. Between $2x10^4$ and $1x10^5$ $CD34^+$ CB cells, in complete IMDM supplemented with 100ng/ml rhTPO, 100ng/ml rhFLT3L, 100ng/ml rhSCF, 10ng/ml rhIL-3 and 10ng/ml rhIL-6 were then added onto the retronectin-coated plate and incubated at 37 ºC overnight. 250µl of complete IMDM supplemented with 100ng/ml rhTPO, 100ng/ml rhFLT3L, 100ng/ml rhSCF, 10ng/ml rhIL-3 and 10ng/ml rhIL-6 was added to each well the next day. The transduced $CD34^+$ CB cells were maintained at $0.5\text{-}2x10^6$ per ml in a 24 well plate, in IMDM supplemented with 20% FCS, 100U/ml Penicillin, 100µg/ml Streptomycin, 2mM L-glutamine 100ng/ml TPO, 100ng/ml rhFLT3L, 100ng/ml rhSCF, 10ng/ml rhIL-3 and 10ng/ml rhIL-6, and used for further experiments five days after the transduction.

2.14. shRNA delivery

shRNAs were delivered via lentiviral transduction. Lentiviral supernatant containing shNRAs were generated according to 2.11. The Vesicular Stomatitis Virus Glycoprotein (VSV-G) envelope was used to coat the lentiviral shRNA particles. Lentiviral supernatant was collected 48 hours after transfection and filtered through a 0.45µm filter (Sartorius). For human leukaemic cells, $6x10^5$ cells in complete RPMI, supplemented with 5µg/ml polybrene in 1ml medium, were transduced by spinoculation at 700g, for 45 minutes at 25ºC. 24 hours after the transduction, 1ml per well of complete RPMI was added. Transduced cells were treated with 2µg/ml of puromycin (Invitrogen), two days after transduction, for three days.

For cord blood (CB)-derived immortalised MLL-AF9 cells, $5x10^4$ cells per well, in 100µl complete IMDM supplemented with 5µg/ml polybrene, 100ng/ml rhTPO, 100ng/ml rhFLT3L, 100ng/ml rhSCF, 10ng/ml rhIL-3 and 10ng/ml rhIL-6 in a 96-well plate, were transduced by spinoculation at 700g, for 45 minutes at 25 ºC. 24 hours after the transduction, 100µl per well of complete IMDM supplemented with 100ng/ml rh TPO, 100ng/ml rhFLT3L, 100ng/ml rhSCF, 10ng/ml rhIL-3 and 10ng/ml rhIL-6 was added. Transduced cells were treated with 1µg/ml of puromycin, two days after transduction, for three days. The transduced cells were used for further experiments after five days of transduction.

2.15. Determination of the viral titre

The efficiency of the viral transduction was determined by measuring the percentage of tGFP, EGFP or hCD2 expressing cells. The ecotropic virus titre was determined by the transduction of NIH-3T3 cells. NIH-3T3 cells were seeded at a density of $2x10^5$ per 4ml medium, 24 hours before the transduction. 24 hours later, serially diluted virus was added to the cells, together with 5µg/ml polybrene. The transduced cells were harvested 48 hours after transduction. Viral infection per ml was calculated using the following formula:

$$\text{Inf/ml} = \text{number of cells transduced} \times \frac{(\%\ \text{of EGFP/CD2 expressing cells})}{100} \times \text{dilution factor}$$

2.16. Ultracentrifugation

Ultracentrifugation was performed to concentrate retrovirus in some experiments. Sorvall 12ml centrifuge tubes (Thermo Fisher Scientific) were washed once with 70% ethanol and twice with PBS prior to use, in order to sterilise them. 11.5ml per tube of filtered virus was concentrated by ultracentrifugation at 18,000g for 3 hours at 4 ºC (Thermo Fisher Scientific, Discovery 100). The supernatant was discarded and the viral pellet was re-suspended in fresh medium with a 40-fold reduction in volume. The concentrated virus was left for 30 minutes on ice to re-suspend prior to use.

2.17. Colony formation assay

For human $CD34^+$ CB cells, between $3x10^4$ and $1x10^5$ transduced cells were washed in HPGM and resuspended in 300ul cell resuspension solution (R&D systems). The cells were added to 3ml of human methylcellulose complete media without Epo (R&D system), supplemented with 100ng/ml rhTPO, 100ng/ml rhFLT3L, 100ng/ml rhSCF, 10ng/ml rhIL-3, and 10ng/ml rhIL-6. The cells were cultured for 10 days before re-plating or harvesting for analysis.

For human leukaemic cells, colony formation was optimised and performed by Mr Maurizio Mangolini (MHCB unit, ICH). $1x10^4$ cells were resuspended in 0.6ml of cell resuspension solution (R&D systems) and added to 2.7ml of human methylcellulose base media (R&D systems). The cells were cultured for 14 days before harvesting for analysis.

2.18. Flow cytometry

Cells were washed with 2ml of wash buffer (PBS supplemented with 0.05% v/v sodium azide). Cells were pre-incubated with 50µl of human FcR-binding inhibitor (eBioscience, Hatfield, UK) containing stain buffer (PBS supplemented with 0.05% v/v sodium azide and 0.1% w/v BSA), for 15 minutes on ice, to block non-specific antibody binding. The cells were then stained with florochrome-conjugated antibodies in stain buffer, in a total of 100µl, for 30 minutes on ice, and washed with wash buffer prior to analysis. Anti-human antibodies used are listed in Table 2.4. Appropriate IgG isotype control antibodies were used. Cells were analysed on a Cyan ADP analyser (Dakocytomation, Cambridge UK) or LSRII (BD Bioscience) and the data was analysed with Summit 4.3 software (Dakocytomation).

2.19. Apoptosis assay

Annexin V and 4', 6-diamidino-2-phenylindole (DAPI) were used to detect apoptotic cells. Annexin belongs to a calcium-dependent phospholipid binding protein family. It binds to phosphatidylserine which is transferred to the extracellular membrane early during apoptosis. DAPI is a fluorescent DNA binding dye which is used to detect dead cells. Together, Annexin V and DAPI are used to detect early ($AnnexinV^{+}$ $DAPI^{-}$) and late stage ($Annexin^{+}$ $DAPI^{+}$) apoptotic cells. Cells were washed with PBS followed by 1x binding buffer (50mM Tris [pH7.4], 100nM NaCl, 1% w/v BSA, 0.02% v/v sodium azide [eBioscience]).

Antibody	Isotype	Dilution
hCD2 PE (e Bioscience)	IgG1κ	1 in 25
CD11b PE (Biolegend)	IgG1κ	1 in 5
CD14 APC (BD Bioscience)	IgG2κ	1 in 5
CD15 APC (Biolegend)	IgM1κ	1 in 5
CD33 PE (e Bioscience)	IgG1κ	1 in 5
CD34 PE (BD Bioscience)	IgG1κ	1 in 5
CD38 APC (e Bioscience)	IgG1κ	1 in 5

Table 2.4. Antibodies used for flow cytometric analyses in this study

Cells were then re-suspended in 1x binding buffer at a density of 1-5x10^6/ml and 5µl of Annexin V (eBiosciecnes) was added to 100µl of the cell suspension and incubated for 15 minutes at room temperature. The cell suspension was washed and re-suspended in 200µl of 1x binding buffer and 5µl of DAPI was added to the cell suspension prior to flow cytometric analysis.

2.20. Preparation of total protein lysate for western blot analysis

Cells were harvested and washed with PBS by centrifugation at 300g for 5 minutes at 4ºC. Cell pellets were lysed using 60µl Dithiothreiothreitol (DTT) sample buffer (200mM DTT, 2% sodium dodecyl sulphate (SDS), 10% v/v Glycerol, 0.02% v/v Bromophenol blue, 125mM Tris-HCL [tris(hydroxymethyl)aminomethane] [pH6.8]) per 1x10^6 cells. The lysate was incubated for five minutes at 100°C in a heating block and vortexed for 10 seconds followed by centrifugation at 16,000g for 10 minutes at 4°C. The pellet was discarded and the total cell lysate was stored at -20°C.

2.21. Western blot analysis

Western blot analysis was performed using Hoeffer equipment (GE Healthcare). 4% Sodium Dodecyl Sulfate (SDS)-polyacrylamide gels (stacking gel) and 5%, 10% or 12.5% SDS- polyacrylamide gels (resolving gel) were prepared according to Table 2.5. Protein samples and rainbow molecular weight marker (Amersham Biosciences) were subjected to electrophoresis at 65V overnight at room temperature.

Stacking gel

Reagent	Required volume
30% Acrylamide/Bis Solution (29:1) (BioRad)	0.8ml
Upper Buffer (0.5M TrisHCL[pH6.8] 0.4% w/v SDS)	1.6ml
H_2O	3,8ml
Temed (BioRad)	6.25µl
10% w/v Amonium Persulfate (APS, BioRad)	31.3µl

Resolving gel

Reagent	Required volume		
	5%	10%	12.5%
30% Acrylamide/Bis Solution (29:1) (BioRad)	5ml	10ml	12.5ml
Lower Buffer (1.5M TrisHCL[pH8.8] 0.4% w/v SDS)	7.5ml	7.5ml	7.5ml
H_2O	17.5ml	12.5ml	10ml
Temed (BioRad)	20µl	20µl	20µl
10% w/v Amonium Persulfate (APS, BioRad)	100µl	100µl	100µl

Table 2.5. Stacking gel and resolving gel used for western blot analysis

1X running buffer (0.192 M Glycine, 25nM TrisHCL[pH8.3], 0.1% w/v SDS) was used to perform SDS-polyacrylamide gel electrophoresis (SDS-PAGE). The samples were subsequently transferred onto a polyvinylidenefluoride (PVDF) membrane (Millipore) for 6 hours, at 500mA at 4°C in 1x CAPS (9.5mM CAPS [pH11.0]). Membranes were blocked in PBS with 5% non-fat milk and 0.2% v/v Tween-20, and stained with one of the primary antibodies listed in Table 2.6 for 1 hour, or overnight, depending on the antibody used. The membrane was washed to remove any excess antibody using PBS 0.2% v/v Tween-20, six times over a period of one hour. Proteins were detected using a secondary antibody conjugated with horseradish peroxidise (GE Healthcare, London, UK), as listed in Table 2.6, and visualised using a chemiluminescent reagent (ECL, GE Healthcare), according to the manufacturer's instructions. The rainbow molecular weight marker was used to estimate the protein size. The film was pre-flashed using an Amersham Sensitize Preflash unit (GE Healthcare) and exposed to the membrane. Exposed film was developed using the Xograph CompactX4 developer. A calibrated Densitometer (GS-800, BioRad) was used to scan the film and individual bands were quantified using QuantityOne software (BioRad).

Primary antibodies

Name of antibodies	Suppliers	Dilution
MLL mouse monoclonal (N4.4)	Upstate Milipore	1 in 400
C-MYB moues polyclonal (C-19)	Santa Cruz Biotechnology	1 in 1000
GAPDH goat polyclonal (v-18)	Santa Cruz Biotechnology	1 in 1000
HSP-90 α/β mouse monoclonal (F-8)	Santa Cruz Biotechnology	1 in 1000
β - tubulin mouse monoclonal (D-10)	Santa Cruz Biotechnology	1 in 1000
α - actin goat polyclonal (I-19)	Santa Cruz Biotechnology	1 in 6000
RUVBL1 goat polyclonal (N-15)	Santa Cruz Biotechnology	1 in 500
Clathrin HC mouse monoclonal (TD.1)	Santa Cruz Biotechnology	1 in 1000
RUVBL2 mouse monoclonal (42)	Santa Cruz Biotechnology	1 in 500
TERT rabbit monoclonal (H-231)	Santa Cruz Biotechnology	1 in 500

Secondary antibodies

Name of antibodies	Suppliers	Dilution
Anti-**mouse** IgG HRP-linked whole Antibody (Raised from Sheep)	GE Health Care	1 in 2000
Anti-**goat** IgG HRP-linked whole Antibody (Raised from Donkey)	Santa Cruz Biotechnology	1 in 6000
Anti-**rabbit** IgG HRP-linked whole Antibody (Raised from Donkey)	GE Health Care	1 in 10000

Table 2.6. Primary and secondary antibodies used for western blot analysis

The relative protein expression was calculated by dividing the values of the protein of interest by the value of its loading control. This value was then normalised to relative to control samples.

A membrane was sometimes stripped and re-probed with another antibody. For stripping, the membrane was incubated at 50ºC for 30 minutes with 50ml of stripping buffer (100mM 2-mercaptoethanol, 2% w/v SDS, 62.5mM Tirs-HCL [pH6.7]). The membrane was washed with PBS with 5% non-fat milk and 0.2% Tween-20 every 10 minutes for 30 minutes, before being probed with a primary antibody, as described above.

2.22. MLL-fusion western blot analysis

In order to detect MLL or MLL-fusion protein expression, samples were run on a 4% SDS-polyacrylamide stacking gel and a 5% SDS- polyacrylamide resolving gel at 70V for 9 hours. The samples were subsequently transferred onto a polyvinylidenefluoride (PVDF) membrane (Millipore) overnight, at 300mA at 4°C in 1x CAPS. The membrane was washed as described previously and probed with primary mouse monoclonal MLLN4.4 antibody overnight at 4°C. The membrane was then treated in the same way as described in 2.21.

2.23. RNA isolation

RNA was isolated from cells using the RNeasy Mini kit (Qiagen) according to the manufacturer's protocol. During the isolation, samples were also treated with DNAse (Invitrogen). The concentration of extracted RNA was determined by measuring the absorbance at 260nm using a spectrophotometer (NanoDrop ND-1000, Lebtech International, East Sussex, UK). The purity of the extracted RNA was estimated by measuring the ratio of the absorbance at 260nm and 280nm. A ratio of between 0.8 -2 was considered as pure RNA (NanoDrop user's manual).

2.24. cDNA preparation

Isolated RNA was converted into cDNA using a cDNA synthesis kit (Invitrogen), following the manufacturer's protocol. For synthesising the complementary DNA strand, Moloney Murine Leukaemia Virus Reverse Trasncriptase (M-MLV RT, Invitrogen) was used.

2.25. Real-time PCR (QPCR)

A specific primer and probe set that spanned the MLL-AF9 breakpoint region was previously designed and optimised (Dr Vanessa Walf-Vorderwülbecke, PhD thesis). A forward primer 5'-CAAGTATCCCTGTAAAACAAAAACCA-3' (binds to MLL) and a reverse primer 5'-CATTCACCATTCTTTATTTGCTTATCTG-3' (binds to AF9) and

a probe 5'-TGCTTTGCTTTATTGGACTTTTCACTTCAAGAATCTTT-3' (which spans on the MLL-AF9 breakpoint) were used to detect mRNA expression of MLL-AF9. Table 2.7 shows the Taqman primer probe sets used to detect mRNA for all other genes (Applied Biosystems, Paisley, UK).

Gene	Product code
HPRT	Hs_99999909_ml
ACTB	Hs_00357333_gl
MYB	Hs_00920556_ml
MEIS1	Hs_00180020_ml
TERT	Hs_00972647_ml
RUVBL1	Hs_00186558_ml
RUVBL2	Hs_01090542_ml
MYC	Hs_99999003_ml
HOXA9	Hs_00365956_ml

Table 2.7. Taqman primer probe assays used in this study

2.26. Cytospin analysis

$3x10^4$ cells were washed in PBS at 580xg for five minutes at room temperature and re-suspended in 100µl PBS. The cell suspension was added drop-wise to a cytospin funnel and centrifuged onto a slide at 35xg for five minutes, at low deceleration, using a cytospin 3 machine (Shandon, Thermo Fisher Scientific). The slides were fixed and stained with May-Grünwald-Giemsa (MGG) using a Shandon varistain 24-4 automated

staining machine in the Haematology Department at Great Ormond Street Hospital, London.

2.27. Delivery of siRNA

Three specific siRNA against the 5' sequence of MLL were designed to target both endogenous and MLL-fusion proteins. These were designed by Dr Jasper De Boer (MHCB unit, ICH) (Table2.11). $3x10^6$ cells were electroporated in 300µl complete RPMI with either 500nM SiGLO RED (Thermo Fisher Scientific) or 100nM siRNAs. Electroporation was performed at 330V, for 10 milliseconds (ms) using a pulse generator EPI 2500 electroporator (Heidelberg, Germany). The cells were transferred into a 6 well-plate in complete RPMI. The cells were harvested for further analysis at 72 hours. Targeted sequences of GAPDH, MYB and MLL are also shown in Table 2.8.

Gene	Targeted sequences (5'-3')	Suppliers
MLLA	TTGGTTTGCGAATAAGACCTT	Qiagen
MLL.B	TTATCCTTTCTGTTGATGGAG	Qiagen
MLL.C	TTTGCTTAGAACTATTGCCAT	Qiagen
GAPDH (Pool of 4)	GTCAACGGATTTGGTCGTA CAACGGATTTGGTCGTATT GACCTCAACTACATGGTTT TGGTTTACATGTTCCAATA	Thermo Scientific
MYB (pool of 4)	CCGAAACGTTGGTCTGTTA CAGTCAAGCTCGTAAATAC CCAATTATCTCCCGAATCG TCCATACCCTGTAGCGTTA	Thermo Scientific

Table 2.8. Sequences of siRNAs used in this study

2.28. Polymerase chain reaction (PCR)

PCR was used to amplify the cloned products mentioned in 2.4, 2.7 and 2.30. The typical PCR procedure consisted of 5 steps. The initialisation step initiates heat activation of DNA polymerase. The denaturation step disrupts hydrogen bonds between DNA templates to generate single stranded DNA. The annealing steps allow primers to bind to single stranded DNA via hydrogen bonds. The polymerisation step allows DNA polymerase to synthesize a new DNA strand, which is complementary to the DNA template, in a 5' to 3' direction from the primer. The final extension step ensures full extension of single stranded DNA by DNA polymerase. PCR was performed according to standard manufacturer protocol (Invitrogen) and the reaction was programmed according to Table 2.9.

2.29. Xenotransplantation

All the mice used were maintained in the Western Laboratories animal facilities (UCL Biological Services Unit, London, UK) and experiments were performed according to institutional guidelines and Home Office regulations. Xenotransplantation in this study was performed by Dr. Owen Williams (MHCB Unit, ICH). Sub-lethally γ-irradiated (3.5Gy) NOD.Cg-*Prkdc*^{scid} *Il2rg*^{tm1Wjl}/Sz mice were injected intravenously with 10x10^6 V6MA cells and recipients were monitored for signs of disease. Mice were sacrificed and bone marrow and spleen were harvested for analysis. Bone marrow, from the femur and tibia, and spleen were isolated to generate single cell suspensions.

Cloning

Step	Temperature (°C)	Time (minute)	Cycles
Initial denaturation	94	5	1
Denaturation	94	0.5	35
Annealing	50	1	
Polymerisation	72	1	
Final extension	72	5	1

Mutagenesis

Step	Temperature (°C)	Time (minute)	Cycles
Initial denaturation	95	2	1
Denaturation	95	0.5	30
Annealing	55	0.5	
Polymerisation	72	1.5	
Final extension	72	5	1

Telomerase assay

Step	Temperature (°C)	Time (minute)	Cycles
Primer elongation	20	25	1
Telomease inactivation	94	5	1
Denaturation	94	0.5	20
Annealing	50	0.5	
Polymerisation	72	1.25	
Final extension	72	10	1

Table 2.9. PCR programmes used in this study

Red cells were lysed by incubating cells in Red Cell Lysis buffer (17mM Tris (hydeoxymethyl) methylamine (TrisHCL)[pH7.2] and 0.144M Ammonium Chloride (NH_4CL)) for 10 minutes at room temperature and cells were counted prior to further analysis.

2.30. Determination of telomerase activity

Telomerase activity was measured using the Telo TAGGG Telomerase PCR ELISA^{plus} kit (Roche) and assays were performed according to the manufacturer's protocol. Total protein was extracted from $2x10^5$ cells, and lysate from $1x10^3$ cells was used to perform a single assay. Isolated telomerase was used to add telomeric repeats (TTAGGG) to the 3' end of biotin labelled synthetic primers and the telomerase mediated elongation product was amplified (Table 2.26). This PCR product was then hybridised to a digoxigenin labelled detection probe which is specific to telomeric repeats, immobilised to streptavidin coated plates via biotin. This immobilised product was detected by an antibody specific to digozigenin, conjugated with horseradish peroxidase and developed with a sensitive hydroxidase substrate. Colour change was measured using a plate reader (Bio Rad 680 Microplate reader, Herts UK) at 450nm, with a reference wavelength of 690nm. The relative telomerase activities (RTA) were calculated using the formula (Telo TAGGG telomerase PCR ELISA^{plus} manual):

$$RTA = \frac{(A_S - A_{S.0})/A_{S.IS}}{[(A_{TS8} - A_{S0})/A_{TS8.0}]/A_{TS8.IS}} \times 100$$

A_S: absorbance of sample
$A_{S.0}$: absorbance of heat treated sample
A_{TS8} : absorbance of Internal standard (IS) of the sample
$A_{TS8.0}$: absorbance of Control template
$A_{TS8.IS}$: absorbance of Lysis buffer

2.31. Determination of fold accumulation of proliferating cells

Fold accumulation of cells was determined and plotted using the following formula:

Fold accumulation on day (n+x) = Fold accumulation on day (n) x Fold increase on day (n+x)

Where: Fold increase on day (n+x) = $\frac{\text{Cell number on day (n+x)}}{\text{Cell number plated on day (n)}}$

CHAPTER 3. RESULTS - Generation and characterisation of human cord blood-derived MLL-AF9 immortalised myeloid cells

3.1. Introduction

The generation of MLL-AF9 immortalised myeloid cells from cord blood (CB) is an important step in transfering key findings from murine models to human systems. So far, only two groups have managed to successfully immortalise CB cells using MLL-AF9 (Barabe et al., 2007; Wei et al., 2008), which demonstrates the technical difficulty involved in achieving this process. To create immortalised myeloid cell lines, we decided to set up the conditions required for generating high-titre amphotropic virus. At first, this was done with a control virus, made by transient transfection of packaging cell lines with the pMSCV-IRES-EGFP or pMSCV-PGK-EGFP expression vectors, so that efficiency of transduction could be followed by the expression of EGFP. Once this was satisfactory accomplished, we planned to generate amphotropic virus produced by transiently transfecting a packaging cell line with an MLL-ENL or MLL-AF9 expression vector. Subsequently, we could use these viruses to transduce $CD34^+$ CB cells. In addition, human leukaemic cells were also used for some optimisations.

Barabe *et al* and Wei *et al* both successfully generated immortalised myeloid cell lines using MLL-fusions from human cord blood by retroviral transduction (Barabe et al., 2007; Wei et al., 2008). For this reason, retroviral transduction was initially employed for our experiments. Also, some of their transduction strategies were employed in our optimisation process.

Generating a high titre of retrovirus involves several optimisation steps. First of all, packaging cell lines that allow the production of amphotropic retroviruses need to be chosen. The packaging cells used were derived from human embryonic kidney cells and are necessary for the production of replication defective virus particles. Some of these cell lines contain the genes encoding Group Antigens (gag), reverse transcriptase (pol) and envelope proteins (env), which are all required for the formation of viral particles as well as transduction (Morgenstern and Land, 1990). The envelope protein encoded by the packaging cell lines is vital in viral entry into target cells and determines the viral tropism. For our experiments, it was essential to use packaging cells that did not encode the envelope protein, in order to identify the most efficient envelope for the transduction of $CD34^+$ CB cells. Following selection of the appropriate envelope, we planned to optimise the ratio of expression vector to envelope construct for the transfection.

3.2. Selection of the packaging cell lines

Firstly, we wanted to select a retroviral packaging cell that generates high-titre retroviral supernatant, capable of efficient transduction of $CD34^+$ CB cells. Platinum-GP (Plat-GP) (Cambridge Biosciences, Cambridge, UK) (Morita et al., 2000) and GP2-293 (Clontech) packaging cells are both derived from human 293 embryonic kidney cells, transfected with the *gag* and *pol* genes. LinXE cells contain the ecotropic *env* gene as well as *gag* and *pol* genes, and produce high-titre virus. Initially we compared the packaging ability of Plat-GP and GP2-293 cells to that of LinXE cells by testing their ability to generate ecotropic retroviral supernatant. Plat-GP and GP2-293 cells were

transiently co-transfected with the EGFP control retroviral vector (pMSCV-IRES-EGFP) and the envelope construct which encodes the murine specific envelope (pEco), while LinXE cells were transiently transfected with pMSCV-IRES-EGFP only. NIH-3T3 cells were used as target cells for retrovirus produced by these packaging cell lines. The percentage of cells expressing EGFP was used as an indicator of the efficiency of transduction. The retroviral supernatant was serially diluted to obtain a quantitative measurement of retroviral titre. Figure 3.1 shows that Plat-GP cells produced a higher titre retroviral supernatant (0.56×10^6 inf/ml) than GP2-293 cells (0.37×10^6 inf/ml). However, a further two independent experiments showed that this difference was not always obvious. Nevertheless, Plat-GP cells were used in subsequent experiments.

3.3. Selection of the envelope constructs

The envelope gene codes for the viral envelope which is responsible for the target cell tropism of the retrovirus. In order to produce amphotropic virus with Plat-GP cells, an envelope construct capable of transducing human cells is required and therefore different envelope constructs were tested. Plat-GP cells were transiently co-transfected with the pMSCV-IRES-EGFP vector and envelope constructs coding for the vesicular stomatitis glycoprotein (pVSV-G) (Emi et al., 1991), or the envelope protein from the feline endogenous virus (pCMV-RD114) (Sandrin et al., 2002). We initially chose these VSV-G and RD114 envelope constructs for testing because they were previously employed to generate CB-derived MLL-AF9 immortalised cells by Barabe *et al* and Wei *et al*, respectively (Barabe et al., 2007; Wei et al., 2008). $CD34^+$ CB cells were purified and transduced with the retrovirus generated using the respective envelope constructs.

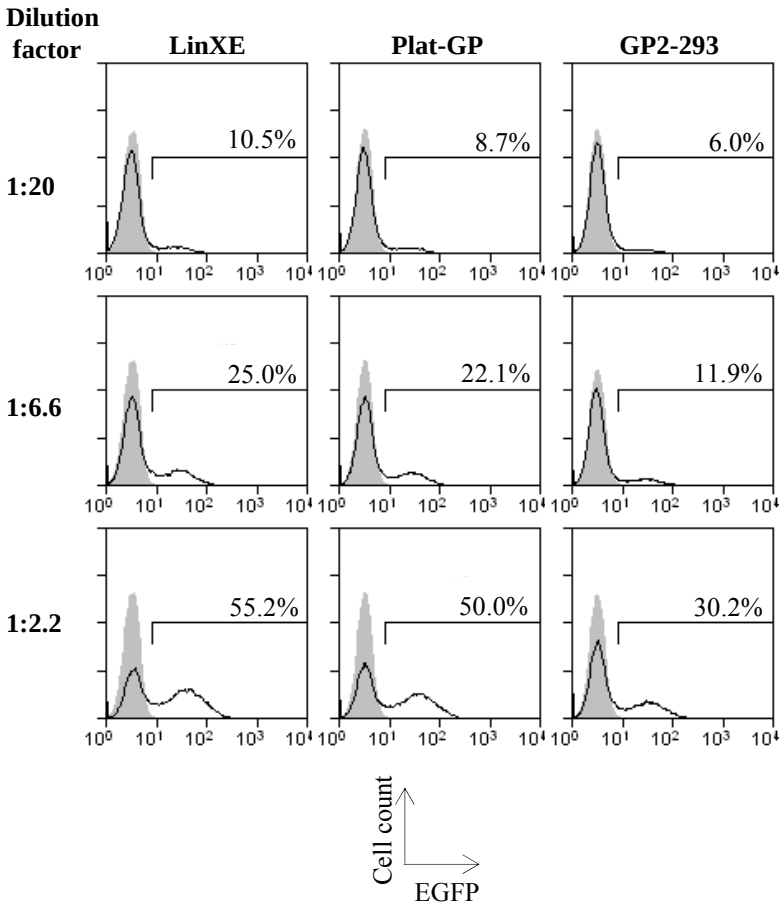

Cell lines	Average inf/ml
LinXE	0.68×10^6
Plat-Gp	0.56×10^6
Gp-293	0.37×10^6

Figure 3.1. Plat-GP provides more efficient retroviral transduction than Gp2-293 cells

The histograms represent the percentage expression of EGFP in transduced 3T3 cells 48 hours after the transduction. Plat-GP and Gp2-293 cells were transiently co-transfected with pMSCV-IRES-EGFP and pEco. LinXE cells were transiently transfected with pMSCV-IRES-EGFP only. Filled grey areas represent un-transduced NIH-3T3 cells. Serial dilution was used to determine average infection unit per ml (inf/ml). Similar results were observed in two independent experiments.

A higher percentage of cells transduced with RD114 coated retrovirus expressed EGFP than those transduced with VSV-G coated retrovirus (Figure 3.2A). Interestingly, $CD34^+$ CB cells transduced with VSV-G coated retrovirus expressed higher levels of CD38, which is characteristic of differentiation (Figure 3.2B). This suggests that the VSV-G envelope may induce differentiation of $CD34^+$ CB cells. This effect is not ideal since oncogene activity may be limited to $CD34^+CD38^-$ HSC. However, a further two independent experiments showed that this difference was not consistently observed. Nevertheless, this data suggest that RD114 envelope was at least as good as VSV-G. Therefore, the RD114 envelope was chosen for subsequent experiments.

Additionally, Di Nunzio *et al* showed that a chimeric RD114TR envelope provides higher virus titre than the RD114 envelope (Di Nunzio et al., 2007). This envelope is comprised of the RD114 extracellular and transmembrane domains and the Moloney murine leukemia virus (MoLV) amphotropic cytoplasmic tail (Di Nunzio et al., 2007). We therefore compared the efficiency of virus production using RD114TR and RD114. For these experiments, SEMK-2 cells, a human cell line derived from an MLL-AF4 associated ALL patient sample, were used as target cells (Pocock et al., 1995). SEMK-2 cells transduced with RD114TR coated retrovirus expressed a higher percentage of EGFP than those transduced with virus coated with RD114 envelope (2.7% versus 4.7%, data not shown). Based on this observation, the RD114TR envelope was selected for the following experiments.

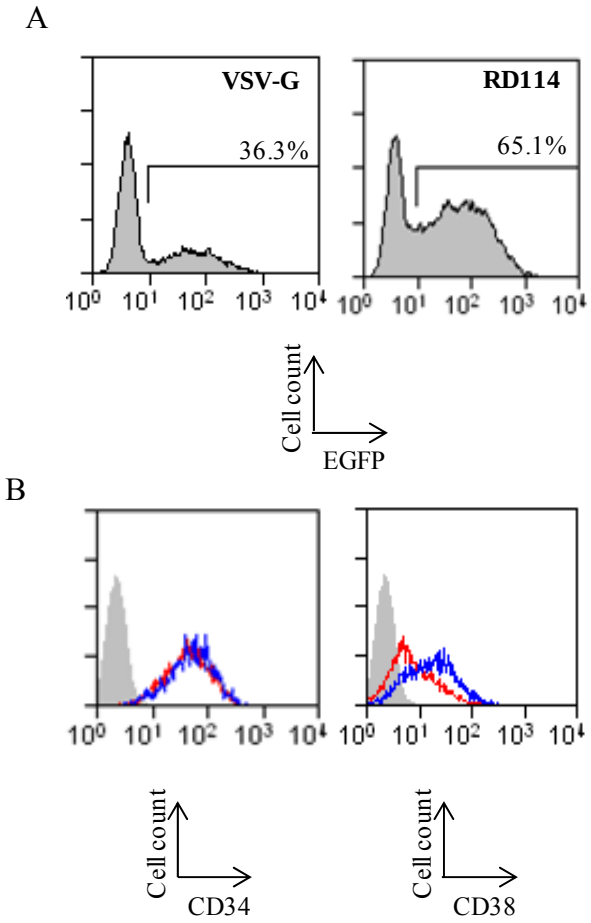

Figure 3.2. The RD114 envelope construct provides more efficient transduction of CD34+ CB cells

A) The grey areas in the histograms show the percentage expression of EGFP in transduced $CD34^+$ CB cells with virus coated with VSV-G (left) or RD114 (right) envelopes, five days after the transduction. B) The histograms represent the percentage expression of EGFP positive gated CD34 (left) and CD38 (right) in the $CD34^+$ CB cells transduced with the virus coated with VSV-G (blue) or RD114 (red) envelopes, five days after the transduction. Filled grey areas represent un-transduced $CD34^+$ CB cells. This experiment was carried out a total of three times.

3.4. Concentration of retrovirus

So far, all the retroviral transductions were done using un-concentrated MSCV-EGFP virus. One problem with generating immortalised myeloid cell lines from $CD34^+$ CB cells, using MLL-ENL and MLL-AF9 fusions, is the size of retroviral inserts in these vectors (8.9Kb and 7.3Kb respectively). The maximum insert capacity of retroviruses is between approximately 7 and 8Kb. Therefore they are both close to the limit of efficient packaging capacity of the packaging cell lines, which inevitably results in lower retroviral titres (Shin et al., 2000; Walther and Stein, 2000).

In order to overcome this difficulty, we decided to concentrate the retrovirus and examine whether this would increase the retroviral titre. Initially, size exclusion filter columns were used to concentrate the retrovirus (Reiser, 2000; Sena-Esteves et al., 2004). However using this approach, there was a loss of virus during the process, resulting in insufficient concentration of retrovirus. A second approach employed was ultracentrifugation. The retroviral supernatant produced from Plat-GP cells transiently transfected with pMSCV-PGK-EGFP and pSMV-RD114TR was ultracentrifuged at 18,000g for 3 hours at 4°C. The retroviral pellet was then re-suspended in fresh medium, resulting in a 40-fold reduction in volume. The retroviral concentration resulted in an increase in transduction of SEMK-2 cells from 2.5% to 37.8%, with an increase in mean florescence intensity (MFI), suggesting an increase in the copy number of integrated provirus (Figure 3.3 A). However, when $CD34^+$ CB cells were transduced with MSCV-ME (MSCV-ME virus) virus, and concentrated using the same approach, only a marginal increase in the percentage of EGFP positive cells was observed (from 5.9% to 8.9%) (Figure 3.3 B).

Figure 3.3. Ultracentrifugation increases the efficiency of retroviral transduction with a control vector but not with the MLL-ENL expression vector

A) The histograms represent the percentage of EGFP expressing SEMK-2 cells transduced with MSCV-PGK-EGFP virus five days after the transduction. The numbers in the histogram represent the percentage expression of EGFP and the numbers in parentheses indicate mean fluorescence intensity (MFI). The top histogram shows the percentage of EGFP expressing cells transduced with un-concentrated virus and the bottom histogram with ultracentrifuged virus (18,000g, 3hours, at 4°C). The pellet of the concentrated retrovirus was re-suspended to a concentration of 40-fold. A similar pattern of percentage expression of EGFP was observed in one other independent experiment. B) The histograms show the percentage of EGFP expressing CB cells transduced with MSCV-PGK-EGFP or MSCV-PGK-MLLENL virus. The top two histograms show the transduction with un-concentrated virus and the bottom two histograms with virus concentrated to 40-fold. This experiment was carried out once.

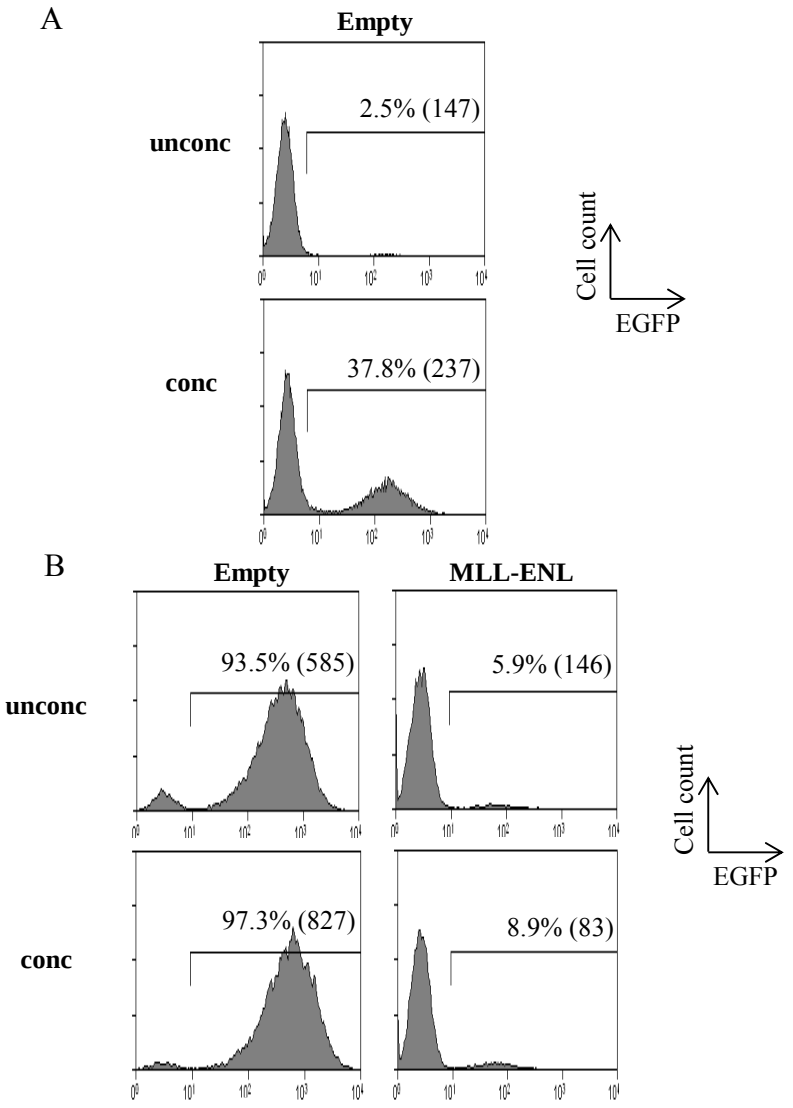
A
Empty
unconc
2.5% (147)
conc
37.8% (237)
Cell count
EGFP
B
Empty
MLL-ENL
unconc
93.5% (585)
5.9% (146)
conc
97.3% (827)
8.9% (83)
Cell count
EGFP

In addition, for unknown reasons, the intensity of EGFP expression decreased from 146 to 83. This suggests, that in our hands, ultracentrifugation of MSCV-ME virus did not improve the efficiency of $CD34^+$ CB cell transduction.

3.5. Selection of reagents to enhance transduction

Polybrene is a cationic polymer that improves the efficiency of transduction by increasing virus adsorption to target cells (Davis et al., 2002). Retronectin provides an alternative approach to increase efficiency of transduction. It is a recombinant human fibronectin fragment that acts as a co-localizer of the virions and the target cells. Since viral particles can be bound by retronectin, inhibitory factors that may be contained within the viral supernatant can be removed after binding of the virus onto retronectin coated plates (Chono et al., 2001). In order to compare the efficiency of transduction using polybrene and retronectin, we transduced $CD34^+$ CB cells with retrovirus produced by transiently transfecting Plat-GP cells with pMSCV-IRES-EGFP (MSCV-EGFP virus) and pCMV-RD114TR. Retronectin was found to achieve a higher percentage of $CD34^+$ CB cell transduction than polybrene (32.2% versus 12.5%, data not shown). In addition, a further two experiments also showed 1.1-fold and 1.4-fold increases in the percentage of $CD34^+$ CB cells transduced using retronectin in comparison to polybrene. For this reason, retronectin was selected for the following experiments.

3.6. Retroviral transduction of human cord blood

Following this series of optimisations, the most effective conditions were applied to retroviral transduction of $CD34^+$ CB cells with expression vectors containing MLL-fusions. Plat-GP cells were transiently transfected with pMCV-RD114TR and either the control pMSCV-PGK-EGFP or the MLL-fusion expression vectors, pMSCV-MLL-ENL-PGK-EGFP and pMSCV-MLL-AF9-PGK-EGFP (MSCV-MA). In addition, we also used an expression vector which encodes the AML1-ETO9a fusion protein, pMIG-AE9a (MIG-AE9a). Since MIG-AE9a has a smaller insert size (3.3Kb) than MLL-fusions expression vectors, it was expected to provide higher retroviral titre and be more efficient at transducing $CD34^+$ CB cells. For this reason, it was used as a positive control. The ratio of the retroviral expression construct to the envelope construct used was 8 to 2. A serial transduction method to improve retroviral transduction was employed, since ultracentrifugation was not successful in this study. $CD34^+$ CB cells were transduced four times, consecutively, within a 48 hour period, with MSCV-MA and MSCV-ME viruses, and only once with MSCV-EGFP and MIG-AE9a viruses, since these were both shown to generate high retroviral titre (data not shown). Transduced $CD34^+$ CB cells were then plated into methylcellulose culture supplemented with TPO (100ng/ml), FLT3L (100ng/ml), SCF (100ng/ml), IL-3(10ng/ml) and IL-6 (10ng/ml) and serially re-plated every 7 to 10 days. The number of cells and colonies produced in each round, as well as EGFP expression, was analysed. Figure 3.4 shows a schematic diagram of the retroviral transduction steps used for this experiment.

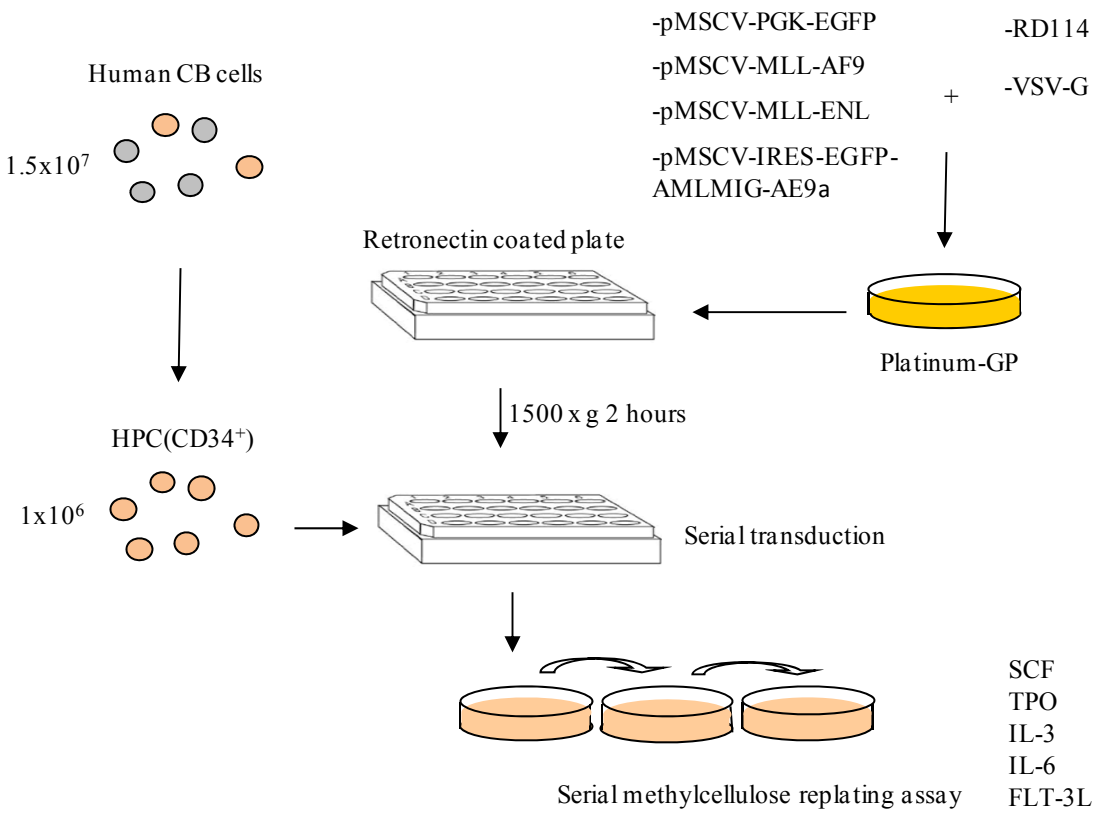

Figure 3.4. Schematic diagram of retroviral transduction used in this study

The diagram illustrates the retroviral transduction approach. 8µg of expression vector and 2µg of envelope construct were used to transfect Plat-GP cells. Retroviral supernatant collected 48 hours after transfection was added to a retronectin-coated plate and was centrifuged at 1,500g for two hours at room temperature. The viral supernatant was then removed and $2x10^4$ $CD34^+$ CB cells in complete IMDM supplemented with 100ng/ml TPO, 100ng/ml rhFLT3L, 100ng/ml rhSCF, 10ng/ml rhIL-3 and 10ng/ml rhIL-6, were then added onto the retronectin-coated plate and incubated at 37 ºC. $3x10^4$ or $1x10^5$ transduced cells were added to 3ml of human methylcellulose complete media (without Epo), supplemented with 100ng/ml TPO, 100ng/ml rhFLT3L, 100ng/ml rhSCF, 10ng/ml rhIL-3, and 10ng/ml rhIL-6. The cells were cultured for 7 to 10 days before re-plating or harvesting for analysis.

The initial percentage expression of EGFP in $CD34^+$ CB cells transduced with MSCV-EGFP and MIG-AE9a virus was significantly higher than in the cells transduced with MSCV-MA and MSCV-ME (Figure 3.5A). Colony formation by MSCV-EGFP cells ceased on the 3rd round of re-plating, whereas the MIG-AE9a culture continued to re-plate, maintaining a high percentage of EGFP expressing cells (Figure 3.5B). The MSCV-ME and MSCV-MA cells did not become immortalised (Figure 3.5B and C). Colony formation ceased by the 3rd round for the MSCV-ME culture and the 4th round for the MSCV-MA culture (Figure 3.5B). However, these cultures still contained live cells, which did not proliferate. It may be possible that these cells require closer contact with each other in order to continue to proliferate. For this reason, the cells were transferred into liquid culture at higher density, in complete IMDM supplemented with TPO, FLT3L, SCF, IL-3 and IL-6. EGFP expression and cell growth were monitored. Regardless of the close contact between the individual cells, the MSCV-ME and MSCV-MA cells failed proliferate despite being EGFP positive (data not shown). From this observation, and four independent experiments with similar results, we reasoned that the $CD34^+$ CB cells transduced with MSCV- ME and MSCV-MA virus may have become senescent.

3.7. Lentiviral transduction of human cord blood

Since the retroviral vectors expressing MLL-ENL and MLL-AF9 failed to immortalise $CD34^+$ CB cells, we decided to switch to using lentiviral vectors, which may be more efficient at transducing $CD34^+$ CB cells (Naldini et al., 1996; Naldini, 1998).

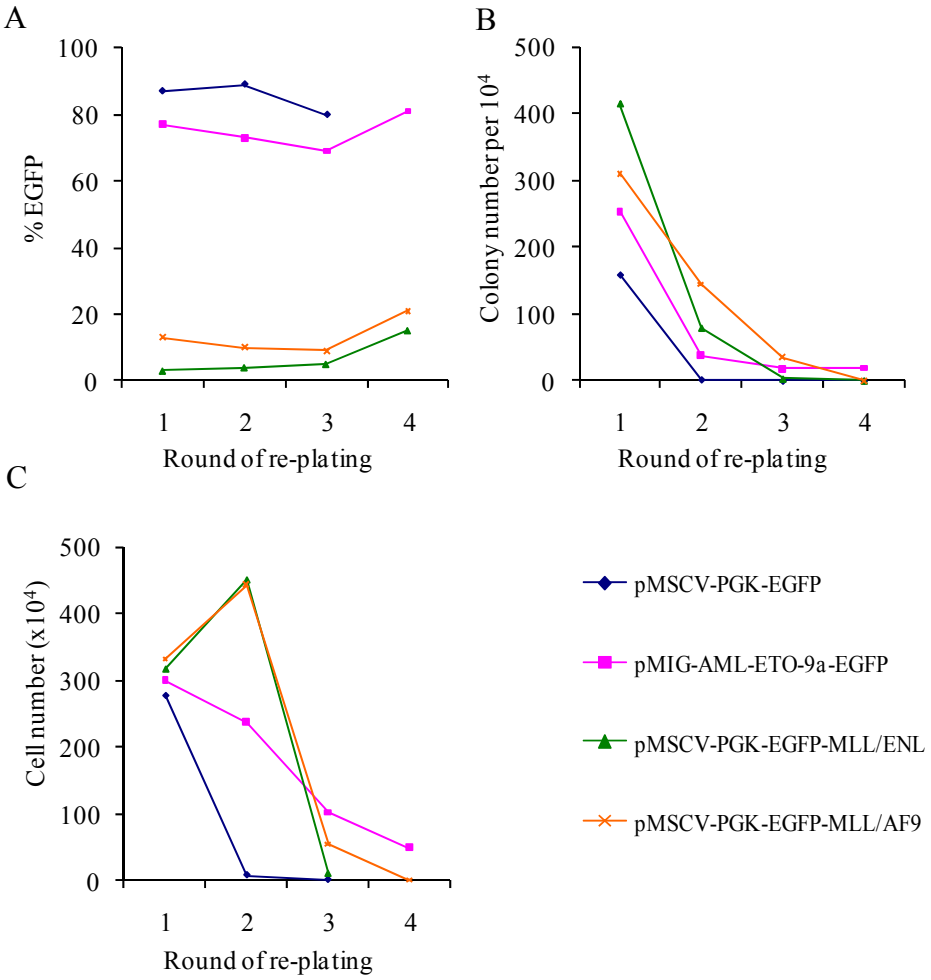

Figure 3.5. CD34$^+$ CB cells were not immortalised following retroviral transduction

The graphs represents: A) the percentage expression of EGFP, B) colony number per 10^4 cells plated, and C) cell number of CB cells per 10^4 cells plated. Transduced CB cells were plated into methylcellulose supplemented with TPO, FLT3L, SCF, IL-3 and IL-6. Cultures were re-plated approximately every seven days. Similar results have been obtained from four other independent experiments.

Unlike retroviruses, lentiviruses do not require a host cell to be in mitosis in order to target the nucleus, and for this reason, lentiviruses can integrate into non-dividing cells as well as dividing cells (Walther and Stein, 2000). The lentiviral expression vectors FUGW-V6 and FUGW-V6MA were kindly supplied by Dr. Sarah Horton, University of Groningen, Netherlands, and Dr. Gianni Morrone, University of Catanzaro Magna Graecia, Italy. See Material and Methods for plasmid maps). For lentiviral transduction, 293FT packaging cells were used. 293FT cells are a variant of 293 cells and contain the SV40 large T antigen, which increases episomal DNA copy number. Unlike Plat-GP cells, these packaging cells do not encode any viral proteins, and therefore co-transfection of the cells with all the packaging genes is necessary. The 293FT cells were transiently co-transfected with the lentiviral expression vectors, FUGW-V6 or FUGW-V6MA, and the pCMV-PAX2 construct, containing the *gag* and *pol* elements, and either the pCMV-RD114TR or the pVSV-G envelope construct. Figure 3.6 shows a schematic diagram of the lentiviral transduction steps used for this experiment. The number of $CD34^+$ CB cells to be transduced was increased from $2x10^4$ to $1x10^5$ in order to provide closer contact between the cells. $CD34^+$ CB cells were only transduced once with FUGW-V6 and four times, serially, with FUGW-V6MA. A high percentage of $CD34^+$ CB cells was transduced with the V6MA vector (Figure 3.7). The percentage of EGFP positive cells increased upon liquid culture of the transduced cells, and reached 99.5% with V6MA virus coated with VSV-G envelope, and 99.9% with V6MA virus coated with RD114TR envelope, by day 40 after the transduction (Figure 3.7). Interestingly, the intensity of EGFP expression in $CD34^+$ CB cells transduced with V6MA (VSV-G) increased from 61 to 128 (Figure 3.7). The increase in intensity of EGFP expression in cells transduced with V6MA (RD114TR) was even higher, from 77 to 291 (Figure 3.7).

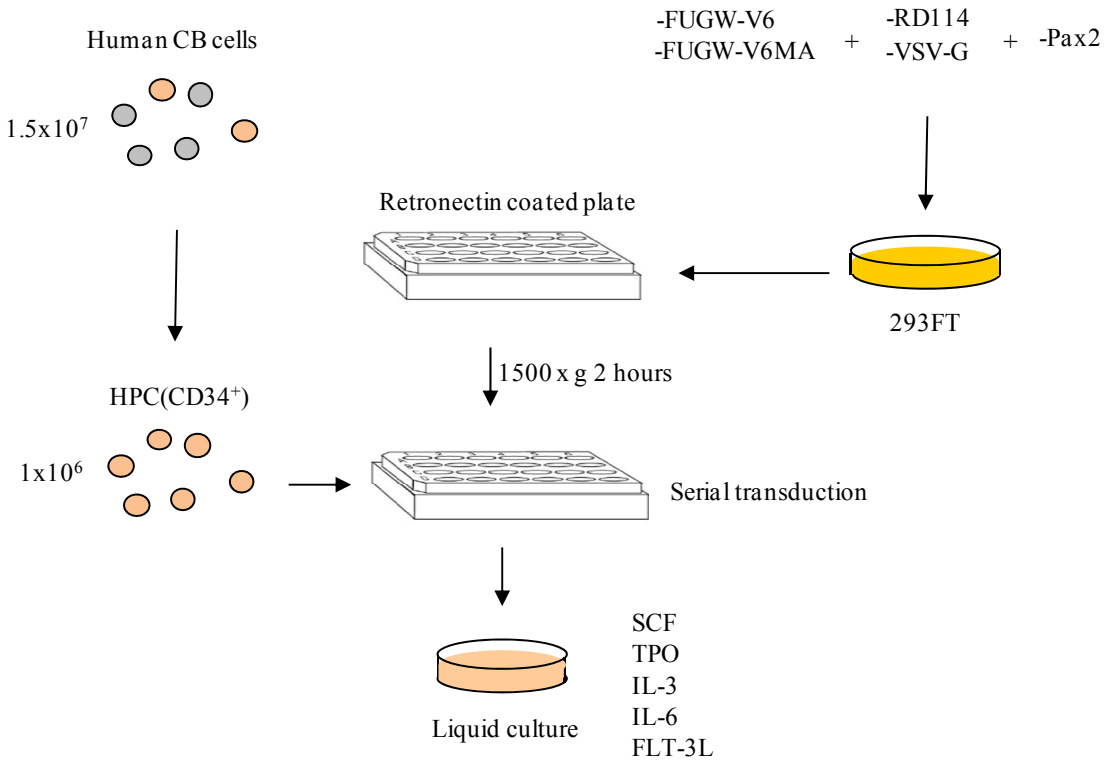

Figure 3.6. Schematic diagram of lentiviral transduction used in this study

The diagram illustrates the lentiviral transduction approach system. 5µg of expression vector, 1.5µg of envelope construct and 3.75 µg of Pax2 were used to transfect 293FT cells. Lentiviral supernatant was collected 48 hours after transfection, added to retronectin-coated plates and was centrifuged at 1,500g for two hours at room temperature. The viral supernatant was then removed and $2x10^5$ $CD34^+$ CB cells in complete IMDM supplemented with 100ng/ml TPO, 100ng/ml rhFLT3L, 100ng/ml rhSCF, 10ng/ml rhIL-3 and 10ng/ml rhIL-6, were added onto the retronectin-coated plate and incubated at 37 ºC. $0.5x10^6$ transduced cells were added to 1ml of complete IMDM supplemented with 100ng/ml TPO, 100ng/ml rhFLT3L, 100ng/ml rhSCF, 10ng/ml rhIL-3 and 10ng/ml rhIL-6. The cells were re-seeded every two to three days at $0.5x10^6$ cell/ml.

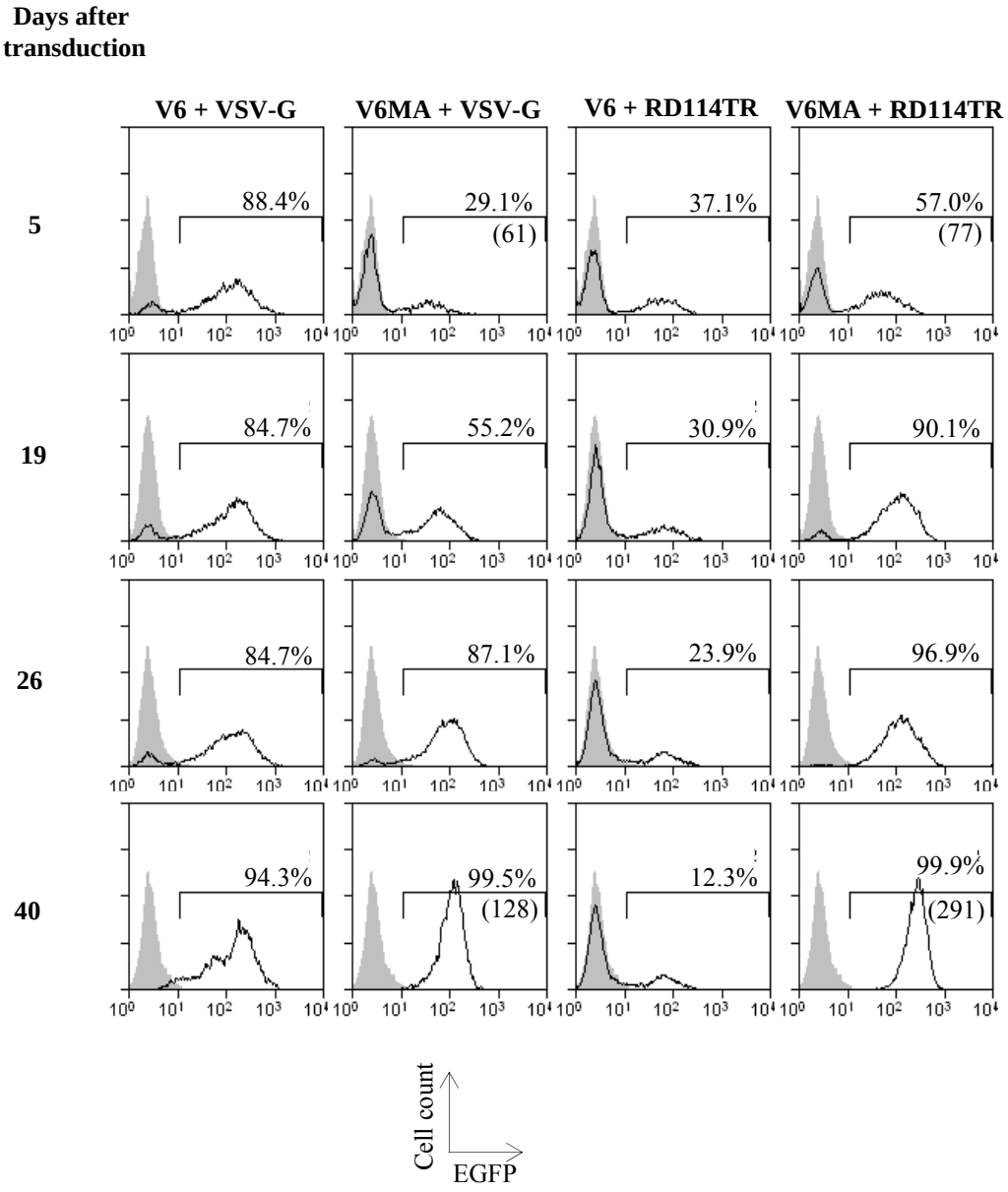

Figure 3.7. Enrichment of EGFP positive V6MA cells following transduction of CD34$^+$ CB cells

The histograms show the percentage of EGFP expressing CB cells after transduction with V6 or V6MA virus, coated either with VSV-G or RD114TR envelopes. The analysis was performed at the indicated times after lentiviral transduction. The numbers in the histograms represent the percentage of EGFP positive cells and the numbers in brackets indicate mean fluorescence intensity. Filled grey areas represent un-transduced CD34$^+$ CB cells. A similar trend was observed in three other independent experiments.

In total, four different human CB samples were used to generate immortalised myeloid cells using MLL-AF9 (V6MA1-4) (Figure 3.8). The CD34$^+$ CB cells transduced with

V6MAr (RD114TR) and V6MAv (VSV-G) continued to proliferate exponentially over the time period analysed, while the proliferation rate of GFP control vector and untransduced $CD34^+$ CB cells plateaued by approximately day 40 of culturing (Figure 3.8).

It should be noted that although V6MA cells were successfully immortalised, none of the V6MA cells proliferated indefinitely. V6MA cells eventually ceased to proliferate and the length of the proliferation varied depending on the CB samples and the particular line. V6MA1v, V6MA1r, V6MA2r, V6MA3v, V6MA3r and V6MA4r proliferated up to days 192, 101, 222, 180, 303 and 104, respectively.

3.8. Validation of MLL-AF9 expression in V6MA cells

The protein and mRNA expression of MLL-AF9 was validated in the V6MA cells. Untransduced $CD34^+$ CB cells, V6.3 cells and V6MA3r cells were tested for MLL-AF9 protein expression by western blot analysis, using a monoclonal antibody directed against the N-terminus of MLL (Figure 3.9A). A 170kDa band corresponding to the MLL-AF9 protein was detected in V6MA3r cells, while this band was absent in both untransduced $CD34^+$ CB cells and V6.3 cells.

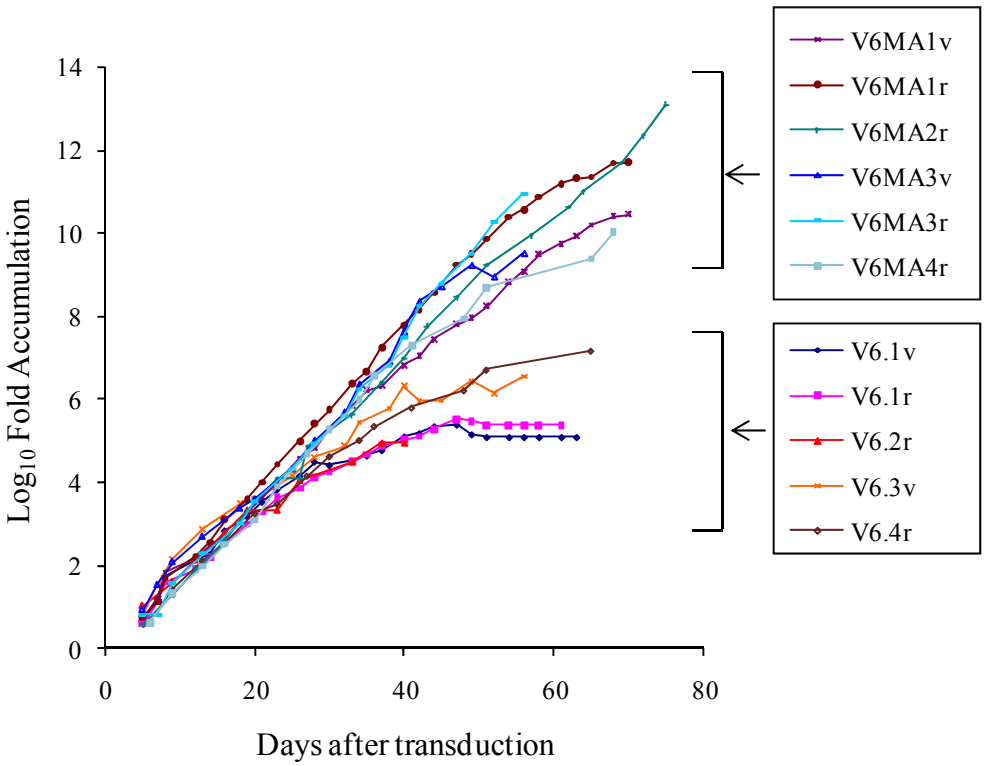

Figure 3.8. Accumulation of V6MA cells *in vitro*

The plot shows the accumulation in CB cell number following transduction with V6 virus coated with VSV-G envelope (V6.1v, V6.3v), V6MA virus coated VSV-G envelope (V6MA1v, V6MA3v), V6 virus coated with RD114TR envelope (V6.1r, V6.2r, V6.4r) and V6MA virus coated with RD114TR envelope (V6MA1r, V6MA2r, V6MA3r, V6MA4r). The numbers after V6 and V6MA represent the CB sample (1-4) used in each transduction. All the cultures were started at a density of $0.5x10^6$ cells per ml.

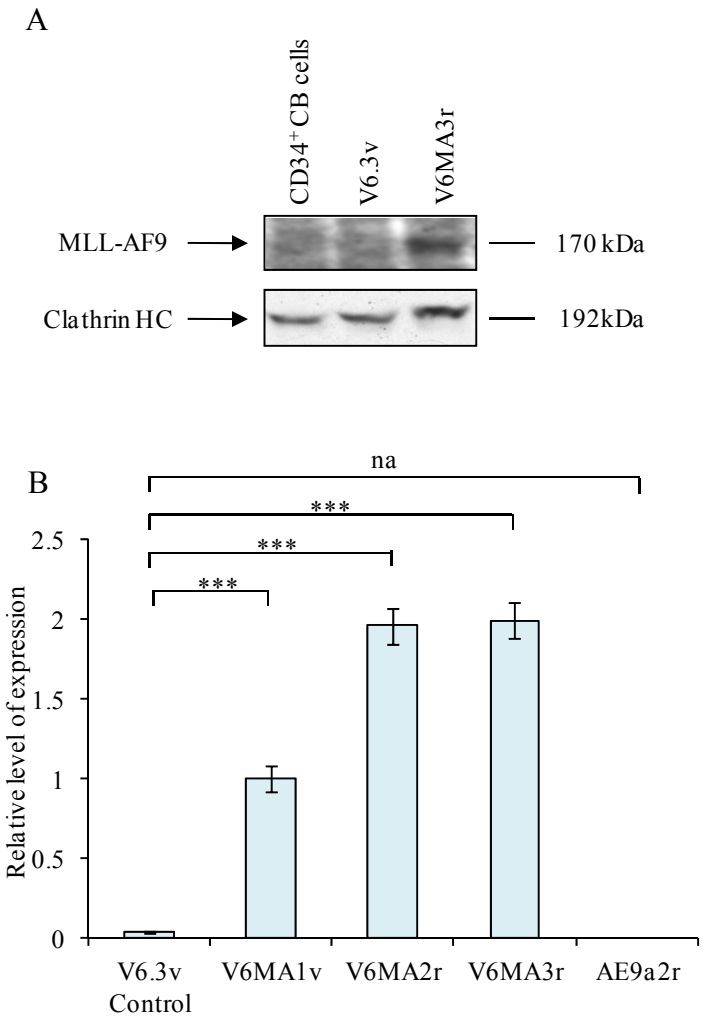

Figure 3.9. Validation of MLL-AF9 mRNA and protein expression in V6MA cells

A) The figure shows western blot analysis of total lysates from human $CD34^+$ CB cells, V6.3v and V6MA3r cells. A mouse anti-human MLLN4.4 antibody and sheep anti-mouse IgG HRP were used as primary and secondary antibodies to probe the western blot. An anti Clathrin-HC antibody was used to control for protein loading. V6.3 and V6MA3r cells were in culture for 14 and 59 days respectively. The same trend of protein expression was observed in all other V6MA cells. B) The bar graphs show the relative levels of MLL-AF9 mRNA expression, measured by QPCR in V6, V6MAs and AE9A cells. Values for each cell line were normalised to the expression in V6MA1v cells. Columns represent the mean of quadruplicate measurements and the error bars represent the SD. *P*-values were calculated using Student's paired t-test. (***) $P \leq 0.001$, (na) not applicable. V6.3v, V6MA1v, V6MA2r and V6MA3r were in culture for 57, 105, 100 and 57 days respectively. This experiment was carried out once.

Next, we validated the mRNA expression of *MLL-AF9* in V6MA cells. *MLL-AF9* mRNA expression was measured using QPCR primers and a probe designed to span the breakpoint of the *MLL-AF9* fusion, in V6.3, V6MA1v, V6MA2r, V6MA34 and AE9a2r cells. Figure 3.9B shows the mRNA expression of *MLL-AF9* in the V6MA cells. Values for each cell line were normalised to the expression in V6MA1v cells. Negligible and no expression of *MLL-AF9* was observed in V6.3v and AE9a2r cells, respectively, while significant *MLL-AF9* expression was observed in all the V6AMA cells analysed. Taken together, these data demonstrate the expression of MLL-AF9 at both the protein and mRNA levels.

3.9. Validation of MLL-AF9 target genes in V6MA cells

Next, we measured the expression of known MLL-AF9 down-stream target genes in the V6MA cells. *HOXA9* and *MEIS1* are two of the best characterised down-stream target genes of MLL-AF9 (Ayton and Cleary, 2003; Zeisig et al., 2004; Horton et al., 2005; Hess et al., 2006; Wong et al., 2007; Faber et al., 2009; Kumar et al., 2009; Somervaille and Cleary, 2010). Therefore, V6, V6MA and AE9a cells were harvested to measure *HOXA9* and *MEIS1* expression by QPCR analysis (Figure 3.10A and B). Expression of both *HOXA9* and *MEIS1* was significantly higher in all of the V6MA cells, compared to that in V6 or AE9a2r cells.

We then measured the expression of other down-stream targets of MLL-AF9, the *MYB* and *MYC* genes.

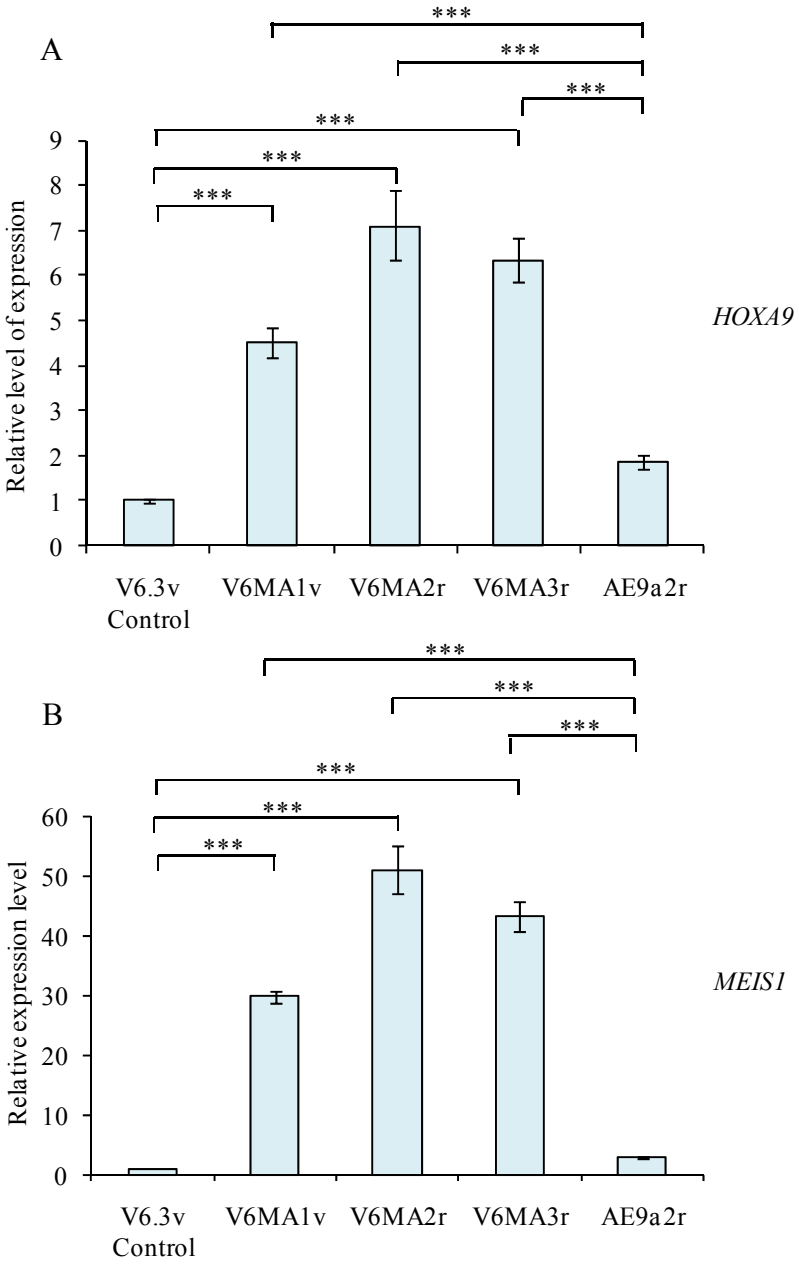

Figure 3.10. HOXA9 and MEIS1 mRNA expression are up-regulated in V6MA cells

The bar graphs show the relative level of A) *HOXA9* and B) *MEIS1* mRNA expression, measured by QPCR in V6, V6MAs and AE9a cells. Values for each cell line were normalised to the expression in V6 cells. Columns represent the mean of quadruplicate measurements and the error bars represent the SD. *P*-values were calculated using Student's paired t-test. (***) $P \leq 0.001$. V6.3v, V6MA1v, V6MA2r and V6MA3r were in culture for 57, 105, 100 and 57 days respectively. These experiments were carried out once.

Their expression has also been found to be increased in the presence of MLL-fusions in conditionally immortalised mouse cells in previous work from our group. In addition, Hess *et al* demonstrated the importance of *c-myb* as a down-stream target gene of HOXA9 and MEIS1 (Hess et al., 2006). Protein and mRNA expression of MYB were analysed in V6MA cells by western blot and QPCR respectively (Figure 3.11A and B). Significantly higher expression of MYB protein and *MYB* mRNA was observed in V6MA cells, compared to that in $CD34^+$ CB cells and V6 cells. A similar expression pattern of *MYC* mRNA was also observed in V6MA cells (Figure 3.11C).

3.10. Immunophenotypic and morphological characterisation of V6MA cells

The immunophenotypes of V6MA cells were also determined (Figure 3.12A). A panel of differentiation associated markers was selected to determine at what stage in myelopoiesis the V6MA cells were positioned. V6 cells and V6MA cells generated with different envelope constructs (VSV-G and RD114TR) were stained and analysed by flow cytometry. The data shows that most of the V6MA population consisted of $CD34^-$ and $CD33^+$ cells, with heterogeneous CD38 expression. In addition, more than half of the cells within each V6MA cell line expressed the CD11b and CD14 surface markers. Interestingly, the percentage expression of the CD15 marker was found to be higher in $CD34^+$ CB cells transduced with V6MA (RD114TR), than those transduced with V6MA (VSV-G). CD15 is initially expressed on GMPs and early monoblasts, as well as throughout granulocyte maturation. In addition, increases in CD15 expression were observed over time in liquid cultures of V6MA1v, V6MA1r, V6MA2r and V6MA3v cells.

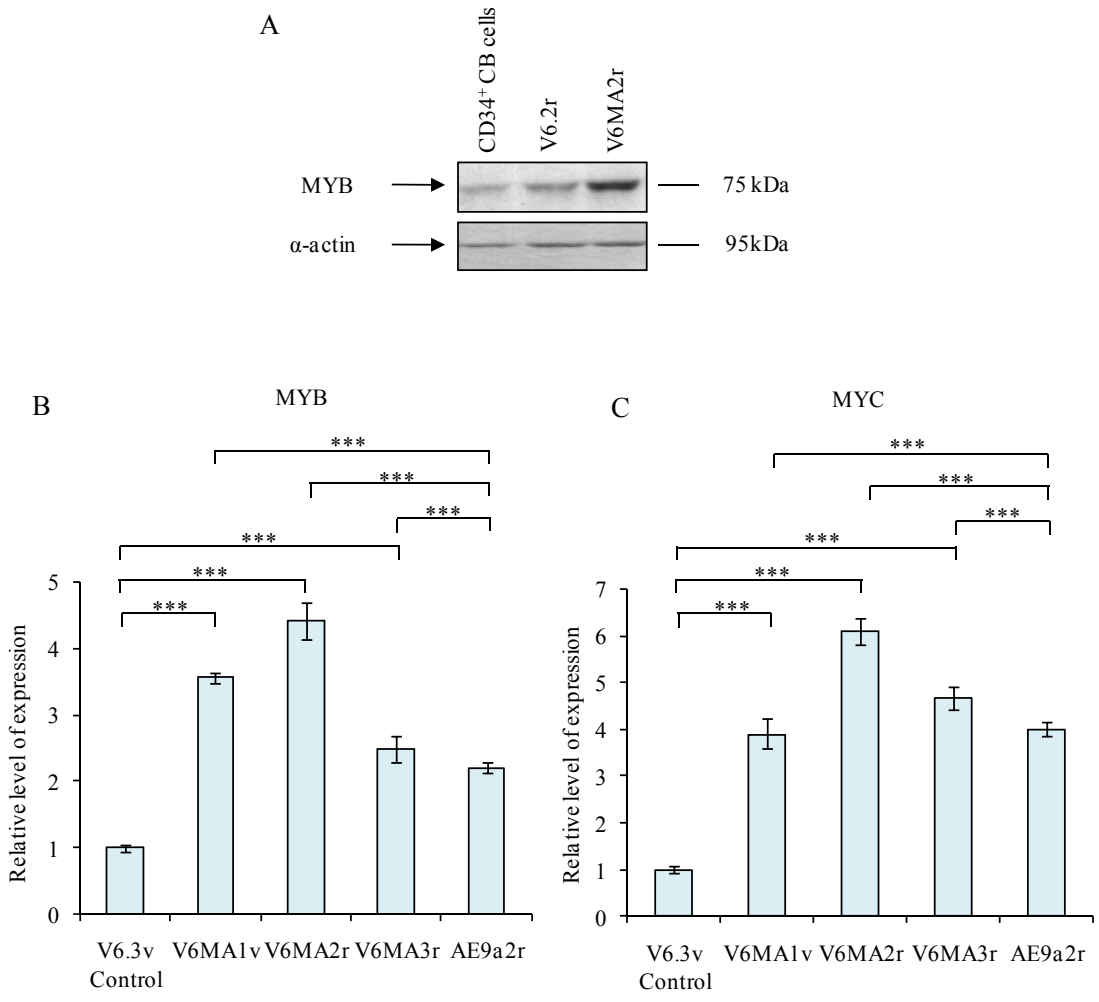

Figure 3.11. MYB and MYC expression are up-regulated in V6MA cells

A) The figure shows a western blot analysis of total lysates from human $CD34^+$ CB cells, V6.2r and V6MA2r cells. The western blot was probed with a primary rabbit polyclonal anti-MYB antibody and a secondary goat anti-rabbit IgG HRP. An anti-α-actin antibody was used to control for protein loading. V6.2r and V6MA2r were in culture for 38 days. The bar graphs show the relative levels of B) *MYB* and C) *MYC* mRNA expression, measured by QPCR in V6, V6MAs and AE9A cells. Values for each cell line was normalised to the expression in V6 cells. Columns represent the mean of quadruplicate measurements and the error bars represent the SD. V6.3v, V6MA1v, V6MA2r and V6MA3r were in culture for 57, 105, 100 and 57 days respectively. *P*-values were calculated using Student's paired t-test. (***) $P \leq 0.001$. These experiments were carried once.

A

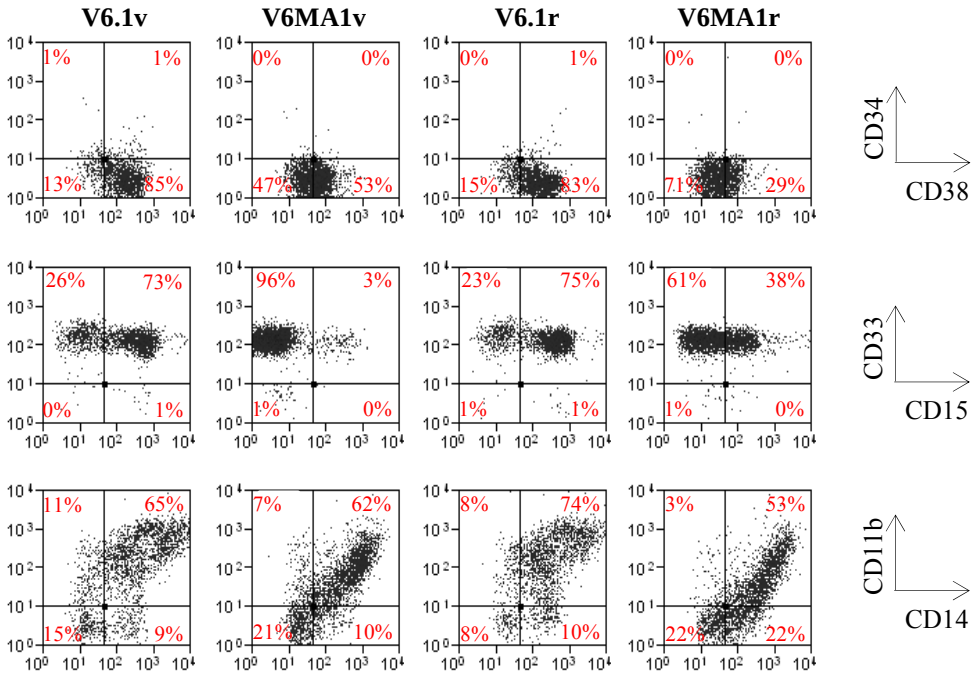

B

Figure 3.12. Immuno and morphological phenotypes of transduced human CB cells

A) The dot plots show flow cytometric analysis of lentivirally transduced CB cells (V6.1 and V6MA1) after 40 days of culture. CD34 and CD38, CD33 and CD15 and CD11b and CD14. Numbers in dot plots represent the percentage of cells within each quadrant. Similar patterns of respective expression were observed in all other V6MA cells. B) Pictures of cytospins (magnification of x100) of V6MA2r, V6MA3r and V6MA4r cells.

The V6MA cells (V6MA2r, V6MA3r and V6MA4r) were also subjected to cytospin and morphological analysis (Figure 3.12B). The data showed that the majority of cells within each V6MA line had a myeloblast morphology.

3.11. Xenotransplantation

Xenotransplantation was then performed in order to establish whether the immortalised V6MA cells were capable of inducing leukaemia. NOD.Cg-Prkdc^{scid} Il2rg^{tm1Wjl}/SzJ mice (commonly known as NOD scid gamma or NSG), deficient in T, B and NK cells and cytokine signalling were used as recipients for transplantation. Sub-lethally irradiated (3.5 Gy) NSG mice were injected with 1-10x10^6 V6MA cells and recipients were monitored for signs of disease (Figure 3.13A). V6MA2r, V6MA3r and V6MA4r cell lines induced AML with a latency of between 51 to 84 days (Figure 3.13B). The leukaemic phenotype of the induced human AML was confirmed by flow cytometric analysis (Figure 3.14).

3.12. Discussion

Modelling myeloid leukaemia using human haematopoietic progenitor cells started approximately 12 years ago and several fusion genes associated with leukaemia were used to generate human immortalised cells [reviewed in (Mulloy et al., 2008)].

A

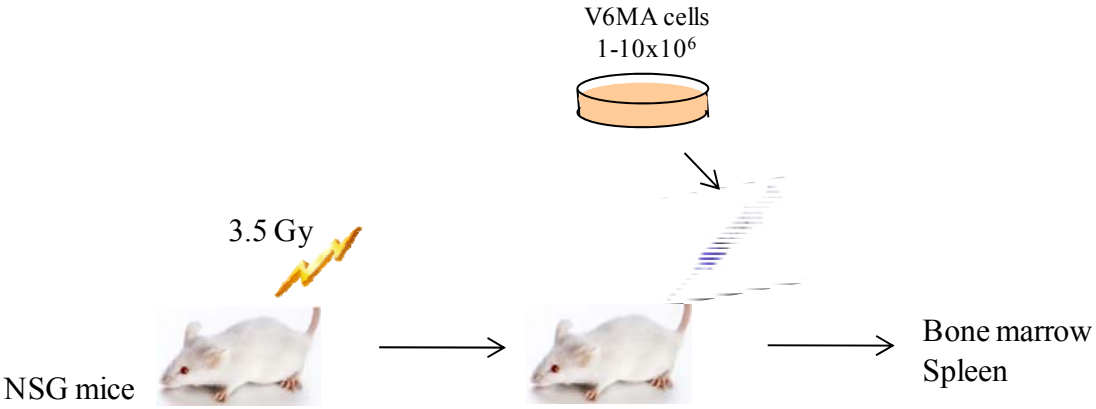

B

Cell line	*In vitro* cultured time (days)	Cell number injected (10^6)	AML latency (days)
V6MA2R	31	10	61
V6MA2R	77	10	-*
V6MA3R	162	10	84
V6MA3R	162	10	63
V6MA4R	48	10	-
V6MA4R	48	1	-
V6MA4R	29	10	51

Figure 3.13. Xenotransplantation of V6MA cells

A) The diagram illustrates the *in vivo* transplantation of V6MA cells. NSG mice were sub-lethally irradiated (3.5Gy) one day before transplantation. V6MA cells were injected and recipients were monitored for signs of disease. B) The table represents a list of transplantations performed in this study. *-: no AML was detected more than 6 months after transplantation

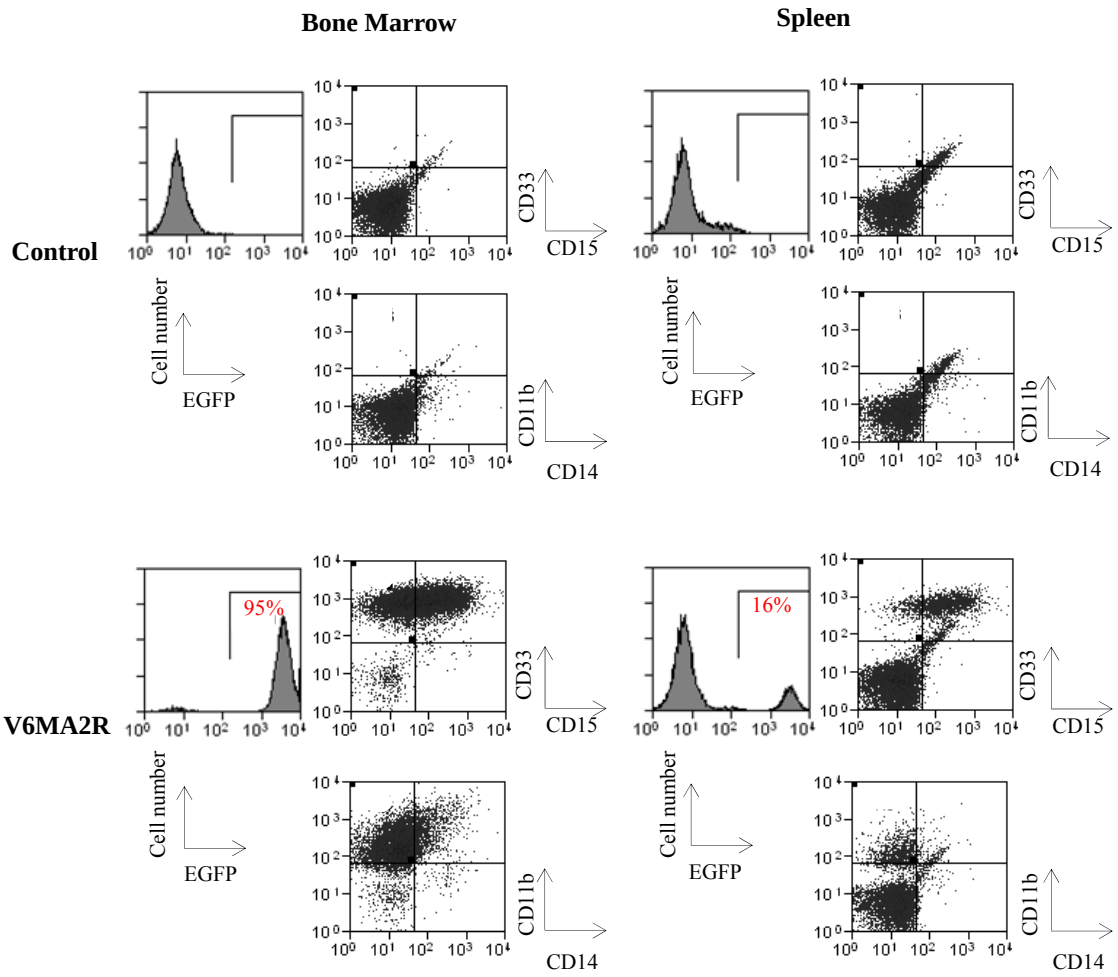

Figure 3.14. Engraftment of V6MA cells in NSG mice

The flow cytometric analysis shows NSG mouse (control) or NSG mice injected with V6MA2R cells (V6MA2R) and scarified 61 days later. The histograms show the percentage of EGFP positive cells in bone marrow and spleen of the NSG mice. The dot plots show flow cytometric analysis of CD15 /CD33, and CD11b/CD14 expression. Similar patterns of respective expression were observed in four other mice that were sacrificed due to leukaemic symptoms.

However, although a number of groups generated murine models of MLL-fusions-associated leukaemia, there are still relatively few reports of human haematopoietic cells immortalized by MLL-fusions (Lavau et al., 1997; Slany et al., 1998; Zeisig et al., 2003; Horton et al., 2005; Krivtsov et al., 2006; Somervaille and Cleary, 2006; Barabe et al., 2007; Wei et al., 2008). Barabe *et al* and Wei *et al* both generated immortalized human cells by transducing human CB cells with retroviral vectors expressing MLL-AF9 (Barabe et al., 2007; Wei et al., 2008). Barabe *et al* used the ultracentrifugation method to concentrate the retroviral supernatant containing MLL-AF9 and then performed four serial transductions of lineage negative CB cells, at 12 hours intervals (Barabe et al., 2007). In addition, this study also used the VSV-G envelope. They cultured MLL-AF9 immortalised CB cells in myeloid conditions, using SCF and IL-3. The MLL-AF9 CB cells in this study only proliferated for approximately 125 days in liquid culture. Our data are consistent with Barabe *et al*, in that, although MLL-AF9 transduced CB cells proliferated exponentially over the period analysed, the proliferation eventually slowed down and ceased (data not shown). In contrast, Wei *et al* successfully managed to culture the transduced cells indefinitely (Wei et al., 2008). Their CB-derived MLL-AF9 cells were cultured for two years or longer and no phenotypic changes were observed during this period (Mulloy et al., 2008; Wei et al., 2008). In their approach, the retroviral supernatant containing MLL-AF9 was eight-times concentrated and $CD34^+$ CB cells were transduced using retronectin. In addition, the RD114 envelope was used. The transduced CB cells were cultured with SCF, TPO, FLT3L, IL-3 and IL-6. Mulloy *et al* later explained that inclusion of FLT3L in the culture of the transduced CB cells was crucial in the immortalisation process (Mulloy et al., 2008). Although we cultured the CB derived MLL-AF9 cells in the same conditions as Wei *et al*, including FLT3L, our cells did not proliferate indefinitely. Further experiments revealed that only around a third of the human CB samples tested could be

immortalised by MLL-AF9 (Mulloy et al., 2008). This indicates that the difference in CB cell immortalisation by MLL-AF9 in these and our studies may not be completely explained by the growth factors used in each case.

In our study, virus coated with the RD114 envelope was shown to give higher viral titre on CB cells than virus coated with the VSV-G envelope. The VSV-G envelope is believed to interact with host cells via binding to clathrin (Sun et al., 2005; Roche et al., 2008; Cureton et al., 2009). Viral entry is then mediated via the pH-dependent endocytotic pathway (Roche et al., 2008). On the other hand, the RD114 envelope specifically interacts with the RD114 receptors, which are particularly abundant on $CD34^{+}CD38^{-}$ human cells (Di Nunzio et al., 2007). A number of studies have shown that the RD114 envelope gives more efficient $CD34^{+}$ CB cell transduction than the VSV-G envelope (Kelly et al., 2000; Sandrin et al., 2002; Strang et al., 2004). This is consistent with our experiments. It was interesting to observe that transduction of CB cells using the VSV-G envelope increased CD38 expression. Increase in CD38 expression is associated with differentiation (Terstappen et al., 1991). Since the self-renewing capacity of human haematopoietic cells resides within the $CD34^{+}CD38^{-}$ fraction of the CB sample, we decided to use the RD114 envelope construct in subsequent experiments. There is no report in the literature demonstrating that the VSV-G envelope induces CD38 expression or differentiation in human haematopoietic cells. However, it has been reported that human $CD34^{+}CD38^{+}$ cells were more efficiently transduced with retrovirus coated with VSV-G envelope than were $CD34^{+}$ $CD38^{-}$ cells (von Laer et al., 2000). Therefore, it is possible that the $CD34^{+}$ $CD38^{+}$ cells were preferentially transduced by retrovirus coated with VSV-G in our study.

In our study, $CD34^+$ CB cells were successfully immortalised by lentiviral transduction. It is not clear why $CD34^+$ CB cells were not immortalized by retroviral transduction in our experiments. It is possible that the quality of the cord blood may influence the outcome of retroviral transduction. Thus, frozen cord blood was used in our study, while fresh cord blood was used in the previously published studies. Another possible reason for the greater efficiency of lentiviral transduction in comparison to retroviral transduction is the ability of lentiviruses to integrate into non-dividing cells. Furthermore, lentiviruses can package inserts of up to 10 kb in size, which is considerably larger than retroviruses (Walther and Stein, 2000). An increase in EGFP expressing transduced CB cells, as well as an increase in EGFP intensity over time (Figure 3.7), suggested that immortalised CB cells were outgrowing the cultures due to the expression of MLL-AF9. In addition, the initial intensity of EGFP expression was higher in the CB cells transduced with V6MA (RD114TR) than those transduced with V6MA (VSV-G) (Figure 3.7). This indicates that RD114TR was more efficient at transducing the CB cells, leading to higher numbers of proviral intergrations. In contrast, although EGFP expression in $CD34^+$ CB cells transduced with V6MA (RD114) was higher than those transduced with V6MA (VSV-G), it was lower in control V6(RD114) than V6(VSV-G) transductions. Despite these differences in transduction efficiency, immortalised MLL-AF9 expressions cells were generated with both RD114 and VSV-G coated lentiviral particles.

Detection of MLL-AF9 protein and mRNA expression in V6MA cells confirmed that they did indeed express the fusion. Variation in the level of MLL-AF9 detected in V6MA cells may be explained by heterogeneous genotypes of the different human CB, differences in the developmental stage of the transduced cells and/or the viral titres

achieved in each of the transductions. MLL-AF9 expression by the CB cells was found to result in up-regulation of *HOXA9, MEIS1, MYB* and *MYC* mRNA expression. Several studies using murine MLL-fusion models suggest that *Hoxa9* and *Meis1* are major target genes of MLL fusions (Ayton and Cleary, 2001; Zeisig et al., 2004; Horton et al., 2005; Wong et al., 2007; Faber et al., 2009; Kumar et al., 2009). Indeed, *Hoxa9* and *Meis1* are both up-regulated in MLL-AF9 and MLL-ENL transformed cells, yet they are down-regulated in mature cells such as neutrophils (Milne et al., 2005). A key study performed by Zeisig *et al* used murine inducible cells in which MLL-ENL expression was induced by 4-hydroxy-tamoxifen (4-OHT). The group showed, using this model and microarray analysis, that *Hoxa9* and *Meis1* are crucial down-stream targets of MLL-ENL (Zeisig et al., 2004). Furthermore, our laboratory has previously demonstrated that *Hoxa* gene expression is reduced upon loss of MLL-ENL, but not upon differentiation induced by granulocyte colony-stimulating factor (G-CSF). This work demonstrated that *Hoxa* genes are targets of MLL-ENL (Horton et al., 2005). In the human model, *HOXA9* up-regulation was also found by Wei *et al,* although mRNA was only increased by two-fold in comparison to control cells (Wei et al., 2008).

The up-regulation of MYB protein and mRNA in V6MA cells in our study is in agreement with previously published data from Hess *et al* (Hess et al., 2006). In this study, *c-Myb* was demonstrated to be a down-steam target gene of HOXA9 and MEIS1, which in turn were regulated by the conditionally expressed MLL-ENL (Hess et al., 2006). Although *c-Myb* itself was not sufficient to cause transformation, it was found to be necessary for MLL-ENL-mediated transformation (Hess et al., 2006). Similar up-regulation was seen with *MYC* mRNA expression in V6MA cells. These data are consistent with a previous study, showing that *c-Myc* expression is required for the

differentiation block imposed my MLL-ENL (Schreiner et al., 2001). In summary, we confirmed that previously published MLL-fusion target genes were also up-regulated in the human system.

Various combinations of antibodies were used to determine the differentiation block in V6MA cells. Our flow cytometric analyses showed that V6MA cells express high levels of CD33 and CD14, and were heterogeneous for CD11b, CD15 and CD38 expression. Immunophenotypic characterisation of CB-derived MLL-AF9 cells was also performed by Wei et al (Wei et al., 2008). Interestingly, this study used two different MLL-AF9 expression constructs, and slightly different immunophyenotypes were observed depending on the construct used. The pREW-MLL-AF9 vector used the pREW 5'LTR retroviral promoter to drive expression of EGFP followed by MLL-AF9, with 2A peptide links between the two cDNAs. The pMSCV-MLL-AF9 vector used the pMSCV 5'LTR retroviral promoter to drive the expression of MLL-AF9, while the PGK promoter was used to drive the expression of the puromycin resistance gene. The immunophentype of our V6MA cells resembles that of MLL-AF9 cells generated using the pREW-MLL-AF9 expression construct (Wei et al., 2008). The FUGW vector used in the present study also employs an EGFP expression cassette, similar to the pREW-MLL-AF9 vector used in Wei *et al* (Wei et al., 2008). It is possible that puromycin selection, used in the pMSCV-MA transduced cells, may have selected for a highly transduced population, compared to our strategy, which relied on monitoring outgrowth of immortalised V6MA cells by examining EGFP expression. For this reason, our cultures may have contained more heterogeneous populations than the pMSCV-MA transduced cells from Wei *et al.* Furthermore, the MLL-AF9 cDNA sequence used in

our study differs from both of the sequences used in Wei *et al* (Wei et al., 2008), which may also reflect the difference in immunophenotypes between the two studies.

It was interesting to note that CD15 expression was higher in the V6MA (RD114TR) cells, than in the V6MA (VSV-G) cells (Figure 3.12A). CD15 expression is up-regulated after the GMP stage of myeloid development, and its expression remains up-regulated throughout the maturation of granulocytes, while it is lost during monocyte maturation (Figure 1.3). This suggests that the V6MA (RD114TR) transduced cells were more mature than the V6MA (VSV-G) cells. However, it is also possible that the latter culture contained more mature monocytes. In addition, we observed an increase in CD15 expression over time in the liquid cultures (data not shown). Since V6MA cells do not proliferate indefinitely, CD15 expression may inversely correlate with the proliferation capacity of V6MA cells. However, how CD15 expression is related to proliferation is not clear. Further phenotypic characterisation will have to be performed to clarify these possibilities.

Xenotransplantation experiments confirmed that CB-derived V6MA cells have the potential to induce leukaemia *in vivo*. Upon injection of 1 x10^7 V6MA cells, not all of the NSG mice came down with leukaemia in our experiments. These data are in agreement with Wei et al (Wei et al., 2008). Despite the identical phenotypes and morphology of the different lines used, this study found variation in induction of leukaemia *in vivo*, depending on which immortalised MLL-AF9 line was used (Mulloy et al., 2008). It is known that not all AML patient samples, including 11q23 rearranged AML, engraft upon xenotransplantation (Pearce et al., 2006). The similarity in leukaemia induction between our study and that of Wei *et al*, suggests that the capacity

of the MLL-AF9 immortalised cells to proliferate indefinitely *in vitro* may not correlate with their ability to cause AML. These results illustrate the complexity of interpreting experiments using heterogeneous human CB samples, in comparison to murine model experiments with haematopoietic cells from inbred strains of mice. Nevertheless, some NSG mice did develop leukaemia upon transplantation with V6MA cells. The technical challenges involved in the culture of human primary AML patient samples, make the use of CB-derived V6MA cells an attractive alternative in the analysis of MLL-AF9 function in human cells.

CHAPTER 4. RESULTS – Approaches to gene knock-down in human leukaemia cells

4.1. Introduction

Human leukaemic cell lines are valuable models for cancer research. Derived from patient samples under appropriate conditions, these cell lines can be maintained in culture for extensive periods of time. We have successfully generated MLL-AF9 immortalised human CB-derived (V6MA) cells in the previous chapter. Since these cells are immortalised by expression of MLL-AF9 in the absence of any other genetic mutations, they are invaluable in studying the function of this fusion in leukaemia. They also allow us to validate information, gained from mouse cell experiments, in human leukaemia models. However, these cells are growth factor dependent, do not proliferate indefinitely and are less robust than leukaemia cell lines. In order to test and develop different strategies to knock-down gene expression, we decided to use leukaemic cell lines. Therefore in this chapter, we planned to characterise and study a panel of human leukaemic cells prior to using them as a human model. As a first step in analysing MLL-fusion function in human cells, we tested various human leukaemic cell lines containing endogenous MLL-rearrangements. Before we could use the cell lines in this way, it was important to verify that they indeed expressed the respective MLL-fusions. Following confirmation of this, we planned to knock-down the expression of MLL-fusions, to observe the dependence of the cell lines on these oncogenes. We first employed the siRNA to produce knock-down of gene expression, as this technique was previously optimised in our laboratory. This would then allow us to study the roles of

MLL-fusion target genes in leukaemogenesis in human leukaemic cells and to extend these studies to the CB-derived MLL-AF9 immortalised cells.

4.2. Detection of MLL-fusion expression

A list of human leukaemic cells used for this study is shown in Table 4.1. Several human leukaemic cell lines containing chromosomal translocations involving the *MLL* gene were tested for the expression of the appropriate MLL-fusion protein using a monoclonal antibody directed against the N-terminus of MLL (common to all the fusions) (Figure 4.1A and B). Murine MLL-AF9 myeloid cells generated previously in our lab were used as a positive control for MLL-fusion expression, and α-tubulin and clathrin HC protein expression was measured as a loading control. We also used several human leukaemic cells such as KCL-22, OCI-AML3, YCUB-2 and KASUMI-1 that are not associated with MLL-fusions, as negative controls. Bands corresponding to MLL-fusions were detected in most of the appropriate cells, such as the 360kDa band corresponding to MLL-AF6, the 240kDa band corresponding to MLL-AF4, and the 170kDa band corresponding to MLL-AF9, except KOPN-8 cells. KOPN-8 cells are described as being derived from a patient with the MLL-ENL fusion (Drexler et al., 2004). However, a 220kDa band corresponding to this fusion protein was not detected in our experiments. In addition, the 320kDa band corresponding to the N-terminal MLL fragment was also observed in most of the human leukaemic cells. The clearest band corresponding to MLL-AF9 was observed in THP-1 cells. For this reason, we decided to primarily use THP-1 cells to study MLL-AF9-associated leukaemia.

Cell line	Fusion protein	Type of leukaemia
THP-1	MLL-AF9	human acute monocytic leukemia
NOMO-1	MLL-AF9	human acute myeloid leukemia
SHI-1	MLL-AF6	human acute myelocytic leukemia
MOLM-13	MLL-AF9	human acute myeloid leukemia
MONO-MAC-6	MLL-AF9	human acute monocytic leukemia
MV4-11	MLL-AF4	human acute monocytic leukemia
KCL-22	BCR-ABL	human chronic myeloid leukemia in blast crisis
OCI-AML3	NPM mutated	human acute myeloid leukemia
KASUMI-1	AML1-ETO	human acute myeloid leukemia
KOPN-8	MLL-ENL	human B cell precursor acute lymphoblastic leukemia
SEMK-2	MLL-AF4	human acute lymphoblastic leukemia
YCUB-2	E2A-HLF	human B-lineage acute lymphoblastic leukemia

Table 4.1. A panel of human leukaemic cell lines used in this study

The list shows a panel of human leumaemic cell lines used in this study. *DSMZ* - the German Resource Centre for Biological Material, was used as a source for most of the cell lines and a source for this information (www.dsmz.de).

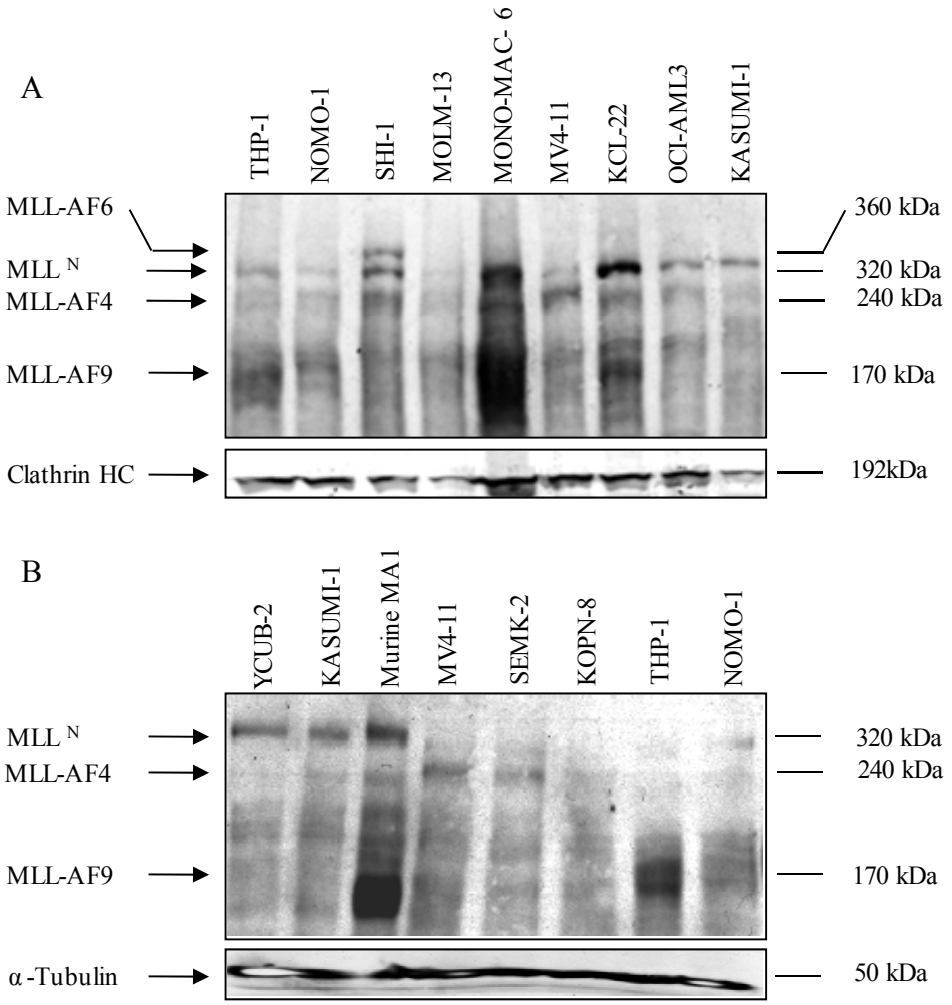

Figure 4.1. Human leukaemic cells express their MLL-fusion proteins

Figures A and B show western blot analyses of total lysates from human leukaemic cell lines. Mouse anti-human MLL-N4.4 antibody and sheep anti-mouse IgG HRP were used for primary and secondary antibodies to probe the western blot. Total lysates from YCUB-2, KCL-22, OCI-AML3 and KASUMI-1 cells were used as negative controls, and murine cells expressing MLL-AF9 were used as a positive control (kindly provided by Dr Vanessa Walf-Vorderwülbecke). Anti-α tubulin and anti-Clathrin HC antibody were used to control for protein loading. MLLN, the N-terminal MLL fragment.

Since most of the human leukaemic cells did indeed express their respective MLL-fusions, mRNA expression of known target genes was then examined (Figure 4.2). mRNA expression of *HOXA9* and *MEIS1* was analysed first, due to the importance of these target genes to MLL-fusion function (see chapter 3.9). All the human leukaemic cells expressed *HOXA9* and *MEIS1* apart from THP-1 cells, in which only a very low level of *MEIS1* expression was detected, when compared to that of other MLL-associated leukaemic cells. *HOXA9* and *MEIS1* expression was undetectable in YCUB-2 cells and was negligible in KASUMI-1 cells. In addition, the highest expression of *HOXA9* and *MEIS1* was observed in NOMO-1 cells. Moreover, despite undetectable MLL-ENL protein expression, *HOXA9* and *MEIS1* expression was also detectable in KOPN-8 cells.

In order to further characterise THP-1 cells, their immunophenotype was then analysed. Surface antigen expression by THP-1 cells is documented in the literature (Pession et al., 2003). In order to compare the differentiation state of THP-1 cells to that of V6MA cells, we used the same maturation markers as used in Chapter 3, namely CD11b, CD14, CD15, CD33, CD34 and CD38 (Figure 4.3). Flow cytometric analysis showed that THP-1 cells expressed high levels of CD15 and CD38, were heterogeneous for CD11b expression, and had no or very low expression of CD34 and CD14.

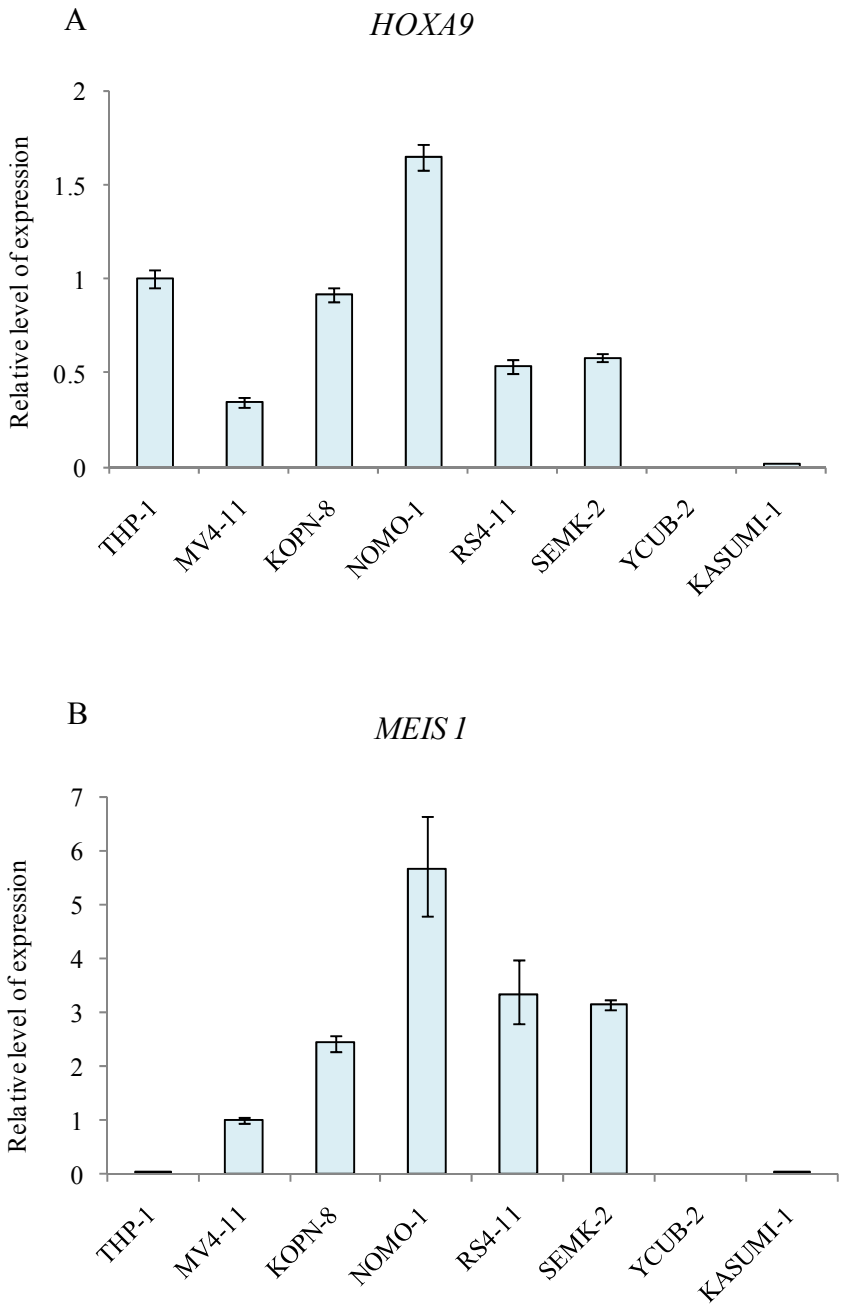

Figure 4.2. mRNA expression of HOXA9 and MEIS1 in human leukaemic cells

The bar graphs show the relative levels of A) *HOXA9* and B) *MEIS1* mRNA expression, measured by QPCR in human leukaemic cells. Values for each cell line were normalised to the expression in A) THP-1 cells B) MV4-11 cells. Columns represent the mean of quadruplicate measurements and the error bars represent the SD. A similar pattern of expression was observed in one independent experiment. The same trend was observed in one other experiment.

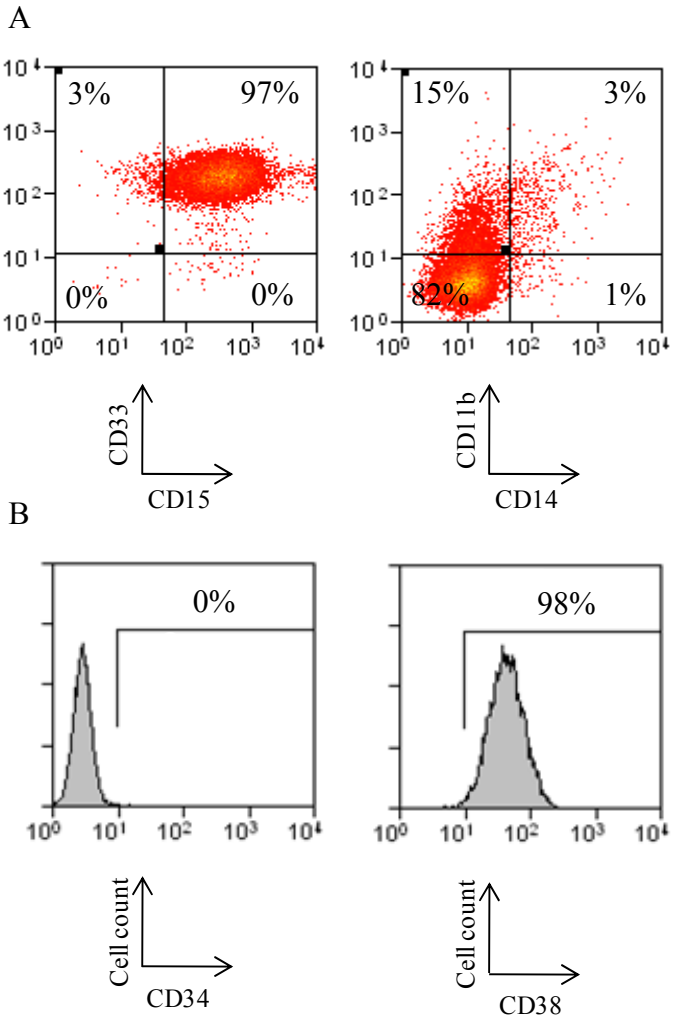

Figure 4.3. Imunophenotype of THP-1 cells

A) Dot plots show flow cytometric analysis of THP-1 cells with antibodies against CD33 and CD15 (left panel), and CD11b and CD14 (right panel). Numbers below dot plots represent the percentage of cells within each quadrant. B) Histograms show flow cytometric analysis of THP-1 cells with antibodies against CD34 (left) and CD38 (right). Numbers within the histograms represent the percentage of cells within each gate. Similar patterns of CD33, CD15, CD11b and CD14 expression were observed in at least three other experiments.

4.3. Optimisation of siRNA delivery

To determine whether the human leukaemic cell lines were dependent on MLL-fusions for survival and proliferation, we decided to knock down the expression of the relevant MLL-fusion using small interfering RNA (siRNA). siRNAs are incorporated into an RNA-induced silencing complex (RISC), which unwinds and cleaves target mRNA, causing the silencing of the target gene (Dykxhoorn et al., 2003; Mittal, 2004). siRNA was delivered by electroporation in our study. Initially, we used siGLO Red to measure how efficiently siRNA was delivered, using the pulse generator EPI 2500 electroporator (Heidelberg, Germany). siGLO Red is a double stranded RNA that is chemically labelled with fluorophores and serves as a transfection indicator. We electroporated THP-1, MV4-11, SEMK-2 and YCUB-2 cells, and the expression of siGLO Red was monitored after 72 hours by flow cytometry (Figure 4.4). All electroporated cell lines showed an increase in the expression of siGLO Red, except YCUB-2 cells. The data indicates that despite the variation in efficiency between human leukaemic cells, siRNA can be delivered efficiently using the pulse generator EPI 2500 electroporator.

Prior to knocking down MLL-fusion expression in human leukaemic cells, we used a positive control siRNA to ensure that it was possible to knock down gene expression in these cells. For this experiment, a pool of four siRNAs targeting *GAPDH* was used as a positive control. This mixture of four validated siRNAs against *GAPDH*, purchased from Dharamcon (Thermo Fisher Scientific Leicestershire, UK), was designed to perform more efficient knock-down than a single siRNA.

Figure 4.4. siRNA transfer using electroporation

A) A schematic diagram illustrates the electroporation process to deliver siRNA used in this study. $3x10^6$ human leukaemic cells were transferred into a cuvette with 100nM siRNA or 500nM siGLO Red. The cells were then electroporated at various voltages, ranging from 330-900V for 10ms. The cells were harvested for flow cytometric analysis 72 hours later. B) Histograms show flow cytometric analysis of human leukaemic cells before (grey-filled areas) and after (solid lines) siGLO Red delivery using electroporation. Numbers in the histograms indicate the percentage of siGLO Red expressing human leukaemic cells. Human leukaemic cells were electroporated at 330V for 10ms with siGLO Red (500nM). The cells were analysed 72 hours later. The experiment was repeated one other time with THP-1, MV4-11 and KASUMI-1 cells and expression of siGLO Red was confirmed using florescence microscopy.

A

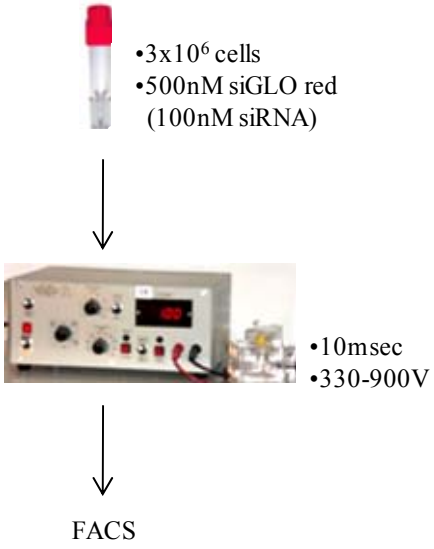
•3x10^6 cells
•500nM siGLO red
(100nM siRNA)
•10msec
•330-900V
FACS

B

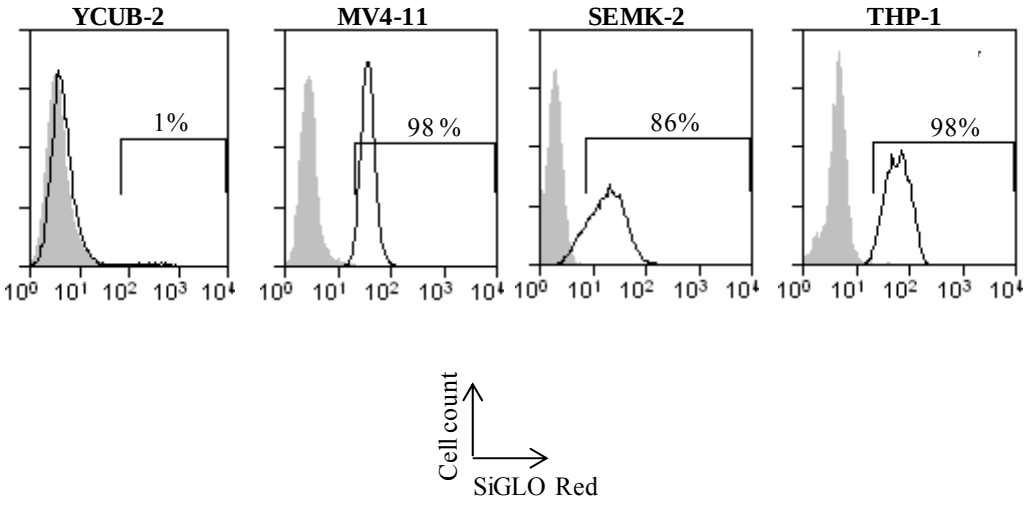
YCUB-2
MV4-11
SEMK-2
THP-1
1%
98 %
86%
98%
Cell count
SiGLO Red

A negative control siRNA used for this experiment was designed to have no homology to mammalian genes, and this was validated by Dharmacon using Affymetrix GeneChip arrays (Thermo Fisher Scientific). THP-1 cells were electroporated with the GAPDH siRNA and harvested 72 hours later. A western blot analysis showed a 36kDa band, corresponding to GAPDH, in THP-1 cells electroporated with negative control siRNA (Figure 4.5A). Electroporation of THP-1 cells with GAPDH siRNA decreased GAPDH protein expression down to 0.2 of the negative control. This result demonstrates that it is possible to knock-down target gene expression using electroporation-delivered siRNA.

We then tested whether any of the MLL-fusion target genes could be knocked down by siRNA. For this experiment, a pool of four validated siRNAs targeting the *MYB* gene was used. THP-1 cells were electroporated in the same way as described above and protein was harvested 72 hours later for western blot analysis (Figure 4.5B). Protein expression of the 72kDa band corresponding to MYB was detected in THP-1 cells transfected with negative control siRNA. Upon electroporation with siRNA against *MYB*, MYB protein expression showed a modest decrease, down to 0.6 of that of the negative control. These results indicate that although it is possible to perform efficient knock-down using siRNA in human leukaemic cells, variation in efficiency occurs, depending on the gene being targeted.

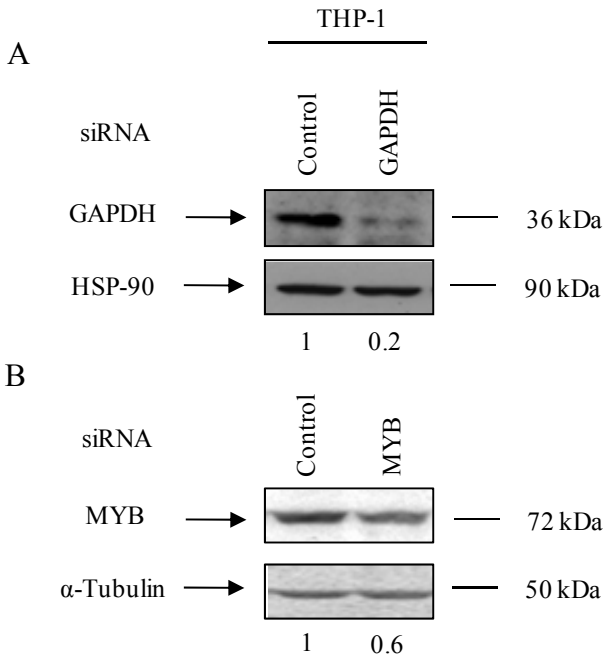

Figure 4.5. GAPDH and MYB knock-down using siRNA

Figures represent western blot analyses of total lysates from electroportated THP-1 cells with siRNA against A) *GAPDH* or B) *MYB*. Cells were electroporated at 330V for 10ms and harvested at 72 hours to make cell lysates. The western blots were probed with a primary goat polyclonal anti-GAPDH or a primary rabbit polyclonal anti-MYB antibody and a secondary donkey anti-goat IgG HRP or a secondary goat anti-rabbit IgG HRP. Anti-HSP90 or anti-αTubulin antibodies were used to control for protein loading. Values for protein expression were normalised to THP-1 cells transfected with control siRNA**.** These experiments were carried out once.

4.4. Knock-down of MLL-fusions by siRNA

To perform knock-down of MLL-fusion expression, we used three siRNAs (MLL siRNA A, MLL siRNA B and MLL siRNA C). These siRNAs target 5' sequences of *MLL* and would therefore be expected to target both the endogenous *MLL* gene and the *MLL*-fusions. The THP-1 cell line was electroporated as described previously and expression of the MLL-AF9 fusion protein was examined after 72 hours (Figure 4.6A). A marked decrease of MLL-fusion protein expression in the THP-1 cells electroporated with MLL siRNA A (down to 0.1) and with MLL siRNA B (down to 0.2), was observed. However, during replicate experiments, we noticed that the efficiency of knock-down varied considerably. This experiment (Figure 4.6A) was repeated seven times and efficient knock-down was achieved three times. The voltage of the electroporation was increased up to 900V to determine whether this would provide more consistent results (Figure 4.6B and Figure 4.6C). Although use of higher voltage of siRNA delivery did achieve efficient knock-down of MLL-AF9 protein expression in THP-1 cells in some experiments (Figure 4.6B), consistent results could not be obtained (Figure 4.6C). Furthermore, there was no consistency in the proliferation of THP-1 cells electroporated with siRNA targeting *MLL* (Figure 4.7). We performed two additional independent experiments with similar results for proliferation. Due to this inconsistency in siRNA mediated knock-down of gene expression, an alternative approach to study the function of MLL-fusions in these cells was undertaken.

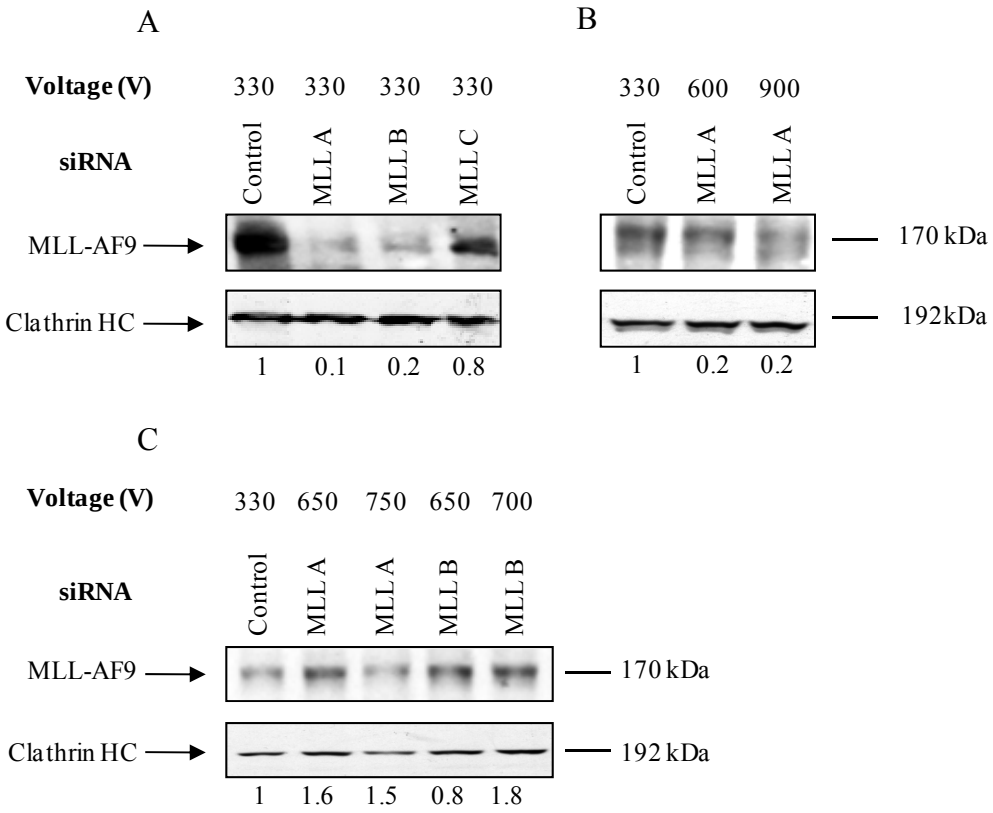

Figure 4.6. Knock-down of MLL-fusion protein expression in THP-1 cells

Figures represent Western blot analyses of total lysates from THP-1 cells electroporated with siRNA. Cells were electroporated in the range of 330V to 900V for 10ms and harvested at 72 hours. Western blots were probed with primary mouse anti-human MLL-N4.4 antibody and secondary sheep-anti mouse IgG HRP. An Anti Clathrin-HC antibody was used to control for protein loading. Values for protein expression were normalised to THP-1 cells electroporated with control siRNA. A)-C) Figures represent three individual experiments.

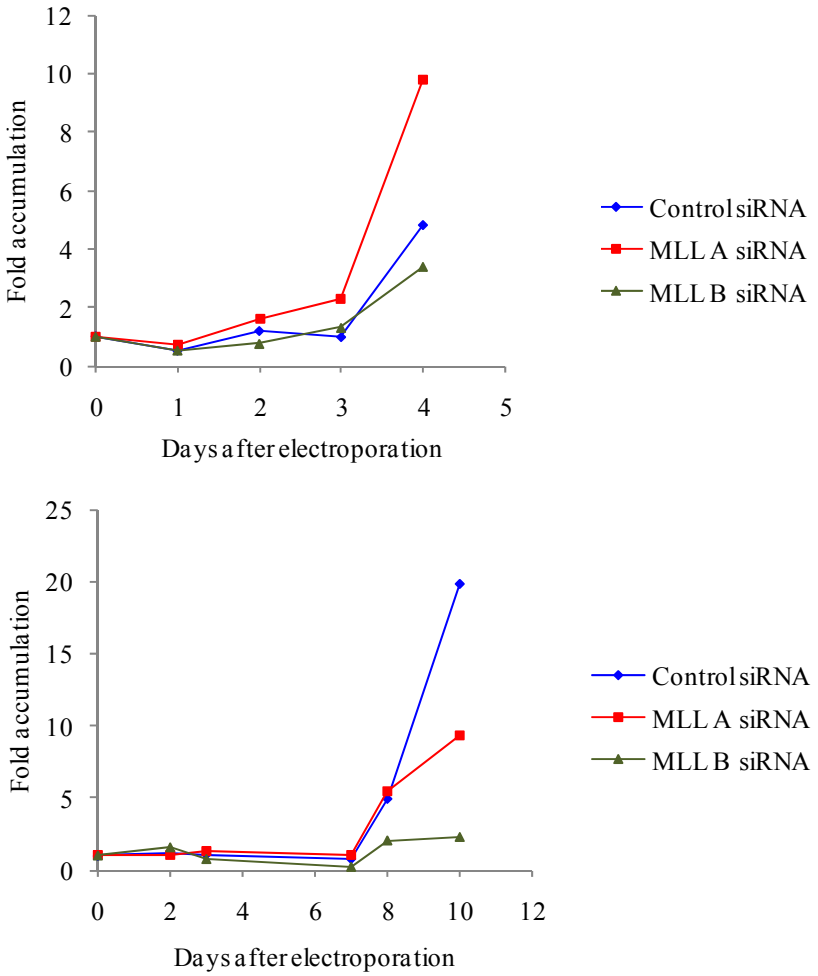

Figure 4.7. siRNA targeting MLL does not decrease the proliferation of THP-1 cells

The graphs represent the fold-accumulation in THP-1 cell number after electroporation with siRNA, against control (red diamonds), MLL A (blue squares) and MLL B (black triangles) and MLL C (green triangle) shRNA. Cells were electroporated at 330V for 10ms and counted at various time points. All the cultures started at a density of $0.5x10^6$ cells per ml. Viable cell numbers were evaluated using trypan blue exclusion. No consistency in results was observed in two other independent experiments.

4.5. Knock-down study by shRNA

As an alternative approach to siRNA delivery to knock-down MLL-AF9 expression, lentiviral short hairpin RNA (shRNA) delivery was undertaken. Unlike siRNA, shRNA are delivered by retroviral or lentiviral expression vectors, which provide a stable knock-down. Initially, we tested the efficiency of gene expression knock-down by shRNA, by knocking down *GPADH*. An shRNA sequence specific for the *GAPDH* gene, embedded within the mir-30 microRNA, was purchased from Open Biosystems (Surrey, UK). This shRNA mir-30 was cloned into the SFFV-GIPZ vector, in which the CMV promoter of the GIPZ vector was replaced with the SFFV promoter. THP-1 cells were transduced with shRNA targeting *GAPDH*, or a negative control which was designed to have no homology to mammalian genes, and this was validated by Open Biosystems using Affymetrix GeneChip arrays (Open Biosystems). Transduced THP-1 cells were selected by puromycin two days later for three days and the transduction efficiency was estimated by measuring the percentage of EGFP expressing cells by flow cytometry (data not shown). Figure 4.8 shows that *GAPDH* mRNA expression in THP-1 cells transduced with GAPDH shRNA decreased down to 10% of negative control shRNA. This suggests that lentiviral shRNA-mir30 delivery would be an effective approach for gene expression knock-down in these leukaemic cells.

This shRNA delivery system was used to perform knock-down of established MLL-fusion target gene expression.

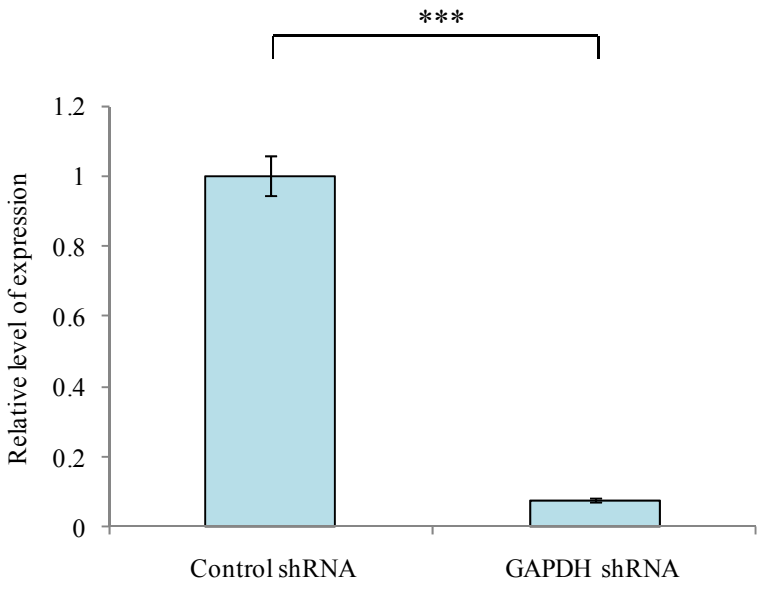

Figure 4.8. Knock-down of GAPDH expression using shRNA in THP-1 cells

The bar graph shows the relative levels of *GAPDH* mRNA expression, measured by QPCR in THP-1 cells after lentiviral transduction with shRNA targeting *GAPDH*. RNA was harvested five days after the transduction. Values for gene expression were normalised to THP-1 cells transduced with control shRNA. Columns represent the mean of quadruplicate measurements and the error bars represent the SD. *P*-values were calculated using Student's paired t-test. (***) $P \leq 0.001$. This experiment was carried out once.

Initially, we knocked down *HOXA9* expression, as it is one of the most critical down-stream target genes of MLL-fusions, and its expression has been demonstrated to be regulated directly by these fusions (Ayton and Cleary, 2001; Zeisig et al., 2004; Horton et al., 2005). shRNA sequences specific for *HOXA9*, embedded within the mir-30 microRNA, were purchased from Open Biosystems (Surrey UK). These shRNA mir-30 were then cloned into the SFFV-GIPZ vector, as described previously. THP-1 cells were transduced with various shRNAs targeting *HOXA9*. RNA was then harvested six days after transduction and *HOXA9* expression was measured by QPCR (Figure 4.9A). The efficiency of knock-down of *HOXA9* expression varied depending on the shRNA used. Transduction of THP-1 cells with HOXA9.5 shRNA reduced *HOXA9* mRNA expression by 69% compared to that of control shRNA, while HOXA9.4 and HOXA9.6 shRNA only reduced *HOXA9* expression by 29% and 24% respectively. Since *MYB* expression was found to be a down-stream target of HOXA9 and MEIS1 (Hess et al., 2006), *MYB* mRNA expression was also measured in THP-1 cells transduced with HOXA9.4 and HOXA9.5 shNRAs (Figure 4.9B). Only HOXA9.5 shRNA was found to significantly reduce *MYB* mRNA, down to 78% of that of the control. In addition, we tested the HOXA9.5 shRNA in MOLM-13 cells, also derived from a patient with the MLL-AF9 translocation. MOLM-13 cells transduced with control or HOXA9.5 shRNA were harvested seven days after transduction (Figure 4.9C). HOXA9.5 shRNA reduced *HOXA9* mRNA by 27% compared to that of control shRNA. This reduction was less marked compared to that of THP-1 cells (Figure 4.9A). Next, we knocked-down MYC expression in THP-1 cells using the same shRNA approach (Figure 4.9C). THP-1 cells transduced with all three shRNA against *MYC* reduced *MYC* mRNA expression significantly, by 31%, 59% and 31%. Taken together, these data suggest that lentiviral shRNA mediated knock-down of gene expression can be effective, although the knock-down efficiency varied depending on the shRNA and type of cell lines used.

Figure 4.9. Knock-down of gene expression using shRNA in THP-1 cells

The bar graph shows the relative level of A) *HOXA9 B) MYB* mRNA expression, measured by QPCR in THP-1cells and C) *HOXA9* in MOLM-13 cells after lentiviral transduction with shRNA targeting *HOXA9*. RNA was harvested A-B) six and C) seven days after the transduction. Values for gene expression were normalised to THP-1 cells or MOLM-13 cells transduced with control shRNA. Columns represent the mean of quadruplicate measurements and the error bars represent the SD. *P*-values were calculated using Student's paired t-test. (***) $P \leq 0.001$, (**) $P \leq 0.01$, (ns) not significant. D) The bar graph shows the relative level of *MYC* expression, measured by QPCR, in THP-1 cells after lentiviral transduction with shRNA targeting *MYC*. RNA was harvested six days after the transduction. Values for gene expression were normalised to THP-1 cells transduced with control shRNA. Columns represent the mean of quadruplicate measurements and the error bars represent the SD. *P*-values were calculated using Student's paired t-test. (***) $P \leq 0.001$, (**) $P \leq 0.01$, (*) $P \leq 0.05$. These experiments were carried out once.

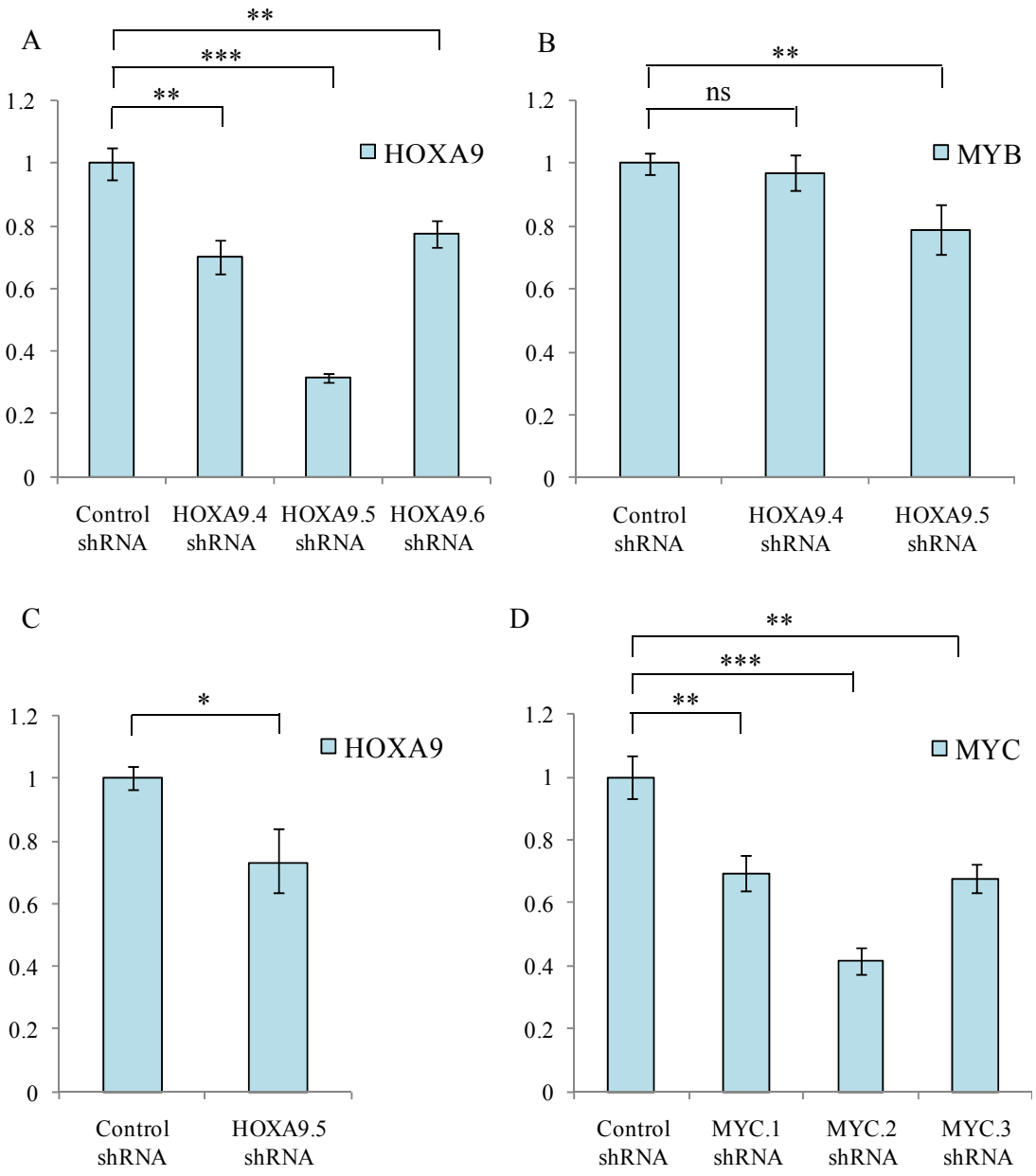
A
**
***
**
1.2
1
0.8
0.6
0.4
0.2
0
HOXA9
Control shRNA
HOXA9.4 shRNA
HOXA9.5 shRNA
HOXA9.6 shRNA
B
**
ns
1.2
1
0.8
0.6
0.4
0.2
0
MYB
Control shRNA
HOXA9.4 shRNA
HOXA9.5 shRNA
C
*
1.2
1
0.8
0.6
0.4
0.2
0
HOXA9
Control shRNA
HOXA9.5 shRNA
D
**
***
**
1.2
1
0.8
0.6
0.4
0.2
0
MYC
Control shRNA
MYC.1 shRNA
MYC.2 shRNA
MYC.3 shRNA

4.6. Discussion

A large number of leukaemic cells have been established and widely used in scientific research in the last two to three decades (Drexler et al., 2004). These cell lines have advantages and disadvantages as models to study oncogene function. The former are their robustness in tissue culture, lack of growth factor requirement and relevance to the disease being studied. Disadvantages include the length of time the cells have spent in culture, the consequent genetic drift from the original leukaemia and acquisition of confounding secondary mutations. In this chapter, we tested and characterised a panel of commercially available human leukaemic cells. Our study showed that all of the human leukaemic cell lines we tested, apart from the KOPN-8 cells, expressed their respective MLL-fusions at the protein level. It is unclear why we could not detect MLL-ENL protein expression in the KOPN-8 cell line. KOPN-8 cells were derived from the peripheral blood of a three-month-old girl with B cell precursor acute lymphoblastic leukaemia in 1977 (Matsuo and Drexler, 1998). The expression of MLL-ENL in KOPN-8 cells was previously validated by QPCR (Drexler et al., 2004). In addition, our result showed that despite the lack of MLL-ENL expression at the protein level in KOPN-8 cells, both *HOXA9* and *MEIS1* mRNA were detectable. It is possible that the expression level of the fusion was too low to detect. Alternatively, it is possible that the KOPN-8 cells lost the expression of MLL-ENL. In this case, *HOXA9* and *MEIS1* are likely to have lost their dependency on MLL-ENL, possibly due to acquisition of further mutations or epigenetic changes during the extended time the cell line has spent in culture.

The lack of *MEIS1* mRNA expression in THP-1 cells was surprising. THP-1 cells were established from the peripheral blood of a one-year-old boy with acute monocytic leukaemia in 1980 (Tsuchiya et al., 1980). MEIS1 and HOXA9 expression is associated with MLL-fusion positive leukaemia (Armstrong et al., 2002; Ayton and Cleary, 2003; Quentmeier et al., 2004; Zeisig et al., 2004; Wong et al., 2007). Indeed, *HOXA9* and *MEIS1* are crucial down-stream target genes of MLL-fusions and over-expression of these genes by retroviral transduction was sufficient to cause leukaemia, indicating that these genes play an important role in the induction and maintenance of MLL-fusion (Kroon et al., 1998; Armstrong et al., 2002; Zeisig et al., 2004; Wong et al., 2007). There are a couple of studies in the literature describing *MEIS1* expression in THP-1 cells (Quentmeier et al., 2004; Wong et al., 2007). It is therefore possible that the THP-1 cells from DMSZ lost *MEIS1* expression at some point during the time spent in culture, and that down-stream transcriptional regulation of target genes is no longer dependent on MEIS1. Wong *et al* showed that unlike murine progenitor cells transduced with MLL-fusions, human leukaemic cells express *MEIS2* as well as *MEIS1* (Wong et al., 2007). The relative expression ratio of *MEIS1* to *MEIS2* in THP-1 cells was 1:1 in this study. Previous work from our laboratory also suggested that *Meis1* expression in murine cells with conditional MLL-ENL expression may be substituted by *Meis2* expression (Horton et al., 2005). Taken together, this suggests the possibility that *MEIS2* expression may have substituted the requirement for *MEIS1* in the THP-1 cells used in the present study.

One apparent problem of using commercially available human leukaemic cells is the physiological similarity between these cells and the actual human leukaemia. Since these cells can be maintained in culture for substantial periods of time, one cannot

exclude the possibility that the cell lines are no longer dependent on MLL-fusions. To resolve this issue, we decided to knock-down MLL-fusion expression to observe the dependency of these cells on MLL-fusions. siRNA transfer is a widely used technique for silencing the gene of interest (Hannon, 2002). In addition, we chose electroporation as a method of siRNA delivery, because other common methods such as the use of cationic lipid formulations were reported to be inefficient in suspension cells, especially in haematopoietic cells (Walters and Jelinek, 2002; Dunne et al., 2003). Several studies have successfully performed siRNA delivery into leukaemic cells using this approach (Dunne et al., 2003; Heidenreich et al., 2003; Scherr et al., 2003). Electroporation was performed using a pulse generator EPI 2500 electroporator in our study (Heidenreich et al., 2003), that, unlike conventional electroporators, delivers a high voltage discharge in a square-wave pulse, which reduces heat produced in the culture. siGLO Red delivery using the electroporator confirmed that electroporation efficiently transfered siRNA into human leukaemic cells.

There are few studies regarding the knock-down of MLL-fusion expression in human leukaemic cell lines. Thomas *et al* used a similar method to our approach to knock-down the expression of *MLL-AF4*, except that their siRNA targeted the fusion sequence (Thomas et al., 2005). Their group used electroporation as a means of siRNA delivery and demonstrated a decrease in protein expression of MLL-AF4 after 48 hours. In our study, cells were harvested for analysis 72 hours after electroporation, since no knock-down was observed at 48 hours (data not shown). This discrepancy can be explained by the different cell lines used and the difference in their proliferation rate. Pession *et al* and Kawagoe *et al* both used anti-sense oligodeoxyribonucleotide (ODN) as a method for the knock-down of MLL-AF9 expression in THP-1 cells. These studies showed an

increase in apoptosis following ODN delivery (Kawagoe et al., 2001; Pession et al., 2003). However, neither terminal differentiation nor immunophenotypic changes were observed. Although siRNA transfer was successfully performed in the first instance in our study, we noticed that the knock-down level of MLL-AF9/MLL expression differed considerably in subsequent experiments. Increases in the voltage of electroporation did not alter the knock-down efficiency. Furthermore, there was no consistency in proliferation of THP-1 cells electroporated with MLL siRNA, suggesting ineffective knock-down of the fusion gene. Based on these results, we decided to change our approach to stable shRNA delivery. Lentiviral transfer of shRNA overcomes the transient nature of siRNA knock-down. The lentiviral vector used in the present study contains the SFFV promoter to drive the expression of the shRNA, embedded within the miR-30 sequence, that is then cleaved by the Dicer enzyme to generate siRNA (Leung and Whittaker, 2005). This system enables continuous synthesis of shRNA by the host cells, to provide stable knock-down of gene expression. In addition, a number of studies suggest that shRNA is a more efficient method of silencing gene expression than siRNA (Leung and Whittaker, 2005; Rao et al., 2009). In agreement with this, we have shown that shRNA targeting *GAPDH* reduced *GAPDH* mRNA expression down to 0.1 of the negative control. We also knocked down *HOXA9* and *MYC* mRNA expression in THP-1 cells, and significant reductions in both genes were observed. However, we noticed that knock-down efficiency varied depending on shRNA used and that only the HOXA9.5 shRNA, that knocked-down *HOXA9* mRNA expression by 69%, also reduced *MYB* mRNA expression. This suggests that more than 70% knock-down may be necessary in order to study target gene function. Furthermore, less marked reduction of *HOXA9* mRNA expression was observed when the same shNRA was used in MOLM-13, suggesting that efficiency of gene expression knock-down using shRNA may vary depending on the cell lines used. Based on our data, we decided to employ

stable silencing of MLL-fusion target genes using shRNAs in the rest of our experiments and to test a number of shRNAs to obtain high knock-down of gene expression.

CHAPTER 5. RESULTS - Validation of MLL-AF9 transcriptional target genes

5.1. Introduction

We have successfully generated human immortalized myeloid cell lines, using MLL-AF9, from human CB cells (V6MA cells) and characterised several human myeloid leukaemic cell lines in previous chapters. This enabled us to validate the MLL-fusion transcriptional target genes established from a murine conditional MLL-fusion expression model (Dr Vanessa Walf-Vorderwülbecke, PhD thesis), in these two human systems. Two of the target genes found to be up-regulated by MLL-fusions, *Ruvbl1* (also known as Tip49a, NMP238, ECP54, TAP54α, TIH1, Pontin and Rvb1) and *Rvbl2* (also known as Tip49b, ECP51,CGI-46, INO80J, TIH2 Tip48, Reptin and Rvb2), encode ATPases belonging to the ATPase family associated with various cellular activities (AAA+), that have multiple roles in telomerase and chromatin-remodelling complexes (Gallant, 2007; Grigoletto et al., 2011). RUVBL1 and RUVBL2 have been demonstrated to interact with telomerase reverse transcriptase (TERT) to form a pre-telomerase complex and recruit TERT in a cell-cycle dependent manner (Venteicher et al., 2008).

Previous studies have identified a possible mechanism for regulation of *Ruvbl1* and *Ruvbl2* by MLL-fusions. Hess *et al* identified *Ruvbl1* and *Ruvbl2* as down-stream targets of *Hoxa9* and *Meis1* transcription factors in conditionally immortalised mouse MLL-ENL cells. In their work, transduction of conditionally immortalised mouse MLL-ENL cells with *Hoxa9* and *Meis1* prevented reduction of both *Ruvbl1* and *Ruvbl2*

expression upon loss of MLL-ENL (Hess et al., 2006). Evidence from our laboratory showed that the expression of *Ruvbl1* and *Ruvbl2* is decreased by 3.9 and 3.6-fold, respectively, upon loss of MLL-fusion expression. Loss of expression was previously demonstrated at the protein and mRNA levels by western blot and QPCR analysis (Dr Vanessa Walf-Vorderwülbecke, PhD thesis). Interestingly, shRNA-mediated knock-down of either *Ruvbl* or *Ruvbl2* led to a loss of mouse MLL-fusion immortalised cells from cell cultures (Dr Vanessa Walf-Vorderwülbecke, PhD thesis). Through a knock-down study, RUVBL1 and RUVBL2 were demonstrated to be important in assembly and remodelling of the telomerase complex (Venteicher et al., 2008). Other work also suggests both proteins are necessary for telomerase regulation (Li et al., 2010; Menard et al., 2010). This is particularly interesting because CB-derived MLL-AF9 cells have been shown to exhibit higher telomerase activity compared to that of untransduced CB cells (Wei et al., 2008). One possibility is that MLL-AF9 alters telomerase activity by regulating expression of RUVBL1 and RUVBL2. Based on these results, and previously published work, we decided to study the role of *RUVBL1* and *RUVBL2* in the oncogenic activity of MLL-AF9 in human cells, using the immortalised CB-derived and leukaemic cell lines.

5.2. RUVBL1 expression is maintained by MLL-AF9 in conditionally immortalised murine cells

Reduced *Ruvbl1* expression upon loss of MLL-AF9 in the conditionally immortalised mouse myeloid cells may have been a consequence of differentiation, rather than regulation, by the MLL-fusion. In order to distinguish between these two possibilities, we treated the conditionally immortalised mouse cells with Granulocyte Colony-

Stimulating Factor (G-CSF). G-CSF has previously been shown to cause terminal differentiation of mouse MLL-ENL immortalised cell lines (Lavau et al., 1997). Previous work from our laboratory has also demonstrated that despite the induction of terminal neutrophil differentiation by G-CSF, established MLL-fusion transcriptional target genes of the *Hoxa* cluster remained unchanged in the conditionally immortalised cells (Horton et al., 2005). The murine conditional MLL-AF9 cell lines were generated by retroviral delivery of the "Tet-off" expression system (Horton et al., 2005). In this system, the tetracycline-responsive promoter element (TRE) drives the MLL-AF9 expression, which is dependent on the binding of the tetracycline-controlled transactivator protein (tTA). In the presence of doxycycline (Dox), tTA undergoes a conformational change which prevents TRE from binding to tTA and therefore blocks the expression of MLL-AF9. Since the rate of differentiation in the conditional cells induced by Dox and G-CSF was comparable (Horton et al., 2005), G-CSF treatment can be used to exclude gene expression changes resulting from myeloid differentiation *per se*. RUVBL1 protein expression was examined in cells treated with Dox or G-CSF. The treated cells were harvested after 72 hours for detection of protein expression by western blot analysis (Figure 5.1). A 52kDa band corresponding to the RUVBL1 protein was detected in untreated cells. Addition of Dox caused a decrease in RUVBL1 protein expression, down to 0.3 of that of the untreated control. However, treatment with G-CSF did not cause a similar decrease in expression. These data suggest that MLL-AF9 is indeed required in order to maintain RUVBL1 expression in the conditionally immortalised mouse cells.

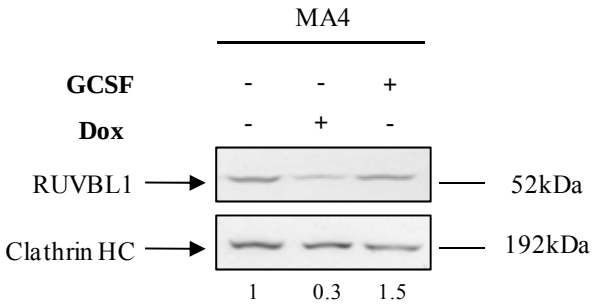

Figure 5.1. RUVBL1 expression is regulated by MLL-AF9

The figure shows western blot analysis of total lysates from murine conditionally immortalised MLL-AF9 cells (MA4). Cells were treated with Dox (2µg/ml) or G-CSF (10ng/ml) and harvested after 72 hours. The western blot was probed with a primary goat polyclonal anti-RUVBL1 antibody and a secondary donkey anti-goat IgG HRP. An anti-Clathrin-HC antibody was used to control for protein loading. Values for protein expression were normalised to untreated MA4 cells. A similar pattern of expression was observed in one independent experiment.

5.3. *RUVBL1* expression is up-regulated in V6MA cells

The mRNA expression of *RUVBL1* was examined in V6MA cells, generated in this study (Chapter 3) (Figure 5.2). QPCR analysis revealed that the expression of *RUVBL1* mRNA was significantly up-regulated in the V6MA cells (V6MA1v, V6MA2r, V6MA3r), compared to the expression in control human myeloid cells, transduced with the empty lentiviral expression construct FUGW-V6 (V6 cells). CB cells immortalised using the *AML-ETO-9a* fusion gene were used as a further control, in order to examine *RUVBL1* expression in non-MLL-fusion immortalised cells. The expression of *RUVBL1* in V6MA3r cells was significantly higher than in the AML1-ETO9a cells. However, AML-ETO9a cells also expressed high levels of *RUVBL1*, suggesting alternative mechanisms of regulating this gene may exist. These results validate the findings from the mouse immortalised cells and extend them to human cells.

5.4. *RUVBL1* is regulated by MLL-AF9 and/or endogenous MLL in THP-1 cells

In order to further establish the importance of RUVBL1 expression in MLL-AF9 expressing leukaemia cells, and its dependence on the fusion, we knocked down MLL-AF9 expression in THP-1 cells. The shRNAs used target 5' sequences of the *MLL* gene and therefore both endogenous *MLL* and *MLL-AF9* were subject to inhibition of gene expression. Two independent shRNAs against *MLL* were used for this experiment, to eliminate the possibility of off-target effects.

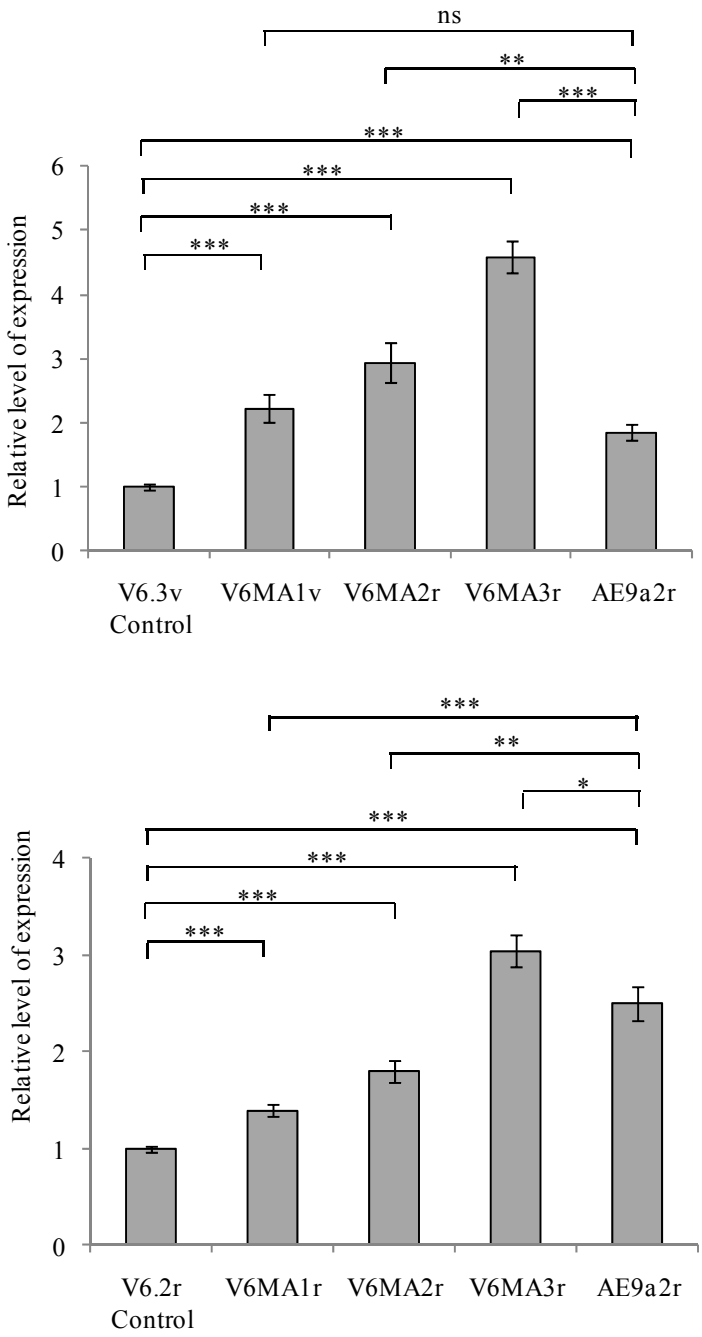

Figure 5.2. mRNA expression of RUVBL1 is up-regulated in human immortalised myeloid cells

The bar graphs show the relative levels of *RUVBL1* mRNA expression, measured by QPCR in V6, V6MAs and AE9a cells in two independent experiments. Values for each cell line were normalised to the expression in V6 cells. Columns represent the mean of quadruplicate measurements and the error bars represent the SD. V6.3v, V6MA1v, V6MA2r and V6MA3r were in culture for 57, 105, 100 and 57 days respectively (top). V6.2r, V6MA1v, V6MA2r and V6MA3r were in culture for approximately 69, 53, 55 and 165 days respectively (bottom). *P*-values were calculated using Student's paired t-test. (***) $P \leq 0.001$, (**) $P \leq 0.01$, (*), $P \leq 0.05$, (ns) not significant.

THP-1 cells were chosen because they were previously shown to express high levels of the MLL-AF9 protein among the human myeloid leukaemic cells we studied. THP-1 cells were harvested five days after transduction with lentiviral shRNA constructs, to measure the protein expression of MLL-AF9 by western blot analysis (Figure 5.3A). MLL-AF9 protein expression was reduced by approximately 50% following transduction of THP-1 cells with the shRNA against *MLL,* compared to the transduction with control shRNA. The control shRNA was validated to have no homology to any mammalian genes by Open Biosystems (Surry, UK). The inhibition of *MLL-AF9/MLL* expression in THP-1 cells also decreased proliferation of the cells in liquid culture (Figure 5.3B). In addition, mRNA was harvested 22 days (Figure 5.4 A) or five days (Figure 5.4 B) after transduction to determine MLL-AF9 target gene expression, in two independent experiments (Figure 5.4). *HOXA9* is one of the most critical down-stream target genes of MLL-fusions and its expression has been demonstrated to be regulated directly by these fusions (Ayton and Cleary, 2001; Zeisig et al., 2004; Horton et al., 2005). The expression of *HOXA9* would therefore be predicted to decrease if inhibition of MLL-AF9 expression was successful. The expression of *HOXA9* mRNA decreased to approximately 60% to 40% of control when THP-1 cells were transduced with shRNA against *MLL*. The mRNA expression of *RUVBL1* was also slightly down-regulated, by 15% in both experiments. Together, these results suggest that the expression of *RUVBL1* may be regulated directly or indirectly by MLL-AF9 and/or endogenous MLL in THP-1 cells.

Figure 5.3. Inhibition of MLL-AF9 (and/or MLL) expression decreases the proliferation of THP-1 cells

A) The figure shows western blot analysis of total cell lysates from THP-1 cells. THP-1 cells were lentivirally transduced with control, MLL.2 and MLL.5 shRNA. The cells were harvested five days after the transduction. The western blot was probed with a primary mouse anti-human MLL-N4.4 antibody and a secondary sheep anti-mouse HRP. An anti-Clathrin-HC antibody was used to control for protein loading. Values for protein expression were normalised to THP-1 cells transduced with control shRNA. Values for endogenous MLL protein expression were 1, 0.5 and 0.5 respectively. B) The plots show the accumulation in THP-1 cell number after lentiviral transduction with control shRNA (diamonds), MLL.2 shRNA (squares) and MLL.5 shRNA (triangles). All the cultures started at a density of $0.5x10^6$ cells per ml. Viable cell numbers were evaluated using trypan blue exclusion. In the plot on the left, each point represents the mean of triplicate measurements and the error bars represent the SD. In the plot on the right, each point represents a single measurement.

A

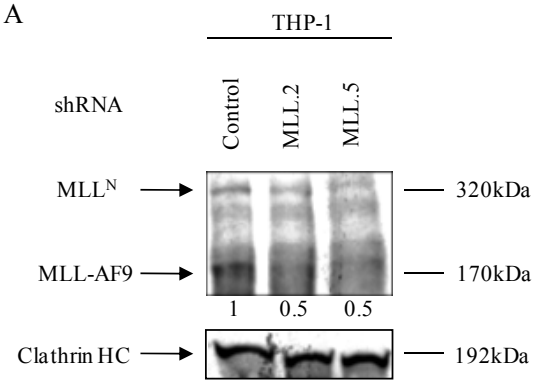
THP-1
shRNA
Control
MLL.2
MLL.5
MLL^N
320kDa
MLL-AF9
170kDa
1
0.5
0.5
Clathrin HC
192kDa

B

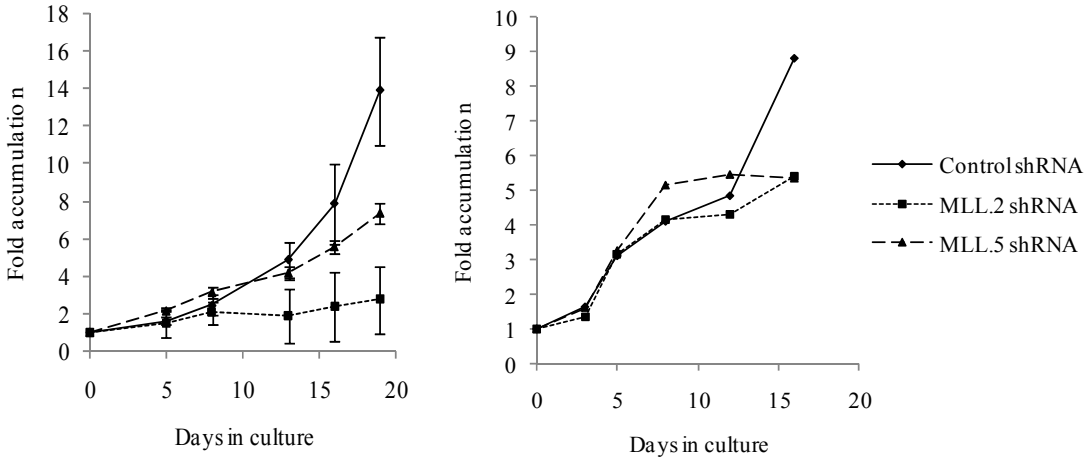
Fold accumulation
Days in culture
Fold accumulation
Days in culture
Control shRNA
MLL.2 shRNA
MLL.5 shRNA

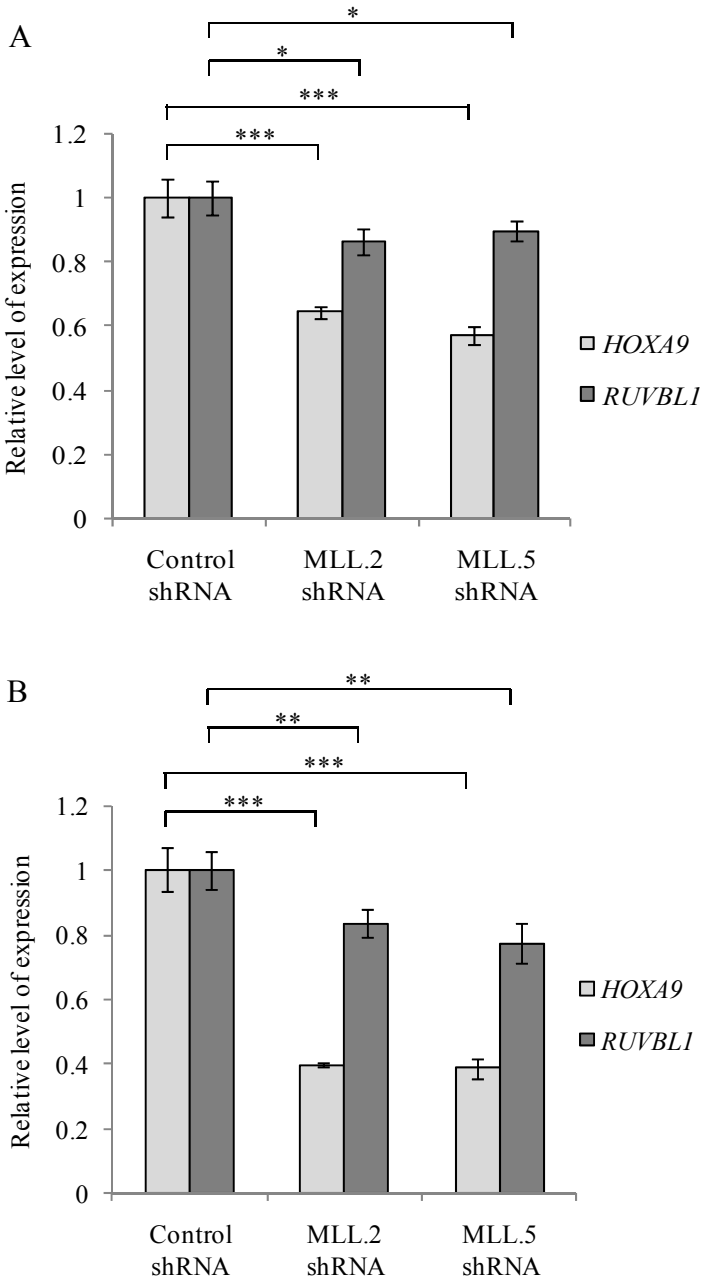

Figure 5.4. Inhibition of MLL-AF9 (and/or MLL) decreases RUVBL1 mRNA expression in THP-1 cells

The bar graphs show the relative level of *HOXA9* (light grey) and *RUVBL1* (dark grey) mRNA expression, measured by QPCR in THP-1 cells after transduction with shRNA targeting *MLL*. RNA was harvested 22 days A) and five days B) after transduction. Values for gene expression were normalised to THP-1 cells transduced with control shRNA. Columns represent the mean of quadruplicate measurements and the error bars represent the SD. *P*-values were calculated using Student's paired t-test. (***) $P \leq 0.001$, (**) $P \leq 0.01$, (*) $P \leq 0.05$.

5.5. Human leukaemic cell lines require RUVBL1 expression to persist in culture

Since *RUVBL1* expression appears to be regulated by MLL-AF9 in both human immortalised myeloid cells, as well as in THP-cells, it is possible that over-expression of this gene plays an important role in mediating part of the MLL-fusion leukaemogenic activity. To assess the role of *RUVBL1* expression in human leukaemic cells, its expression was inhibited in THP-1 cells using shRNAs. Various shRNAs that target different sequences of *RUVBL1* were tested to obtain the highest knock-down of gene expression. mRNAs were harvested from cells five days after transduction to measure the expression of *RUVBL1* by QPCR analysis (Figure 5.5). Transduction of THP-1 cells with all three shRNAs reduced RUVBL1 mRNA expression by at least 60%. Next, we examined the effect of inhibiting *RUVBL1* expression on the persistence of human leukaemic myeloid cells *in vitro*. NOMO-1, MV4-11, KASUMI-1, and OCI-AML3 cells were transduced with shRNA targeting *RUVBL1* (RUVBL1.1, RUVBL1.2, and RUVBL1.2 shRNAs) and the percentage of transduced EGFP expressing cells in these cultures was monitored (Figure 5.6A). The leukaemic cells transduced with RUVBL1.1 and RUVBL1.2 shRNA were gradually lost from the culture, compared to that of control shRNA. The data also showed that the RUVBL1.2 shRNA induced the strongest reduction in the percentage of EGFP positive cells in transduced leukaemic cells, over the period analysed, among other shRNAs.

The effect of inhibiting *RUVBL1* expression on the persistence of a panel of human myeloid leukaemic lines, expressing MLL-fusions or distinct fusion, was then analysed.

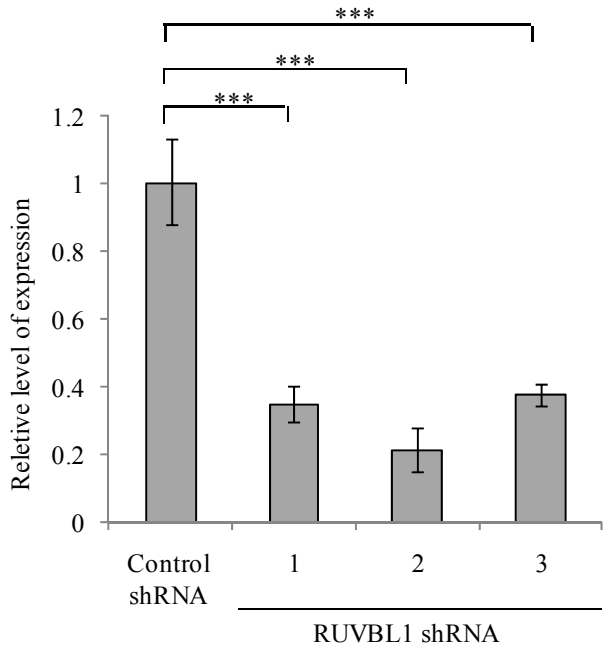

Figure 5.5. Knock-down of the RUVBL1 expression in THP-1 cells

The bar graph shows the relative level of *RUVBL1* mRNA expression, measured by QPCR, in THP-1cells after lentiviral transduction with shRNA targeting *RUVBL1*. RNA was harvested five days after the transduction. Values for gene expression were normalised to THP-1 cells transduced with control shRNA. Columns represent the mean of quadruplicate measurements and the error bars represent the SD. *P*-values were calculated using Student's paired t-test. (***) $P \leq 0.001$.

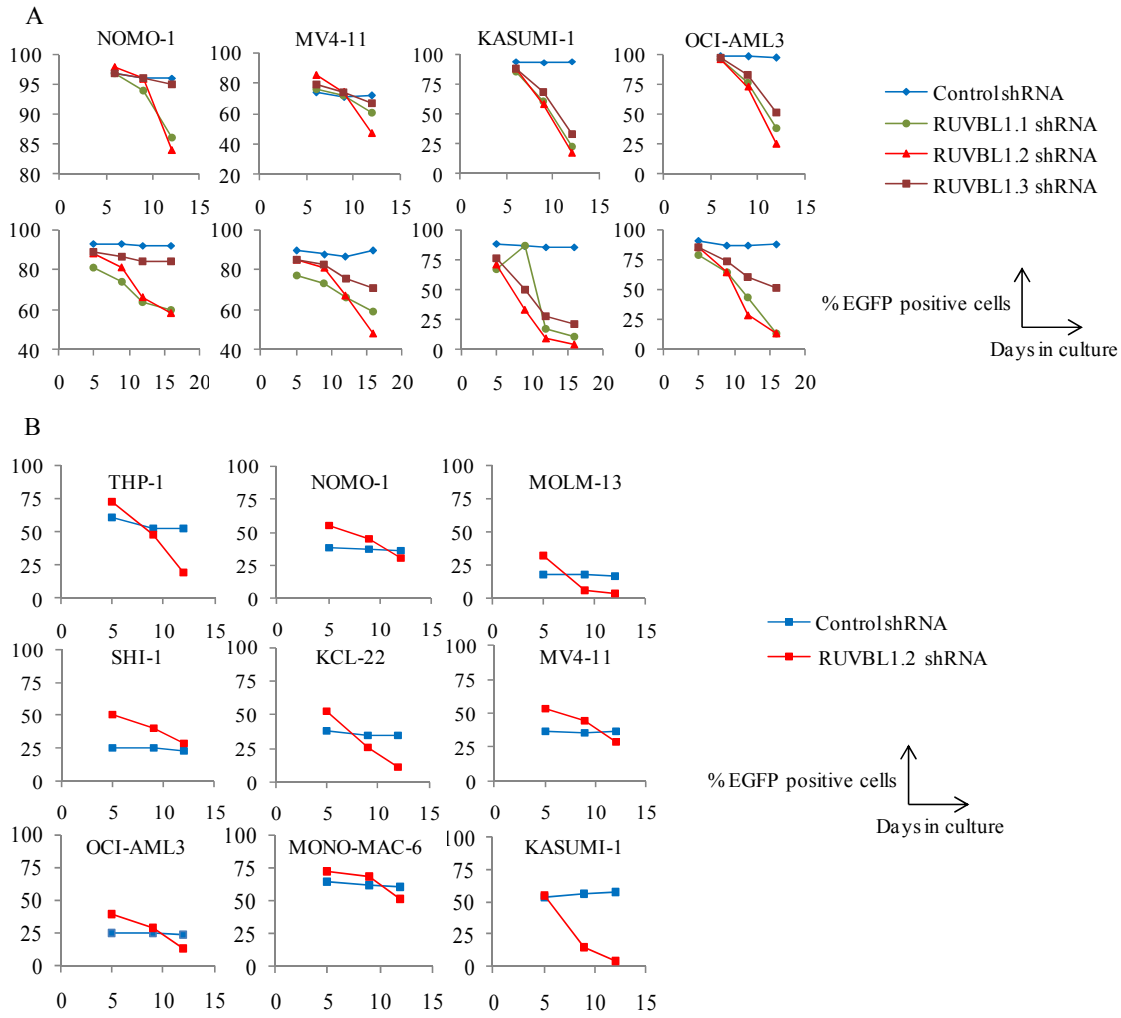

Figure 5.6. Inhibition of the RUVBL1 expression results in loss of transduced cells from culture

A) The graphs represent the persistence of EGFP positive human leukaemic cells (NOMO-1, MV4-11 KASUMI-1 and OCI-AML3). Lentivirally transduced leukaemic cells were transduced with control shRNA (blue), RUVBL1.2 shRNA (green), RUVBL1.2 shRNA (red) or RUVBL1.3 shRNA (brown). EGFP expression was determined by flow cytometric analysis at the indicated time points. Cultures were re-plated approximately every three to four days. B) The graphs represent the persistence of EGFP positive human leukaemic cells. Lentivirally transduced human leukaemic cells were transduced with control shRNA (blue) or *RUVBL1.2* shRNA (red). EGFP expression was determined by flow cytometric analysis at the indicated time points. Cultures were re-plated approximately every three to four days. Viral supernatant was diluted to 6% prior to transduction.

The human myeloid leukaemic cells were transduced with RUVBL1.2 shRNA and the percentage of transduced EGFP expressing cells in these cultures was monitored (Figure 5.6B). RUVBL1.2 shRNA was used to target *RUVBL1* in this experiment, since it was previously shown to cause the strongest inhibition of leukaemic cell proliferation (Figure 5.6A). The percentage of EGFP positive cells in all the cultures transduced with the RUVBL1.2 shRNA declined over the 12 days analysed. In particular, the strongest effect was seen in THP-1 and KASUMI-1 cells. This data suggests that *RUVBL1* expression is not only important in MLL-fusion associated leukaemia, but may be necessary to maintain proliferation and or survival of human myeloid leukaemia cells in general.

5.6. The conserved Walker B motif in RUVBL1 is required for normal THP-1 proliferation

So far, we have obtained evidence to suggest that the expression of *RUVBL1* is important for the maintenance of human myeloid leukaemia cells in culture, including cell lines expressing different MLL-fusions. RUVBL1 was previously demonstrated to have ATPase activity, which was found to be important for c-Myc mediated oncogenic transformation of rat embryonic fibroblasts (Wood et al., 2000). The Walker B motif within RUVBL1 is highly conserved from yeast to humans and is responsible for hydrolysing ATP as well as binding to DNA (Mezard et al., 1997). Introduction of a missense mutation within the Walker B motif (DEVH→NEVH) results in a dominant negative mutant, capable of inhibiting RUVBL1 activity (Mezard et al., 1997; Wood et al., 2000). The RUVBL1 (D302N) mutant retains the ability to bind c-Myc and to form homotypic and heterotypic complexes with RUVBL1 and RUVBL2, respectively.

However, this mutant is unable to hydrolyse ATP or to bind DNA (Mezard et al., 1997 6; Wood et al., 2000). The D302N point mutation was introduced within the full-length cDNA of *RUVBL1* and the mutated cDNA was cloned into the SFFV-GIPZ lentiviral expression vector, replacing the EGFP cDNA. The SFFV-GIPZ vector with the EGFP cDNA deleted was used as the empty vector negative control in these experiments. THP-1 cells were transduced with the RUVBL1 (D302N) expression vector or the empty vector negative control. Two days after transduction, puromycin was added to the cultures, to select for transduced cells. Viable cell counts were then taken at various time-points over a 12-day period (Figure 5.7). THP-1 cells transduced with the negative control vector proliferated exponentially, whereas the THP-1 cells transduced with RUVBL1 (D302N) showed a marked reduction in their proliferation rate over the period analysed. These data suggest that the Walker B motif, conferring ATP hydrolysis and DNA binding, was necessary to maintain proliferation of THP-1 cells.

5.7. RUVBL2 expression is also maintained by MLL-AF9 in mouse cells

Since RUVBL1 and RUVBL2 can function synergistically, as well as antagonistically, we also decided to examine the function of RUVBL2 in the MLL-AF9 expressing cells. First of all, it was important to establish whether RUVBL2 expression was maintained by MLL-fusions, as was found to be case for RUVBL1. To answer this question, MLL-AF9 conditionally immortalised mouse cells were treated with Dox or G-CSF, as previously described in section 5.1. Treatment with Dox resulted in decreased RUVBL2 expression, down to 0.1 or 0.2 of that of the control, after 72 hours (Figure 5.8).

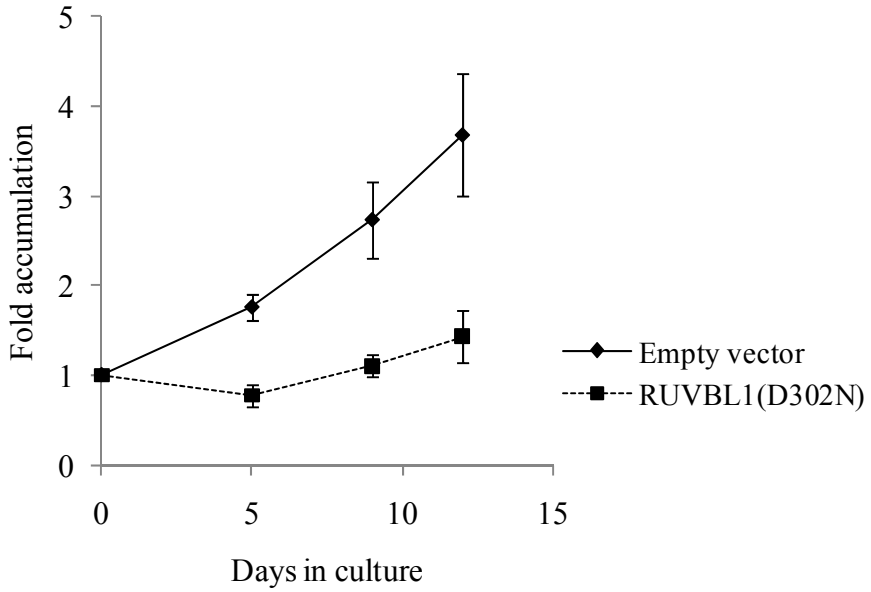

Figure 5.7. The Walker B motif of RVBL1 is necessary to maintain proliferation of THP-1 cells

The plot shows the accumulation in THP-1 cell number after lentiviral transduction with empty vector (diamonds) and RUVBL1 (D302N) (squares). Transduced cells were selected with purimycin two days later and treated for three days. All the cultures started at a density of $0.5x10^6$ cells per ml. Viable cell numbers were evaluated using trypan blue exclusion. Each point represents the mean of triplicate measurement and the error bars represent the SD.

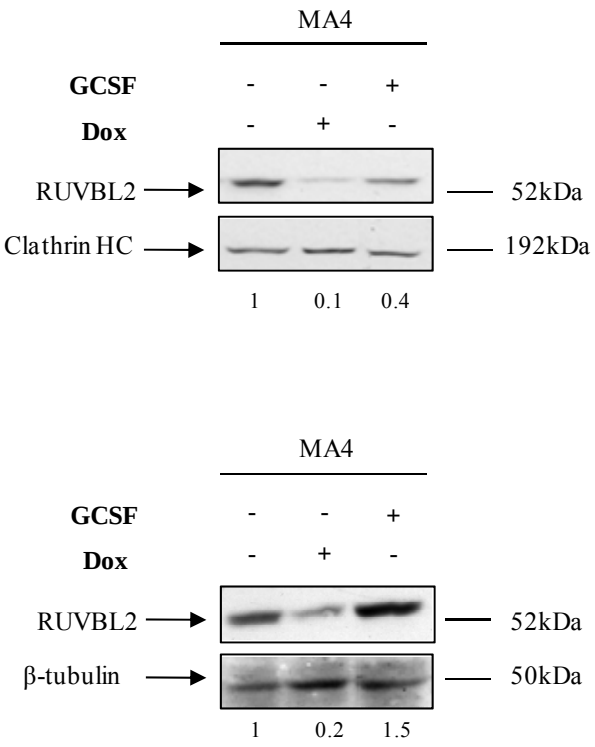

Figure 5.8. MLL-AF9 regulates RUVBL2 expression in mouse cells

The figures show two independent western blot analyses of total lysates from conditionally immortalised mouse MLL-AF9 cells (MA4). Cells were treated with Dox or G-CSF and harvested after 72 hours. The western blot was probed with a primary mouse monoclonal anti-RUVBL2 antibody and a secondary sheep anti-mouse IgG HRP. An anti-Clathrin-HC antibody or an anti-β-tubulin antibody was used to control for protein loading. Values for protein expression were normalised to untreated MA4 cells.

Although treatment of cells with G-CSF also resulted in a decrease in RUVBL2 protein expression in one of the experiments, this was less marked, down to 0.4 of that of the control . In contrast, treatment with G-CSF did not cause a reduction in expression in the other experiment. These data indicate that RUVBL2 expression is a least in part regulated by MLL-AF9 in the mouse cells.

5.8. *RUVBL2* expression is up-regulated in V6MA cells

RUVBL2 mRNA expression was then examined in V6MA cells (Figure 5.9). The expression of *RUVBL2* was significantly up-regulated in V6MA cells compared to that in V6 cells. Expression of V6MA3r cells was also significantly higher than in the AE9a2r cells. These data confirm that mRNA expression of *RUVBL2* is also up-regulated following immortalisation of CB-derived human cells by MLL-AF9.

To determine whether *RUVBL2* expression was regulated by MLL-AF9 and/or endogenous MLL in these human cells, MLL-AF9 was targeted using shRNA directed against 5' sequences of *MLL*. V6MA2r cells were transduced with the same shRNAs against *MLL* as used in section 5.4. Transduced V6MA2r cells were selected by addition of puromycin two days later and transduction was confirmed by flow cytometric analysis of EGFP expression. mRNA was harvested 10 days following transduction to examine *MLL* and *RUVBL2* expression by QPCR analysis (Figure 5.10A).

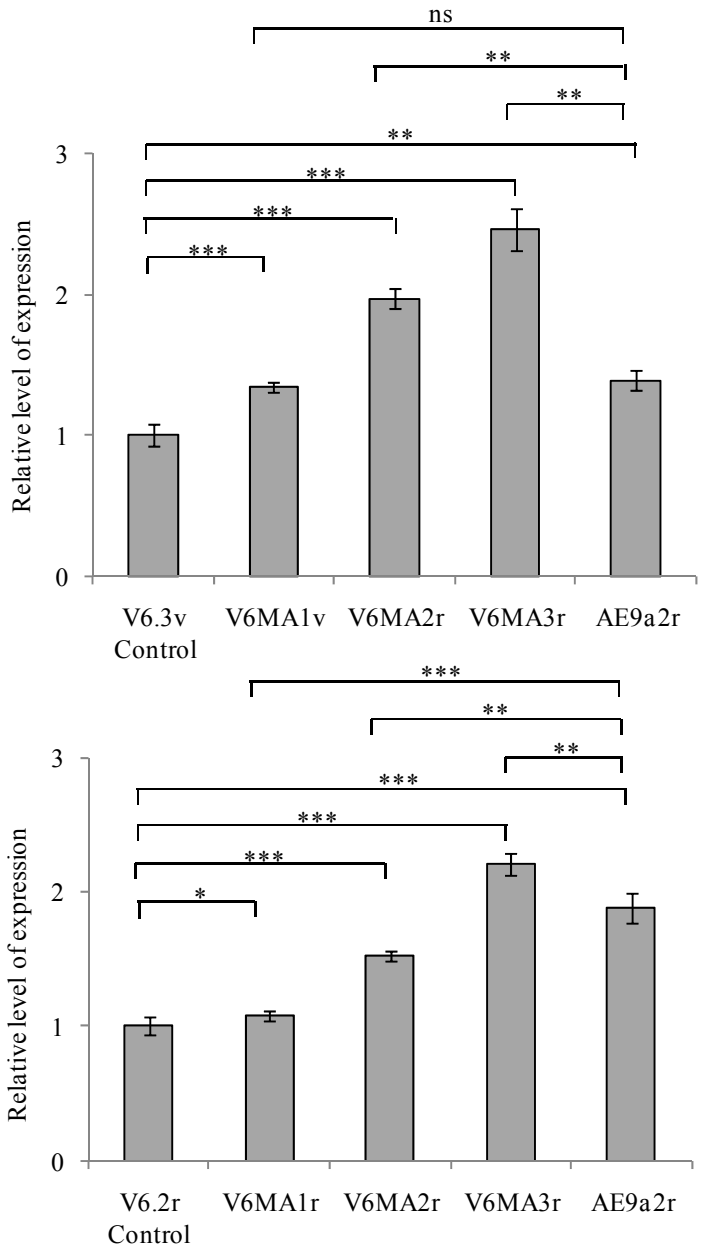

Figure 5.9. mRNA expression of RUVBL2 is up-regulated in human immortalised myeloid cells

The bar graphs show two independent measurements of the relative levels of *RUVBL2* mRNA expression, measured by QPCR in V6, V6MAs and AE9A2r cells. Values for each cell line were normalised to the expression in V6 cells. V6.3v, V6MA1v, V6MA2r and V6MA3r were in culture for 57, 105, 100 and 57 days respectively (top). V6.2r, V6MA1v, V6MA2r and V6MA3r were in culture for 29, 13, 15 and 125 days respectively (bottom). Columns represent the mean of quadruplicate measurements and the error bars represent the SD. *P*-values were calculated using Student's paired t-test. (***) $P \leq 0.001$, (**) $P \leq 0.01$, (*) $P \leq 0.05$, (ns) not significant.

Figure 5.10. Inhibition of MLL-AF9 (and/or MLL) decreases the RUVBL2 mRNA expression in human MLL-AF9 immortalised myeloid cells

A) The bar graph shows the relative level of *MLL* (light grey) and *RUVBL2* (dark grey) mRNA expression, measured by QPCR in V6MA2R cells following lentiviral transduction with shRNA against *MLL* and control shRNA. The transduced cells were selected with puromycin two days later and treated for three days. RNA was harvested 10 days after the transduction. Values for gene expression were normalised to V6MA2r cells transduced with control shRNA. V6MA2r cells were in culture for approximately 66 days after confirmation that the cells expressed 100% EGFP. Columns represent the mean of quadruplicate measurements and the error bars represent the SD. *P*-values were calculated using Student's paired t-test. (*) $P \leq 0.05$, (**) $P \leq 0.01$. This experiment was repeated with V6MA2r and RNA was harvested 25 days later. The relative expression level of RUVBL2 was 1, 0.8 and 0.92 respectively. B) The plots show the accumulation in V6MA2r (right) and V6MA3r (left) cell number following transduction with control shRNA (diamonds), MLL.2 shRNA (squares) and MLL.5 shRNA (triangles). The transduced cells were selected with puromycin two days later and treated for four (left) and six (right) days. All the cultures started at a density of 0.25×10^6 cells per ml. V6MA2r and V6MA3r cells were in culture for approximately 66 and 73 days respectively. In the plots, measurement of the fold accumulation started on the day the cells came out of puromycin selection. Viable cell numbers were evaluated using trypan blue exclusion. In the plot on the left, each point represents the mean of triplicate measurements and the error bars represents the SD. In the plot on the right, each point represents a single measurement.

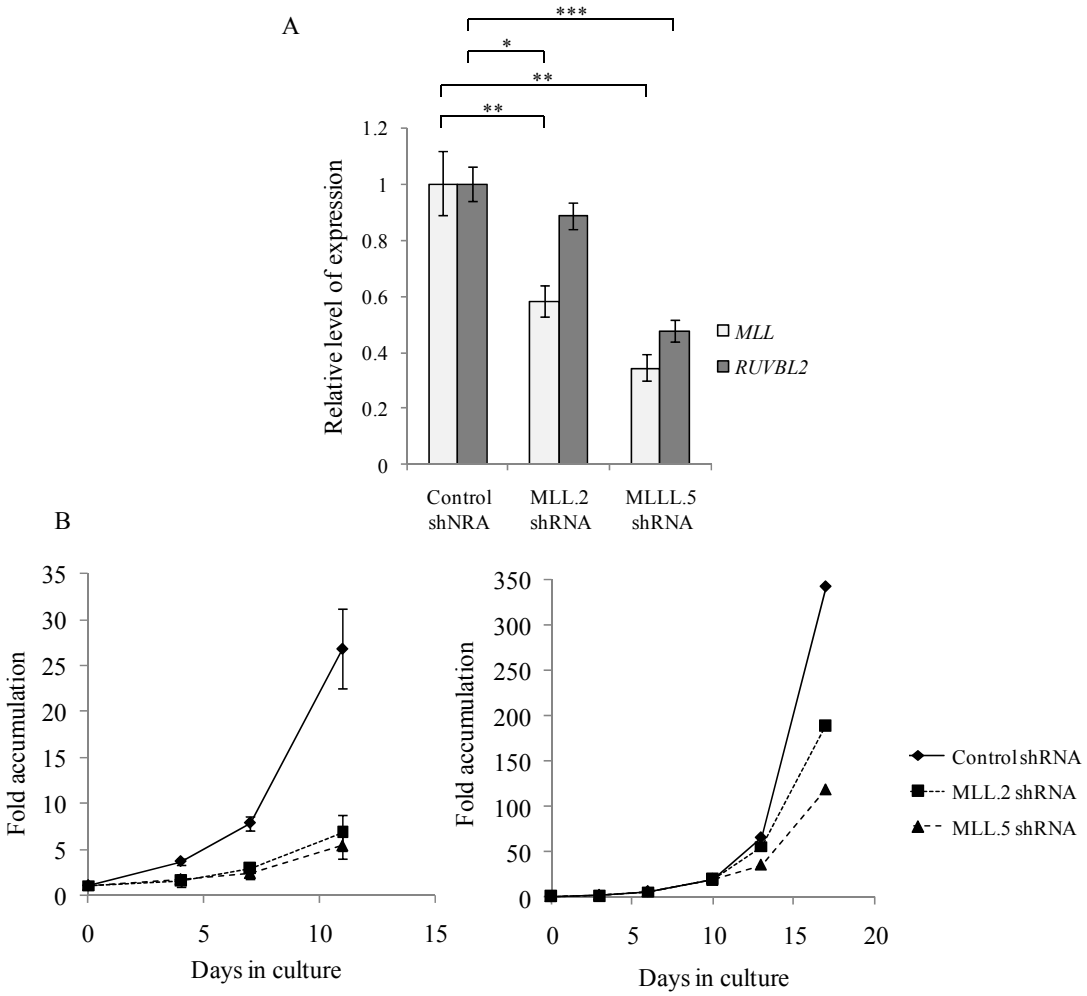
A
***
*
**
**
1.2
1
0.8
0.6
0.4
0.2
0
Relative level of expression
MLL
RUVBL2
Control shNRA
MLL.2 shRNA
MLLL.5 shRNA
B
35
30
25
20
15
10
5
0
Fold accumulation
0
5
10
15
Days in culture
350
300
250
200
150
100
50
0
Fold accumulation
0
5
10
15
20
Days in culture
Control shRNA
MLL.2 shRNA
MLL.5 shRNA

The shRNAs against *MLL* reduced *MLL* expression down to 58% (MLL.2 shRNA) and 45% (MLL.5 shNRA) in V6MA2r cells, compared to that of V6MA2r cells transduced with the control shRNA. This resulted in decreases of *RUVBL2* expression of 12% (MLL.2 shRNA) and 53% (MLL.5 shRNA). These results indicate that expression of *RUVBL2*, as well as that of *RUVBL1*, is likely to be induced by MLL-AF9 in the human immortalised cells. In order to confirm that reduction of *MLL-AF9* expression (and/or *MLL*) was sufficient for functional consequences in the V6MA cells, proliferation of the transduced cells was examined. The proliferation of V6MA2r cells and V6MA3r cells transduced with the MLL shRNA was monitored in liquid culture (Figure 5.10B). Compared to the accumulation of V6MA2r and VMA3r cells transduced with the control shRNA, there was a reduction in the accumulation of V6MA2r and V6MA3r cells transduced with the two shRNA against *MLL*.

5.9. Human leukaemic cell lines require *RUVBL2* expression to persist in culture

In order to examine whether *RUVBL2* expression was necessary for proliferation of human myeloid leukaemic cells, as *RUVBL1* expression was found to be, *RUVBL2* expression was silenced by shRNAs in THP-1 cells. THP-1 cells were transduced with five shRNAs against *RUVBL2* and mRNA was harvested five days (Figure 5.11A left) and 14 days (Figure 5.11A right) after transduction to measure *RUVBL2* expression by QPCR analysis (Figure 5.11A). The data show that all of the shRNAs tested led to 80% reductions in *RUVBL2* expression, compared to THP-1 cells transduced with control shRNA (Figure 5.11A left). The same data were also observed when the experiment was repeated with RUVBL2.3 and RUVBL2.5 shRNA (Figure 5.11A right).

Figure 5.11. Inhibition of the RUVBL2 expression decreases proliferation rate of THP-1 cells

A) The bar graph shows the relative level of *RUVBL2* mRNA expression, measured by QPCR in THP-1 cells after lentiviral transduction with control shRNA and several different shRNAs targeting *RUVBL2*. RNA was harvested five days (left) and 14 days (right) after transduction. Values for gene expression were normalised to THP-1 cells transduced with control shRNA. Columns represent the mean of quadruplicate measurements and the error bars represent the SD. *P*-values were calculated using Student's paired t-test. (***) $P \leq 0.001$. B) The plots represent two independent experiments measuring the accumulation in THP-1 cell number after transduction with control shRNA (diamonds), RUVBL2.3 shRNA (squares) and RUVBL2.5 shRNA (triangles). All the cultures started at a density of 0.5×10^6 cells per ml. The transduced cells were selected with puromycin two days later and treated for three days. Viable cell numbers were evaluated using trypan blue exclusion. In the plot, each point represents the mean of triplicate measurements and the error bars represent the SD.

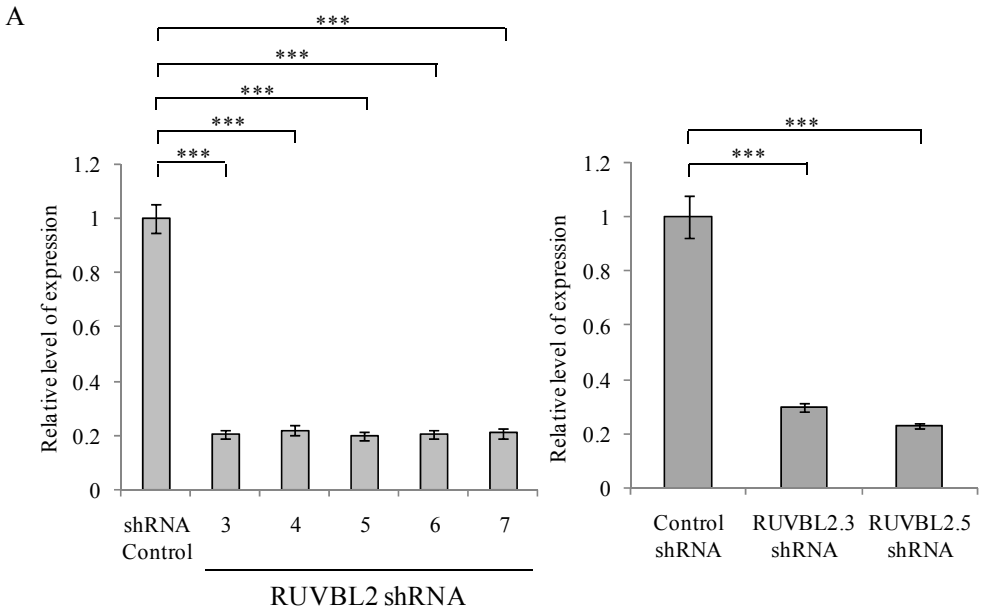
A
***
***
***
***
***
1.2
1
0.8
0.6
0.4
0.2
0
Relative level of expression
shRNA Control
3
4
5
6
7
RUVBL2 shRNA
***
***
Control shRNA
RUVBL2.3 shRNA
RUVBL2.5 shRNA

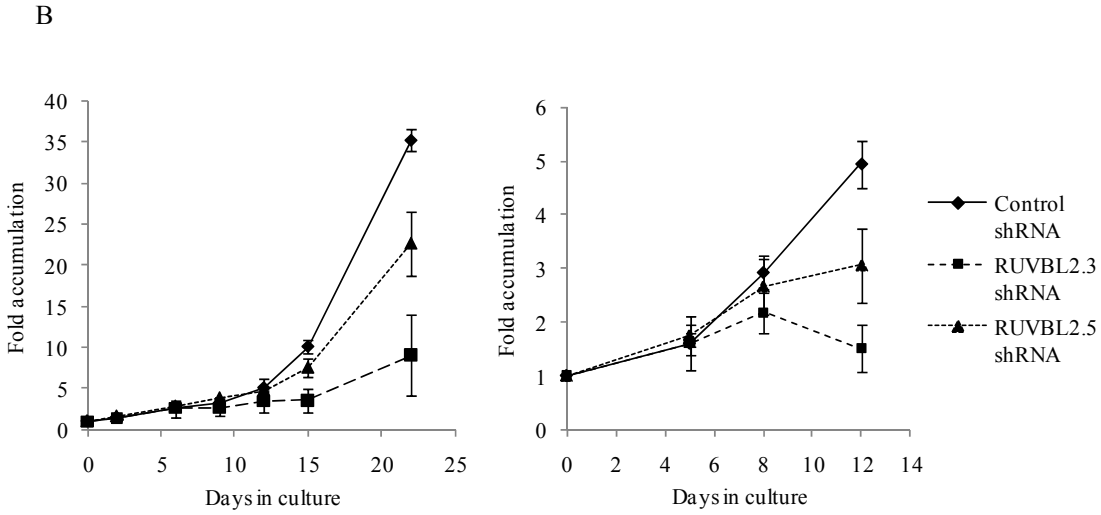
B
Fold accumulation
Days in culture
Control shRNA
RUVBL2.3 shRNA
RUVBL2.5 shRNA

The effect of *RUVBL2* knock-down on the proliferation capacity of THP-1 cells was also measured (Figure 5.11B). RUVBL2.3 and RUVB2.5 shRNAs were used to silence *RUVBL2* expression for this experiment. Whereas control THP-1 cells proliferated exponentially, THP-1 cells transduced with RUVBL2.3 and RUVBL2.5 shRNA accumulated at a significantly slower rate. Taken together, these data indicate that *RUVBL2*, as well as *RUVBL1*, expression is necessary for the proliferation of human leukaemic cells.

Since the loss of *RUVBL2* expression affected the proliferation capacity of THP-1 cells, we sought to determine the effect of decreased RUVBL2 expression in other human myeloid leukaemic lines. We first tested all the RUVBL2 shNRAs to determine which shRNA causes the strongest effect in THP-1 and NOMO-1 cells (Figure 5.12A). The data showed that RUVBL2.3 shRNA induced the strongest reduction in the percentage of EGFP positive cells in transduced NOMO-1 and THP-1 cells over the 12 days analysed. A panel of human myeloid leukaemic cells was then transduced with RUVBL2 shRNA and the percentages of EGFP positive leukaemic cells were followed over time (Figure 5.12B). The percentage of EGFP positive cells in all of the leukaemic cells transduced with RUVBL2.3 shRNA declined over the 16 days analysed. In particular, the strongest reductions were observed in THP-1, MONO-MAC6 and KASUMI-1 cells. These results suggest that, consistent with a requirement for *RUVBL1*, the expression of *RUVBL2* was necessary to maintain proliferation of human myeloid leukaemic cells.

Figure 5.12. Inhibition of RUVBL2 expression results in loss of transduced cells from culture

A) The graphs represent the persistence of EGFP positive human leukaemic cells (THP-1 and NOMO-1). Lentivirally transduced leukaemic cells (viral supernatant diluted to 6% and 50% for transducing THP-1 and NOMO-1 cells respectively) were transduced with shRNA against control (blue), RUVBL2.3 (red), RUVBL2.4 (green), RUVBL2.4 (pink), RUVBL2.5 (purple), and RUVBL2.6 (orange). EGFP expression was determined by flow cytometric analysis at the indicated time points. Cultures were re-plated approximately every three to four days. B) Each graph represents the persistence of EGFP positive human leukaemic cells. Human leukaemic cells were transduced with control shRNA (blue) or RUVBL2.3 shRNA (red). EGFP expression was determined by flow cytometric analysis at the indicated time point. Cultures were re-plated approximately every 3 to 4 days. Viral supernatant was diluted to 6% prior to transduction.

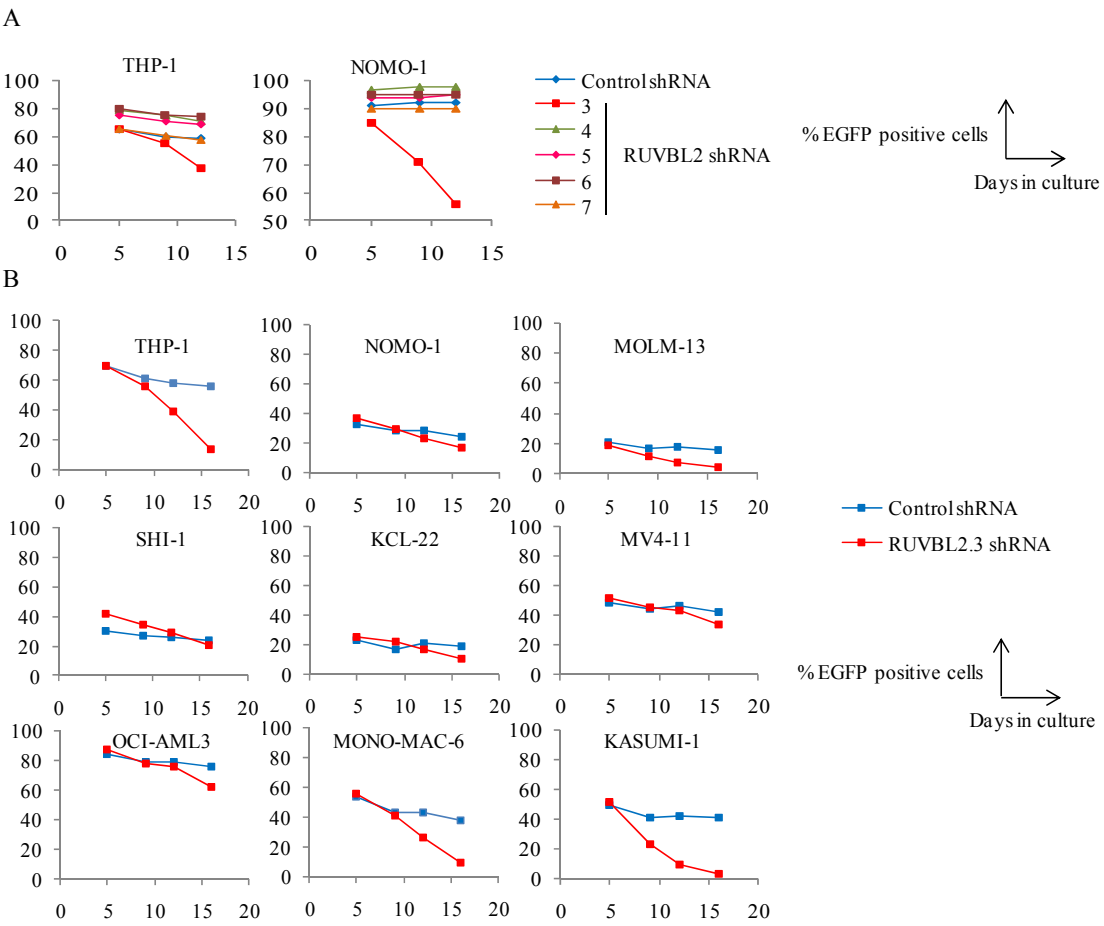
A
THP-1
NOMO-1
Control shRNA
3
4
5
6
7
RUVBL2 shRNA
% EGFP positive cells
Days in culture
B
THP-1
NOMO-1
MOLM-13
SHI-1
KCL-22
MV4-11
OCI-AML3
MONO-MAC-6
KASUMI-1
Control shRNA
RUVBL2.3 shRNA
% EGFP positive cells
Days in culture

5.10. The conserved Walker B motif in *RUVBL2* is required for normal THP-1 proliferation

In order to establish whether the Walker B motif in RUVBL2 is also required for proliferation of THP-1 cells, as was the case for RUVBL1, THP-1 cells were transduced with the RUVBL2 (D299N) expression lentiviral vector, or the empty vector negative control. Transduced THP-1 cells were selected with puromycin two days after transduction. Cell counts were then taken at various time-points to calculate the fold accumulation over 12 days (Figure 5.13). THP-1 cells transduced with RUVBL2 (D299N) initially accumulated, but decreased in cell number after five days of culture. In contrast, the THP-1 cells transduced with the negative control vector proliferated exponentially. This result suggests that the Walker B motif in RUVBL2 is also necessary to maintain the cell proliferation of THP-1 cells.

The protein expression of RUVBL2 was also measured following shRNA transduction of THP-1 cells. Transduced THP-1 cells were selected with puromycin two days after transduction. Protein was then harvested nine days (Figure 5.14 A) and five days (Figure 5.14 B) after transduction, in two independent experiments. Upon inhibition of *RUVBL2* expression using *RUVBL2.3* and *RUVBL2.5* shRNA, RUVBL2 protein expression decreased to 0.3 and 0.4 of that of the control, respectively (Figure 5.14 A), and 0.3 and 0.2 of that of the control, respectively (Figure 5.14 B). In addition, RUVBL1 protein expression was also reduced, to 0.2 and 0.3 upon RUVBL2 inhibition, which is consistent with previous studies (Venteicher et al., 2008).

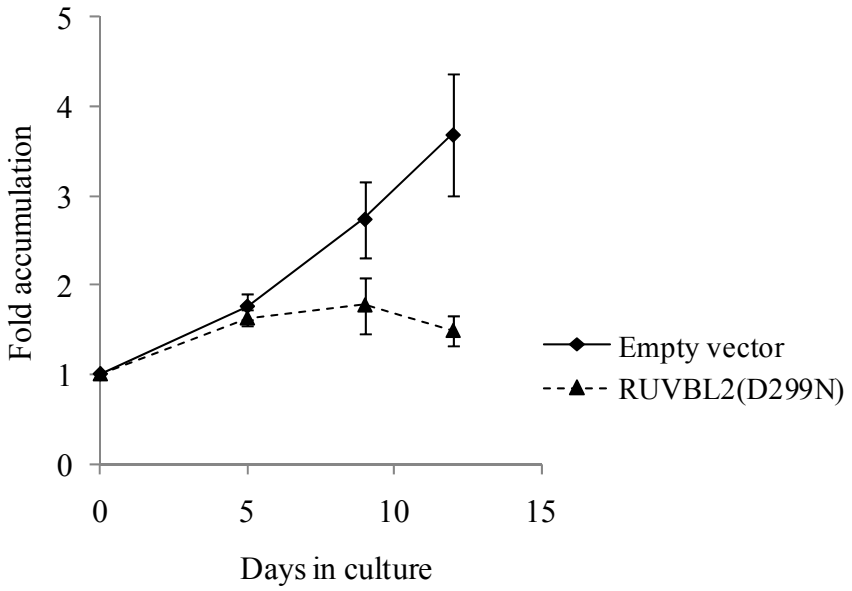

Figure 5.13. The Walker B motif of RUVBL2 is necessary to maintain proliferation of THP-1 cells

The diagram shows the accumulation in THP-1 cell number after lentiviral transduction with empty vector (diamonds) and RUVBL2 (D299N) (triangle). The transduced cells were selected with puromycin two days after transduction for three days. All the cultures started at a density of $0.5x10^6$ cells per ml. Viable cell numbers were evaluated using trypan blue exclusion. Each point represents the mean of triplicate measurements and the error bars represent the SD. Similar results have since been obtained from two independent experiments by others in the laboratory.

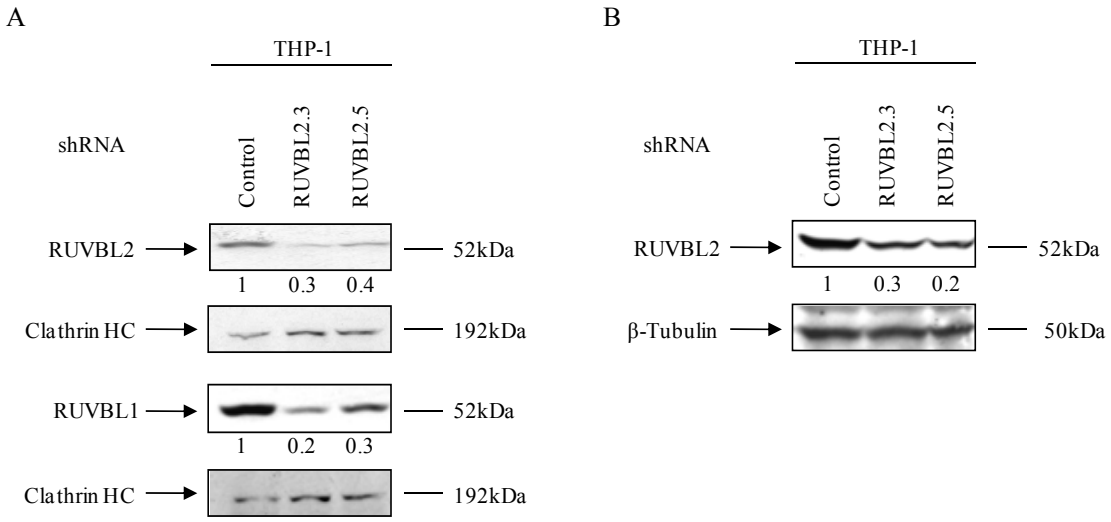

Figure 5.14. shRNA causes efficient knock-down of RUVBL2 protein expression

The figure shows western blot analyses of total lysates from THP-1 cells lentivirally transduced with control, RUVBL2.3 or RUVBL2.5 shRNA in two independent experiments. The transduced cells were selected with puromycin two days after transduction for three days. RNA was harvested A) nine and B) five days after transduction. The western blots were probed with either a primary goat polyclonal anti-RUVBL1 antibody or a primary mouse monoclonal anti-RUVBL2 antibody and either with a secondary donkey anti-goat or sheep anti-mouse HRP. An Anti-Clathrin-HC or anti-βTubulin antibody was used to control for protein loading. Values for protein expression were normalised to THP-1 cells transduced with control shRNA.

This co-depletion of RUVBL1 and RUVBL2 protein expression suggests that *RUVBL2* silencing destabilises a heterotypic complex formation of RUVBL1 and RUVBL2. We therefore decided to address the function of RUVBL1 and RUVBL2 in human leukaemic cells using RUVBL2 shRNA in subsequent experiments.

5.11. Inhibition of *RUVBL2* expression decreases cell proliferation in V6MA cells

Since *RUVBL2* expression is required for normal proliferation in human leukaemic cells, the effect of inhibiting *RUVBL2* expression in V6MA cells was then addressed. V6MA3r and V6MA2r cells were transduced with RUVBL2.3 shRNA and treated with puromycin two days after transduction, for three days. Following the confirmation of transduction by cytometric analysis (data not shown), RNA was harvested from the transduced cells 22 days (Figure 5.15A right) and 12 days (Figure 5.15A left) later, to determine the *RUVBL2* expression, in two independent experiments. QPCR analysis showed that RUVBL2.2 shRNA reduced *RUVBL2* expression down to 25% in V6MA3r (Figure 5.15A left) and to 67% in V6MA2r (Figure 5.15A right) compared to that of control shNRA. The corresponding fold accumulation of V6MA3r and V6MA2r cells was then monitored (Figure 5.15B). While control V6MA3r and V6MA2r proliferated exponentially, V6MA cells transduced with RUVBL2.3 shRNA accumulated at a significantly slower rate. Taken together, these data suggest that *RUVBL2* expression is also essential for the proliferation of CB-derived immortalised MLL-AF9 cells.

Figure 5.15. Inhibition of the RUVBL2 expression decreases proliferation rate of human MLL-AF9 immortalised myeloid cells

A) The bar graphs show the relative levels of *RUVBL2* mRNA expression, measured by QPCR in V6MA3r cells (left) and V6MA2r cells (right), and after lentiviral transduction with control shRNA and RUVBL2.3 shNRA. RNA was harvested 22 days (right) and 12 days (left) after transduction. Values for gene expression were normalised to V6MA cells transduced with control shRNA. Columns represent the mean of quadruplicate measurements and the error bars represent the SD. *P*-values were calculated using Student's paired t-test. (***) $P \leq 0.001$. B) The plots show the accumulation in V6MA3r (left) and V6MA4r cell (right) number after transduction with control shRNA (diamonds), RUVBL2.3 shRNA (squares). All the cultures started at a density of 0.25×10^6 cells per ml. V6MA2r and V6MA3r were in culture for approximately 52 and 73 days, after confirmation that these lines expressed 100% EGFP expression, respectively. The transduced cells were selected with puromycin two days later and treated for seven (left) and four (left) days. Viable cell numbers were evaluated using trypan blue exclusion. In the plots, measurement of the fold accumulation started on the day the cells came out of puromycin selection. In the plot on the left, each point represents the mean of triplicate measurements and the error bars represent the SD. In the plot on the right, each point represents a single measurement.

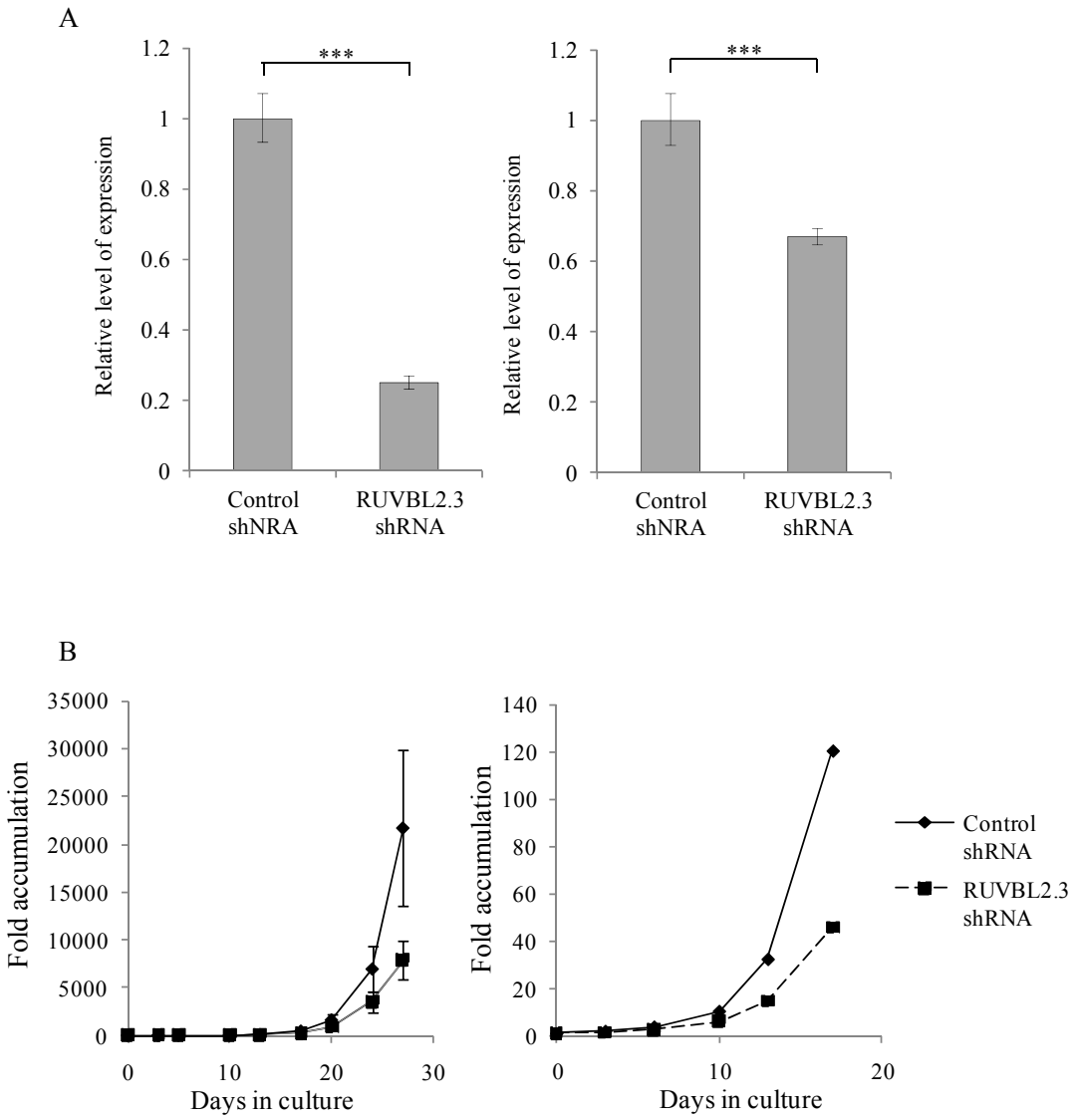
A
1.2
1
0.8
0.6
0.4
0.2
0
***
Relative level of expression
Control shNRA
RUVBL2.3 shRNA
1.2
1
0.8
0.6
0.4
0.2
0
***
Relative level of epxression
Control shNRA
RUVBL2.3 shRNA
B
35000
30000
25000
20000
15000
10000
5000
0
Fold accumulation
0
10
20
30
Days in culture
140
120
100
80
60
40
20
0
Fold accumulation
0
10
20
Days in culture
Control shRNA
RUVBL2.3 shRNA

5.12. Knock-down of *RUVBL2* induces apoptosis and differentiation of THP-1 cells

To address the functional basis for the decrease in cell proliferation upon inhibition of *RUVBL2* in human myeloid leukaemic cells, apoptosis was measured in THP-1 cells transduced with RUVBL2 shRNA, 19 days after the transduction. The transduced cells were stained with Annexin V and DAPI to detect early (AnnexinV^{+} DAPI^{-}) and late stage (Annexin^{+} DAPI^{+}) apoptotic cells (Figure 5.16A, 5.16B and 5.16C). An increase in the percentage of Annexin V positive THP-1 cells transduced with the shRNA targeting *RUVBL2* was observed when compared with THP-1 cells transduced with control shRNA. This result indicates that the inhibition of *RUVBL2* expression induces apoptosis in THP-1 cells.

CD15 expression was previously analysed in human CB-derived immortalised cells in Chapter Three. V6MA cells generated in this study were found to express intermediate levels of CD15 and this expression varied depending on the maturation states of the cells. The expression of CD15 in THP-1 cells was previously used to examine their differentiation (Prieto et al., 1994). For these reasons, we decided to analyse the expression of CD15 in THP-1 cells following knock-down of *RUVBL2* expression. THP-1 cells were transduced with shRNA against *RUVBL2* and cultured for 19 days. The transduced THP-1 cells were then stained for CD15 expression and analysed by flow cytometry (Figure 5.16D and Figure 5.16E). Knock-down of *RUVBL2* expression resulted in a uniform increase in average CD15 mean fluorescence intensity in the transduced THP-1 cells.

Figure 5.16. Inhibition of the RUVBL2 expression increases apoptosis in THP-1 cells

A) The dot plots show flow cytometric analysis of lentivirally transduced THP-1 cells with control, RUVBL2.3 or RUVBL2.5 shRNA, 19 days after transduction. The cells were stained with Annexin V and DAPI. Numbers below represent the percentage of cells within each quadrant. B) The bar graph shows the percentage of Annexin V positive THP-1 cells. Columns represent the mean of triplicate measurements and the error bars represent the SD. *P*-values were calculated using Student's paired t-test. (*) $P \leq 0.05$, (***) $P \leq 0.001$. C) The bar graph shows the average fold increase over control cells of Annexin V positive cells in three independent experiments. D) The bars represent the average mean fluorescence intensity of CD15 expression from the same experiment. Columns represent the mean of triplicate measurements and the error bars represent the SD. *P*-values were calculated using Student's paired t-test. (**) $P \leq 0.01$. E) The histogram shows an example of mean intensity of CD15 expression resulting from the control (black), RVBL2.3 (red) and RUVBL2.5 (blue) shRNAs. Filled grey areas represent unstained THP-1 cells.

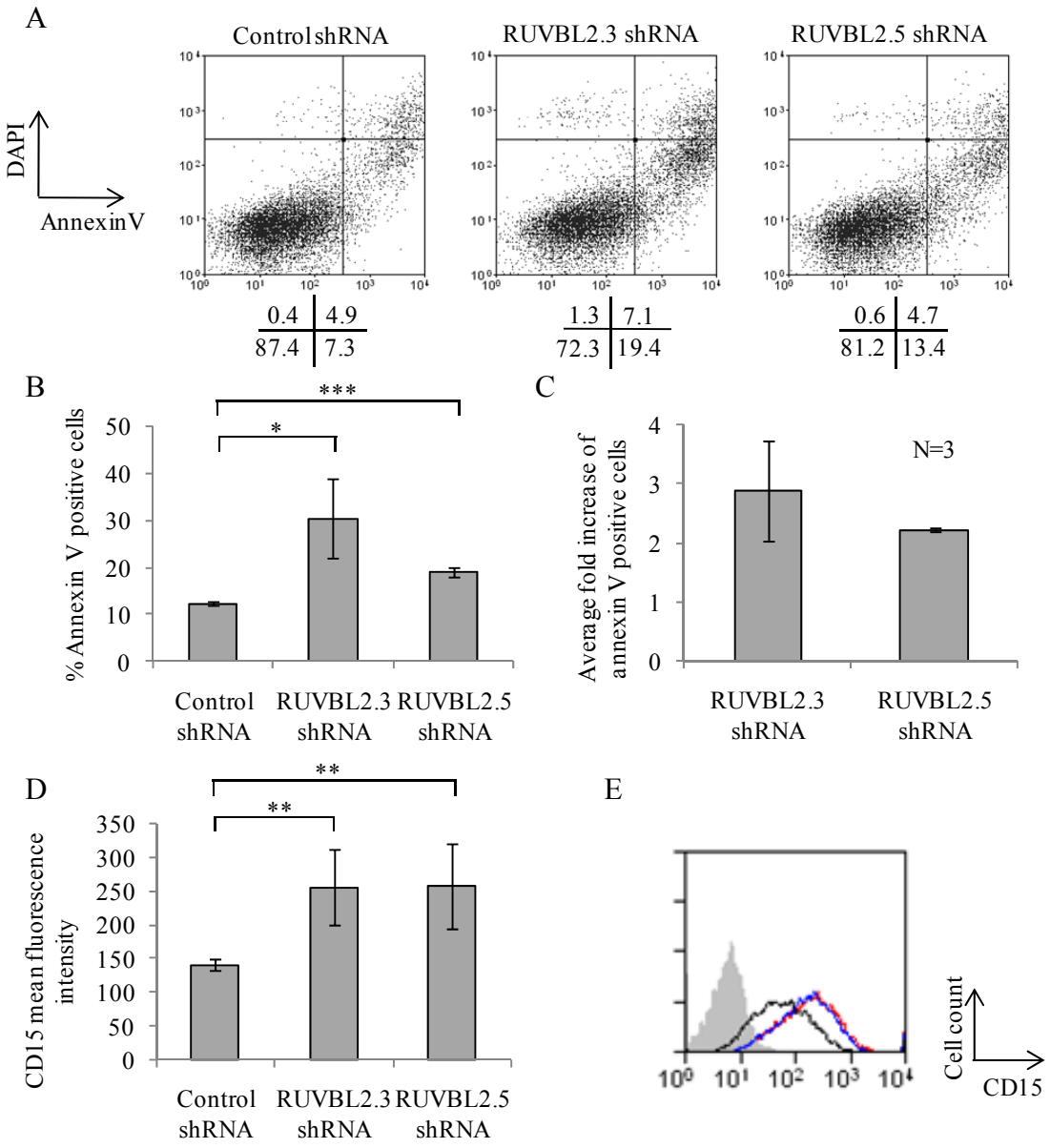
A
Control shRNA
RUVBL2.3 shRNA
RUVBL2.5 shRNA
DAPI
AnnexinV
0.4 4.9
87.4 7.3
1.3 7.1
72.3 19.4
0.6 4.7
81.2 13.4
B
% Annexin V positive cells
Control shRNA
RUVBL2.3 shRNA
RUVBL2.5 shRNA
C
Average fold increase of annexin V positive cells
N=3
RUVBL2.3 shRNA
RUVBL2.5 shRNA
D
CD15 mean fluorescence intensity
Control shRNA
RUVBL2.3 shRNA
RUVBL2.5 shRNA
E
Cell count
CD15

This result indicates that the decreased accumulation of cells associated with inhibition of *RUVBL2* expression was likely to result from a combination of the induction of apoptosis and differentiation.

5.13. *TERT* expression is up-regulated in V6MA cells

Until recently, the major role of RUVBL1 and RUVBL2 was believed to be that of chromatin re-modelling cofactors and transcriptional cofactors for c-Myc and β-catenin (Gallant, 2007). However, another important function of RUVBL1 and RUVBL2 was recently discovered when both were found to form part of the telomerase complex (Venteicher et al., 2008). Telomerase is a ribonucleoprotein enzyme complex that prevents shortening of telomeres by adding specific DNA sequences at their ends (Blackburn, 1991; Blasco et al., 1997; Blackburn, 2001; Venteicher et al., 2008). The mammalian telomere repeat sequence, TTAGGG, is extended by the telomerase complex, which consists of telomerase reverse transcriptase (TERT) and telomerase RNA (TERC) components (Blackburn, 1991; Blasco et al., 1997; Blackburn, 2001). RUVBL1 was shown to interact with TERT and RUVBL2 was also demonstrated to be recruited to TERT by RUVBL1 (Venteicher et al., 2008). Since high levels of telomerase activity have previously been demonstrated in CB-derived MLL-AF9 cells (Wei et al., 2008), and since we found both *RUVBL1* and *RUVBL2* to be up-regulated in V6MA cells, we examined the expression of *TERT* in these cells. mRNA was harvested from V6, V6MA and AE9A2r cells and *TERT* mRNA expression was measured by QPCR. It should be noted that the V6MA cells used for this analysis were in culture for different periods of time. V6MA1v cells were cultured for at least 105 days, V6MA2r cells were cultured for 100 days and V6.3v and V6MA3r cells were cultured for 57

days, when the RNA was harvested (Figure 5.17A). *TERT* expression was also measured in an independent experiment in which the V6.3v, V6MA2r and V6MA3v cells were culture for 100 days, 195 days and 182 days respectively (Figure 5.17B). All of the V6MA cells expressed higher levels of *TERT* mRNA compared to V6 control cells. Surprisingly, the expression of *TERT* in V6MA3r cells was much higher than that in the other V6MA cells in one of the experiments (Figure5.17A).

5.14. RUVBL1 and RUVBL2 are required for *TERT* expression and telomerase activity in THP-1 cells

Increased expression of *RUVBL1* and *RUVBL2* was previously implicated in several cancers, including hepatocellular carcinoma, cervical cancer, colorectal cancer and gastric cancer (Lauscher et al., 2007; Li et al., 2010; Menard et al., 2010). Furthermore, silencing of *RUVBL1* and *RUVBL2* expression in cervical and gastric cancer cell lines was shown to reduce *TERT* mRNA expression, and this reduction was accompanied by decreased telomerase activity (Li et al., 2010). Based on this evidence and our results, we hypothesized that RUVBL1 and RUVBL2 are required for MLL-fusion induced telomerase activity in human immortalised and leukaemic cells. To test this hypothesis, we first measured the mRNA expression of *TERT* in THP-1 cells following silencing of *RUVBL2* expression. THP-1 cells were transduced with shRNA targeting *RUVBL2* and harvested six days (Figure 5.18A left) and 14 days (Figure 5.18A right) later to measure *TERT* mRNA expression. We also measured *TERT* mRNA expression in V6MA3r cells following lentiviral transduction with RUVBL2.3 shRNA (Figure 5.18B). In this experiment, transduced V6MA3r cells were harvested 15 days after transduction.

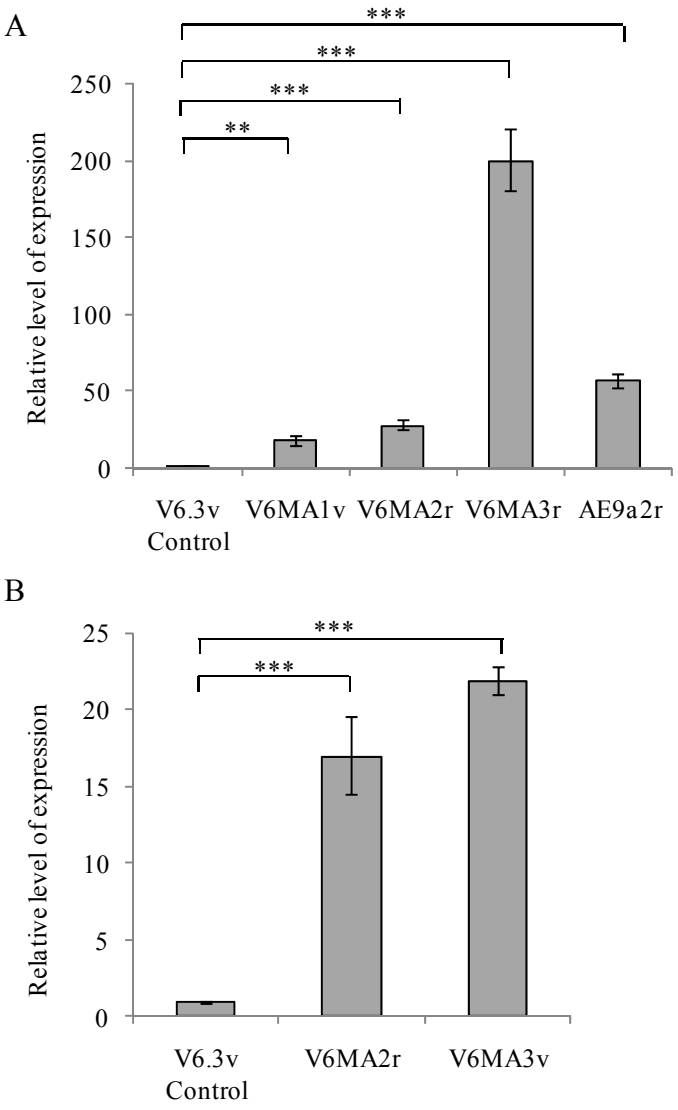

Figure 5.17. TERT mRNA expression is up-regulated in human CB-derived immortalised myeloid cells

The bar graphs show two independent measurements of the relative levels of *TERT* mRNA expression, measured by QPCR in V6, V6MAs and AE9a cells. Values for gene expression were normalised to V6.3v cells. A) V6MA cells exhibited 18–fold (V6MA1v), 27-fold (V6MA2r) and 200-fold (V6MA3r) increases in *TERT* expression over control V6 cells. B) V6MA cells displayed 17-fold (V6MA2r) and 22-fold (V6MA3r) increases in *TERT* expression over control V6 cells (bottom). Columns represent the mean of quadruplicate measurements and the error bars represent the SD. *P*-values were calculated using Student's paired t-test. (***) $P \leq 0.001$ (**) $P \leq 0.01$.

Figure 5.18. RUVBL2 knock-down reduces TERT expression in THP-1 cells and V6MA cells

A) The bar graphs show the relative level of *TERT* mRNA, measured by QPCR in THP-1 cells following lentiviral transduction with shRNA, targeting *RUVBL2*, in two independent experiments. The transduced cells were selected with puromycin two days later for three days. RNA was harvested six days (left) and 14 days (right) after transduction. Values for gene expression were normalised to THP-1 cells transduced with control shRNA. Columns represent the mean of quadruplicate measurements and the error bars represent the SD. *P*-values were calculated using Student's paired t-test. (*) $P \leq 0.05$, (**) $P \leq 0.01$. B) The bar graph shows the relative levels of *TERT* mRNA expression, measured by QPCR, in V6MA3r cells following lentiviral transduction with shRNA targeting RUVBL2. V6MA3r cells were in culture for approximately 52 days after confirming that EGFP expression was 100%. The transduced cells were selected with puromycin in the same way as described in Figure 5.18A and RNA was harvested 15 days after transduction. Values for gene expression were normalised to V6MA cells transduced with control shRNA. (*) $P \leq 0.05$. C) The figure shows western blot analysis of total lysates from THP-1 cells lentivirally transduced with control, RUVBL2.3 or RUVBL2.5 shRNA. The transduced cells were selected with puromycin two days later for three days. Cells were harvested five days after transduction. The western blot was probed with a primary rabbit anti-TERT antibody, and with a secondary donkey anti-rabbit IgG HRP. An anti-Clathrin-HC antibody was used to control for protein loading. Values for protein expression were normalised to THP-1 cells transduced with control shRNA. This experiment was repeated and values for TERT protein expression were 0.6 and 0.6, to that of control respectively.

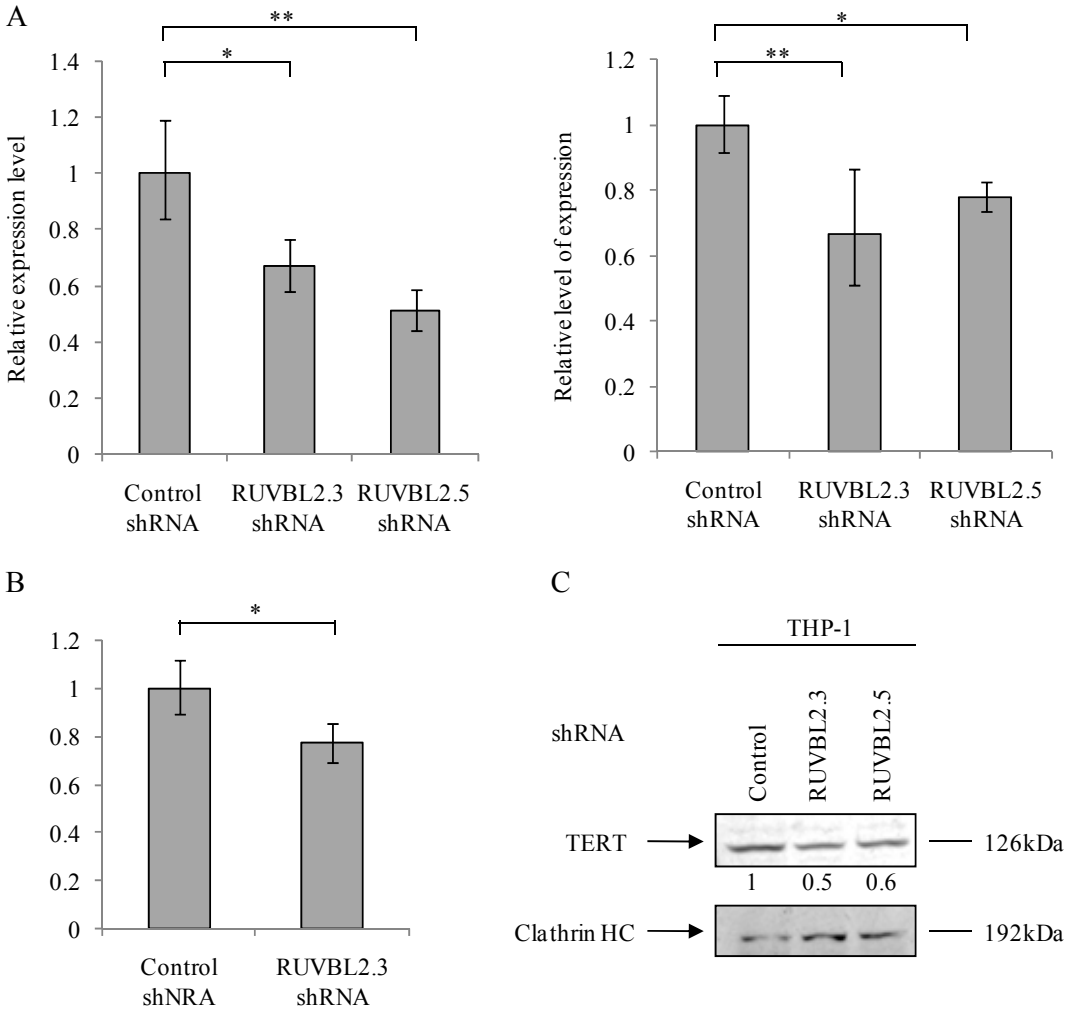
A
**
*
1.4
1.2
1
0.8
0.6
0.4
0.2
0
Relative expression level
Control shRNA
RUVBL2.3 shRNA
RUVBL2.5 shRNA
*
**
1.2
1
0.8
0.6
0.4
0.2
0
Relative level of expression
Control shRNA
RUVBL2.3 shRNA
RUVBL2.5 shRNA
B
*
1.2
1
0.8
0.6
0.4
0.2
0
Control shNRA
RUVBL2.3 shRNA
C
THP-1
shRNA
Control
RUVBL2.3
RUVBL2.5
TERT
126kDa
1
0.5
0.6
Clathrin HC
192kDa

Consistent with Li *et al*'s work, a reduction in *TERT* mRNA expression was observed both in THP-1 and V6MA3r cells (Li et al., 2010). The experiment outlined in Figure 5.18A was repeated to examine TERT protein expression after silencing of *RUVBL2* expression in THP-1 cells (Figure 5.18C). In this experiment, the total cell lysates from Figure 5.14A were analysed for changes in TERT protein expression (Figure 5.18B left). Consistent with the change in *TERT* mRNA expression, a decrease in TERT protein levels was observed in THP-1 cells transduced with RUVBL2.3 and 5 shRNA, compared to the THP-1 cells transduced with control shRNA. This was confirmed in an independent experiment and protein expression after RUVBL2 knock-down was 0.6 and 0.6 respectively (data not shown). We then measured the activity of telomerase in THP-1 cells in which the expression of *RUVBL2* was inhibited. Transduced THP-1 cells were harvested 21 days (Figure 5.19 top) or 12 days (Figure 5.19 bottom) later to measure the telomerase activity in two independent experiments. As expected, telomerase activity was significantly reduced in THP-1 cells transduced with RUVBL2 shRNAs, compared to that in THP-1 cells transduced with control shRNA. These results indicate that the expression of *RUVBL2* is required for the maintenance of the *TERT* expression and for telomerase activity in THP-1 cells.

5.15. *RUVBL2* expression is required in order to maintain the clonogenic potential of THP-1 cells

Loss of *RUVBL2* and *TERT* expression was previously shown to affect the clonogenic potential of gastric cancer cells (Zhang et al., 1999; Li et al., 2010).

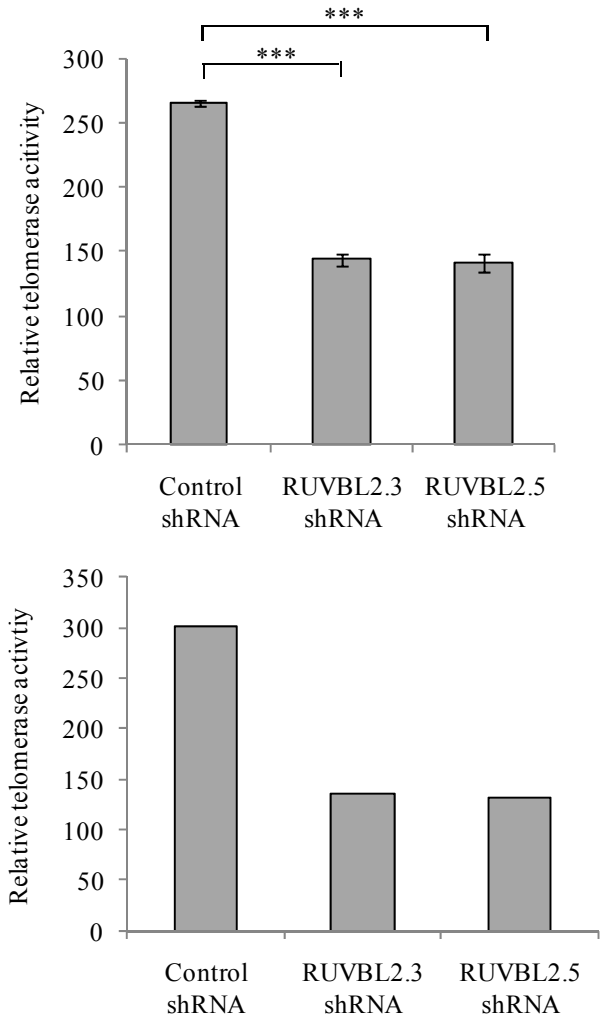

Figure 5.19. Inhibition of RUVBL2 expression results in decreased telomerase activity in THP-1 cells

The bar graphs show the relative telomerase activity (RTA) in THP-1 cells following lentiviral transduction with shRNA targeting *RUVBL2*, in two independent experiments. RNA was harvested 21 days (top) and 12 days (bottom) after transduction. Values for RTA were normalised to THP-1 cells transduced with control shRNA. Columns represent the mean of quadruplicate measurements and the error bars represent the SD. *P*-values were calculated using Student's paired t-test. (*) $P \leq 0.05$, (**) $P \leq 0.01$. A similar pattern of RTA was observed in an independent experiment.

To determine whether *RUVBL2* expression also affected the clonogenic potential of human leukaemic cells, colony formation assays were performed with transduced THP-1 cells. In three independent experiments, THP-1 cells, transduced with shRNA targeting *RUVBL2*, were transferred into methylcellulose 21 days after transduction (Figure 5.20A) and colony formation was measured after a further 14 days (experiment performed by Mr Maurizio Mangolini, MHCB Unit, ICH). Transduction of THP-1 cells with RUVBL2 shRNA reduced the average colony number, down to 0.1 compared to that of control shRNA. These data confirm that RUVBL2, and RUVBL1, are essential in order to maintain the clonogenic potential of THP-1 cells.

5.16. Discussion

In this chapter, we have presented data suggesting that RUVBL1 and RUVBL2 are important key regulators of MLL-AF9 induced leukaemia, in human models. Several studies suggest that RUVBL1 and RUVBL2 also interact with the transcription factor MYC (Wood et al., 2000; Dugan et al., 2002; Bellosta et al., 2005; Maslon et al., 2010). This interaction was shown to take place via the c-Myc domain box II (MBII) of c-Myc, a region critical for the biological activities of c-Myc, including transformation (Wood et al., 2000). C-Myc was found to bind to RUVBL1 in a region between the Walker A and B motifs (Wood et al., 2000). This interaction is evolutionally conserved, also having been demonstrated in *Drosophila* (Bellosta et al., 2005).

Figure 5.20. Knock-down of RUVBL2 expression inhibits the clonological potential of THP-1 cells

A) The pictures show methylcellulose cultures of THP-1 cells transduced with control, RUVBL2.3 or RUVBL2.5 shRNA. THP-1 cells were transduced and puromycin selected two days after transduction and plated 21 days later. The THP-1 colonies were stained with p-iodonitrotetrazolim 14 days after plating. B) The bar graph shows the average fold change in duplicate colony numbers of the transduced THP-1 cells with shRNA, against control and RUVBL2.3, in three independent experiments. Values for colony numbers were normalised to the mean of THP-1 cells transduced with control shRNA. Columns represent the mean of triplicate measurements and the error bars represent the SD. *P*-values were calculated using Student's paired t-test. (***) $P \leq 0.001$.

A

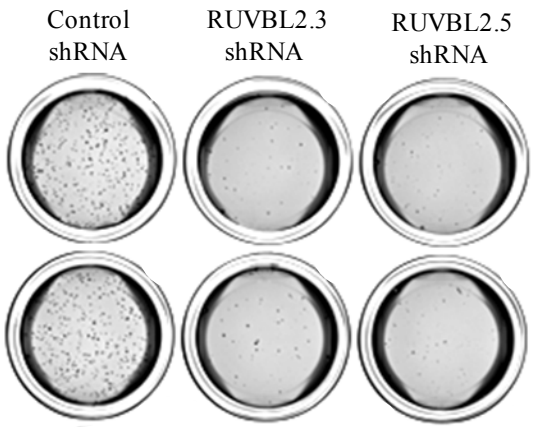
Control shRNA
RUVBL2.3 shRNA
RUVBL2.5 shRNA

B

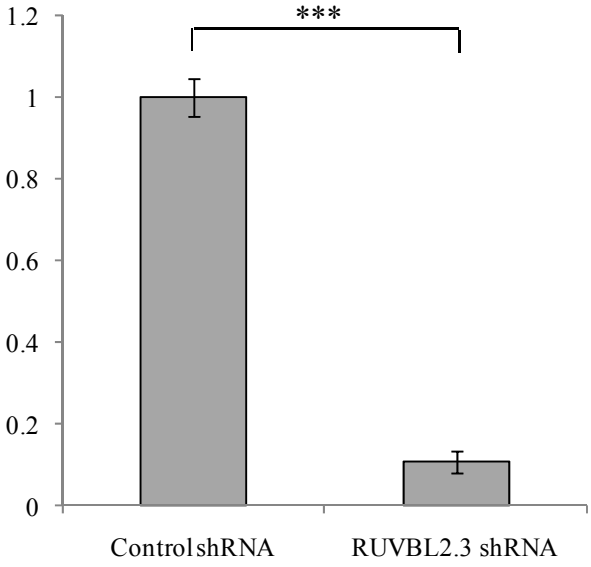
***
1.2
1
0.8
0.6
0.4
0.2
0
Control shRNA
RUVBL2.3 shRNA

Data from a conditional model of c-MYC expression in human Burkitt's lymphoma suggested that *RUVBL1* and *RUVBL2* were also transcriptionally regulated by c-MYC (Fan et al., 2010). Global gene expression data from our laboratory suggested that MLL-fusions may directly or indirectly induce *Ruvbl1* and *Ruvbl2* expression. Furthermore, our data showed that expression of RUVBL1 and RUVBL2, in conditionally immortalised murine MLL-AF9 cells, decreased following Dox treatment, while this decrease was not apparent (RUVBL1), or was less marked (RUVBL2) (in one of the experiments), after G-CSF treatment. This reduction in RUVBL1 and RUVBL2 expression following loss of MLL-fusions is in agreement with previous studies (Hess et al., 2006). Hess *et al* conditionally immortalised murine MLL-ENL cells, which were then co-transduced with constitutive murine *Meis1* and *HoxA9* expression constructs, and performed global gene expression analysis following loss of MLL-ENL expression (Hess et al., 2006). This analysis identified genes that were regulated by HOXA9 and MEIS1 in MLL-fusion immortalised cells. Expression of *Hoxa9*/*Meis1* resulted in a 2.3-and 2.2-fold up-regulation of *Ruvbl1* and *Ruvbl2* expression, respectively, in comparison to control cells, upon loss of MLL-ENL expression. This work suggests that MLL-fusions may induce expression of *Ruvbl1* and *Ruvbl2* via up-regulation of HOXA9 and MEIS1. However, it is still unclear whether HOXA9 and MEIS1 can directly induce *Ruvbl1* and *Ruvbl2* expression, or whether this occurs indirectly via induction of other transcription factors, such as MYC or MYB. Moreover, our work suggests that MLL-AF9, directly or indirectly, is responsible for up-regulation of both RUVBL1 and RUVBL2 in both human and mouse immortalised myeloid cells.

Knock-out of *RUVBL1(pont)* and *RUVBL2(rept)* in *Drosophila* was lethal at the early larval stage, indicating that their expression is crucial from early development, although absence of their expression did not affect embryogenesis (Bauer et al., 2000; Bellosta et al., 2005). Another group over-expressed *RUVBL1(pont)* and *RUVBL2(rept)* in *Xenopus laevis* embryos and showed an increased cell proliferation (Etard et al., 2005). Recently, Nerlov's group generated conditional Ruvbl1 knockout mice using the Cre-loxP approach. Their group demonstrated that a conditional knockout of RUVBL1 in the haematopoietic system in mice caused rapid lethality, similar to constitutive knockout mice, and this effect was due to total bone marrow failure (European Haematology Association 16th Congress, 8th-12th June 2011). We observed that *RUVBL1* and *RUVBL2* expression was important not only for maintaining MLL-AF9 expressing cells in culture, but was also necessary for the maintenance of other myeloid leukaemic cells. *RUVBL1* and *RUVBL2* expression has previously been found to be important for proliferation of other types of cancer cells, for example, human hepatoceullular carcinoma (Haurie et al., 2009; Menard et al., 2010). Considering RUVBL1 and RUVBL2 are involved in different complexes, and function both synergistically and antagonistically, it is difficult to say whether they function in promoting cancer and/or survival in the same way in all these different cell types.

The Walker B motif of RUVBL1 was also shown to be required for transformation by several oncogenes (Wood et al., 2000; Dugan et al., 2002; Feng et al., 2003; Jha and Dutta, 2009; Grigoletto et al., 2011). Wood *et al* showed an inhibition of MYC transforming activity when rat embryo fibroblast cells were co-transfected with c-MYC, H-RAS and RUVBL1 (D302N). A similar observation was also made using E1A and β-catenin with RUVBL1 (D302N) (Dugan et al., 2002; Feng et al., 2003). Although

these studies only used the RUVBL1 (D302N) mutant, our results with RUVBL2 (D299N) suggest that the Walker B motif is also required for RUVBL2 function in proliferating human leukaemic cells. Experiments with the dominant negative forms of RUVBL1 and RUVBL2 confirmed the shRNA knock-down data, suggesting that both these proteins appear to be of critical importance to immortalisation by MLL-AF9. Although our experiments demonstrate the importance of the Walker B motif for RUVBL1 and RUVBL2 function in MLL-fusion associated leukaemia, further work is required to establish whether this is due to DNA binding, or ATP hydrolysis, or both.

Structural analysis of RUVBL1 and RUVBL2 proteins in yeast suggest that they exist as monomers at low concentrations (5μM), whereas high concentrations (40μM) promote hetero-hexameric ring formation between RUVBL1 and RUVBL2 (Gribun et al., 2008). In addition, human recombinant RUVBL1 and RUVBL2 complexes were shown to exhibit higher ATPase activity than either of the proteins individually (Puri et al., 2007). We observed the co-depletion of RUVBL1 protein upon knock-down of *RUVBL2*. This reciprocal depletion of RUVBL1 and RUVBL2 is in agreement with the study by Venteicher *et al* (Venteicher et al., 2008). Their work showed that shRNA knock down of *RUVBL2* expression led to co-depletion of RUVBL1 protein expression in Hela cells, and *vice versa* upon RUVBL1 inhibition. Haurie *et al* made a similar observation using the human hepatocarcinoma model (Haurie et al., 2009). Their analysis suggests that this co-depletion does not affect the respective mRNA expression levels. The author suggested that loss of either RUVBL1 or RUVBL2 expression causes destabilisation of the hetro-hexameric ring, leading to ubiquitination and proteasome-dependent degradation. The same group also tested this effect on different cancer cells, including breast cancer and prostatic cancer cells, to prove that this is not a

cell lineage-specific event. Our data are therefore consistent with previously published work, suggesting that RUVBL1 and RUVBL2 exist in an interdependent manner. However, these proteins do appear to function antagonistically in some pathways.

We found that the inhibition of *RUVBL2* expression in THP-1 cells induced apoptosis and differentiation. Induction of apoptosis was observed in hepatocarcimoma cells upon *RUVBL2* inhibition by both constitutive and inducible shRNA systems (Rousseau et al., 2007; Menard et al., 2010). In constitutive shRNA knock-down experiments, Rousseau *et al* showed an increase in apoptosis following silencing *RUVBL2* in HuH7 hepatocarcinoma cells, and this increase was associated with induction of pro-apoptotic proteins Bad (Bcl-2 antagonist of cell death) and Bid (BH3-interacting domain death agonist). However, whether these members of the pro-apoptotic Bcl-2 family are directly targeted by RUVBL2 is not known (Rousseau et al., 2007). The same group also demonstrated that ectopic expression of RUVBL2 de-sensitizes HuH7 cells to apoptosis induced by C2 ceramide, indicating that RUVBL2 may have a role in cell survival upon exposure to stress (Rousseau et al., 2007).

Several markers have been used to show the differentiation of THP-1 cells. In the work of Kharas *et al*, differentiation of THP-1 cells was shown by increases in the percentage expression of CD16 and CD11b, while CD14 was used to assess THP-1 differentiation in Suzuki's work (Suzuki et al., 2009; Kharas et al., 2010). In our study, CD15 expression was used to assess differentiation in THP-1 cells, since its expression was found to increase upon differentiation of V6MA cells (Chapter 3). It was striking to observe that *RUVBL2* knock-down led to an increase in differentiation measured by CD15 expression. Knock-down of MLL-fusions were previously performed by others,

and although inhibition of proliferation was observed, no terminal differentiation was associated with the knock-down of MLL-fusions (Pession et al., 2003; Martino et al., 2006; Suzuki et al., 2009). In contrast, MYB knock-down in THP-1 cells led to terminal differentiation of THP-1 cells (Suzuki et al., 2009). However, it is not known whether *RUVBL2* mediates part or all of the MYB-induced differentiation block. Our data demonstrate that knock-down of *RUVBL2* expression not only induces apoptosis, but also differentiation. It would therefore be interesting to determine how RUVBL2 induces apoptosis and differentiation, and whether these two functional consequences were results of single or multiple pathways.

Activation of telomerase is a major phenomena in cancer, evident in more than 90% of human cancers (Flores et al., 2006). Since the initial discovery that RUVBL1 and RUVBL2 were part of the telomerase complex (Venteicher et al., 2008), two groups reported a link between telomerase activity and RUVBL2 function in oncogenesis (Li et al., 2010; Menard et al., 2010). One study in gastric and cervical cancer cells demonstrated a requirement of RUVBL2 for constitutive *TERT* expression and telomerase activity (Li et al., 2010). The same group also showed that this regulation was c-MYC dependent. Another group used an inducible shRNA system against *RUVBL2* to demonstrate a decrease in telomerase activity upon knock-down, accompanied by induction of senescence, in hepatocellular carcinoma cells (Menard et al., 2010). We have established the necessity of RUVBL2 to mediate *MLL*-fusion induced telomerase activity in human leukaemic cells. In addition, *TERT* expression decreased when *RUVBL2* was inhibited in THP-1 cells and V6MA3r cells. Furthermore, we provided evidence that *TERT* expression in CB-derived V6MA cells was higher than that in V6 cells. The presence of telomerase activity in CB-derived immortalised MLL-AF9 cells was first shown by Wei *et al* (Wei et al., 2008). This

group showed that CB-derived immortalised MLL-AF9 cells had higher telomerase activity compared to that of untransduced CB cells (Wei et al., 2008). However, they found no change in *TERT* mRNA expression. This discrepancy between Wei *et al.* and our work may be due to the different MLL-AF9 expression constructs used in each case, the exact fusion used, or the expression levels achieved in each system. Increased *TERT* expression has been shown to be associated with MLL-AF4 associated leukaemia (Gessner et al., 2010). Using siRNA directed at sequences in the breakpoint of *MLL-AF4* in SEMK-2 and RS4-11 cells, Gessener *et al* showed that MLL-AF4 knock-down resulted in a reduction in *TERT* expression and telomerase activity (Gessner et al., 2010). The same affect was also observed when *HOXA7*, a down-stream target of MLL-AF4, was silenced by shRNA. Chromatin immunoprecipitation (Chip) analysis further confirmed that HOXA7 binds to the promoter region of TERT (Gessner et al., 2010). Our data showed that RUVBL2, a direct or indirect down-stream target of MLL-fusions, regulates the expression of *TERT* and telomerase activity in THP-1 cells.

So how does RUVBL2 regulate *TERT* expression and telomerase activity? One study on gastric cancer cells suggests that RUVBL2 may regulate telomerase activity by two different mechanisms. RUVBL2 knock-down leads to a significant decrease in *TERT* promoter activity and mRNA expression (Li et al., 2010). Chip analysis further confirmed that RUVBL2 interacts with the *TERT* proximal promoter (Li et al., 2010). Interestingly, MYC was also shown by Chip analysis to bind to the TERT promoter, and this occupancy was diminished upon RUVBL2 depletion, suggesting that RUVBL2 regulates the transcription of *TERT* in a MYC dependent manner. Surprisingly, although RUVBL1 knock-down also caused reduced *TERT* mRNA expression, this may have been via an indirect effect on RUVBL2 protein expression levels, since RUVBL1

loss slightly increased rather than inhibited TERT promoter activity (Li et al., 2010). These data are yet another example of the antagonistic functions of these two proteins in some contexts. These findings, together with our data, suggest that RUVBL2 is a co-factor directly involved in inducing *TERT* expression.

Telomerase complexes are dynamic and exist in multiple forms, regulated by the cell cycle (Venteicher et al., 2008). Whereas the highly active form of telomerase contains TERT, TERC and Dyskerin (a TERC-binding protein), the TERT-RUVBL1-RUVBL2 complex is specific to the S phase of the cell cycle and is responsible for maintaining low telomearase activity (Baek, 2008; Venteicher et al., 2008). This complex is thought to be a pre-telomerase complex (Venteicher et al., 2008). RUVBL1 and RUVBL2 were also shown to be responsible for the accumulation of TERC and Dyskerin and the subsequent assembly of the highly active form of the telomerase complex (Baek, 2008; Venteicher et al., 2008). Therefore, loss of RUVBL1 or RUVBL2 may deplete the pre-telomerase complex from leukaemic cells and this in turn may result in lower levels of the active telomerase complex. It is therefore possible that RUVBL2 contributes to increased telomerase activity by influencing both transcriptional regulation of *TERT* and telomerase complex assembly.

Our data demonstrate that RUVBL2 expression is required for maintenance of transformation by MLL-AF9. This result is consistent with the findings of the study by Li *et al*, that RUVBL2 expression was essential for clonogenic potential of human gastric cancer cells (Li et al., 2010). In addition, increased colony formation was also shown by over-expression of RUVBL2 in HuH7 hepatocarcinoma cells (Rousseau et al., 2007). It is possible that inhibition of transformation upon RUVBL2 silencing was

a direct consequence of the reduction in *TERT* expression and telomerase activity. Use of dominant negative mutant forms of TERT in LoVo cells (colon cancer cells), causes growth arrest and apoptosis in a telomere length dependent manner, and this is a direct consequence of chromosomal damage due to telomere shortening (Hahn et al., 1999; Zhang et al., 1999). The same group also showed that this TERT mutant inhibits the colony forming potential of 293 cells (Zhang et al., 1999). However, there is also evidence that apoptosis and growth arrest upon TERT inhibition in human prostate cancer cells occurs before the shortening of telomeres, suggesting that telomere shortening may not be the only mechanism to explain our results (Folini et al., 2005). In agreement with this, dominant negative mutant TERT, with no telomerase enzymatic activity, can inhibit apoptosis in breast cancer cells (Cao et al., 2002). Massard *et al* also showed that *TERT* inhibition sensitises HCT116 colon cancer cells to induction of cell death via BCL-2-associated X (Bax) activation, by a post-translational mechanism, rather than as a consequence of telomere shortening (Massard et al., 2006). Finally, *TERT* deficient mice were used to confirm that *TERT* mRNA expression has an alternative anti-apoptotic role that is independent of telomerase activity (Lee et al., 2008). These data suggest that several mechanisms are likely to be involved in the induction of apoptosis and inhibition of clonogenic potential following RUVBL2 knock-down in our experiments.

Telomerase activity has been considered to be a potential target for cancer therapy since its discovery (Harley, 2008). Several approaches have been developed to target the enzymatic activity of telomerase and *TERT* expression. However, ongoing clinical trials have encountered difficulty in targeting the enzymatic activity of telomerase and consequently this has led to some disappointing results (De Cian et al., 2008). One of

the major problems of telomerase inhibition is the considerable delay in the anti-cancer activity of the drug following administration, indicating that this therapy should only be used to compliment other more potent cancer targeting drugs. Our study shows that RUVBL1 and RUVBL2 represent promising alternative candidates for cancer therapies, including treatment of acute myeloid leukaemia. Since *RUVBL2* knock-down induces apoptosis as well as telomerase inhibition, its therapeutic targeting may have considerable advantages over direct telomerase inhibition. Furthermore, although the data in this chapter suggest that *RUVBL1* and *RUVBL2* expression are induced by MLL-fusions, they also suggest that targeting these proteins will be effective against several forms of acute myeloid leukaemia.

CHAPTER 6. CONCLUSION

In this study, we have explored various human models to study MLL-AF9 associated myeloid leukaemia. This step is essential to translate and validate key findings from the mouse system to human systems. Using these systems, we validated down-stream target genes of MLL-fusions.

The lentiviral gene transfer approach was used to generate human CB-derived MLL-AF9 immortalised myeloid cells (V6MA). Four V6MA cell lines were generated from independent CB samples and all of these cells outgrew untransduced cells in culture and proliferated exponentially in medium supplemented with SCF, TPO, FLT3L, IL-3 and IL-6. Protein and mRNA expression of MLL-AF9 were both confirmed in V6MA cells by western blot and QPCR analysis. In addition, MLL-fusion down-stream target genes, *HOXA9*, *MEIS1*, *MYB* and *MYC* were also measured and observed to be over-expressed in V6MA cells. Morphological analysis revealed that V6MA cells displayed myeloblastic phenotypes. Immunophenotypic analysis showed that V6MA cells were $CD33^+$ and $CD34^-$ with heterogeneous CD38 expression, and with more than half of the cells within each V6MA line expressed the CD11b and CD14 markers. CD15 expression varied, depending on the envelope constructs used in the transduction and the length of time V6MA had been in cell liquid culture. Xenotransplantation confirmed that V6MA2r, V6MA3r and V6MA4r cell lines were all capable of inducing AML in NSG mice, with a latency of between 51 to 84 days. Flow cytometric analysis was used to confirm the phenotype of the resulting leukaemia.

In order to develop an efficient gene expression knock-down strategy, human leukaemic cell lines, derived from patients with leukaemia, were used. MLL fusion protein expression was detected in all of the cell lines tested, except KOPN-8 cells. The siRNA delivery using a square pulse electroporator was initially employed to knock-down gene expression. The siGLO Red fluorescent siRNA showed that siRNA were efficiently delivered using this approach. siRNA targeting 5' sequences of *MLL* was used to knock-down expression of *MLL/MLL-AF9* in THP-1 cells. Although knock-down of MLL and/or MLL-AF9 was observed in some experiments, the data were inconsistent. For this reason, lentiviral shRNA delivery was then used to knock-down gene expression. *GADPH* mRNA expression was efficiently knocked-down in THP-1 cells using this approach. MLL-fusion down-stream target genes, such as *HOXA9* and *MYC*, were also knocked down and consistent knock-down of these genes expression was achieved. Therefore the lentiviral shRNA delivery system was used to knock-down gene expression in subsequent experiments.

We studied the novel MLL-fusion down-stream target genes, *RUVBL1* and *RUVBL2*. These genes were over-expressed in immortalised myeloid MLL-AF9 cells derived from both mouse and human cells, and their expression was shown to be directly or indirectly regulated by MLL-fusions. Expression of these genes was required for human myeloid leukemic cell lines to persist in liquid culture. Knock-down of *RUVBL2* expression decreased RUVBL1 protein expression in THP-1 cells, indicating that these proteins exist in an interdependent manner. In addition, inhibition of *RUVBL2* expression induced apoptosis and differentiation of THP-1 cells. RUVBL1 and RUVBL2 were previously implicated in telomerase activity (Venteicher et al., 2008). *TERT* expression was found to be up-regulated in V6MA cells and knock-down of

RUVBL2 expression reduced *TERT* mRNA expression both in THP-1 cells and V6MA cells. In addition, this reduction of *TERT* expression was accompanied by a decrease in telomerase activity. Furthermore, maintenance of clonogenic potential of THP-1 cells required *RUVBL2* expression. Taken together, the data we have presented in this thesis suggest that RUVBL2 can be a potential therapeutic target for myeloid leukaemia, which may compliment currently clinically available telomerase inhibitors.

CHAPTER 7. REFERENCES

ADOLFSSON, J., MANSSON, R., BUZA-VIDAS, N., HULTQUIST, A., LIUBA, K., JENSEN, C. T., BRYDER, D., YANG, L. P., BORGE, O. J., THOREN, L. A. M., ANDERSON, K., SITNICKA, E., SASAKI, Y., SIGVARDSSON, M. & JACOBSEN, S. E. W. 2005. Identification of flt3(+) lympho-myeloid stem cells lacking erythro-megakaryocytic potential: A revised road map for adult blood lineage commitment. *Cell,* 121**,** 295-306.

AKASHI, K., TRAVER, D., MIYAMOTO, T. & WEISSMAN, I. L. 2000. A clonogenic common myeloid progenitor that gives rise to all myeloid lineages. *Nature,* 404**,** 193-197.

AL-HAJJ, M., WICHA, M. S., BENITO-HERNANDEZ, A., MORRISON, S. J. & CLARKE, M. F. 2003. Prospective identification of tumorigenic breast cancer cells. *Proc Natl Acad Sci U S A,* 100**,** 3983-8.

ARINOBU, Y., MIZUNO, S., CHONG, Y., SHIGEMATSU, H., IINO, T., IWASAKI, H., GRAF, T., MAYFIELD, R., CHAN, S., KASTNER, P. & AKASHI, K. 2007. Reciprocal activation of gata-1 and pu.1 marks initial specification of hematopoietic stem cells into myeloerythroid and myelolymphoid lineages. *Cell Stem Cell,* 1**,** 416-27.

ARMSTRONG, S. A., STAUNTON, J. E., SILVERMAN, L. B., PIETERS, R., DE BOER, M. L., MINDEN, M. D., SALLAN, S. E., LANDER, E. S., GOLUB, T. R. & KORSMEYER, S. J. 2002. Mll translocations specify a distinct gene expression profile that distinguishes a unique leukemia. *Nature Genetics,* 30**,** 41-47.

AYTON, P. M. & CLEARY, M. L. 2001. Molecular mechanisms of leukemogenesis mediated by mll fusion proteins. *Oncogene,* 20**,** 5695-5707.

AYTON, P. M. & CLEARY, M. L. 2003. Transformation of myeloid progenitors by mll oncoproteins is dependent on hoxa7 and hoxa9. *Genes & Development,* 17**,** 2298-2307.

BAEK, S. H. 2008. When atpases pontin and reptin met telomerase. *Developmental Cell,* 14**,** 459-461.

BARABE, F., KENNEDY, J. A., HOPE, K. J. & DICK, J. E. 2007. Modeling the initiation and progression of human acute leukemia in mice. *Science,* 316**,** 600-4.

BAUER, A., CHAUVET, S., HUBER, O., USSEGLIO, F., ROTHBACHER, U., ARAGNOL, D., KEMLER, R. & PRADEL, J. 2000. Pontin52 and reptin52 function as antagonistic regulators of beta-catenin signalling activity. *Embo Journal,* 19**,** 6121-6130.

BELLOSTA, P., HULF, T., BALLA DIOP, S., USSEGLIO, F., PRADEL, J., ARAGNOL, D. & GALLANT, P. 2005. Myc interacts genetically with

tip48/reptin and tip49/pontin to control growth and proliferation during drosophila development. *Proc Natl Acad Sci U S A,* 102**,** 11799-804.

BENEDIKT, A., BALTRUSCHAT, S., SCHOLZ, B., BURSEN, A., ARREY, T. N., MEYER, B., VARAGNOLO, L., MUELLER, A. M., KARAS, M., DINGERMANN, T. & MARSCHALEK, R. 2011. The leukemogenic af4-mll fusion protein causes p-tefb kinase activation and altered epigenetic signatures. *Leukemia,* 25**,** 135-144.

BETTI, C. J., VILLALOBOS, M. J., DIAZ, M. O. & VAUGHAN, A. T. M. 2001. Apoptotic triggers initiate translocations within the mll gene involving the nonhomologous end joining repair system. *Cancer Research,* 61**,** 4550-4555.

BHATIA, M., BONNET, D., MURDOCH, B., GAN, O. I. & DICK, J. E. 1998. A newly discovered class of human hematopoietic cells with scid-repopulating activity. *Nature Medicine,* 4**,** 1038-1045.

BIONDI, A., CIMINO, G., PIETERS, R. & PUI, C. H. 2000. Biological and therapeutic aspects of infant leukemia. *Blood,* 96**,** 24-33.

BITOUN, E., OLIVER, P. L. & DAVIES, K. E. 2007. The mixed-lineage leukemia fusion partner af4 stimulates rna polymerase ii transcriptional elongation and mediates coordinated chromatin remodeling. *Hum Mol Genet,* 16**,** 92-106.

BLACKBURN, E. H. 1991. Structure and function of telomeres. *Nature,* 350**,** 569-573.

BLACKBURN, E. H. 1992. Telomerases. *Annual Review of Biochemistry,* 61**,** 113-129.

BLACKBURN, E. H. 2001. Switching and signaling at the telomere. *Cell,* 106**,** 661-73.

BLASCO, M. A., LEE, H. W., HANDE, M. P., SAMPER, E., LANSDORP, P. M., DEPINHO, R. A. & GREIDER, C. W. 1997. Telomere shortening and tumor formation by mouse cells lacking telomerase rna. *Cell,* 91**,** 25-34.

BONNET, D. 2002. Haematopoietic stem cells. *J Pathol,* 197**,** 430-40.

BONNET, D. 2005. Normal and leukaemic stem cells. *Br J Haematol,* 130**,** 469-79.

BONNET, D. & DICK, J. E. 1997. Human acute myeloid leukemia is organized as a hierarchy that originates from a primitive hematopoietic cell. *Nature Medicine,* 3**,** 730-737.

BURSEN, A., SCHWABE, K., RUESTER, B., HENSCHLER, R., RUTHARDT, M., DINGERMANN, T. & MARSCHALEK, R. 2010. The af4.Mll fusion protein is capable of inducing all in mice without requirement of mll.Af4. *Blood,* 115**,** 3570-3579.

BUTLER, L. H., SLANY, R., CUI, X. M., CLEARY, M. L. & MASON, D. Y. 1997. The hrx proto-oncogene product is widely expressed in human tissues and localizes to nuclear structures. *Blood,* 89**,** 3361-3370.

CAO, Y., LI, H., DEB, S. & LIU, J. P. 2002. Tert regulates cell survival independent of telomerase enzymatic activity. *Oncogene,* 21**,** 3130-3138.

CASLINI, C., YANG, Z., EL-OSTA, M., MILNE, T. A., SLANY, R. K. & HESS, J. L. 2007. Interaction of mll amino terminal sequences with menin is required for transformation. *Cancer Research,* 67**,** 7275-7283.

CHEUNG, K. L., HUEN, J., KAKIHARA, Y., HOURY, W. A. & ORTEGA, J. 2010. Alternative oligomeric states of the yeast rvb1/rvb2 complex induced by histidine tags. *J Mol Biol,* 404**,** 478-92.

CHONO, H., YOSHIOKA, H., UENO, M. & KATO, I. 2001. Removal of inhibitory substances with recombinant fibronectin-ch-296 plates enhances the retroviral transduction efficiency of cd34(+)cd38(-) bone marrow cells. *J Biochem,* 130**,** 331-4.

COLLINS, E. C., APPERT, A., ARIZA-MCNAUGHTON, L., PANNELL, R., YAMADA, Y. & RABBITTS, T. H. 2002. Mouse af9 is a controller of embryo patterning, like mll, whose human homologue fuses with af9 after chromosomal translocation in leukemia. *Molecular and Cellular Biology,* 22**,** 7313-7324.

COLLINS, E. C., PANNELL, R., SIMPSON, E. M., FORSTER, A. & RABBITTS, T. H. 2000. Inter-chromosomal recombination of mll and af9 genes mediated by cre-loxp in mouse development. *EMBO Rep,* 1**,** 127-132.

CONAWAY, R. C. & CONAWAY, J. W. 2009. The ino80 chromatin remodeling complex in transcription, replication and repair. *Trends in Biochemical Sciences,* 34**,** 71-77.

CORRAL, J., LAVENIR, I., IMPEY, H., WARREN, A. J., FORSTER, A., LARSON, T. A., BELL, S., MCKENZIE, A. N., KING, G. & RABBITTS, T. H. 1996. An mll-af9 fusion gene made by homologous recombination causes acute leukemia in chimeric mice: A method to create fusion oncogenes. *Cell,* 85**,** 853-61.

COULOMBEL, L. 2004. Identification of hematopoietic stem/progenitor cells: Strength and drawbacks of functional assays. *Oncogene,* 23**,** 7210-22.

COZZIO, A., PASSEGUE, E., AYTON, P. M., KARSUNKY, H., CLEARY, M. L. & WEISSMAN, I. L. 2003. Similar mll-associated leukemias arising from self-renewing stem cells and short-lived myeloid progenitors. *Genes Dev,* 17**,** 3029-35.

CULLEN, B. R. 2005. Rnai the natural way. *Nature Genetics,* 37**,** 1163-1165.

CUMANO, A. & GODIN, I. 2001. Pluripotent hematopoietic stem cell development during embryogenesis. *Curr Opin Immunol,* 13**,** 166-71.

CURETON, D. K., MASSOL, R. H., SAFFARIAN, S., KIRCHHAUSEN, T. L. & WHELAN, S. P. J. 2009. Vesicular stomatitis virus enters cells through vesicles incompletely coated with clathrin that depend upon actin for internalization. *Plos Pathogens,* 5.

DASER, A. & RABBITTS, T. H. 2005. The versatile mixed lineage leukaemia gene mll and its many associations in leukaemogenesis. *Semin Cancer Biol,* 15**,** 175-88.

DAVIS, H. E., MORGAN, J. R. & YARMUSH, M. L. 2002. Polybrene increases retrovirus gene transfer efficiency by enhancing receptor-independent virus adsorption on target cell membranes. *Biophys Chem,* 97**,** 159-72.

DE BRUIJN, M., SPECK, N. A., PEETERS, M. C. E. & DZIERZAK, E. 2000. Definitive hematopoietic stem cells first develop within the major arterial regions of the mouse embryo. *Embo Journal,* 19**,** 2465-2474.

DE CIAN, A., LACROIX, L., DOUARRE, C., TEMIME-SMAALI, N., TRENTESAUX, C., RIOU, J. F. & MERGNY, J. L. 2008. Targeting telomeres and telomerase. *Biochimie,* 90**,** 131-155.

DEBERNARDI, S., BASSINI, A., JONES, L. K., CHAPLIN, I., LINDER, B., DE BRUIJN, D. R. H., MEESE, E. & YOUNG, B. D. 2002. The mll fusion partner af10 binds gas41, a protein that interacts with the human swi/snf complex. *Blood,* 99**,** 275-281.

DEFTOS, M. L., HE, Y. W., OJALA, E. W. & BEVAN, M. J. 1998. Correlating notch signaling with thymocyte maturation. *Immunity,* 9**,** 777-86.

DEXTER, T. M., ALLEN, T. D. & LAJTHA, L. G. 1977. Conditions controlling the proliferation of haemopoietic stem cells in vitro. *J Cell Physiol,* 91**,** 335-44.

DI NUNZIO, F., PIOVANI, B., COSSET, F. L., MAVILIO, F. & STORNAIUOLO, A. 2007. Transduction of human hematopoietic stem cells by lentiviral vectors pseudotyped with the rd114-tr chimeric envelope glycoprotein. *Hum Gene Ther,* 18**,** 811-20.

DICK, J. E. 2008. Stem cell concepts renew cancer research. *Blood,* 112**,** 4793-4807.

DIMARTINO, J. F., MILLER, T., AYTON, P. M., LANDEWE, T., HESS, J. L., CLEARY, M. L. & SHILATIFARD, A. 2000. A carboxy-terminal domain of ell is required and sufficient for immortalization of myeloid progenitors by mll-ell. *Blood,* 96**,** 3887-3893.

DJABALI, M., SELLERI, L., PARRY, P., BOWER, M., YOUNG, B. D. & EVANS, G. A. 1992. A trithorax-like gene is interrupted by chromosome 11q23 translocations in acute leukemias. *Nature Genetics,* 2**,** 113-118.

DOBSON, C. L., WARREN, A. J., PANNELL, R., FORSTER, A., LAVENIR, I., CORRAL, J., SMITH, A. J. H. & RABBITTS, T. H. 1999. The mll-af9 gene fusion in mice controls myeloproliferation and specifies acute myeloid leukaemogenesis. *Embo Journal,* 18**,** 3564-3574.

DOBSON, C. L., WARREN, A. J., PANNELL, R., FORSTER, A. & RABBITTS, T. H. 2000. Tumorigenesis in mice with a fusion of the leukaemia oncogene mll and the bacterial lacz gene. *Embo Journal,* 19**,** 843-851.

DOU, Y., MILNE, T. A., TACKETT, A. J., SMITH, E. R., FUKUDA, A., WYSOCKA, J., ALLIS, C. D., CHAIT, B. T., HESS, J. L. & ROEDER, R. G. 2005. Physical association and coordinate function of the h3 k4 methyltransferase mll1 and the h4 k16 acetyltransferase mof. *Cell,* 121**,** 873-85.

DREXLER, H. G., QUENTMEIER, H. & MACLEOD, R. A. 2004. Malignant hematopoietic cell lines: In vitro models for the study of mll gene alterations. *Leukemia,* 18**,** 227-32.

DUGAN, K. A., WOOD, M. A. & COLE, M. D. 2002. Tip49, but not trrap, modulates c-myc and e2f1 dependent apoptosis. *Oncogene,* 21**,** 5835-43.

DUNNE, J., DRESCHER, B., RIEHLE, H., HADWIGER, P., YOUNG, B. D., KRAUTER, J. & HEIDENREICH, O. 2003. The apparent uptake of fluorescently labeled sirnas by electroporated cells depends on the fluorochrome. *Oligonucleotides,* 13**,** 375-380.

DYKXHOORN, D. M., NOVINA, C. D. & SHARP, P. A. 2003. Killing the messenger: Short rnas that silence gene expression. *Nat Rev Mol Cell Biol,* 4**,** 457-67.

EGUCHI, M., EGUCHI-ISHIMAE, M. & GREAVES, M. 2003. The role of the mll gene in infant leukemia. *Int J Hematol,* 78**,** 390-401.

EMI, N., FRIEDMANN, T. & YEE, J. K. 1991. Pseudotype formation of murine leukemia virus with the g protein of vesicular stomatitis virus. *J Virol,* 65**,** 1202-7.

ENGELHARDT, M., MACKENZIE, K., DRULLINSKY, P., SILVER, R. T. & MOORE, M. A. S. 2000. Telomerase activity and telomere length in acute and chronic leukemia, pre- and post-ex vivo culture. *Cancer Research,* 60**,** 610-617.

ERFURTH, F., HEMENWAY, C. S., DE ERKENEZ, A. C. & DOMER, P. H. 2004. Mll fusion partners af4 and af9 interact at subnuclear foci. *Leukemia,* 18**,** 92-102.

ERNST, P., FISHER, J. K., AVERY, W., WADE, S., FOY, D. & KORSMEYER, S. J. 2004. Definitive hematopoiesis requires the mixed-lineage leukemia gene. *Developmental Cell,* 6**,** 437-443.

ERNST, P., WANG, J., HUANG, M., GOODMAN, R. H. & KORSMEYER, S. J. 2001. Mll and creb bind cooperatively to the nuclear coactivator creb-binding protein. *Molecular and Cellular Biology,* 21**,** 2249-2258.

ESTEY, E. & DOHNER, H. 2006. Acute myeloid leukaemia. *Lancet,* 368**,** 1894-907.

ETARD, C., GRADL, D., KUNZ, M., EILERS, M. & WEDLICH, D. 2005. Pontin and reptin regulate cell proliferation in early xenopus embryos in collaboration with c-myc and miz-1. *Mechanisms of Development,* 122**,** 545-556.

FABER, J., KRIVTSOV, A. V., STUBBS, M. C., WRIGHT, R., DAVIS, T. N., VAN DEN HEUVEL-EIBRINK, M., ZWAAN, C. M., KUNG, A. L. & ARMSTRONG, S. A. 2009. Hoxa9 is required for survival in human mll-rearranged acute leukemias. *Blood,* 113**,** 2375-2385.

FAIR, K., ANDERSON, M., BULANOVA, E., MI, H. F., TROPSCHUG, M. & DIAZ, M. O. 2001. Protein interactions of the mll phd fingers modulate mll target gene regulation in human cells. *Molecular and Cellular Biology,* 21**,** 3589-3597.

FAN, J. S., ZELLER, K., CHEN, Y. C., WATKINS, T., BARNES, K. C., BECKER, K. G., DANG, C. V. & CHEADLE, C. 2010. Time-dependent c-myc transactomes mapped by array-based nuclear run-on reveal transcriptional modules in human b cells. *Plos One,* 5**,** e9691.

FELIX, C. A. & LANGE, B. J. 1999. Leukemia in infants. *Oncologist,* 4**,** 225-40.

FENG, Y., LEE, N. & FEARON, E. R. 2003. Tip49 regulates beta-catenin-mediated neoplastic transformation and t-cell factor target gene induction via effects on chromatin remodeling. *Cancer Research,* 63**,** 8726-8734.

FLORES, I., BENETTI, R. & BLASCO, M. A. 2006. Telomerase regulation and stem cell behaviour. *Current Opinion in Cell Biology,* 18**,** 254-260.

FOLINI, M., BRAMBILLA, C., VILLA, R., GANDELLINI, P., VIGNATI, S., PADUANO, F., DAIDONE, M. G. & ZAFFARONI, N. 2005. Antisense oligonucleotide-mediated inhibition of htert, but not hterc, induces rapid cell growth decline and apoptosis in the absence of telomere shortening in human prostate cancer cells. *European Journal of Cancer,* 41**,** 624-634.

FORD, A. M., RIDGE, S. A., CABRERA, M. E., MAHMOUD, H., STEEL, C. M., CHAN, L. C. & GREAVES, M. 1993. Inutero rearrangements in the trithorax-related oncogene in infant leukemias. *Nature,* 363**,** 358-360.

FORSTER, A., PANNELL, R., DRYNAN, L. F., MCCORMACK, M., COLLINS, E. C., DASER, A. & RABBITTS, T. H. 2003. Engineering de novo reciprocal chromosomal translocations associated with mll to replicate primary events of human cancer. *Cancer Cell,* 3**,** 449-58.

FUJIWARA, Y., BROWNE, C. P., CUNNIFF, K., GOFF, S. C. & ORKIN, S. H. 1996. Arrested development of embryonic red cell precursors in mouse embryos lacking transcription factor gata-1. *Proc Natl Acad Sci U S A,* 93**,** 12355-8.

GALE, K. B., FORD, A. M., REPP, R., BORKHARDT, A., KELLER, C., EDEN, O. B. & GREAVES, M. F. 1997. Backtracking leukemia to birth: Identification of clonotypic gene fusion sequences in neonatal blood spots. *Proceedings of the National Academy of Sciences of the United States of America,* 94**,** 13950-13954.

GALLANT, P. 2007. Control of transcription by pontin and reptin. *Trends in Cell Biology,* 17**,** 187-192.

GEKAS, C., DIETERLEN-LIEVRE, F., ORKIN, S. H. & MIKKOLA, H. K. A. 2005. The placenta is a niche for hematopoietic stem cells. *Developmental Cell,* 8**,** 365-375.

GESSNER, A., THOMAS, M., CASTRO, P. G., BUCHLER, L., SCHOLZ, A., BRUMMENDORF, T. H., SORIA, N. M., VORMOOR, J., GREIL, J. & HEIDENREICH, O. 2010. Leukemic fusion genes mll/af4 and aml1/mtg8 support leukemic self-renewal by controlling expression of the telomerase subunit tert. *Leukemia,* 24**,** 1751-1759.

GILLERT, E., LEIS, T., REPP, R., REICHEL, M., HOSCH, A., BREITENLOHNER, I., ANGERMULLER, S., BORKHARDT, A., HARBOTT, J., LAMPERT, F., GRIESINGER, F., GREIL, J., FEY, G. H. & MARSCHALEK, R. 1999. A DNA damage repair mechanism is involved in the origin of chromosomal translocations t(4;11) in primary leukemic cells. *Oncogene,* 18**,** 4663-4671.

GOODELL, M. A., ROSENZWEIG, M., KIM, H., MARKS, D. F., DEMARIA, M., PARADIS, G., GRUPP, S. A., SIEFF, C. A., MULLIGAN, R. C. & JOHNSON, R. P. 1997. Dye efflux studies suggest that hematopoietic stem cells expressing low or undetectable levels of cd34 antigen exist in multiple species. *Nature Medicine,* 3**,** 1337-1345.

GRIBUN, A., CHEUNG, K. L. Y., HUEN, J., ORTEGA, J. & HOURY, W. A. 2008. Yeast rvb1 and rvb2 are atp-dependent DNA helicases that form a heterohexameric complex. *Journal of Molecular Biology,* 376**,** 1320-1333.

GRIGOLETTO, A., LESTIENNE, P. & ROSENBAUM, J. 2011. The multifaceted proteins reptin and pontin as major players in cancer. *Biochimica Et Biophysica Acta-Reviews on Cancer,* 1815**,** 147-157.

GU, Y., ALDER, H., NAKAMURA, T., SCHICHMAN, S. A., PRASAD, R., CANAANI, O., SAITO, H., CROCE, C. M. & CANAANI, E. 1994. Sequence-analysis of the breakpoint cluster region in the all-1 gene involved in acute-leukemia. *Cancer Research,* 54**,** 2327-2330.

GU, Y., NAKAMURA, T., ALDER, H., PRASAD, R., CANAANI, O., CIMINO, G., CROCE, C. M. & CANAANI, E. 1992. The t(4-11) chromosome-translocation of human acute leukemias fuses the all-1 gene, related to drosophila-trithorax, to the af-4 gene. *Cell,* 71**,** 701-708.

GUENTHER, M. G., LAWTON, L. N., ROZOVSKAIA, T., FRAMPTON, G. M., LEVINE, S. S., VOLKERT, T. L., CROCE, C. M., NAKAMURA, T., CANAANI, E. & YOUNG, R. A. 2008. Aberrant chromatin at genes encoding stem cell regulators in human mixed-lineage leukemia. *Genes & Development,* 22**,** 3403-3408.

HAHN, W. C., STEWART, S. A., BROOKS, M. W., YORK, S. G., EATON, E., KURACHI, A., BEIJERSBERGEN, R. L., KNOLL, J. H. M., MEYERSON, M. & WEINBERG, R. A. 1999. Inhibition of telomerase limits the growth of human cancer cells. *Nature Medicine,* 5**,** 1164-1170.

HALL, P. A. & RUSSELL, S. E. H. 2004. The pathobiology of the septin gene family. *Journal of Pathology,* 204**,** 489-505.

HANNON, G. J. 2002. Rna interference. *Nature,* 418**,** 244-251.

HAO, Q. L., THIEMANN, F. T., PETERSEN, D., SMOGORZEWSKA, E. M. & CROOKS, G. M. 1996. Extended long-term culture reveals a highly quiescent and primitive human hematopoietic progenitor population. *Blood,* 88**,** 3306-3313.

HARLEY, C. B. 2008. Telomerase and cancer therapeutics. *Nature Reviews Cancer,* 8**,** 167-179.

HARRIS, N. L., JAFFE, E. S., DIEBOLD, J., FLANDRIN, G., MULLER-HERMELINK, H. K., VARDIMAN, J., LISTER, T. A. & BLOOMFIELD, C. D. 2000. The world health organization classification of hematological malignancies report of the clinical advisory committee meeting, airlie house, virginia, november 1997. *Modern Pathology,* 13**,** 193-207.

HARS, E. S., LYU, Y. L., LIN, C. P. & LIU, L. F. 2006. Role of apoptotic nuclease caspase-activated dnase in etoposide-induced treatment-related acute myelogenous leukemia. *Cancer Research,* 66**,** 8975-8979.

HAURIE, V., MENARD, L., NICOU, A., TOURIOL, C., METZLER, P., FERNANDEZ, J., TARAS, D., LESTIENNE, P., BALABAUD, C., BIOULAC-SAGE, P., PRATS, H., ZUCMAN-ROSSI, J. & ROSENBAUM, J. 2009. Adenosine triphosphatase pontin is overexpressed in hepatocellular carcinoma and coregulated with reptin through a new posttranslational mechanism. *Hepatology,* 50**,** 1871-83.

HEIDENREICH, O., KRAUTER, J., RIEHLE, H., HADWIGER, P., JOHN, M., HEIL, G., VORNLOCHER, H. P. & NORDHEIM, A. 2003. Aml1/mtg8 oncogene suppression by small interfering rnas supports myeloid differentiation of t(8;21)-positive leukemic cells. *Blood,* 101**,** 3157-3163.

HESS, J. L. 2004. Mll: A histone methyltransferase disrupted in leukemia. *Trends Mol Med,* 10**,** 500-7.

HESS, J. L., BITTNER, C. B., ZEISIG, D. T., BACH, C., FUCHS, U., BORKHARDT, A., FRAMPTON, J. & SLANY, R. K. 2006. C-myb is an essential downstream target for homeobox-mediated transformation of hematopoietic cells. *Blood,* 108**,** 297-304.

HESS, J. L., YU, B. D., LI, B., HANSON, R. & KORSMEYER, S. J. 1997. Defects in yolk sac hematopoiesis in mll-null embryos. *Blood,* 90**,** 1799-1806.

HORTON, S. J., GRIER, D. G., MCGONIGLE, G. J., THOMPSON, A., MORROW, M., DE SILVA, I., MOULDING, D. A., KIOUSSIS, D., LAPPIN, T. R., BRADY, H. J. & WILLIAMS, O. 2005. Continuous mll-enl expression is necessary to establish a "hox code" and maintain immortalization of hematopoietic progenitor cells. *Cancer Res,* 65**,** 9245-52.

HORTON, S. J., WALF-VORDERWULBECKE, V., CHATTERS, S. J., SEBIRE, N. J., DE BOER, J. & WILLIAMS, O. 2009. Acute myeloid leukemia induced by mll-enl is cured by oncogene ablation despite acquisition of complex genetic abnormalities. *Blood,* 113**,** 4922-4929.

HSIEH, J. J. D., CHENG, E. H. Y. & KORSMEYER, S. J. 2003a. Taspase1: A threonine aspartase required for cleavage of mll and proper hox gene expression. *Cell,* 115**,** 293-303.

HSIEH, J. J. D., ERNST, P., ERDJUMENT-BROMAGE, H., TEMPST, P. & KORSMEYER, S. J. 2003b. Proteolytic cleavage of mll generates a complex of n- and c-terminal fragments that confers protein stability and subnuclear localization. *Molecular and Cellular Biology,* 23**,** 186-194.

HUEN, J., KAKIHARA, Y., UGWU, F., CHEUNG, K. L., ORTEGA, J. & HOURY, W. A. 2010a. Rvb1-rvb2: Essential atp-dependent helicases for critical complexes. *Biochem Cell Biol,* 88**,** 29-40.

HUEN, J., KAKIHARA, Y., UGWU, F., CHEUNG, K. L. Y., ORTEGA, J. & HOURY, W. A. 2010b. Rvb1-rvb2: Essential atp-dependent helicases for critical complexes. *Biochemistry and Cell Biology-Biochimie Et Biologie Cellulaire,* 88**,** 29-40.

HUNTLY, B. J. P. & GILLILAND, D. G. 2005. Leukaemia stem cells and the evolution of cancer-stem-cell research. *Nature Reviews Cancer,* 5**,** 311-321.

HUNTLY, B. J. P., SHIGEMATSU, H., DEGUCHI, K., LEE, B. H., MIZUNO, S., DUCLOS, N., ROWAN, R., AMARAL, S., CURLEY, D., WILLIAMS, I. R., AKASHI, K. & GILLILAND, D. G. 2004. Moz-tif2, but not bcr-abl, confers properties of leukemic stem cells to committed murine hematopoietic progenitors. *Cancer Cell,* 6**,** 587-596.

HURET, J. L., DESSEN, P. & BERNHEIM, A. 2001. An atlas of chromosomes in hematological malignancies. Example: 11q23 and mll partners. *Leukemia,* 15**,** 987-9.

IDA, K., KITABAYASHI, I., TAKI, T., TANIWAKI, M., NORO, K., YAMAMOTO, M., OHKI, M. & HAYASHI, Y. 1997. Adenoviral e1a-associated protein p300 is involved in acute myeloid leukemia with t(11;22)(q23;q13). *Blood,* 90**,** 4699-4704.

IKUTA, K. & WEISSMAN, I. L. 1992. Evidence that hematopoietic stem-cells express mouse c-kit but do not depend on steel factor for their generation. *Proceedings of the National Academy of Sciences of the United States of America,* 89**,** 1502-1506.

ISNARD, P., CORE, N., NAQUET, P. & DJABALI, M. 2000. Altered lymphoid development in mice deficient for the maf4 proto-oncogene. *Blood,* 96**,** 705-710.

IWASAKI, H. & AKASHI, K. 2007. Myeloid lineage commitment from the hematopoietic stem cell. *Immunity,* 26**,** 726-40.

IWASAKI, H., SOMOZA, C., SHIGEMATSU, H., DUPREZ, E. A., IWASAKI-ARAI, J., MIZUNO, S., ARINOBU, Y., GEARY, K., ZHANG, P., DAYARAM, T., FENYUS, M. L., ELF, S., CHAN, S., KASTNER, P., HUETTNER, C. S., MURRAY, R., TENEN, D. G. & AKASHI, K. 2005. Distinctive and indispensable roles of pu.1 in maintenance of hematopoietic stem cells and their differentiation. *Blood,* 106**,** 1590-600.

JHA, S. & DUTTA, A. 2009. Rvb1/rvb2: Running rings around molecular biology. *Molecular Cell,* 34**,** 521-533.

JHA, S., SHIBATA, E. & DUTTA, A. 2008. Human rvbl/tip49 is required for the histone acetyltransferase activity of tip60/nua4 and for the downregulation of phosphorylation on h2ax after DNA damage. *Molecular and Cellular Biology,* 28**,** 2690-2700.

KAMELREID, S. & DICK, J. E. 1988. Engraftment of immune-deficient mice with human hematopoietic stem-cells. *Science,* 242**,** 1706-1709.

KAWAGOE, H., KAWAGOE, R. & SANO, K. 2001. Targeted down-regulation of mll-af9 with antisense oligodeoxyribonucleotide reduces the expression of the hoxa7 and -a10 genes and induces apoptosis in a human leukemia cell line, thp-1. *Leukemia,* 15**,** 1743-9.

KELLY, P. F., VANDERGRIFF, J., NATHWANI, A., NIENHUIS, A. W. & VANIN, E. F. 2000. Highly efficient gene transfer into cord blood nonobese diabetic/severe combined immunodeficiency repopulating cells by oncoretroviral vector particles pseudotyped with the feline endogenous retrovirus (rd114) envelope protein. *Blood,* 96**,** 1206-14.

KHARAS, M. G., LENGNER, C. J., AL-SHAHROUR, F., BULLINGER, L., BALL, B., ZAIDI, S., MORGAN, K., TAM, W., PAKTINAT, M., OKABE, R., GOZO, M., EINHORN, W., LANE, S. W., SCHOLL, C., FROHLING, S., FLEMING, M., EBERT, B. L., GILLILAND, D. G., JAENISCH, R. & DALEY, G. Q. 2010. Musashi-2 regulates normal hematopoiesis and promotes aggressive myeloid leukemia. *Nature Medicine,* 16**,** 903-U101.

KIM, J. H., KIM, B., CAI, L., CHOI, H. J., OHGI, K. A., TRAN, C., CHEN, C., CHUNG, C. H., HUBER, O., ROSE, D. W., SAWYERS, C. L., ROSENFELD, M. G. & BAEK, S. H. 2005. Transcriptional regulation of a metastasis suppressor gene by tip60 and beta-catenin complexes. *Nature,* 434**,** 921-926.

KONDO, M., WEISSMAN, I. L. & AKASHI, K. 1997. Identification of clonogenic common lymphoid progenitors in mouse bone marrow. *Cell,* 91**,** 661-672.

KRIVTSOV, A. V. & ARMSTRONG, S. A. 2007. Mll translocations, histone modifications and leukaemia stem-cell development. *Nature Reviews Cancer,* 7**,** 823-833.

KRIVTSOV, A. V., FENG, Z., LEMIEUX, M. E., FABER, J., VEMPATI, S., SINHA, A. U., XIA, X., JESNECK, J., BRACKEN, A. P., SILVERMAN, L. B., KUTOK, J. L., KUNG, A. L. & ARMSTRONG, S. A. 2008. H3k79 methylation profiles define murine and human mll-af4 leukemias. *Cancer Cell,* 14**,** 355-368.

KRIVTSOV, A. V., TWOMEY, D., FENG, Z., STUBBS, M. C., WANG, Y., FABER, J., LEVINE, J. E., WANG, J., HAHN, W. C., GILLILAND, D. G., GOLUB, T. R. & ARMSTRONG, S. A. 2006. Transformation from committed progenitor to leukaemia stem cell initiated by mll-af9. *Nature,* 442**,** 818-22.

KROON, E., KROSL, J., THORSTEINSDOTTIR, U., BABAN, S., BUCHBERG, A. M. & SAUVAGEAU, G. 1998. Hoxa9 transforms primary bone marrow cells through specific collaboration with meis1a but not pbx1b. *Embo Journal,* 17**,** 3714-3725.

KUMAR, A. R., LI, Q., HUDSON, W. A., CHEN, W., SAM, T., YAO, Q., LUND, E. A., WU, B., KOWAL, B. J. & KERSEY, J. H. 2009. A role for meis1 in mll-fusion gene leukemia. *Blood,* 113**,** 1756-8.

LAPIDOT, T., PFLUMIO, F., DOEDENS, M., MURDOCH, B., WILLIAMS, D. E. & DICK, J. E. 1992. Cytokine stimulation of multilineage hematopoiesis from immature human-cells engrafted in scid mice. *Science,* 255**,** 1137-1141.

LAPIDOT, T., SIRARD, C., VORMOOR, J., MURDOCH, B., HOANG, T., CACERESCORTES, J., MINDEN, M., PATERSON, B., CALIGIURI, M. A. & DICK, J. E. 1994. A cell initiating human acute myeloid-leukemia after transplantation into scid mice. *Nature,* 367**,** 645-648.

LAUSCHER, J. C., LODDENKEMPER, C., KOSEL, L., GRONE, J., BUHR, H. J. & HUBER, O. 2007. Increased pontin expression in human colorectal cancer tissue. *Hum Pathol,* 38**,** 978-85.

LAVAU, C., DU, C. C., THIRMAN, M. & ZELEZNIK-LE, N. 2000a. Chromatin-related properties of cbp fused to mll generate a myelodysplastic-like syndrome that evolves into myeloid leukemia. *Embo Journal,* 19**,** 4655-4664.

LAVAU, C., LUO, R. T., DU, C. C. & THIRMAN, M. J. 2000b. Retrovirus-mediated gene transfer of mll-ell transforms primary myeloid progenitors and causes acute myeloid leukemias in mice. *Proceedings of the National Academy of Sciences of the United States of America,* 97**,** 10984-10989.

LAVAU, C., SZILVASSY, S. J., SLANY, R. & CLEARY, M. L. 1997. Immortalization and leukemic transformation of a myelomonocytic precursor by retrovirally transduced hrx-enl. *EMBO J,* 16**,** 4226-37.

LAWRENCE, H. J., SAUVAGEAU, G., HUMPHRIES, R. K. & LARGMAN, C. 1996. The role of hox homeobox genes in normal and leukemic hematopoiesis. *Stem Cells,* 14**,** 281-291.

LEE, J., SUNG, Y. H., CHEONG, C., CHOI, Y. S., JEON, H. K., SUN, W., HAHN, W. C., ISHIKAWA, F. & LEE, H. W. 2008. Tert promotes cellular and organismal survival independently of telomerase activity. *Oncogene,* 27**,** 3754-3760.

LEUNG, R. K. M. & WHITTAKER, P. A. 2005. Rna interference: From gene silencing to gene-specific therapeutics. *Pharmacology & Therapeutics,* 107**,** 222-239.

LI, W., ZENG, J., LI, Q., ZHAO, L., LIU, T., BJORKHOLM, M., JIA, J. & XU, D. 2010. Reptin is required for the transcription of telomerase reverse transcriptase and over-expressed in gastric cancer. *Mol Cancer,* 9**,** 132.

LIBURA, J., SLATER, D. J., FELIX, C. A. & RICHARDSON, C. 2005. Therapy-related acute myeloid leukemia-like mll rearrangements are induced by etoposide in primary human cd34(+) cells and remain stable after clonal expansion. *Blood,* 105**,** 2124-2131.

LOWENBERG, B., DOWNING, J. R. & BURNETT, A. 1999. Medical progress - acute myeloid leukemia. *New England Journal of Medicine,* 341**,** 1051-1062.

MANZ, M. G., MIYAMOTO, T., AKASHI, K. & WEISSMAN, I. L. 2002. Prospective isolation of human clonogenic common myeloid progenitors. *Proc Natl Acad Sci U S A,* 99**,** 11872-7.

MARSHALL, C. J. & THRASHER, A. J. 2001. The embryonic origins of human haematopoiesis. *Br J Haematol,* 112**,** 838-850.

MARTINEZ, P. & BLASCO, M. A. 2011. Telomeric and extra-telomeric roles for telomerase and the telomere-binding proteins. *Nat Rev Cancer,* 11**,** 161-76.

MARTINO, V., TONELLI, R., MONTEMURRO, L., FRANZONI, M., MARINO, F., FAZZINA, R. & PESSION, A. 2006. Down-regulation of mll-af9, mll and myc expression is not obligatory for monocyte-macrophage maturation in aml-m5 cell lines carrying t(9;11)(p22;q23). *Oncology Reports,* 15**,** 207-211.

MASLON, M. M., HRSTKA, R., VOJTESEK, B. & HUPP, T. R. 2010. A divergent substrate-binding loop within the pro-oncogenic protein anterior gradient-2 forms a docking site for reptin. *J Mol Biol,* 404**,** 418-38.

MASSARD, C., ZERMATI, Y., PAULEAU, A. L., LAROCHETTE, N., WETIVIER, D., SABATIER, L., KROEMER, G. & SORIA, J. C. 2006. Htert: A novel endogenous inhibitor of the mitochondrial cell death pathway. *Oncogene,* 25**,** 4505-4514.

MATIAS, P. M., GORYNIA, S., DONNER, P. & CARRONDO, M. A. 2006. Crystal structure of the human aaa(+) protein ruvbl1. *Journal of Biological Chemistry,* 281**,** 38918-38929.

MATSUO, Y. & DREXLER, H. G. 1998. Establishment and characterization of human b cell precursor-leukemia cell lines. *Leuk Res,* 22**,** 567-79.

MAZO, A. M., HUANG, D. H., MOZER, B. A. & DAWID, I. B. 1990. The trithorax gene, a trans-acting regulator of the bithorax complex in drosophila, encodes a protein with zinc-binding domains. *Proceedings of the National Academy of Sciences of the United States of America,* 87**,** 2112-2116.

MCMAHON, K. A., HIEW, S. Y. L., HADJUR, S., VEIGA-FERNANDES, H., MENZEL, U., PRICE, A. J., KIOUSSIS, D., WILLIAMS, O. & BRADY, H. J. M. 2007. Mii has a critical role in fetal and adult hematopoietic stem cell self-renewal. *Cell Stem Cell,* 1**,** 338-345.

MEDVINSKY, A. & DZIERZAK, E. 1996. Definitive hematopoiesis is autonomously initiated by the agm region. *Cell,* 86**,** 897-906.

MENARD, L., TARAS, D., GRIGOLETTO, A., HAURIE, V., NICOU, A., DUGOT-SENANT, N., COSTET, P., ROUSSEAU, B. & ROSENBAUM, J. 2010. In vivo silencing of reptin blocks the progression of human hepatocellular carcinoma in xenografts and is associated with replicative senescence. *J Hepatol,* 52**,** 681-9.

MEYER, C., SCHNEIDER, B., JAKOB, S., STREHL, S., ATTARBASCHI, A., SCHNITTGER, S., SCHOCH, C., JANSEN, M. W., VAN DONGEN, J. J., DEN BOER, M. L., PIETERS, R., ENNAS, M. G., ANGELUCCI, E., KOEHL, U., GREIL, J., GRIESINGER, F., ZUR STADT, U., ECKERT, C., SZCZEPANSKI, T., NIGGLI, F. K., et al. 2006. The mll recombinome of acute leukemias. *Leukemia,* 20**,** 777-84.

MEZARD, C., DAVIES, A. A., STASIAK, A. & WEST, S. C. 1997. Biochemical properties of ruvb(d113n): A mutation in helicase motif ii of the ruvb hexamer affects DNA binding and atpase activities. *Journal of Molecular Biology,* 271**,** 704-717.

MILNE, T. A., BRIGGS, S. D., BROCK, H. W., MARTIN, M. E., GIBBS, D., ALLIS, C. D. & HESS, J. L. 2002. Mll targets set domain methyltransferase activity to hox gene promoters. *Molecular Cell,* 10**,** 1107-1117.

MILNE, T. A., DOU, Y., MARTIN, M. E., BROCK, H. W., ROEDER, R. G. & HESS, J. L. 2005. Mll associates specifically with a subset of transcriptionally active target genes. *Proc Natl Acad Sci U S A,* 102**,** 14765-70.

MILNE, T. A., KIM, J., WANG, G. G., STADLER, S. C., BASRUR, V., WHITCOMB, S. J., WANG, Z., RUTHENBURG, A. J., ELENITOBA-JOHNSON, K. S. J., ROEDER, R. G. & ALLIS, C. D. 2010. Multiple interactions recruit mll1 and mll1 fusion proteins to the hoxa9 locus in leukemogenesis. *Molecular Cell,* 38**,** 853-863.

MITTAL, V. 2004. Improving the efficiency of rna interference in mammals. *Nat Rev Genet,* 5**,** 355-65.

MORGENSTERN, J. P. & LAND, H. 1990. Advanced mammalian gene transfer: High titre retroviral vectors with multiple drug selection markers and a complementary helper-free packaging cell line. *Nucleic Acids Res,* 18**,** 3587-96.

MORITA, S., KOJIMA, T. & KITAMURA, T. 2000. Plat-e: An efficient and stable system for transient packaging of retroviruses. *Gene Ther,* 7**,** 1063-6.

MORRISON, S. J., LAGASSE, E. & WEISSMAN, I. L. 1994. Demonstration that thy(lo) subsets of mouse bone marrow that express high levels of lineage markers are not significant hematopoietic progenitors. *Blood,* 83**,** 3480-90.

MORRISON, S. J., WANDYCZ, A. M., HEMMATI, H. D., WRIGHT, D. E. & WEISSMAN, I. L. 1997. Identification of a lineage of multipotent hematopoietic progenitors. *Development,* 124**,** 1929-1939.

MORRISON, S. J. & WEISSMAN, I. L. 1994. The long-term repopulating subset of hematopoietic stem cells is deterministic and isolatable by phenotype. *Immunity,* 1**,** 661-73.

MUELLER, D., BACH, C., ZEISIG, D., GARCIA-CUELLAR, M. P., MONROE, S., SREEKUMAR, A., ZHOU, R., NESVIZHSKII, A., CHINNAIYAN, A., HESS, J. L. & SLANY, R. K. 2007. A role for the mll fusion partner enl in transcriptional elongation and chromatin modification. *Blood,* 110**,** 4445-54.

MULLER, A. M., MEDVINSKY, A., STROUBOULIS, J., GROSVELD, F. & DZIERZAK, E. 1994. Development of hematopoietic stem-cell activity in the mouse embryo. *Immunity,* 1**,** 291-301.

MULLOY, J. C., WUNDERLICH, M., ZHENG, Y. & WEI, J. P. 2008. Transforming human blood stem and progenitor cells a new way forward in leukemia modeling. *Cell Cycle,* 7**,** 3314-3319.

NAKAMURA, T., MORI, T., TADA, S., KRAJEWSKI, W., ROZOVSKAIA, T., WASSELL, R., DUBOIS, G., MAZO, A., CROCE, C. M. & CANAANI, E. 2002. All-1 is a histone methyltransferase that assembles a supercomplex of proteins involved in transcriptional regulation. *Molecular Cell,* 10**,** 1119-1128.

NALDINI, L. 1998. Lentiviruses as gene transfer agents for delivery to non-dividing cells. *Curr Opin Biotechnol,* 9**,** 457-63.

NALDINI, L., BLOMER, U., GALLAY, P., ORY, D., MULLIGAN, R., GAGE, F. H., VERMA, I. M. & TRONO, D. 1996. In vivo gene delivery and stable transduction of nondividing cells by a lentiviral vector. *Science,* 272**,** 263-7.

NIE, Z. Q., YAN, Z. J., CHEN, E. H., SECHI, S., LING, C., ZHOU, S. L., XUE, Y. T., YANG, D. F., MURRAY, D., KANAKUBO, E., CLEARY, M. L. & WANG, W. D. 2003. Novel swi/snf chromatin-remodeling complexes contain a mixed-lineage leukemia chromosomal translocation partner. *Molecular and Cellular Biology,* 23**,** 2942-2952.

OHYASHIKI, J. H., OHYASHIKI, K., IWAMA, H., HAYASHI, S., TOYAMA, K. & SHAY, J. W. 1997. Clinical implications of telomerase activity levels in acute leukemia. *Clinical Cancer Research,* 3**,** 619-625.

OKADA, Y., FENG, Q., LIN, Y. H., JIANG, Q., LI, Y. Q., COFFIELD, V. M., SU, L. S., XU, G. L. & ZHANG, Y. 2005. Hdot1l links histone methylation to leukemogenesis. *Cell,* 121**,** 167-178.

OKUNO, Y., IWASAKI, H., HUETTNER, C. S., RADOMSKA, H. S., GONZALEZ, D. A., TENEN, D. G. & AKASHI, K. 2002. Differential regulation of the human and murine cd34 genes in hematopoietic stem cells. *Proceedings of the National Academy of Sciences of the United States of America,* 99**,** 6246-6251.

ORKIN, S. H. 2000. Diversification of haematopoietic stem cells to specific lineages. *Nat Rev Genet,* 1**,** 57-64.

ORKIN, S. H. & ZON, L. I. 2008. Hematopoiesis: An evolving paradigm for stem cell biology. *Cell,* 132**,** 631-44.

OSAWA, M., HANADA, K., HAMADA, H. & NAKAUCHI, H. 1996. Long-term lymphohematopoietic reconstitution by a single cd34-low/negative hematopoietic stem cell. *Science,* 273**,** 242-245.

PALIS, J., ROBERTSON, S., KENNEDY, M., WALL, C. & KELLER, G. 1999. Development of erythroid and myeloid progenitors in the yolk sac and embryo proper of the mouse. *Development,* 126**,** 5073-5084.

PEARCE, D. J., TAUSSIG, D., ZILBARA, K., SMITH, L. L., RIDLER, C. M., PREUDHOMME, C., YOUNG, B. D., ROHATINER, A. Z., LISTER, T. A. & BONNET, D. 2006. Aml engraftment in the nod/scid assay reflects the outcome of aml: Implications for our understanding of the heterogeneity of aml. *Blood,* 107**,** 1166-1173.

PESSION, A., MARTINO, V., TONELLI, R., BELTRAMINI, C., LOCATELLI, F., BISERNI, G., FRANZONI, M., FRECCERO, F., MONTEMURRO, L.,

PATTACINI, L. & PAOLUCCI, G. 2003. Mll-af9 oncogene expression affects cell growth but not terminal differentiation and is downregulated during monocyte-macrophage maturation in aml-m5 thp-1 cells. *Oncogene,* 22**,** 8671-6.

PINEAULT, N., HELGASON, C. D., LAWRENCE, H. J. & HUMPHRIES, R. K. 2002. Differential expression of hox, meis1, and pbx1 genes in primitive cells throughout murine hematopoietic ontogeny. *Experimental Hematology,* 30**,** 49-57.

PLOEMACHER, R. E., VANDERSLUIJS, J. P., VOERMAN, J. S. A. & BRONS, N. H. C. 1989. An invitro limiting-dilution assay of long-term repopulating hematopoietic stem-cells in the mouse. *Blood,* 74**,** 2755-2763.

POCOCK, C. F., MALONE, M., BOOTH, M., EVANS, M., MORGAN, G., GREIL, J. & COTTER, F. E. 1995. Bcl-2 expression by leukaemic blasts in a scid mouse model of biphenotypic leukaemia associated with the t(4;11)(q21;q23) translocation. *Br J Haematol,* 90**,** 855-67.

PRASAD, R., YANO, T., SORIO, C., NAKAMURA, T., RALLAPALLI, R., GU, Y., LESHKOWITZ, D., CROCE, C. M. & CANAANI, E. 1995. Domains with transcriptional regulatory activity within the all1 and af4 proteins involved in acute leukemia. *Proceedings of the National Academy of Sciences of the United States of America,* 92**,** 12160-12164.

PRIETO, J., EKLUND, A. & PATARROYO, M. 1994. Regulated expression of integrins and other adhesion molecules during differentiation of monocytes into macrophages. *Cellular Immunology,* 156**,** 191-211.

PUI, C. H. 1995. Childhood leukemias. *New England Journal of Medicine,* 332**,** 1618-1630.

PURI, T., WENDLER, P., SIGALA, B., SAIBIL, H. & TSANEVA, I. R. 2007. Dodecameric structure and atpase activity of the human tip48/tip49 complex. *Journal of Molecular Biology,* 366**,** 179-192.

QUENTMEIER, H., DIRKS, W. G., MACLEOD, R. A. F., REINHARDT, J., ZABORSKI, M. & DREXLER, H. G. 2004. Expression of hox genes in acute leukemia cell lines with and without mll translocations. *Leukemia & Lymphoma,* 45**,** 567-574.

RANDALL, T. D., LUND, F. E., HOWARD, M. C. & WEISSMAN, I. L. 1996. Expression of murine cd38 defines a population of long-term reconstituting hematopoietic stem cells. *Blood,* 87**,** 4057-67.

RAO, D. D., VORHIES, J. S., SENZER, N. & NEMUNAITIS, J. 2009. Sirna vs. Shrna: Similarities and differences. *Advanced Drug Delivery Reviews,* 61**,** 746-759.

REISER, J. 2000. Production and concentration of pseudotyped hiv-1-based gene transfer vectors. *Gene Ther,* 7**,** 910-3.

REYA, T., MORRISON, S. J., CLARKE, M. F. & WEISSMAN, I. L. 2001. Stem cells, cancer, and cancer stem cells. *Nature,* 414**,** 105-111.

ROCHE, S., ALBERTINI, A. A. V., LEPAULT, J., BRESSANELLI, S. & GAUDIN, Y. 2008. Structures of vesicular stomatitis virus glycoprotein: Membrane fusion revisited. *Cellular and Molecular Life Sciences,* 65**,** 1716-1728.

ROTH, A., VERCAUTEREN, S., SUTHERLAND, H. J. & LANDSORP, P. M. 2003. Telomerase is limiting the growth of acute myeloid leukemia cells. *Leukemia,* 17**,** 2410-2417.

ROUSSEAU, B., MENARD, L., HAURIE, V., TARAS, D., BLANC, J. F., MOREAU-GAUDRY, F., METZLER, P., HUGUES, M., BOYAULT, S., LEMIERE, S., CANRON, Z., COSTET, P., COLE, M., BALABAUD, C., BIOULAC-SAGE, P., ZUCMAN-ROSSI, J. & ROSENBAUM, J. 2007. Overexpression and role of the atpase and putative DNA helicase ruvb-like 2 in human hepatocellular carcinoma. *Hepatology,* 46**,** 1108-1118.

ROWLEY, J. D., RESHMI, S., SOBULO, O., MUSVEE, T., ANASTASI, J., RAIMONDI, S., SCHNEIDER, N. R., BARREDO, J. C., CANTU, E. S., SCHLEGELBERGER, B., BEHM, F., DOGGETT, N. A., BORROW, J. & ZELEZNIKLE, N. 1997. All patients with the t(11;16)(q23;p13.3) that involves mll and cbp have treatment-related hematologic disorders. *Blood,* 90**,** 535-541.

ROZENBLATT-ROSEN, O., ROZOVSKAIA, T., BURAKOV, D., SEDKOV, Y., TILLIB, S., BLECHMAN, J., NAKAMURA, T., CROCE, C. M., MAZO, A. & CANAANI, E. 1998. The c-terminal set domains of all-1 and trithorax interact with the ini1 and snr1 proteins, components of the swi/snf complex. *Proceedings of the National Academy of Sciences of the United States of America,* 95**,** 4152-4157.

RUTHENBURG, A. J., WANG, W. K., GRAYBOSCH, D. M., LI, H. T., ALLIS, C. D., PATEL, D. J. & VERDINE, G. L. 2006. Histone h3 recognition and presentation by the wdr5 module of the mll1 complex. *Nature Structural & Molecular Biology,* 13**,** 704-712.

SANDRIN, V., BOSON, B., SALMON, P., GAY, W., NEGRE, D., LE GRAND, R., TRONO, D. & COSSET, F. L. 2002. Lentiviral vectors pseudotyped with a modified rd114 envelope glycoprotein show increased stability in sera and augmented transduction of primary lymphocytes and cd34+ cells derived from human and nonhuman primates. *Blood,* 100**,** 823-32.

SAUVAGEAU, G., LANSDORP, P. M., EAVES, C. J., HOGGE, D. E., DRAGOWSKA, W. H., REID, D. S., LARGMAN, C., LAWRENCE, H. J. & HUMPHRIES, R. K. 1994. Differential expression of homeobox genes in functionally distinct cd34(+) subpopulations of human bone-marrow cells. *Proceedings of the National Academy of Sciences of the United States of America,* 91**,** 12223-12227.

SCANDURA, J. M., BOCCUNI, P., CAMMENGA, J. & NIMER, S. D. 2002. Transcription factor fusions in acute leukemia: Variations on a theme. *Oncogene,* 21**,** 3422-3444.

SCHERR, M., BATTMER, K., WINKLER, T., HEIDENREICH, O., GANSER, A. & EDER, M. 2003. Specific inhibition of bcr-abl gene expression by small interfering rna. *Blood,* 101**,** 1566-1569.

SCHREINER, S., BIRKE, M., GARCIA-CUELLAR, M. P., ZILLES, O., GREIL, J. & SLANY, R. K. 2001. Mll-enl causes a reversible and myc-dependent block of myelomonocytic cell differentiation. *Cancer Res,* 61**,** 6480-6.

SCHULTZ, D. C., FRIEDMAN, J. R. & RAUSCHER, F. J. 2001. Targeting histone deacetylase complexes via krab-zinc finger proteins: The phd and bromodomains of kap-1 form a cooperative unit that recruits a novel isoform of the mi-2 alpha subunit of nurd. *Genes & Development,* 15**,** 428-443.

SCHULZE, J. M., WANG, A. Y. & KOBOR, M. S. 2009. Yeats domain proteins: A diverse family with many links to chromatin modification and transcription. *Biochem Cell Biol,* 87**,** 65-75.

SENA-ESTEVES, M., TEBBETS, J. C., STEFFENS, S., CROMBLEHOLME, T. & FLAKE, A. W. 2004. Optimized large-scale production of high titer lentivirus vector pseudotypes. *J Virol Methods,* 122**,** 131-9.

SHIN, N. H., HARTIGAN-O'CONNOR, D., PFEIFFER, J. K. & TELESNITSKY, A. 2000. Replication of lengthened moloney murine leukemia virus genomes is impaired at multiple stages. *J Virol,* 74**,** 2694-702.

SHULTZ, L. D., SCHWEITZER, P. A., CHRISTIANSON, S. W., GOTT, B., SCHWEITZER, I. B., TENNENT, B., MCKENNA, S., MOBRAATEN, L., RAJAN, T. V., GREINER, D. L. & LEITER, E. H. 1995. Multiple defects in innate and adaptive immunological function in nod/ltsz-scid mice. *Journal of Immunology,* 154**,** 180-191.

SIERRA, J., YOSHIDA, T., JOAZEIRO, C. A. & JONES, K. A. 2006. The apc tumor suppressor counteracts beta-catenin activation and h3k4 methylation at wnt target genes. *Genes & Development,* 20**,** 586-600.

SILVA, J. M., LI, M. Z., CHANG, K., GE, W., GOLDING, M. C., RICKLES, R. J., SIOLAS, D., HU, G., PADDISON, P. J., SCHLABACH, M. R., SHETH, N., BRADSHAW, J., BURCHARD, J., KULKARNI, A., CAVET, G., SACHIDANANDAM, R., MCCOMBIE, W. R., CLEARY, M. A., ELLEDGE, S. J. & HANNON, G. J. 2005. Second-generation shrna libraries covering the mouse and human genomes. *Nature Genetics,* 37**,** 1281-1288.

SINGH, S. K., CLARKE, I. D., TERASAKI, M., BONN, V. E., HAWKINS, C., SQUIRE, J. & DIRKS, P. B. 2003. Identification of a cancer stem cell in human brain tumors. *Cancer Res,* 63**,** 5821-8.

SIRVEN, A., RAVET, E., CHARNEAU, P., ZENNOU, V., COULOMBEL, L., GUETARD, D., PFLUMIO, F. & DUBART-KUPPERSCHMITT, A. 2001. Enhanced transgene expression in cord blood cd34(+)-derived hematopoietic cells, including developing t cells and nod/scid mouse repopulating cells, following transduction with modified trip lentiviral vectors. *Molecular Therapy,* 3**,** 438-448.

SLANY, R. K. 2009. The molecular biology of mixed lineage leukemia. *Haematologica,* 94**,** 984-93.

SLANY, R. K., LAVAU, C. & CLEARY, M. L. 1998. The oncogenic capacity of hrx-enl requires the transcriptional transactivation activity of enl and the DNA binding motifs of hrx. *Molecular and Cellular Biology,* 18**,** 122-129.

SO, C. W., LIN, M., AYTON, P. M., CHEN, E. H. & CLEARY, M. L. 2003. Dimerization contributes to oncogenic activation of mll chimeras in acute leukemias. *Cancer Cell,* 4**,** 99-110.

SOMERVAILLE, T. C. P. & CLEARY, M. L. 2006. Identification and characterization of leukemia stem cells in murine mll-af9 acute myeloid leukemia. *Cancer Cell,* 10**,** 257-268.

SOMERVAILLE, T. C. P. & CLEARY, M. L. 2010. Grist for the mll: How do mll oncogenic fusion proteins generate leukemia stem cells? *International Journal of Hematology,* 91**,** 735-741.

SOUTHALL, S. M., WONG, P. S., ODHO, Z., ROE, S. M. & WILSON, J. R. 2009. Structural basis for the requirement of additional factors for mll1 set domain activity and recognition of epigenetic marks. *Molecular Cell,* 33**,** 181-191.

SPANGRUDE, G. J., HEIMFELD, S. & WEISSMAN, I. L. 1988. Purification and characterization of mouse hematopoietic stem-cells. *Science,* 241**,** 58-62.

STRANG, B. L., IKEDA, Y., COSSET, F. L., COLLINS, M. K. & TAKEUCHI, Y. 2004. Characterization of hiv-1 vectors with gammaretrovirus envelope glycoproteins produced from stable packaging cells. *Gene Ther,* 11**,** 591-8.

SUN, X. J., YAU, V. K., BRIGGS, B. J. & WHITTAKER, G. R. 2005. Role of clathrin-mediated endocytosis during vesicular stomatitis virus entry into host cells. *Virology,* 338**,** 53-60.

SUTHERLAND, H. J., EAVES, C. J., EAVES, A. C., DRAGOWSKA, W. & LANSDORP, P. M. 1989. Characterization and partial purification of human marrow cells capable of initiating long-term hematopoiesis in vitro. *Blood,* 74**,** 1563-70.

SUTHERLAND, H. J., LANSDORP, P. M., HENKELMAN, D. H., EAVES, A. C. & EAVES, C. J. 1990. Functional-characterization of individual human hematopoietic stem-cells cultured at limiting dilution on supportive marrow stromal layers. *Proceedings of the National Academy of Sciences of the United States of America,* 87**,** 3584-3588.

SUZUKI, H., FORREST, A. R. R., VAN NIMWEGEN, E., DAUB, C. O., BALWIERZ, P. J., IRVINE, K. M., LASSMANN, T., RAVASI, T., HASEGAWA, Y., DE HOON, M. J. L., KATAYAMA, S., SCHRODER, K., CARNINCI, P., TOMARU, Y., KANAMORI-KATAYAMA, M., KUBOSAKI, A., AKALIN, A., ANDO, Y., ARNER, E., ASADA, M., et al. 2009. The transcriptional network that controls growth arrest and differentiation in a human myeloid leukemia cell line. *Nature Genetics,* 41**,** 553-562.

TAKI, T., SAKO, M., TSUCHIDA, M. & HAYASHI, Y. 1997. The t(11;16)(q23;p13) translocation in myelodysplastic syndrome fuses the mll gene to the cbp gene. *Blood,* 89**,** 3945-3950.

TAVIAN, M. & PEAULT, B. 2005. The changing cellular environments of hematopoiesis in human development in utero. *Exp Hematol,* 33**,** 1062-9.

TERSTAPPEN, L., HUANG, S., SAFFORD, M., LANSDORP, P. M. & LOKEN, M. R. 1991. Sequential generations of hematopoietic colonies derived from single nonlineage-committed cd34+cd38- progenitor cells. *Blood,* 77**,** 1218-1227.

THIEL, A. T., BLESSINGTON, P., ZOU, T., FEATHER, D., WU, X. J., YAN, J. Z., ZHANG, H., LIU, Z. G., ERNST, P., KORETZKY, G. A. & HUA, X. X. 2010. Mll-af9-induced leukemogenesis requires coexpression of the wild-type mll allele. *Cancer Cell,* 17**,** 148-159.

THOMAS, M., GESSNER, A., VORNLOCHER, H. P., HADWIGER, P., GREIL, J. & HEIDENREICH, O. 2005. Targeting mll-af4 with short interfering rnas inhibits clonogenicity and engraftment of t(4;11)-positive human leukemic cells. *Blood,* 106**,** 3559-3566.

TKACHUK, D. C., KOHLER, S. & CLEARY, M. L. 1992. Involvement of a homolog of drosophila-trithorax by 11q23 chromosomal translocations in acute leukemias. *Cell,* 71**,** 691-700.

TRAVER, D., AKASHI, K., MANZ, M., MERAD, M., MIYAMOTO, T., ENGLEMAN, E. G. & WEISSMAN, I. L. 2000. Development of cd8 alpha-positive dendritic cells from a common myeloid progenitor. *Science,* 290**,** 2152-2154.

TSUCHIYA, S., YAMABE, M., YAMAGUCHI, Y., KOBAYASHI, Y., KONNO, T. & TADA, K. 1980. Establishment and characterization of a human acute monocytic leukemia cell line (thp-1). *Int J Cancer,* 26**,** 171-6.

VENTEICHER, A. S., MENG, Z. J., MASON, P. J., VEENSTRA, T. D. & ARTANDI, S. E. 2008. Identification of atpases pontin and reptin as telomerase components essential for holoenzyme assembly. *Cell,* 132**,** 945-957.

VERSTOVSEK, S., MANSHOURI, T., SMITH, F. O., GILES, F. J., CORTES, J., ESTEY, E., KANTARJIAN, H., KEATING, M., JEHA, S. & ALBITAR, M. 2003. Telomerase activity is prognostic in pediatric patients with acute myeloid leukemia - comparison with adult acute myeldid leukemia. *Cancer,* 97**,** 2212-2217.

VON LAER, D., COROVIC, A., VOGT, B., HERWIG, U., ROSCHER, S., FEHSE, B. & BAUM, C. 2000. Amphotropic and vsv-g-pseudotyped retroviral vectors transduce human hematopoietic progenitor cells with similar efficiency. *Bone Marrow Transplantation,* 25**,** S75-S79.

VORMOOR, J., LAPIDOT, T., PFLUMIO, F., RISDON, G., PATTERSON, B., BROXMEYER, H. E. & DICK, J. E. 1994. Immature human cord-blood progenitors engraft and proliferate to high-levels in severe combined immunodeficient mice. *Blood,* 83**,** 2489-2497.

WALTERS, D. K. & JELINEK, D. F. 2002. The effectiveness of double-stranded short inhibitory rnas (sirnas) may depend on the method of transfection. *Antisense & Nucleic Acid Drug Development,* 12**,** 411-418.

WALTHER, W. & STEIN, U. 2000. Viral vectors for gene transfer - a review of their use in the treatment of human diseases. *Drugs,* 60**,** 249-271.

WANG, Q. F., WU, G., MI, S. L., HE, F. H., WU, J., DONG, J. F., LUO, R. T., MATTISON, R., KABERLEIN, J. J., PRABHAKAR, S., JI, H. K. & THIRMAN, M. J. 2011. Mll fusion proteins preferentially regulate a subset of wild-type mll target genes in the leukemic genome. *Blood,* 117**,** 6895-6905.

WANG, Y. Z., KRIVTSOV, A. V., SINHA, A. U., NORTH, T. E., GOESSLING, W., FENG, Z. H., ZON, L. I. & ARMSTRONG, S. A. 2010. The wnt/beta-catenin pathway is required for the development of leukemia stem cells in aml. *Science,* 327**,** 1650-1653.

WEI, J., WUNDERLICH, M., FOX, C., ALVAREZ, S., CIGUDOSA, J. C., WILHELM, J. S., ZHENG, Y., CANCELAS, J. A., GU, Y., JANSEN, M., DIMARTINO, J. F. & MULLOY, J. C. 2008. Microenvironment determines lineage fate in a human model of mll-af9 leukemia. *Cancer Cell,* 13**,** 483-95.

WONG, P., IWASAKI, M., SOMERVAILLE, T. C. P., SO, C. W. E. & CLEARY, M. L. 2007. Meis1 is an essential and rate-limiting regulator of mll leukemia stem cell potential. *Genes & Development,* 21**,** 2762-2774.

WOOD, M. A., MCMAHON, S. B. & COLE, M. D. 2000. An atpase/helicase complex is an essential cofactor for oncogenic transformation by c-myc. *Mol Cell,* 5**,** 321-30.

XIA, Z. B., ANDERSON, M., DIAZ, M. O. & ZELEZNIK-LE, N. J. 2003. Mll repression domain interacts with histone deacetylases, the polycomb group proteins hpc2 and bmi-1, and the corepressor c-terminal-binding protein. *Proceedings of the National Academy of Sciences of the United States of America,* 100**,** 8342-8347.

XU, D. W., GRUBER, A., PETERSON, C. & PISA, P. 1998. Telomerase activity and the expression of telomerase components in acute myelogenous leukaemia. *Br J Haematol,* 102**,** 1367-1375.

YAGI, H., DEGUCHI, K., AONO, A., TANI, Y., KISHIMOTO, T. & KOMORI, T. 1998. Growth disturbance in fetal liver hematopoiesis of mll-mutant mice. *Blood,* 92**,** 108-117.

YEOH, E. J., ROSS, M. E., SHURTLEFF, S. A., WILLIAMS, W. K., PATEL, D., MAHFOUZ, R., BEHM, F. G., RAIMONDI, S. C., RELLING, M. V., PATEL, A., CHENG, C., CAMPANA, D., WILKINS, D., ZHOU, X. D., LI, J. Y., LIU, H. Q., PUI, C. H., EVANS, W. E., NAEVE, C., WONG, L. S., et al. 2002. Classification, subtype discovery, and prediction of outcome in pediatric acute lymphoblastic leukemia by gene expression profiling. *Cancer Cell,* 1**,** 133-143.

YOKOYAMA, A. & CLEARY, M. L. 2008. Menin critically links mll proteins with LEDGF on cancer-associated target genes. *Cancer Cell,* 14**,** 36-46.

YOKOYAMA, A., KITABAYASHI, I., AYTON, P. M., CLEARY, M. L. & OHKI, M. 2002. Leukemia proto-oncoprotein mll is proteolytically processed into 2 fragments with opposite transcriptional properties. *Blood,* 100**,** 3710-3718.

YOKOYAMA, A., LIN, M., NARESH, A., KITABAYASHI, I. & CLEARY, M. L. 2010. A higher-order complex containing af4 and enl family proteins with p-tefb facilitates oncogenic and physiologic mll-dependent transcription. *Cancer Cell,* 17**,** 198-212.

YOKOYAMA, A., SOMERVAILLE, T. C. P., SMITH, K. S., ROZENBLATT-ROSEN, O., MEYERSON, M. & CLEARY, M. L. 2005. The menin tumor suppressor protein is an essential oncogenic cofactor for mll-associated leukemogenesis. *Cell,* 123**,** 207-218.

YOKOYAMA, A., WANG, Z., WYSOCKA, J., SANYAL, M., AUFIERO, D. J., KITABAYASHI, I., HERR, W. & CLEARY, M. L. 2004. Leukemia proto-oncoprotein mll forms a set1-like histone methyltransferase complex with menin to regulate hox gene expression. *Molecular and Cellular Biology,* 24**,** 5639-5649.

YU, B. D., HESS, J. L., HORNING, S. E., BROWN, G. A. J. & KORSMEYER, S. J. 1995. Altered hox expression and segmental identity in mll-mutant mice. *Nature,* 378**,** 505-508.

ZEISIG, B. B., GARCIA-CUELLAR, M. P., WINKLER, T. H. & SLANY, R. K. 2003. The oncoprotein mll-enl disturbs hematopoietic lineage determination and transforms a biphenotypic lymphoid/myeloid cell. *Oncogene,* 22**,** 1629-1637.

ZEISIG, B. B., MILNE, T., GARCIA-CUELLAR, M. P., SCHREINER, S., MARTIN, M. E., FUCHS, U., BORKHARDT, A., CHANDA, S. K., WALKER, J., SODEN, R., HESS, J. L. & SLANY, R. K. 2004. Hoxa9 and meis1 are key targets for mll-enl-mediated cellular immortalization. *Mol Cell Biol,* 24**,** 617-28.

ZEISIG, D. T., BITTNER, C. B., ZEISIG, B. B., GARCIA-CUELLAR, M. P., HESS, J. L. & SLANY, R. K. 2005. The eleven-nineteen-leukemia protein enl connects nuclear mll fusion partners with chromatin. *Oncogene,* 24**,** 5525-5532.

ZELEZNIKLE, N. J., HARDEN, A. M. & ROWLEY, J. D. 1994. 11q23-translocations split the at-hook cruciform DNA-binding region and the transcriptional repression domain from the activation domain of the mixed-lineage leukemia (mll) gene. *Proceedings of the National Academy of Sciences of the United States of America,* 91**,** 10610-10614.

ZHANG, X. L., MAR, V., ZHOU, W., HARRINGTON, L. & ROBINSON, M. O. 1999. Telomere shortening and apoptosis in telomerase-inhibited human tumor cells. *Genes & Development,* 13**,** 2388-2399.

ZIEMINVANDERPOEL, S., MCCABE, N. R., GILL, H. J., ESPINOSA, R., PATEL, Y., HARDEN, A., RUBINELLI, P., SMITH, S. D., LEBEAU, M. M., ROWLEY, J. D. & DIAZ, M. O. 1991. Identification of a gene, mll, that spans the breakpoint in 11q23 translocations associated with human leukemias. *Proceedings of the National Academy of Sciences of the United States of America,* 88**,** 10735-10739.